UILU-ENG-96-2006

CIVIL ENGINEERING STUDIES
Transportation Engineering Series No. 94
Illinois Cooperative Highway and Transportation
Series No. 260

ISSN-0197-9191

INTERLAYER STRESS ABSORBING COMPOSITE (ISAC) FOR MITIGATING REFLECTION CRACKING IN ASPHALT CONCRETE OVERLAYS

Final Report

by

M. T. Mukhtar
B. J. Dempsey

A Report of the Findings of:

The Mitigation of Reflection Cracking in Asphalt Concrete Overlays

Project IHR-533
ILLINOIS COOPERATIVE HIGHWAY RESEARCH PROGRAM

Conducted by

DEPARTMENT OF CIVIL ENGINEERING
UNIVERSITY OF ILLINOIS AT URBANA-CHAMPAIGN

and the

ILLINOIS DEPARTMENT OF TRANSPORTATION
in cooperation with the
U.S. DEPARTMENT OF TRANSPORTATION
FEDERAL HIGHWAY ADMINISTRATION

JUNE 1996

Technical Report Documentation Page

1. Report No.	2. Government Accession No.	3. Recipient's Catalog No.
UILU-ENG-96-2006		

4. Title and Subtitle

INTERLAYER STRESS ABSORBING COMPOSITE (ISAC) FOR MITIGATING REFLECTION CRACKING IN ASPHALT CONCRETE OVERLAYS

5. Report Date

June 1996

6. Performing Organization Code

7. Author(s)

Muhammad T. Mukhtar
Barry J. Dempsey

8. Performing Organization Report No.

UILU-ENG-96-2006

9. Performing Organization Name and Address

Department of Civil Engineering
University of Illinois at Urbana-Champaign

10. Work Unit (TRAIS)

11. Contract or Grant No.

IHR-533

12. Sponsoring Agency Name and Address

Illinois Department of Transportation
Bureau of Materials & Physical Research
126 East Ash Street
Springfield, IL 62706

13. Type of Report and Period Covered

14. Sponsoring Agency Code

15. Supplementary Notes

Study was conducted in cooperation with the U.S. Department of Transportation, Federal Highway Administration.

16. Abstract

To approach the reflection cracking problem in AC overlays systematically the properties of the materials intended to be used in an ISAC system were first identified. Various thermal/structural models and laboratory equipment were used for this purpose. A number of woven and nonwoven geotextiles were selected and tested for their engineering properties such as tensile strength, initial modulus, modulus at failure, and percent shrinkage. Several samples of rubber asphalt were prepared by blending different ratios of crumb rubber with various types and ratios of asphalt cements at 400 F. These rubber asphalts were tested at different temperatures and the effects of temperature and rate of deformation on their stiffness were evaluated.

An interlayer stress absorbing composite, ISAC layer was fabricated in the laboratory using the materials considered appropriate. Testing equipment was developed to evaluate the interfacial shear strength and laboratory testing was performed to determine the shear strength of the fabricated ISAC layer under an AC overlay.

The ISAC layer was evaluated for its effectiveness against reflection cracking. A laboratory pavement section with an AC overlay over a jointed PCC slab was constructed and placed in an environmental chamber. A mechanical device was used to simulate thermal strain in the slab and the joint was opened and closed at an extremely slow rate. The testing was conducted at 30F and deterioration in the overlay was monitored using a sensitive LVDT device.

The results from the laboratory evaluation testing program indicated that the ISAC layer was highly effective in preventing reflection cracking in a 2.5 in. AC overlay. When compared to a control test section and a section using a commercially available reflection cracking control material the ISAC layer provided for superior performance. A field pavement test section utilizing the ISAC layer was constructed in the Summer 1994 and field evaluation is ongoing.

17. Key Words

Asphalt Concrete Overlays, Reflection Cracking, Crack Control, Geosynthetic Materials

18. Distribution Statement

19. Security Classif. (of this report)	20. Security Classif. (of this page)	21. No. of Pages	22. Price
Unclassified	Unclassified	235	

Form DOT F 1700.7 (8-72) Reproduction of completed page authorized

ACKNOWLEDGMENTS

This report was prepared as part of the Illinois Cooperative Highway Transportation Research Program, project IHR–533: Interlayer Stress Absorbing Composite (ISAC) for Mitigating Reflection Cracking in Asphalt Concrete Overlays, by the Department of Civil Engineering, University of Illinois at Urbana–Champaign, in cooperation with the Illinois Department of Transportation and the United States Department of Transportation, Federal Highway Administration.

DEDICATION

This report is dedicated to the memory of Harold "Hap" Dalyrmple who set up the hydraulics and electronics for the laboratory testing device used to simulate pavement joint movement. Hap was a major contributor to the success of Transportation research in the Department of Civil Engineering. His innovation, dedication, and willing participation in our research programs will be sorely missed.

DISCLAIMER

The contents of this report reflect the views of the authors who are responsible for the facts and the accuracy of the date presented herein. The contents do not necessarily reflect the official views or policies of the Illinois Department of Transportation of the Federal Highway Administration. This report does not constitute a standard, specification, or regulation.

TABLE OF CONTENTS

LIST OF TABLES

LIST OF FIGURES

Figure **Page**

CHAPTER 1

INTRODUCTION

1.1 General

Many highways constructed during the 1960's and 1970's have reached the end of their design life and some are now deteriorating rapidly due to lack of effective rehabilitation programs. Present rehabilitation programs are consuming a very high percentage of available funds and are seriously affecting future development programs for the expansion of the existing road network.

Asphalt concrete (AC) overlay is the most commonly used method for rehabilitating deteriorated pavements. However, many times this doesn't perform as satisfactorily as is desirable. One major type of distress affecting the life of AC overlay is reflection cracking, in which an existing crack in the old pavement propagates up through the newly constructed overlay. Reflection cracking is caused by one or more cycles of thermal contraction, by repeated traffic loads, or by a combination of these two mechanisms.

Reflection cracking in the overlay not only allows the water to percolate into the pavement structure and weaken the sub base but also contributes to rapid roadway deterioration. Existing methods of overlay design do not address this problem well. A number of studies have, however, been conducted and effort has been made to devise the means to minimize or delay the occurrence of reflection cracking(1, 2, 3, 4, 5 ,6 , 7 , 8 , 9 , 10 , 11 , 12). Various techniques such as increasing the thickness of overlay, cracking and seating the existing pavement, modification of asphalt properties, and pre–overlay repair with placement of crack arresting interlayers (geotextiles) and stress absorbing membrane interlayers (SAMIs) have been used. None of these techniques have completely eradicated the problem of reflection cracking. Some of these treatments have shown positive results under certain conditions but most have given poor performance once subjected to the range of field conditions(1, 2, 3, 4, 5, 7, 8).

1.2 Research Objectives

The goal of this study is to develop a composite material system which can effectively alleviate/mitigate the problem of reflection cracking in an AC overlay. This complex task was approached systematically and a series of research tasks were identified as follows:

a) Literature Review.

b) Identification of properties of the materials needed for the composite material system using various thermal/structural models and laboratory testing procedures

c) Fabrication of the system, using the materials found appropriate.

d) Checking the fabricated system against slippage by using structural models and laboratory testing procedures.

e) Development of a laboratory pavement system for testing and evaluation of the composite material system for its effectiveness against reflection cracking.

1.3 Study Approach

To fully understand the problem, an in depth study was conducted by reviewing various case histories, problem areas were identified, reasons for failure of various techniques were established, and useful conclusions were drawn. Based on these conclusions a new composite material consisting of two geotextile layers containing a thin viscoelastic rubber asphalt layer named, "Interlayer Stress Absorbing Composite (ISAC)" was proposed. Although in the literature review, reflection cracking was attributed to both vertical and horizontal movement of the slab at the joint/crack, most of the researchers concluded that major damage to an overlay occurs because of the horizontal movement of the slab due to temperature variance (2, 6, 13). To achieve simplicity, it was proposed to initially design and evaluate the ISAC system by considering only the horizontal movement of the slab due to thermal effects. The effect of traffic load will be seen later in a separate study in the laboratory and in the field.

To effectively approach the design problem of an ISAC system, it was considered necessary to identify the properties of the materials intended to be used in the system. Various thermal/structural models and laboratory testing procedures were used for this purpose. A Climate–Materials–Structural (CMS) pavement model (model developed at the University of Illinois) (14) was used to establish the pavement temperature range. A number of woven and non woven geotextiles were selected and tested for their engineering properties. Several samples of rubber asphalt were prepared by blending various ratios of crumb rubber with different types and ratios of asphalt cements. These materials were tested at different temperatures and the effects of temperature and rate of deformation on stiffness were investigated.

After having selected the materials suitable for the ISAC system, based on their properties, a prototype ISAC system was designed. The ISAC layer was fabricated in the laboratory and was then checked against slippage under an overlay with a vehicle making a sharp turn or applying sudden brakes. The computer program "CIRCLY" (15) was used for this purpose. Testing equipment was developed to evaluate the interfacial shear strength and laboratory testing was performed to determine the shear strength of the fabricated ISAC layer under an AC overlay. Required stiffness was achieved in the ISAC core material by adding hydrated lime in the rubber asphalt.

After completion of the component property testing program, the ISAC layer was fabricated and prepared for laboratory evaluation. A testing device was developed in the laboratory that simulated field conditions to evaluate an AC overlay over a cracked PCC slab with and without an ISAC system. The performance of the ISAC system was evaluated by comparing crack growth in the overlay of a control pavement section with that in an overlay over the ISAC treated PCC slab.

CHAPTER 2
MECHANICS OF REFLECTION CRACKING

2.1 General

The reflection cracking problem can be effectively addressed if the mechanism is fully understood and performance and behavior of the treatments currently in use are critically analyzed. A detailed literature review was thus completed, various case histories were studied, problem areas were identified, reasons of failure of various techniques were established, and useful conclusions were drawn with the objectives of developing a material system which could effectively alleviate/mitigate the problem of reflection cracking in an AC overlay.

2.2 Phenomenon Of Reflection Cracking

When an overlay is placed on an existing pavement, physical tearing of the overlay takes place as a result of temperature cycles and a crack reflects up

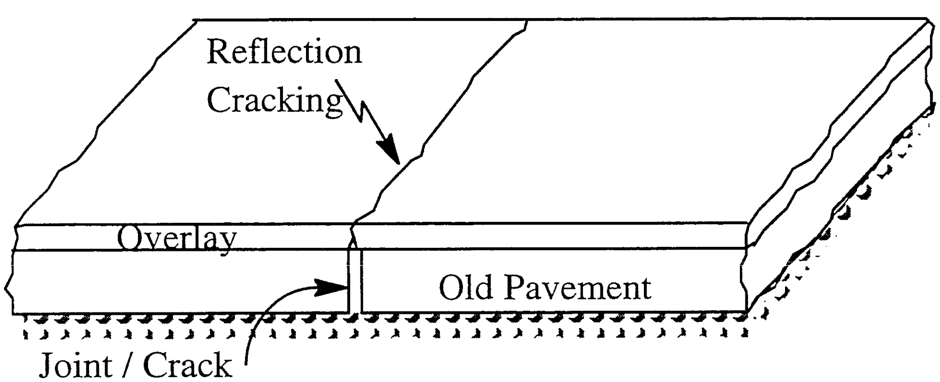

Figure 1: Reflection Cracking in an Overlay

into the new pavement surface just above the "joint/crack " that is already present in the underlying pavement layer. This phenomenon, shown in Figure 1, is called "**Reflection Cracking**".

Reflection cracking has occurred in nearly all types of overlays, but it is more common in AC overlays placed on rigid pavements. When an asphalt concrete overlay is placed on a rigid pavement, the former is fully bonded with the later. Any movement taking place in the underlying pavement at its joint/crack

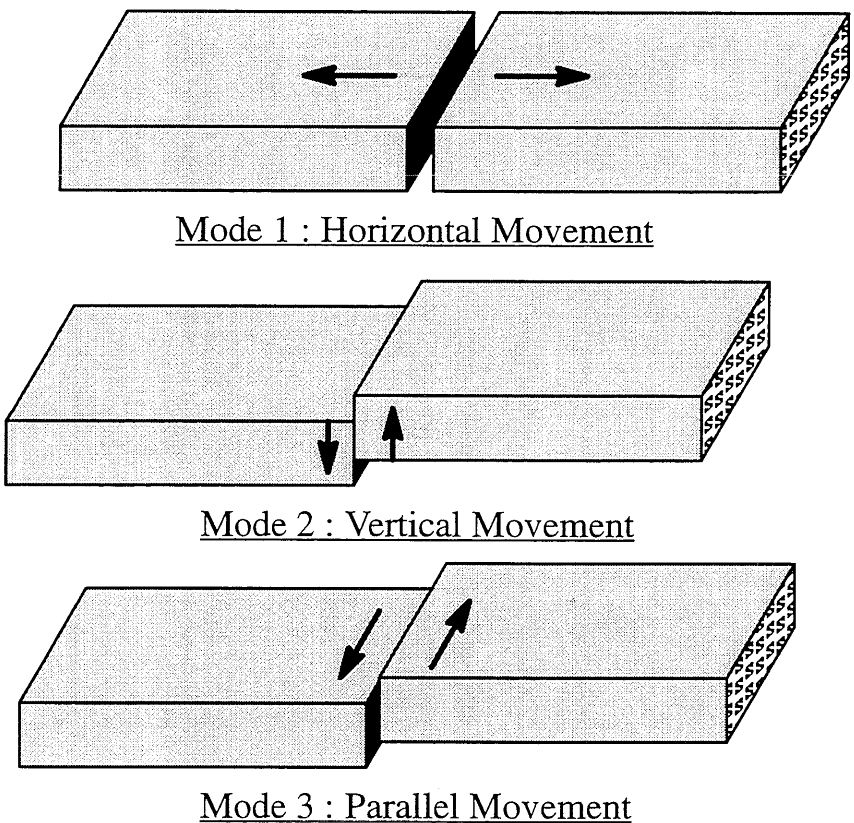

Figure 2: Modes Of Crack Displacement. (Ref 10)

will produce stresses in the overlay and can cause physical tearing if the stresses in the overlay exceed its tensile strength. There are three common modes of failure associated with joint/crack movements. These three movements at the crack interface are shown in Figure 2. Horizontal movement of the slab is the most common mode of reflection cracking. It is usually temperature associated and causes tensile stress in the overlay. Vertical movement is load induced and causes shear stress in the overlay. Parallel movement is less common and occurs only under laterally unstable conditions. The causes of the modes of failure are discussed in the remainder of this chapter.

2.3 Causes Of Reflection Cracking

2.3.1 Seasonal Temperature Changes

Low temperatures in winter cause the existing pavement to contract and open the existing joint/crack. Since the overlay is fully bonded with the underlying pavement, tensile stress is created in the overlay directly above the joint/crack, Figure 3a. This induced stress is proportional to the movement taking place in the joint which in turn is proportional to the slab length,seasonal temperature variance, and the coefficient of thermal expansion of the PCC slab.

The overlay material also contracts in response to low temperature. The reduced length of the overlay, in the area directly above the joint/crack, provides further resistance to the joint opening and induces additional tensile stress in the overlay, Figure 3b. Such stress is proportional to the contraction taking place in the overlay directly above the joint/crack. The contraction in turn is directly proportional to the seasonal temperature change, slab length, coefficient of thermal contraction of the AC overlay, and the length of the overlay directly above the joint/crack which is unbonded with the underlying pavement. The unbonded portion of the overlay above the joint/crack creeps in response to the tensile stress being developed. Some relaxation in the stress takes place due to the creep. This stress relief is directly proportional to the length of overlay immediately above the joint/crack and inversely

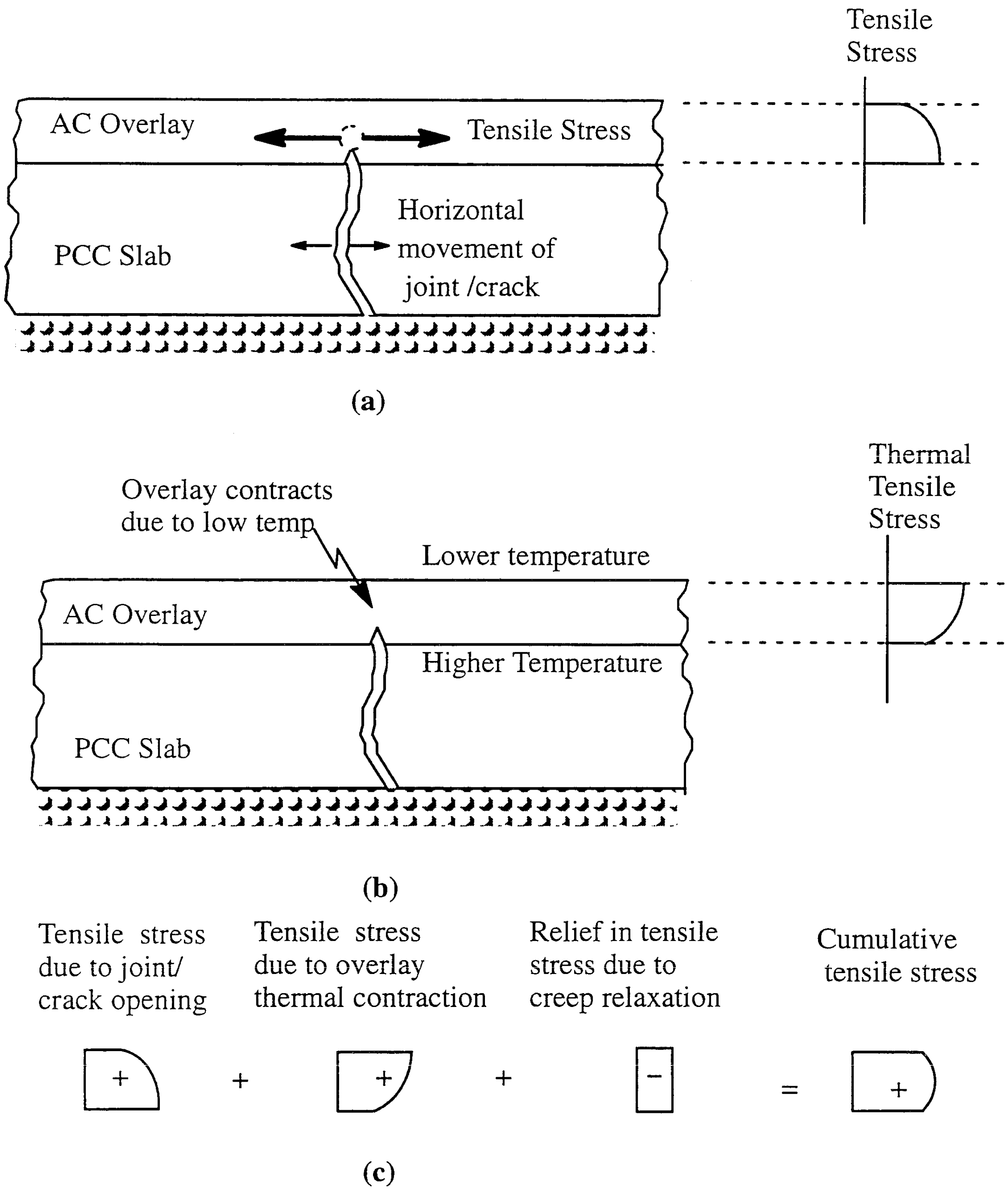

Figure 3: Stress Developed in Overlay Due to Temperature Changes

proportional to the stiffness modulus of the asphalt concrete. The combined effect of the above three phenomenon causes considerable tensile stress in the overlay, Figure 3c. When the induced tensile stress exceeds the tensile strength of the overlay, cracking in the overlay will take place.

2.3.2 Daily Temperature Cycles

Daily temperature cycles produce tensile stresses in the overlay in the same manner as seasonal temperature changes, Figure 3. The only difference is that in this case temperature variance is less but frequency of occurrence is much higher. In addition daily temperature cycling also produces temperature gradients in the PCC slab. Often when the temperature drops in the evening, the upper portion of the slab becomes cooler than the lower portion. The upper surface of the slab contracts more than the bottom and causes the slab to curl upward. This process causes increased opening of the joint/crack at the interface, Figure 4. The increase in opening is over and above that produced

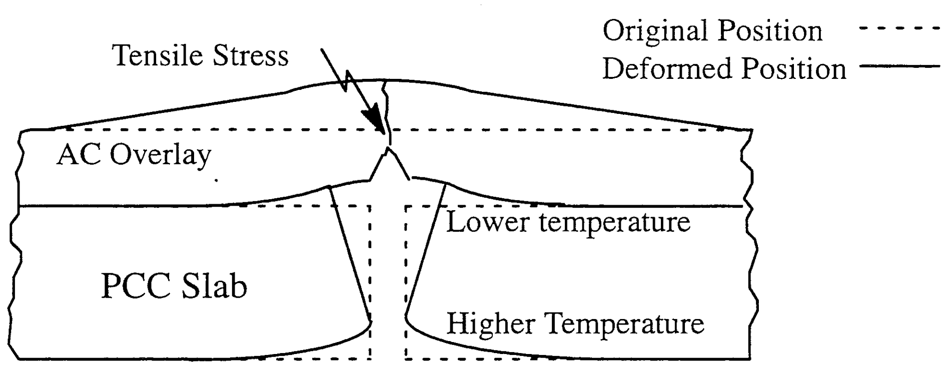

Figure 4: Reflected Crack Due to Daily Temperature Cycle

by thermal contraction of the slab. The cumulative increase in the opening at the joint/crack induces tensile stress in the overlay. Daily temperature stress, though comparatively less severe, occurs more often than that produced by seasonal temperature changes.

2.3.3 Traffic Loads

Moving loads can cause differential vertical settlement of the PCC slab across the joint / crack, Figure 5. Vertical movement of the slab occurs when there is a void under the joint/crack, the load transfer is poor, or there is over-load. Such vertical movement can induce shear stress, Figure 5a, and/or

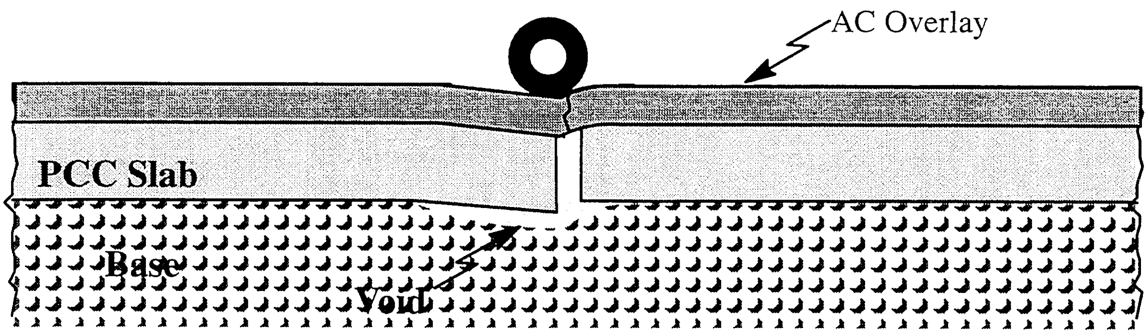

Figure 5 a: Shear Stress Caused by Moving Load

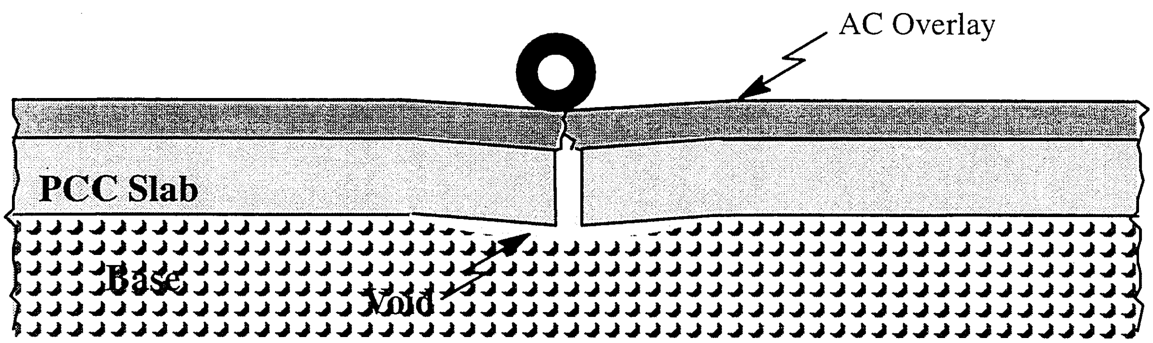

Figure 5 b: Flexural Stress Caused by Moving Load (Ref 8)

flexural stress, Figure 5b, in the overlay which ultimately causes reflection cracking. The larger the void under the joint/crack and poorer the load trans-fer, the more rapidly and severely the crack will reflect and cause deterioration in the pavement.

2.3.4 Moisture

After the crack has reflected through the overlay, water is able to infiltrate through it and cause further pavement deterioration as the crack propagates. Water, infiltrating through the crack, accumulates under the slab and weakens the base. If the load transfer at the joint/crack is not very efficient, pumping will take place and a void will be created under the slab in the vicinity of the joint/crack. Voids will cause vertical settlement of the slab as traffic load is applied and the crack will propagate further, Figure 5a and Figure 5b.

CHAPTER 3
DESIGN AND CONSTRUCTION PROCEDURES TO RETARD REFLECTION CRACKING

3.1 General

The problem of reflection cracking has existed since the 1930's, when highway engineers started using overlays for rehabilitation purposes. Since then various design and construction procedures have been used to find a permanent solution to the problem. These techniques have shown varying degree of success on different projects. The following procedures have been used in the past to alleviate or retard the reflection cracking problem:

a) pre–overlay repair.

b) Increasing overlay thickness.

c) Sawing and sealing joints in AC overlay above the joints of underlying pavement.

d) Cracking and seating.

e) Rubblizing

f) Crack arresting interlayer (granular layer).

g) Bond breaker.

h) Stress absorbing membrane interlayer (SAMI).

i) Geogrid or geotextile reinforcement.

3.2 Design and Construction Procedures

The various design and construction procedures presently being used to control reflection cracking will be discussed in the following paragraphs and evaluated through the use of case histories.

3.2.1 Pre Overlay Repair

A key to eliminating reflection cracking is to control the deformation and reduce the stress produced in the vicinity of the joint/crack. pre–overlay repair is directed towards minimizing horizontal and vertical slab movements at the joint/crack and sealing the joint against water infiltration. Cement grout is injected under the slab in order to fill any voids that have developed. This is completed to prevent any rocking/ vertical deflection of the slab which is one of the major causes of progressive deterioration of a crack. The idea is good, but if not executed properly it can bring disastrous results. There is a tendency to pump grout at very high pressure and overfill the void. This causes the slab to be lifted with creation of a void elsewhere under the slab. This may increase the deflection instead of reducing it. Pressure applied to the injected grout should not exceed the pressure exerted by the self weight of the slab which is about 1 psi for a 12 in. thick slab.

Pre–overlay repair is not a complete cure for reflection cracking. However it provides good results when used in conjunction with other methods and techniques to retard reflection cracking.

3.2.2 Overlay Thickness Increase

Thickness of an overlay can be increased to retard reflection cracking. Gulden and Brown (16) conducted a study in Georgia and presented their results which are shown in the Figures 6,7, and 8. From these figures it is noticed that with increase in overlay thickness reflection cracking decreases considerably. They recommended that for conditions in Georgia a minimum overlay thickness of 4 in. is required when no other treatment is used. Knight (17) also supported these findings.

The NEEP–10 final report in 1984 (9) concluded " No feature delays the development of reflection cracking more than thick (greater than 4 in.) overlays made with high quality dense graded asphalt mix, utilizing lower viscosity asphalt."

The New York DOT experience (2, 18) with thicker overlays, however,is different. It stated that,"Thicker overlays are highly uneconomical with little benefit. Even 7 in. thick overlays completely cracked after 5 years. Its further

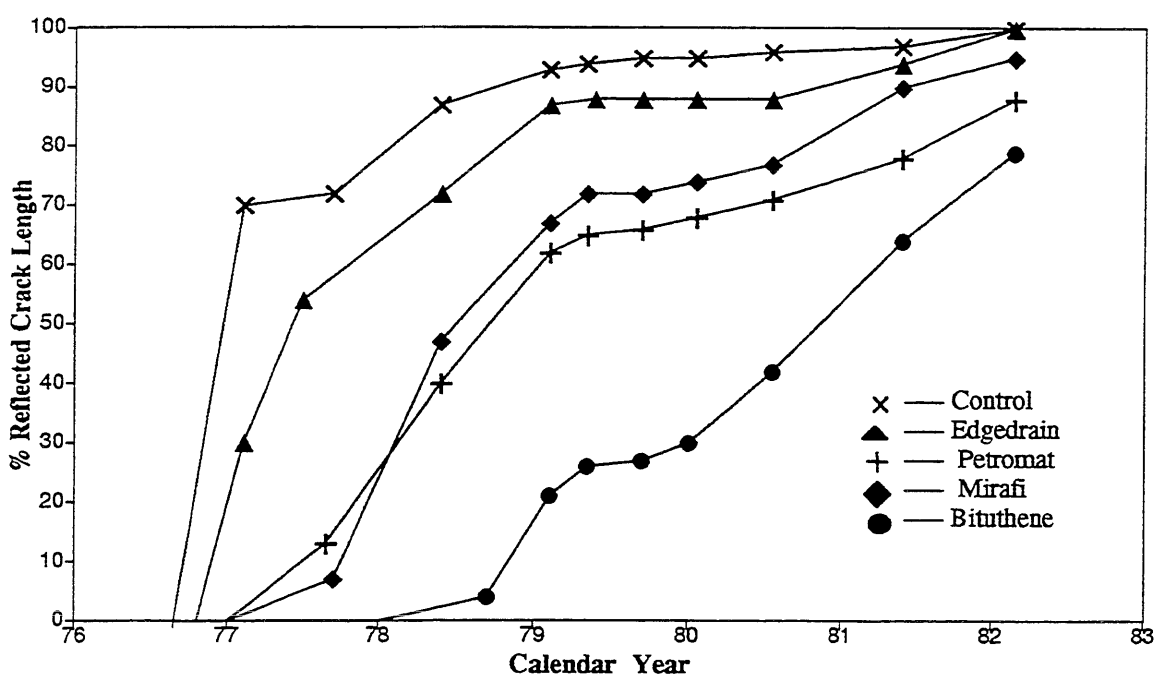

Figure 6: Reflected Crack Length Vs Overlay Life For 2 in. Thick AC Overlay , Georgia DOT (Ref 9)

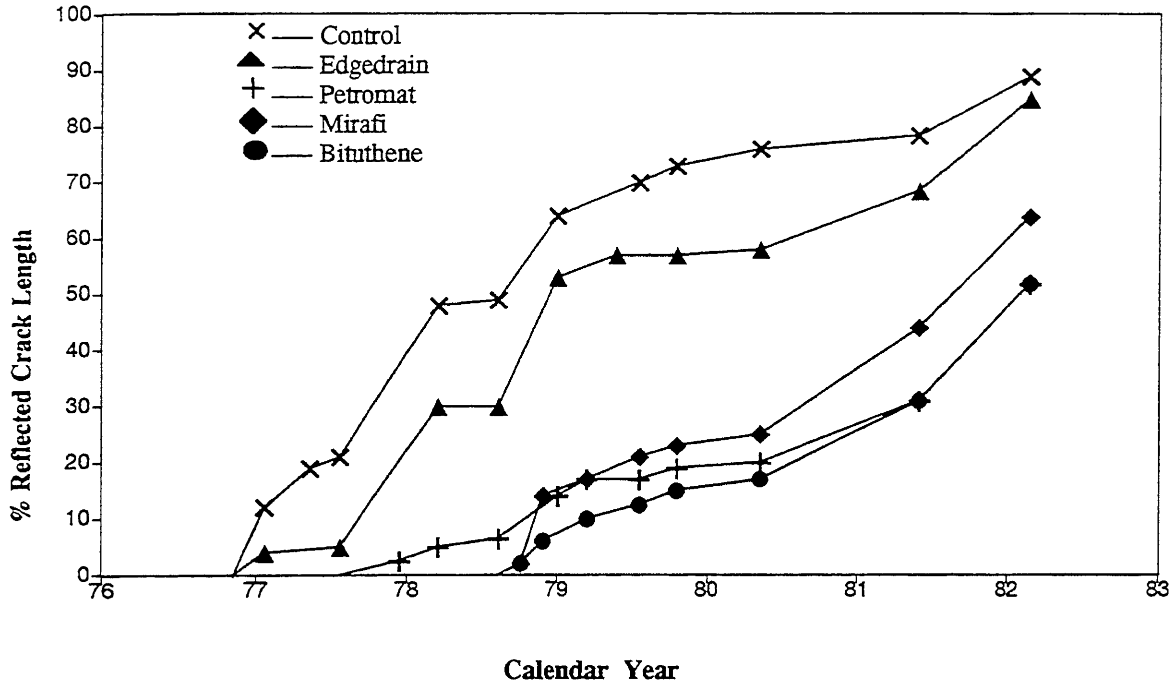

Figure 7: Reflected Crack Length Vs Overlay Life For 4 in. Thick AC Overlay , Georgia DOT (Ref 9)

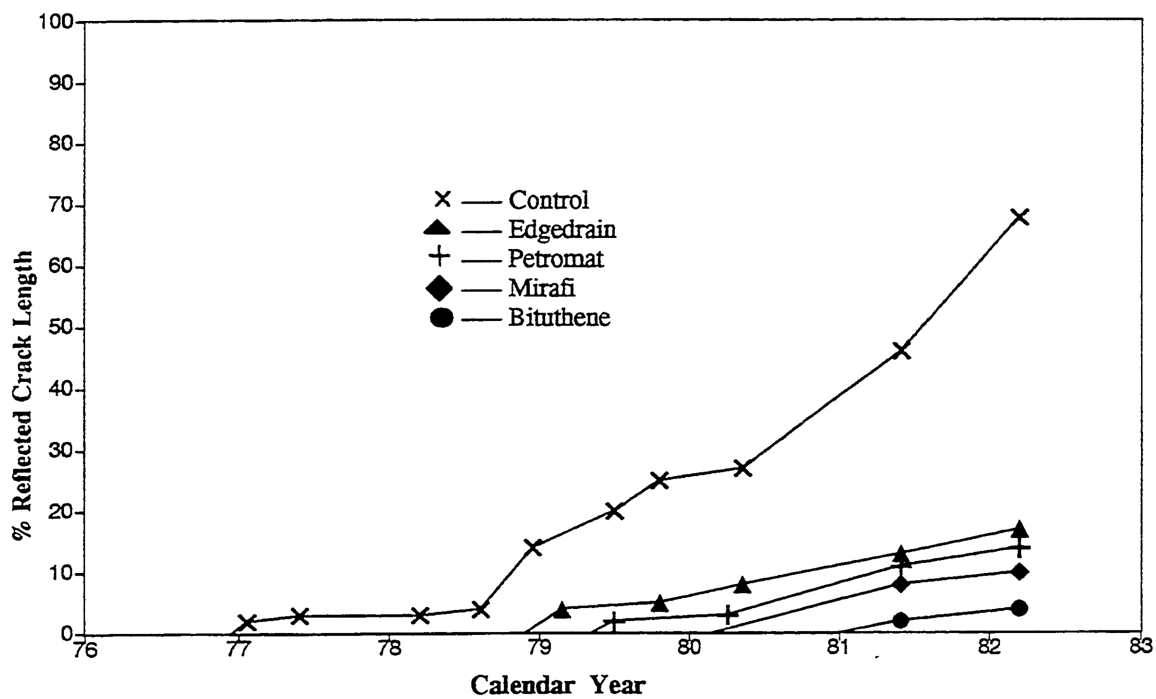

Figure 8: Reflected Crack Length Vs Overlay Life For 6 in. Thick AC Overlay , Georgia DOT (Ref 9)

deterioration was,however, less in the next 14 years due to its thickness".

Failure of thick overlays in New York may have occurred because of longer slabs (78 ft to 100 ft) and high seasonal temperature variation (100 F). Placing thicker overlays is easier but usually the most uneconomical alternative. Cost evaluation should be completed to see which procedure is the most economical alternative. If the cost of placing a thicker overlay is equal to that for thin overlay with any of the present interlayer systems, then the thicker overlay should be selected.

3.2.3 Sawing and Sealing Joints in AC Overlay

Joints in the old pavement can be marked prior to overlaying and then the overlay sawed at the joint, Figure 9. The new saw joint is later filled with a sealant. The concept is to provide a straight clean joint in the overlay which

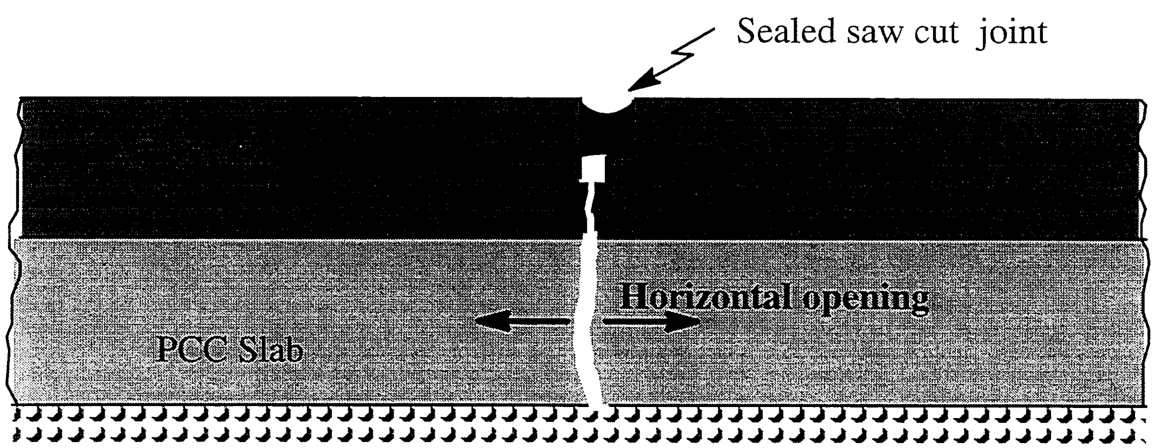

Figure 9: Sawing & Sealing of AC Overlay

can be effectively sealed and provide a plane of stress relief instead of a zig–zag crack. Besides preventing water and other incompressibles into the joints/cracks such a procedure reduces spalling and crack deterioration

In one of the New York studies (2) saw cuts were made in the overlay and sealed. Soon after completion of the work many cracks appeared adjacent to the saw cuts. The cores taken through the overlay showed that most of the saw cuts were not over the concrete joints. Only 174 out of 683 joints were properly located. The remainder were 3 in. to 30 in. away from the joints. None of the 174 saw cuts properly located over transverse joints developed reflection cracking even after 7 years. Later another trial was conducted in which 77 joints were marked with the help of pins. Forty three joints were saw cut and the remaining were left as control. Later these saw cuts were found more or less accurately located. Some cracks appeared over a period of time close to several joints. The results of this trial are shown in Table 1.

Table 1: Reflection Cracking On Overlays With Sawed Joints (Ref 2)

Type Of Treatment Given	No of Total Joints	Reflection Cracking Observations					
		After 1 Year			After 2 Years		
		Joints With No Cracking	Joints With 100% Cracking	% Of Total Length With Cracking	Joints With No Cracking	Joints With 100% Cracking	% Of Total Length With Cracking
Control	34	4	22	78	4	23	79
Sawed	43	15	2	21	13	2	22

The overlay joint sawing and sealing method has also been tried by a few other states including New Jersey and Connecticut with fair amount of success (19). The following observations were made from these studies:

a) The method is successful only on the long jointed reinforced pavement sections which have no mid slab cracking. The joint can be saw cut only above the joint existing in the underlying pavement and not the crack.

b) For shorter jointed pavement (15 ft joint spacing), a large amount of sawing is required and may not be cost effective.

c) Extreme care has to be taken to saw cut the AC overlay exactly above the existing joint. Mismatched joints may reflect another crack adjacent to a saw cut joint reservoir.

3.2.4 Cracking and Seating

Old pavement slabs can be broken into smaller sections (2 ft to 6 ft long/wide) and then seated with the help of a roller before placing an overlay. The concept is used to reduce the effective length /width of the slab so that the change in length due to temperature change is small and the joint opening remains within acceptable limits.

A New York study (2) was conducted in 1970 in which 9 sections (each 1000 ft long) were tested for cracking and seating performance. Each section had different combinations of fragment sizes and overlay thicknesses. Combinations of three fragment sizes, 3 ft, 6 ft, 10 ft, and overlay thicknesses of 2.5 in., 3.5 in., and 4.5 in. were studied. After 12 years, the control sections were found completely cracked, whereas the cracked and seated sections showed much better performance. In the cracked and seated sections, the one with smallest fragment size (3 ft) and maximum overlay thickness (4.5 in.)showed the best results with negligible amount of cracking. Cracking was found to increase with increase in fragment size and decrease with overlay thickness.

Many states like Georgia, Minnesota, California, South Dakota, and Wisconsin (20) have reported excellent results with cracking and seating as a method to control reflection cracking. Several others (20) stated that the results of cracking and seating were quite promising during the first few years but overlay performance during the later years (4 to 5 years later) was not very different from the control section. The stated overall success rate was not more than 40 %. Some of the possible reasons for different observations are as follows:

a) Cracking and seating provides excellent results if the foundation is firm and the broken sections (2 ft to 6 ft) are properly seated and compacted with the help of a pneumatic roller so that no voids are left under the slab. In cases of a weak foundation or underlying voids, the cracked sections may rock or settle due to the traffic load and may cause severe cracking in the surface.

b) If the slab is broken into too small sections (less than 2 ft) aggregate interlock is lost and a very firm foundation is required to ensure that minimum vertical movement of the cracked section takes place. In such a case fatigue cracks can develop in the AC overlay after two to three years. A study by the University of Illinois (21) recommends that to achieve best results, the area of the broken slabs should be 4 sq ft to 6 sq ft and the length and width of the broken sections should be roughly equal. It was noticed that reflection cracking was more severe when the length of the cracked sections was less than the width. For best results, the length of the broken sections should be equal to or slightly greater than the width. In warmer regions the length and width of a broken sections could be increased but should not exceed 6 ft in any case.

c) Cracking and seating has shown better results in plain concrete pavements as compared to jointed reinforced concrete pavement (JRCP). In JRCP the steel, if not cut, creates problems and the seating operation does not take place properly. Rocking and settlement of pavement sections take place due to traffic load and may increase the severity of reflection cracking.

d) Cracking and seating reduces the structural integrity of the existing pavement and may require a much thicker overlay. A thick overlay not only increases the cost but also creates problems with clearances and shoulder elevations. This method should be preferred only when the pavement is severely cracked/ faulted, no longer behaving as a structural section, or needs to be reconstructed.

3.2.5 Rubblizing

The joint and crack pattern of the existing PCC pavement is completely destroyed by rubblizing or pulverizing the slab into small pieces ranging from aggregate size of 12 in. to 6 in. The depressions and week spots are filled with coarse aggregate and the rubblized material is then compacted with the help of steel roller before placing an overlay.

A nationwide research study was conducted (22) by PCS/Law Engineering (PCS/LAW) for the National Asphalt Pavement Association (NAPA) and the State Asphalt Pavement Association Executives (SAPAE). In this study Crack and Seat, Break and Seat (breaking the slab in case of continuous reinforced concrete pavements), rubblizing and saw and sealing techniques were evaluated. The study concluded that rubblization of the existing pavement followed by HMA overlay provided excellent results and graded it as the best out of all the four techniques evaluated. It was also determined in this study that a properly seated rubblized layer is between 1.5 to 3 times as effective as dense graded aggregate base course in terms of contributing to structural capacity of the rehabilitated pavement.

3.2.6 Crack Arresting Granular Interlayer

A granular layer containing large air voids to arrest cracking can be placed on the old pavement before placing an overlay. Such a layer, due to its large interconnecting voids,relieves the stresses caused by the underlying pavement movement before it causes stress in the overlay. It absorbs the crack energy and arrests crack development in the overlay. Arkansas and Tennessee

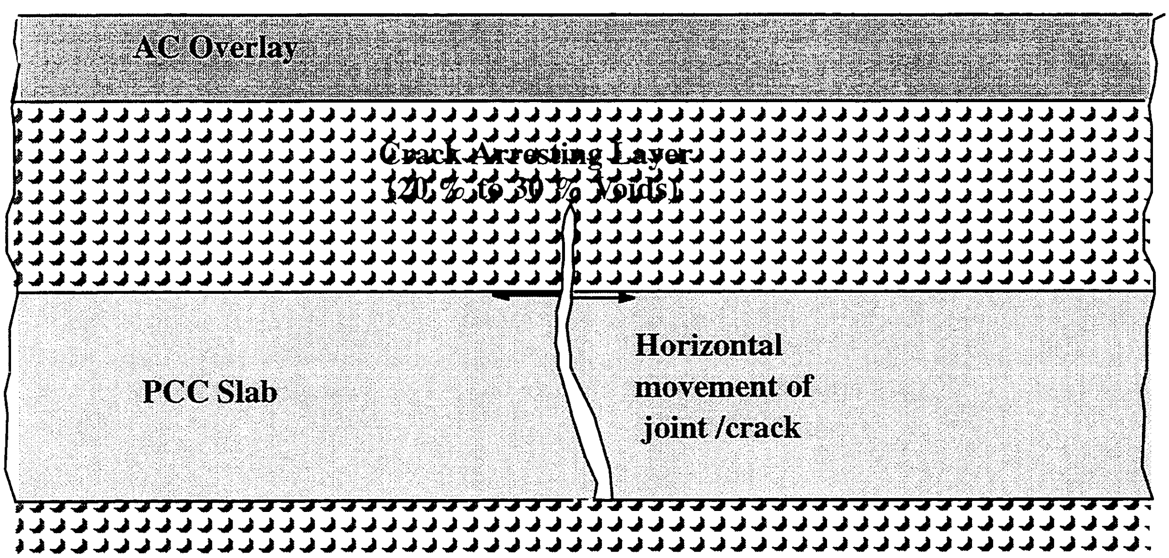

Figure 10: Crack Arresting Granular Interlayer

(23) have pioneered this procedure and have used bituminous stabilized 3.5 in. size aggregate with low fines content and with 25 % to 30 % air voids, Figure 10.

Although the crack arresting granular layer has been somewhat effective. It can experience problems if not installed properly. The following problems may occur with this method:

a) If care is not taken during construction, larger size of aggregate and large void space can lead to instability in the mix and result in rutting problems.

b) Due to larger aggregate size, total overlay thickness is usually 6 in. to 10 in. This thick overlay can cause clearance and shoulder elevation problem.

3.2.7 Bond Breaker

Materials such as wax paper, aluminum foil, roofing paper, or a thin layer of sand / stone dust have been placed on the pavement surface adjacent to the pavement joint/crack before placing an overlay in order to prevent reflection cracking. The width of such a bond breaker strip usually varies from 2 in. to 24 in. on either side of the joint/crack. The concept is to prevent a bond from forming between the old pavement and the overlay in the vicinity of the joint/crack. This extends the area of stress in the asphalt overlay from about 0.25 in. immediately above the concrete joint to a length of several feet. The procedure is used in order to reduce the strain in the AC overlay to a level that reflection cracking does not take place.

Virginia (1) used this technique on three projects. One project did not develop any cracking for 9 years whereas the other two, initially performed well, but developed sever cracking after 3 years. Kentucky (1) also tried this method but reported it to be effective only for a short time. A trial was also conducted in New York (2) to determine the effectiveness of this method. Stone dust, 1/4 in. thick was spread at 40 different locations adjacent to the joints before placing the overlay. It was found that after 4 years all of test sections showed 1/4 in. to 1/2 in. cracks. When cores were taken it was noticed that no free stone dust was present. Some asphalt flow had occurred causing the stone dust, AC overlay, and the PCC slab to bond together. This method experiences problem because of the following reasons:

a) It breaks the bond only in the immediate vicinity of the joint/crack and provides limited degree of relief in the stress because of the small width of the unbonded portion.

b) Use of Wax paper or aluminum foil breaks the bond but does not transfer enough shear force to the underlying pavement. Slippage may occur under the wheels of an accelerating, decelerating, or sharply turning vehicle.

c) Stone dust does not remain an effective bond breaker for a long period of time. Some asphalt usually intermixes and creates bond with the stone dust and the underlying pavement. It is also difficult to spread a uniform thickness of the stone dust around the joint/crack.

3.2.8 Stress Absorbing Membrane Interlayer (SAMI)

SAMI is a layer of soft material which is applied on the old pavement surface prior to placing the overlay. The function of this interlayer is to absorb any type of movement taking place at the joint/crack opening and thus dissipate the stress before it reaches the overlay. Usually a blend of vulcanized rubber and asphalt is prepared at 400 F and a 1/4 in. to 3/8 in. thick layer of the rubber asphalt mix (0.4 gal to 0.6 gal per sq yd) is applied to the old pavement surface. Heated 3/8 in. aggregate chips are then spread over the mix to prevent bleeding and flushing. The aggregate chips are placed on the rubber asphalt layer at a rate of 35 lbs / sq yd to 40 lbs / sq yd. The AC overlay is later placed on the layer of rubber asphalt and aggregate chips. The purpose of this layer is to reduce the tensile stress in the overlay in the vicinity of the joint/crack in the underlying pavement by absorbing the stress. SAMI can either be placed over the entire surface or placed only in the vicinity of joint/crack like a bond breaker.

SAMI was tried by Arizona DOT on I–40 in 1974 (24, 25). It was prepared with 75 % AR–1000 asphalt and 25 % ground rubber tire tread. The asphalt was applied at the rate of 0.6 gal/ sq yd and followed by 3/8 in. aggregate chip placed at the rate of 35 lbs/sq yd. The control section developed reflection cracking during the first year. The sections having SAMI did not show any cracking even after 8 years.

Peredoehl (4) carried out a study in California on 29 flexible pavement sections. He used SAMI along with other treatments. He reported mixed results and indicated poor to good overlay performance in the SAMI sections.

Coetzee and Monismith (11) and Monismith and Coetzee (12) studied the effect of placing SAMI between a PCC pavement and an AC overlay with the help of finite element analysis. Their findings showed that the stress at a crack

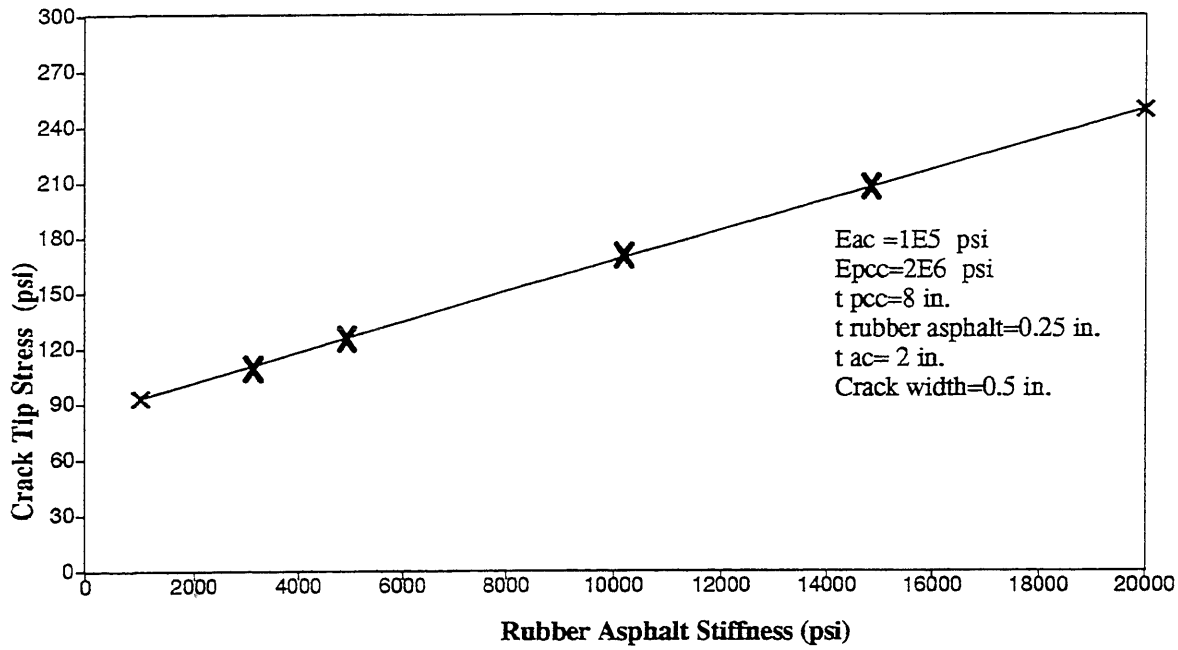

Figure 11: Influence Of Asphalt Rubber Interlayer Stiffness on Effective Stress at Crack Tip (Ref 11)

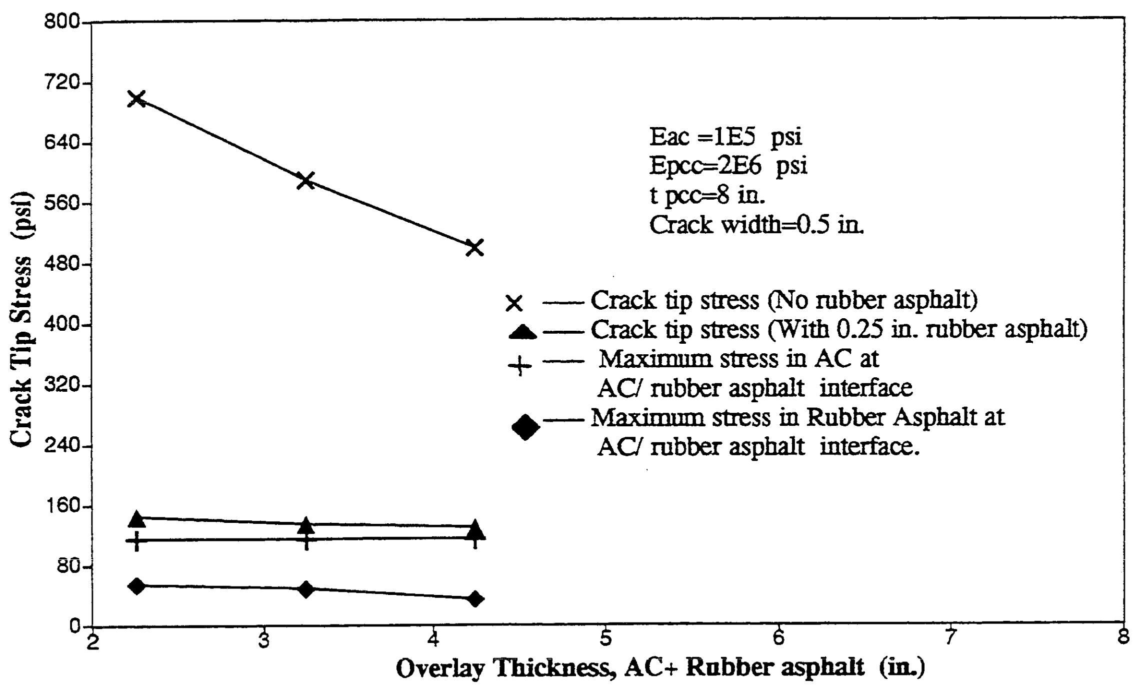

Figure 12: Influence Of Overlay Thickness On Effective Stress At Crack Tip (Ref 12)

tip is reduced considerably by decreasing the stiffness of the SAMI, Figure 11. Since the stiffness of SAMI is inversely proportional to its thickness, crack tip stresses also decrease once a thicker layer of SAMI is used. The effect of overlay thickness on performance was quite significant when SAMI was not used, Figure 12. A small thickness increase in the overlay considerably reduces the stress at the crack tip, Figure 12. With use of SAMI the variation in overlay thickness did not have as much effect on the overlay performance. The effect of crack width on the stress at the crack tip was negligible when the SAMI was used. However, it had some effect when no SAMI was used. Wider crack increased stress at the tip of the crack in the case of no SAMI. In the absence of SAMI, increase in the stiffness of AC overlay reduces the crack tip stress. Even in the absence of SAMI the crack tip stress decreases significantly with a decrease in original pavement stiffness.

According to the NEEP– 10 report (1), of the seven states that used SAMI to retard reflection cracking, four states (Alabama, Arizona, Arkansas, and New York) reported better performance. The other three (Colorado, Pennsylvania, and Nevada) reported it to be a complete failure. After going through all these reports it is concluded that SAMI has given mixed results in the past. The following summary of results is presented from the case history studies:

a) Cracks continue to propagate through the SAMI and the overlay but traveled at comparatively slower rates than in control sections.

b) Performance of SAMI has been better in the overlays on flexible pavements with fatigue cracking as compared to rigid pavements having thermal cracking.

c) Treatment applied on the full width and length of pavement has produced better results than treatment applied only above the joint/crack area

d) A thicker SAMI is more effective. Usually the thickness varies from 0.25 in. to 0.375 in.

e) A SAMI with lower stiffness was more effective. However, it should not provide such low stiffness that slippage occurs because of vehicle movement.

f) Stiffness of the SAMI used in the past has varied from 6500 psi to 7500 psi at temperatures of 70 F to 75 F when no aggregate is used.

3.2.9 Geogrid or Geotextile Reinforcement Studies

Woven or non woven geotextiles made of polypropylene, polyester, nylon, or a combination of these materials have been placed at the bottom or within the AC overlay. The geotextile is added to act as a reinforcing layer for the AC overlay and it is intended to resist the tensile stress being produced in the overlay due to horizontal movement taking place in the underlying pavement. A few of the most common geotextiles currently being used are, Petropave, Petromat, Mirafi, Typar, and Roadglass.

Usually a leveling course is applied to the existing pavement on which a tack coat is sprayed before placing the geotextile interlayer. The geotextile layer is then placed and covered with a tack coat. Finally, a surface coat is placed on the geotextile and compacted. Application of the correct amount of tack coat ensures proper bond between geotextile, overlay, and the underlying pavement and also makes the pavement impervious. Instead of placing the geotextile at the bottom of the overlay, it is often placed either in the center or in the lower third of the overlay.

3.2.9.1 Study Conducted in New York

A study was conducted in New York (2) in order to evaluate the performance of geotextiles. Four pavements were selected for this purpose. A 1 in. thick overlay with geotextile reinforcement was placed on one of the pavements and a 2.5 in. thick overlay with geotextile reinforcement was used on the three remaining pavements.

Figure 13 shows the results for one of the pavements having a 2.5in. thick overlay. In a total of 200 traverse joints, 100 were monitored as control joints and 100 were covered with geotextile. Out of the 100 transverse joints covered with geotextile, 50 joints used 7.5 ft wide geotextile strips, and 50 joints used 15 ft wide geotextile strips prior to placing a 2.5 in. thick overlay. The overlay was completed in January 1974. By December 1974

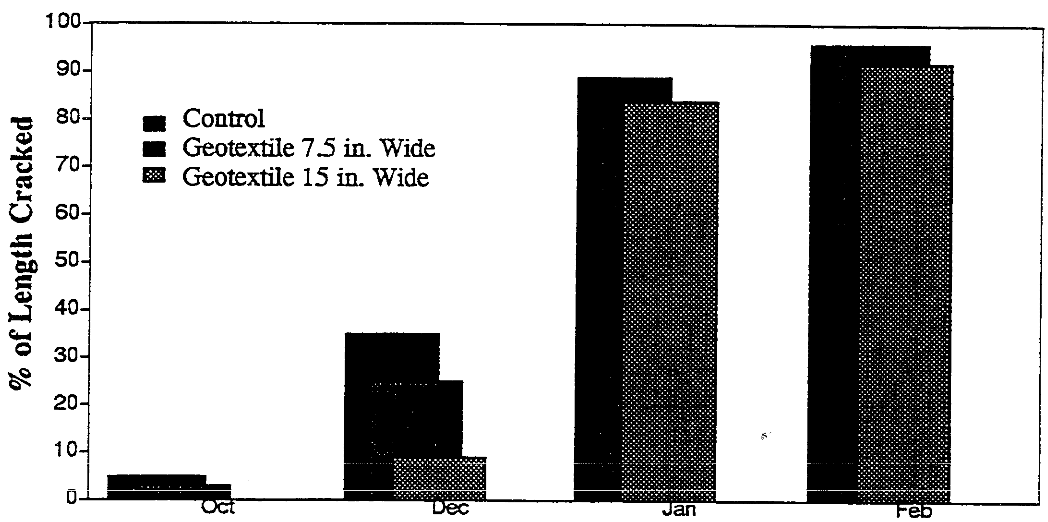

Figure 13: Reflection Cracking on a Test Pavement in New York (Ref 2)

the control joints developed significant cracking whereas the joints with 15 ft wide geotextile strips showed little cracking. By January 1975, 80 % to 89 % cracking developed on all the sections and by February 1975, all the sections had developed more than 95 % cracking. The performances of the other three pavements were similar.

b) On another pavement an AC overlay with paving geotextile was placed over the PCC slab and performance of 40 joints was monitored. On 3 joints, Bituthene (Polypropylene sheet coated with rubberized asphalt on one side) was used and on 5 others Petromat (non woven polypropylene geotextile) was used. The remaining 32 joints were left as control joints. The overlay was completed in May 1974 and the first sign of cracking appeared in November 1974. The results obtained from this study are tabulated in Table 2.

Table 2: Reflection Cracking on a Test Pavement in New York (Ref 18)

Joint Type	% of Joint Length Reflected		
	Nov 1974	**Jan 1975**	**Apr 1976**
Control	82	100	100
Petromat	30	100	100
Bituthene	8	86	100

c) The study concluded that geotextile reinforcement did not work when the joint movement was more than 0.25 in. This was similar to the case in New York, since the slab lengths in New York varied from 78 ft to 100 ft and the seasonal temperature variation was about 100 F.

3.2.9.2 Geotextile Performance Study in California

Predoehl (4) conducted a study in California on 29 flexible pavement sections using an AC overlay with a geotextile interlayer. The overlay thickness varied from 0.7 in. to 4.2 in. He also used a rubber asphalt layer on some of the pavement sections. The test sections were monitored for long term performance of the overlay (up to 13 years) and evaluation was completed based on these results. Some of the results are listed in

Table 3: Performance of Overlays With Geotextiles in California (Ref 4)

Overlay Thickness (ft)	Average Years To Cracking			
	Initial Cracking		Significant Cracking	
	Control	Geotextile	Control	Geotextile
0.20	1	3	1	5
0.25	6.3	7	7.3	7.2*
0.30	2.5	5.5	5	8.1*
0.35	9.5*	9	10*	9.2*
0.40	7*	8.1*	7*	8.4*
0.45	8.8*	8.6*	8.8*	8.8*
0.50	7*	8.5*	7*	8.5*

* 0.1 ft surface course of open graded AC added

Table 4: Average of The Results For Geotextiles in California (Ref 4)

Type of Treat–ment	Average Thick–ness	No of Sections	Average Years to Cracking		
			Initial Cracking	Moderate Cracking	Significant Cracking
Control	0.24 ft	29	5.8	7.2	8.5
Geotex-tiles	0.18 ft	30	6.4	7.8	9.4

Table 3 and Table 4. Performance of overlays using a geotextile interlayer ranged from clear success, such as the one shown in Figure 14, to complete failure in which an overlay with a geotextile interlayer showed poorer performance than the conventional overlay of the same thickness. The discrepancy in the performance was considered to be due to the following factors:

a) The type and extent of existing pavement distress, including the crack width.

b) Amount of preoverlay repair carried out on the old pavement such as crack sealing/filling, pot hole repair, replacement of rocking slabs, etc.

c) Overlay design thickness.

d) Variability in strength/material properties of the PCC slab.

e) Temperature variability and climate.

The success rate of geotextiles for controlling reflection cracking in Cali–

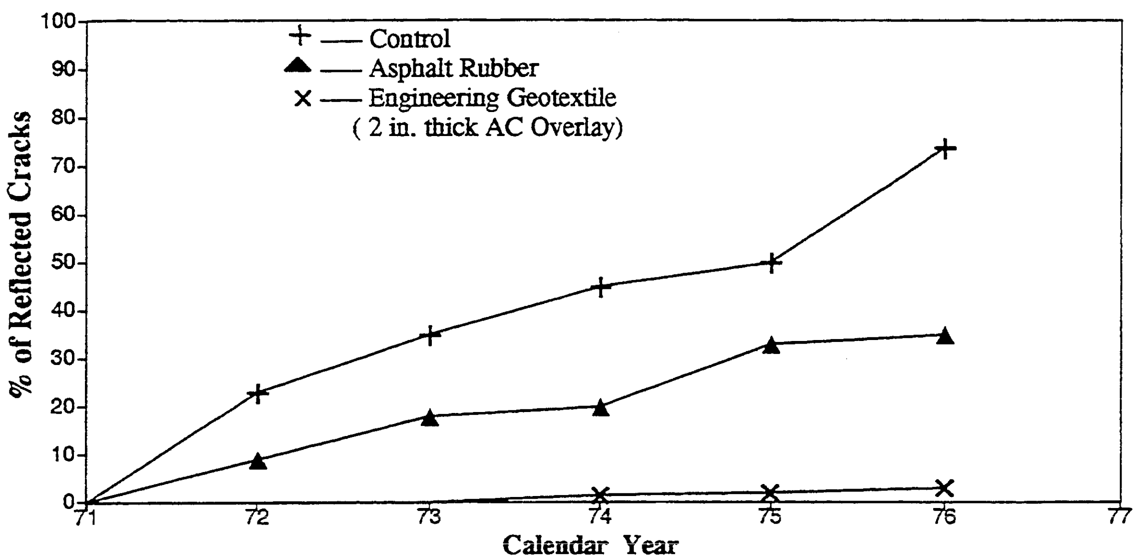

Figure 14: Percent of Reflected Cracks Vs Overlay Life
I – 70, Clifton Colo, California (Ref 33)

fornia was estimated to be 60 %. In cold climates this rate could be less.

3.2.9.3 Experimental Projects in New Mexico

Four test projects were studied in New Mexico in 1989 (3) in which overlays of various thicknesses were placed on badly deteriorated concrete pavement sections using different types of interlayers. The interlayers used for this study consisted of Mirafi 140, Petromat, rubber asphalt membranes, and the Arkansas mix which are described as follows.

Mirafi 140

Mirafi 140 is a non woven geotextile (3) uniquely constructed from two types of continuous filament fibers which includes homo filament polypropylene and hetro filament polypropylene covered with a nylon sheath. During the manufacturing process the hetro filaments were heat bonded or fused together at their intersections.

Petromat

This is a non woven geotextile, manufactured by Philips Fibers Corp. A needle punching process is used to make polypropylene geotextile with low strain properties (3).

Rubber Asphalt Membranes

Sahuaro SAMI This material is a blend of 25 % vulcanized granulated rubber and 75 % 120 to 150 penetration asphalt cement prepared at 350 F (3). This blend was diluted with Kerosene at 5.5 % to 7.5 % by volume. The blend is applied at the rate of 0.6 gal/ sq yd and chips are then placed on the membrane at an average rate of 38 lbs/sq yd.

Arizona SAMI The Arizona Refining Company produced a SAMI (3) by blending 20 % replasticized rubber, 2 % extender oil, and 78 % of 85 to 100 penetration reclaimed asphalt cement and heating at 410 F. The blend is applied at the rate of 0.63 gal/ sq yd and chips are spread over the membrane at an average rate of 38 lbs/sq yd.

Arkansas Mix

This mix consisted of an open graded bituminous pavement material with a coarse graded aggregate less than 2 in. size and with 3 % AC–20 (3).

The performance of the overlays were monitored for 5 years and various treatment procedures were evaluated. The results of this study are shown in the Figure 15 through Figure 18.

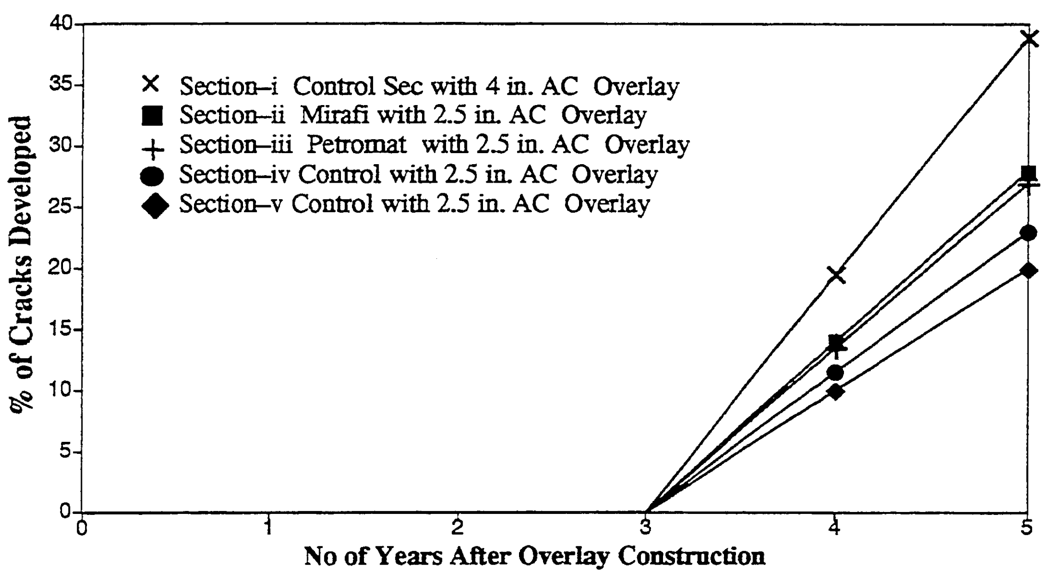

Figure 15: Reflective Cracks Vs Overlay Life On I–27, South of Raton, New Mexico (Ref 3)

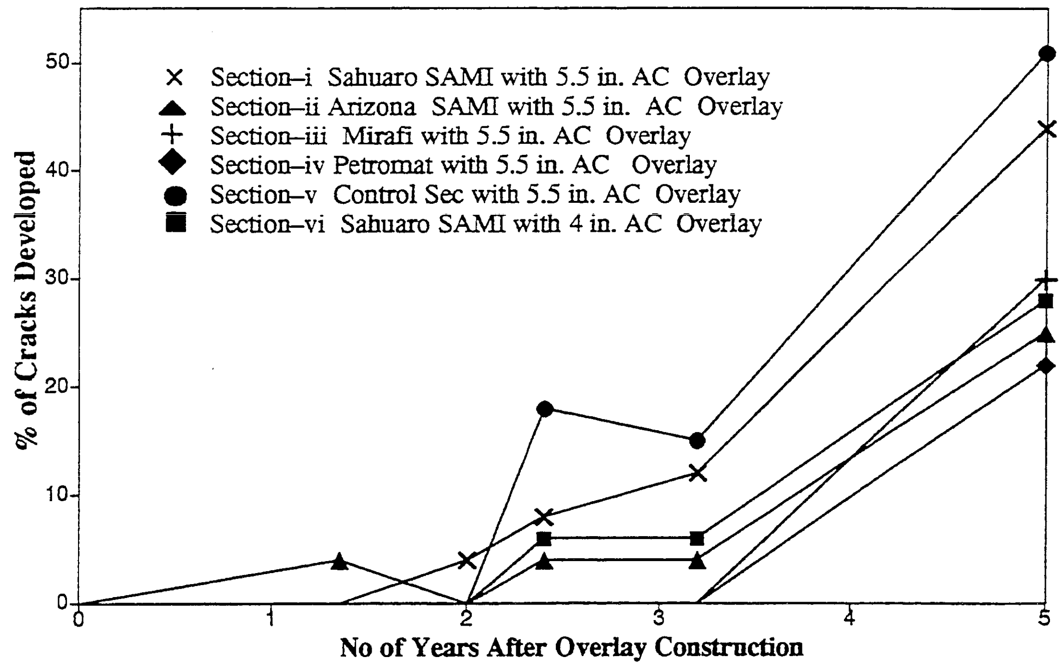

Figure 16: Reflective Cracks Vs Overlay Life On I–40, East of Clines, New Mexico (Ref 3)

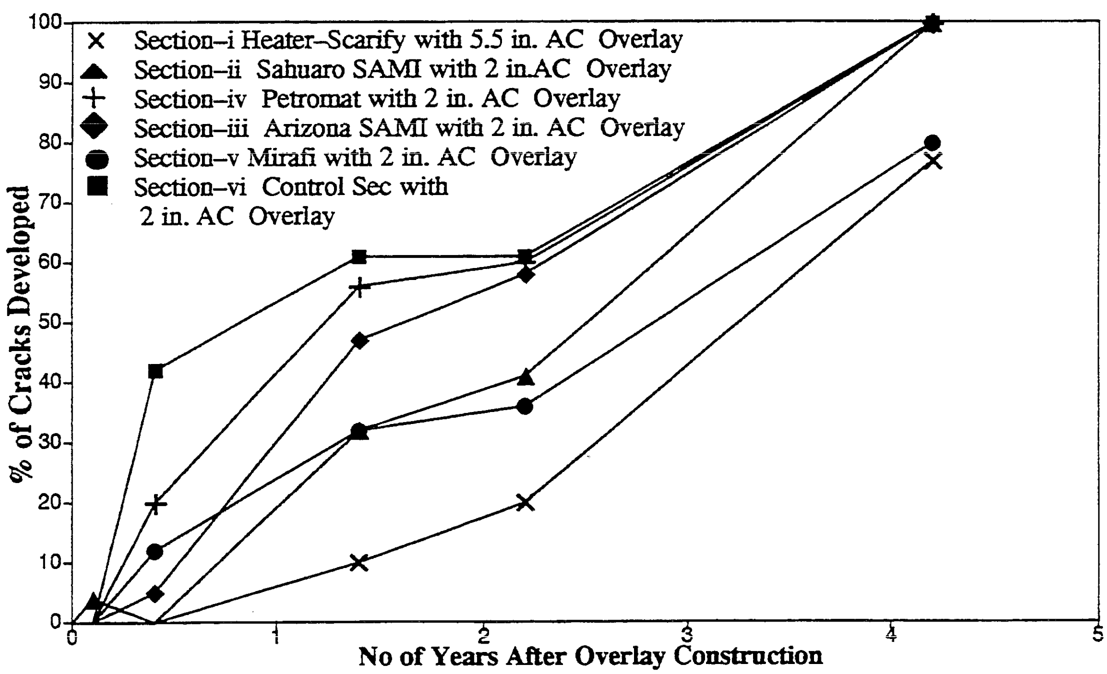

Figure 17: Reflective Cracks Vs Overlay Life On I–25, North of Truth, New Mexico (Ref 3)

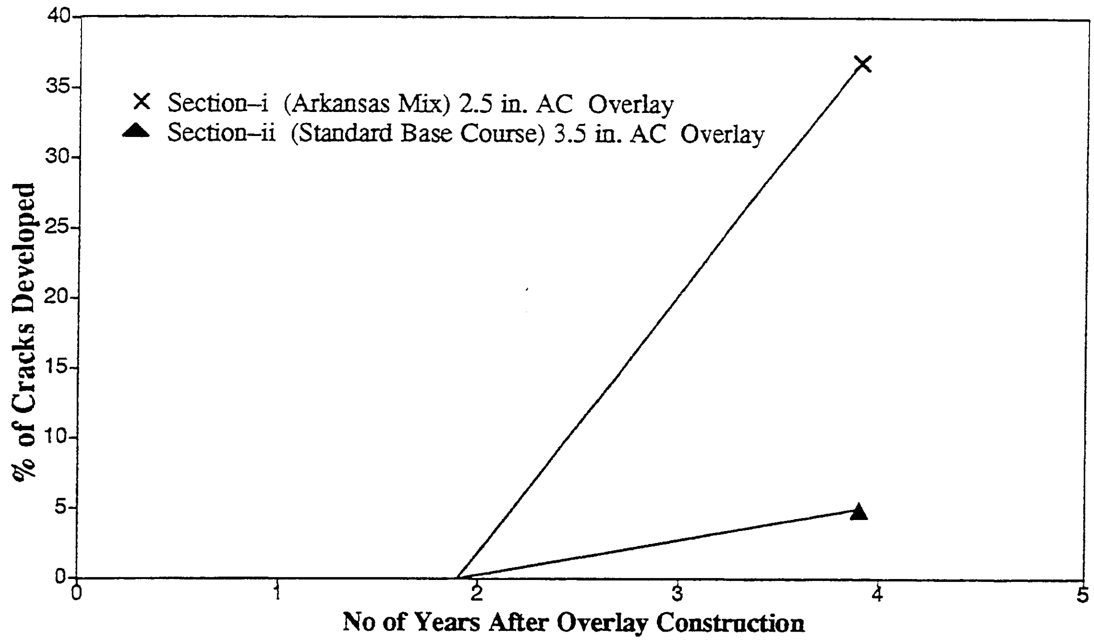

Figure 18: Reflective Cracks Vs Overlay Life On I–40, West of Grants, New Mexico (Ref 3)

The following conclusions were drawn from the New Mexico study:

a) Interlayers do not necessarily prevent reflective cracking. They do retard the rate considerably and can produce savings in maintenance cost.

b) Petromat geotextile performed the best of all the geotextiles tested.

c) The performance of the Arizona SAMI and Sahuaro rubberized asphalt membranes was comparable to that of Petromat.

d) A thicker overlay appears to reduce crack propagation, but it would not be as cost effective as the geotextile or rubberized asphalt membrane.

3.2.9.4 Experimental Projects in Texas

In Texas a study was conducted from 1979 to 1981 to evaluate the performance of different types of geotextiles in overlays (26). Two projects were constructed in 1979, one in 1980, and another in 1981. The AC overlay was installed over the PCC pavement using various types of geotextiles. The descriptions of the different types of geotextiles used in this project are given in Table 5. Performance of the test sections (0.25 miles each) was monitored for 9 years and provided results as shown in Figures 19 through 28.

Table 5: Physical Description Of Geotextiles Used in Texas Study (Ref 7)

Geo- textile Type	Nominal Weight oz/sq yd	Nominal thickness mils	Material	Construc- tion Type	Filament Type	Fiber Bonding
Bidim C–22	4	60	Polyester	Nonwoven	Continuous	Needle Punc- hed (N.P.)
Bidim C–34	8	90	Polyester	Nonwoven	Continuous	N.P.
Old Petromat	4	–	Polypro- pylene	Nonwoven	Staple	N.P. & Heat Bonded 2 side
New Petromat	4	–	Polypro- pylene	Nonwoven	Staple	N.P. & Heat Bonded 1 side
Petromat 8 oz	8	–	Polypro- pylene	Nonwoven	Staple	N.P. & Heat Bonded 1 side
Bidim C–28	6	75	Polyester	Nonwoven	Continuous	N.P.
Reepav 3 oz	3	15	Polyester	Nonwoven	Continuous	Spunbonded & heat bonded
Reepav 4 oz	4	17	Polyester	Nonwoven	Continuous	Spunbonded & heat bonded
Crown Zellerbach	5	60	Polypro- pylene	Nonwoven	Continuous	Spunbonded & N.P.
Mirafi 900 X	5	–	Polyester/ Polyprop- ylene	Woven	Continuous	Woven

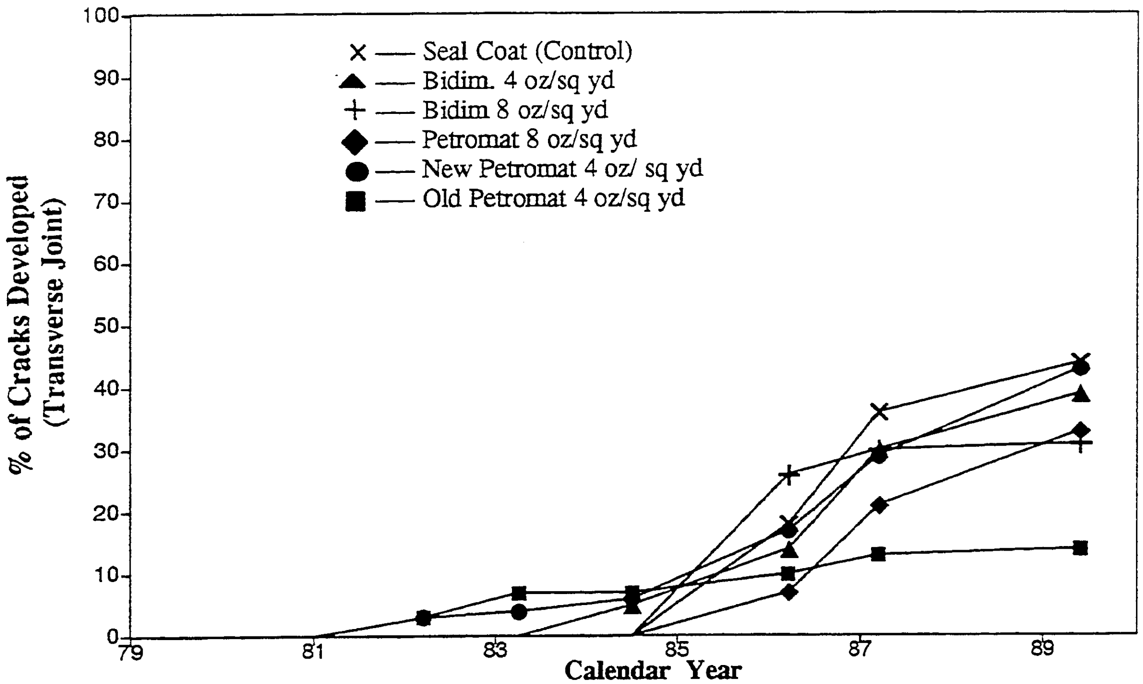

Figure 19: Transverse Reflective Cracks Vs Overlay Life
I H- 10 Near Ozona Westbound, Texas (Ref 7)

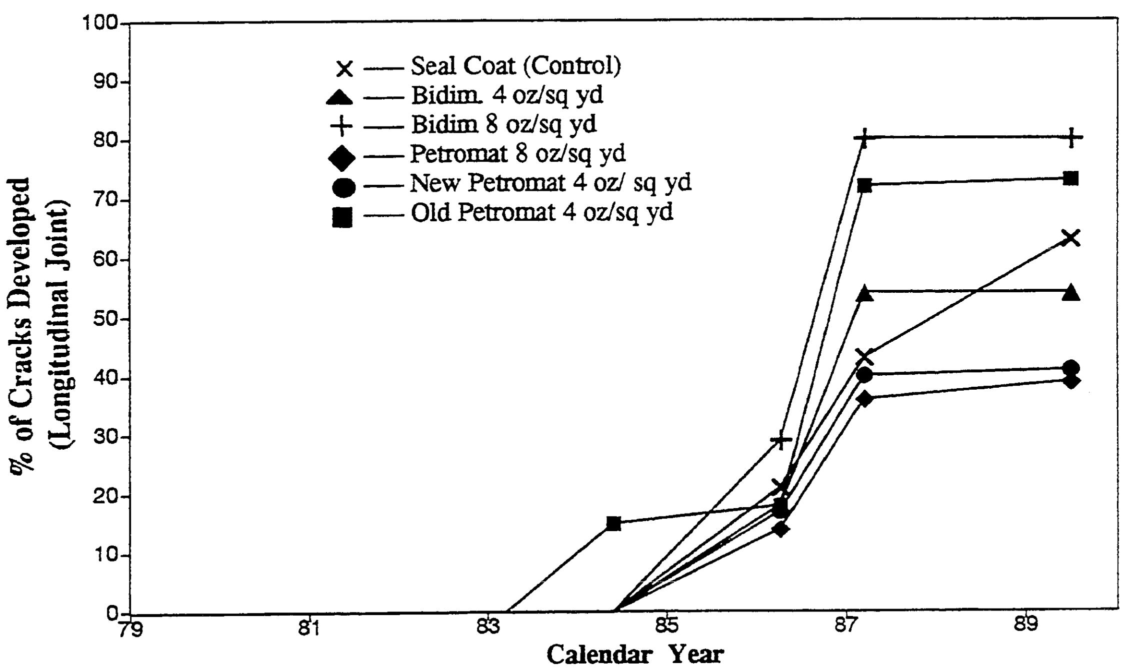

Figure 20: Longitudinal Reflective Cracks Vs Overlay Life
I H- 10 Near Ozona Westbound, Texas (Ref 7)

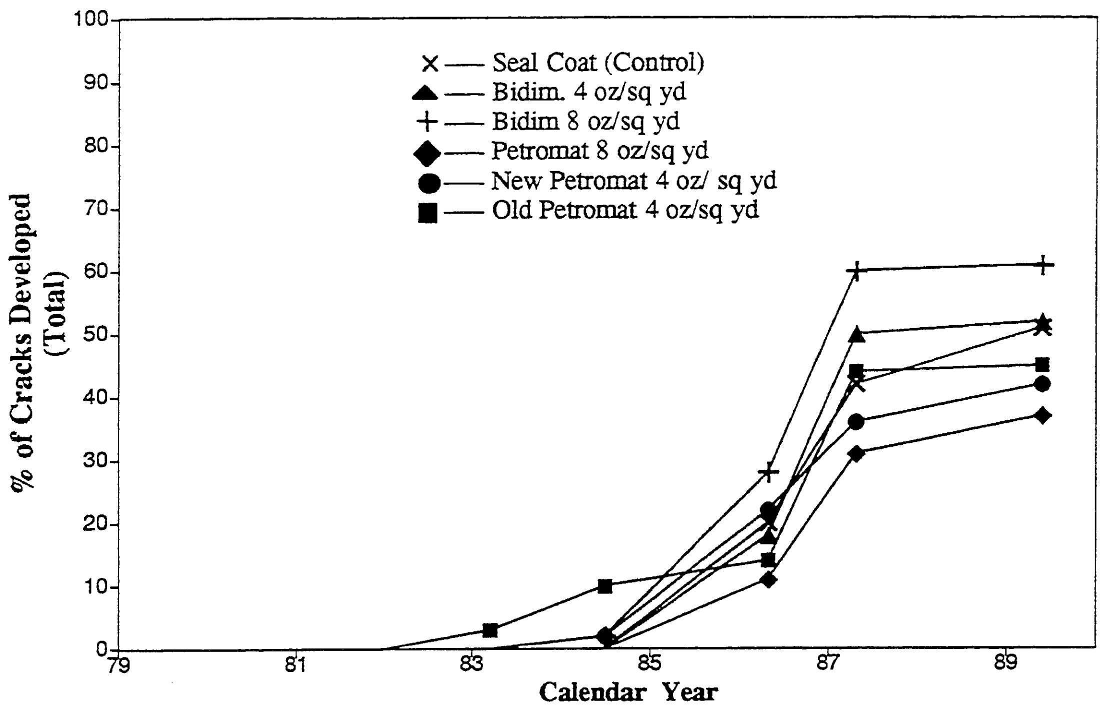

Figure 21: Total Reflective Cracks Vs Overlay Life I H- 10 Near Ozona Westbound, Texas (Ref 7)

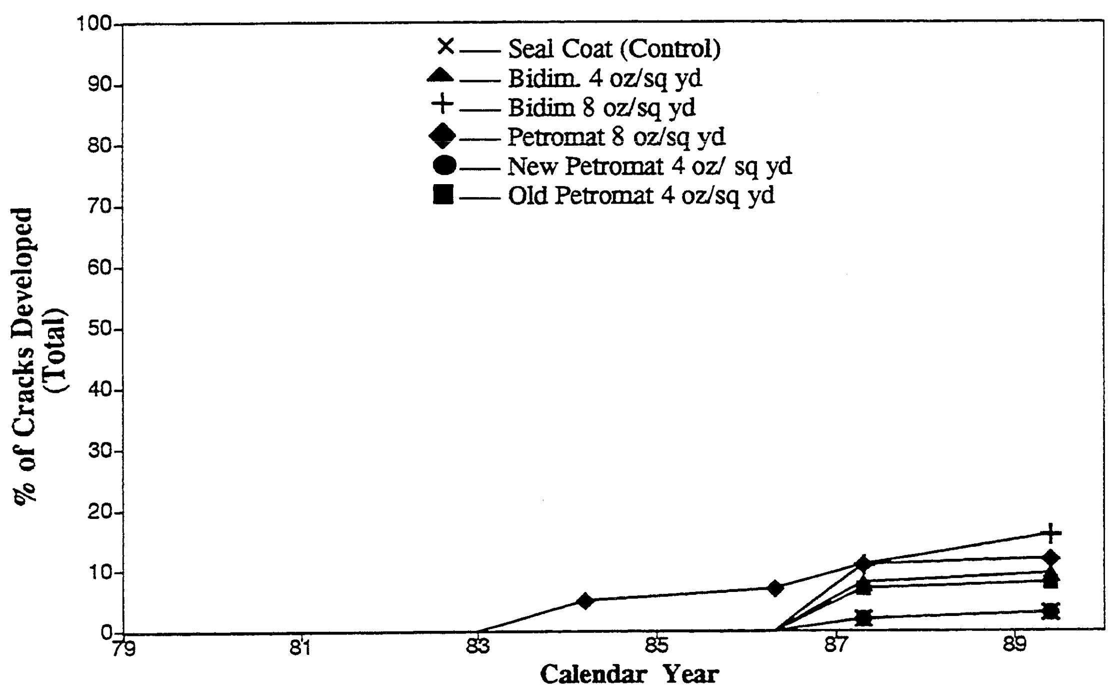

Figure 22: Total Reflective Cracks Vs Overlay Life I H- 10 Near Ozona Eastbound, Texas (Ref 7)

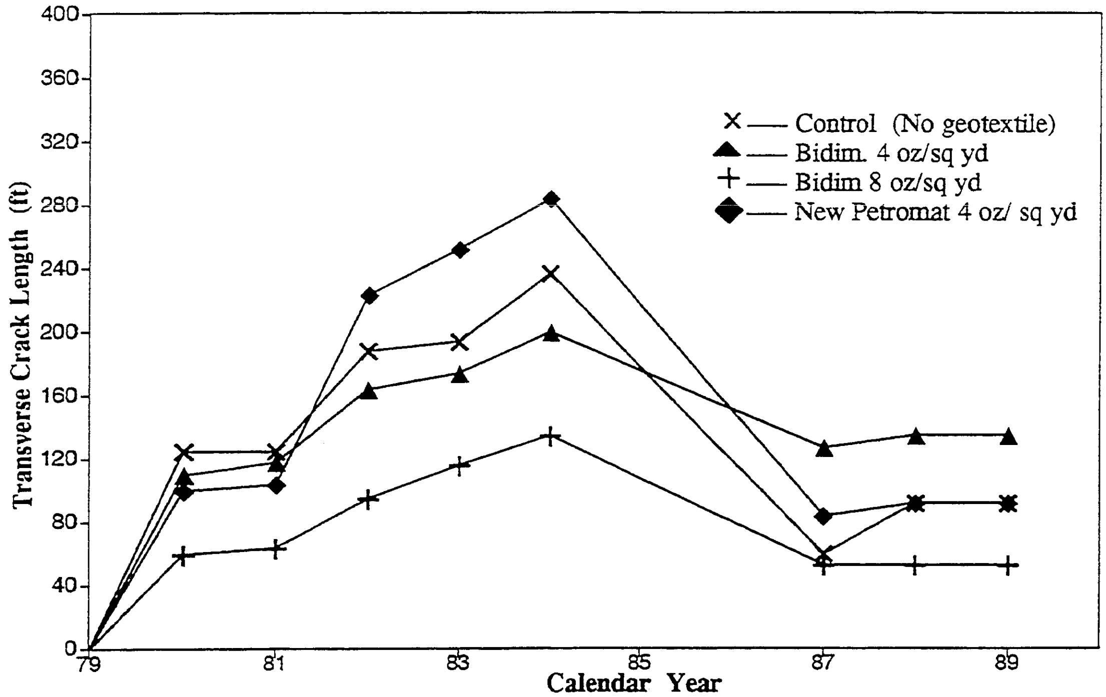

Figure 23: Transverse Crack Length Vs Overlay Life I H- 40 Near Amarillo Eastbound, Texas (Ref 7)

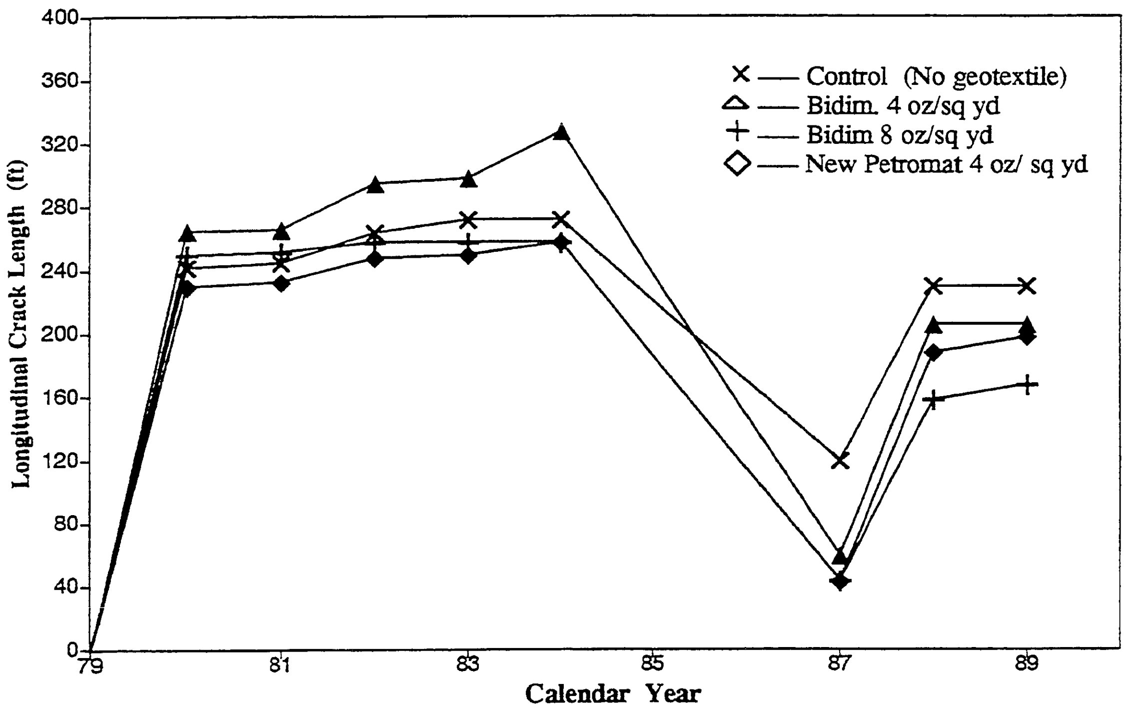

Figure 24: Longitudinal Crack Length Vs Overlay Life I H- 40 Near Amarillo Eastbound, Texas (Ref 7)

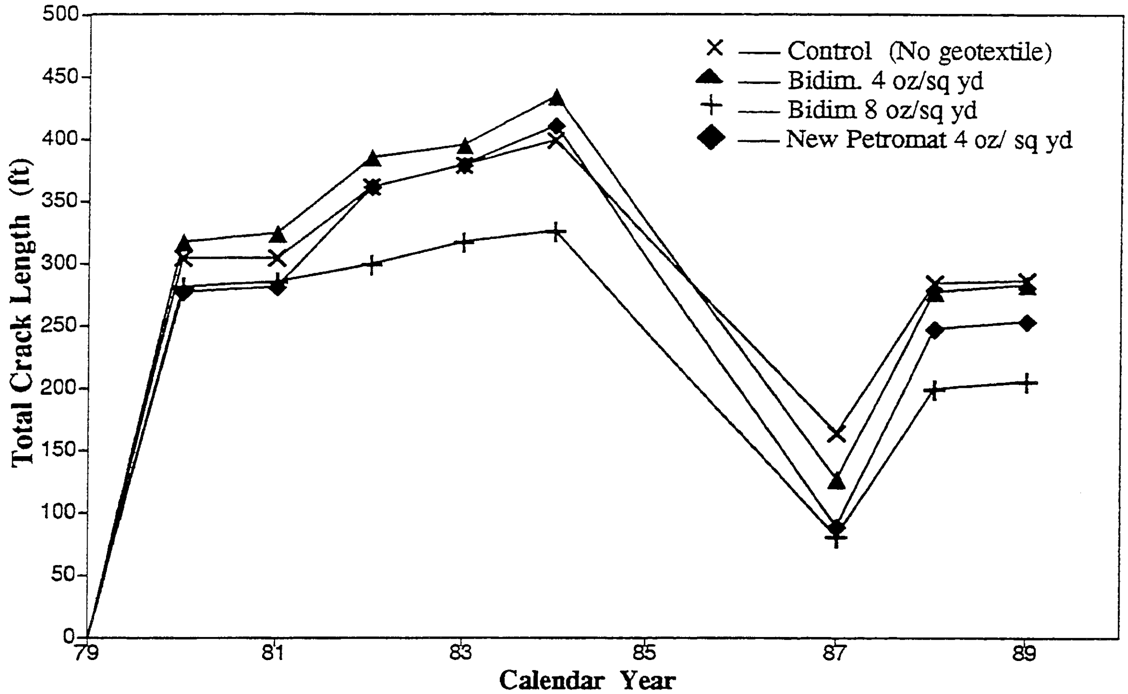

Figure 25: Total Crack Length Vs Overlay Life
I H– 40 Near Amarillo Eastbound, Texas (Ref 7)

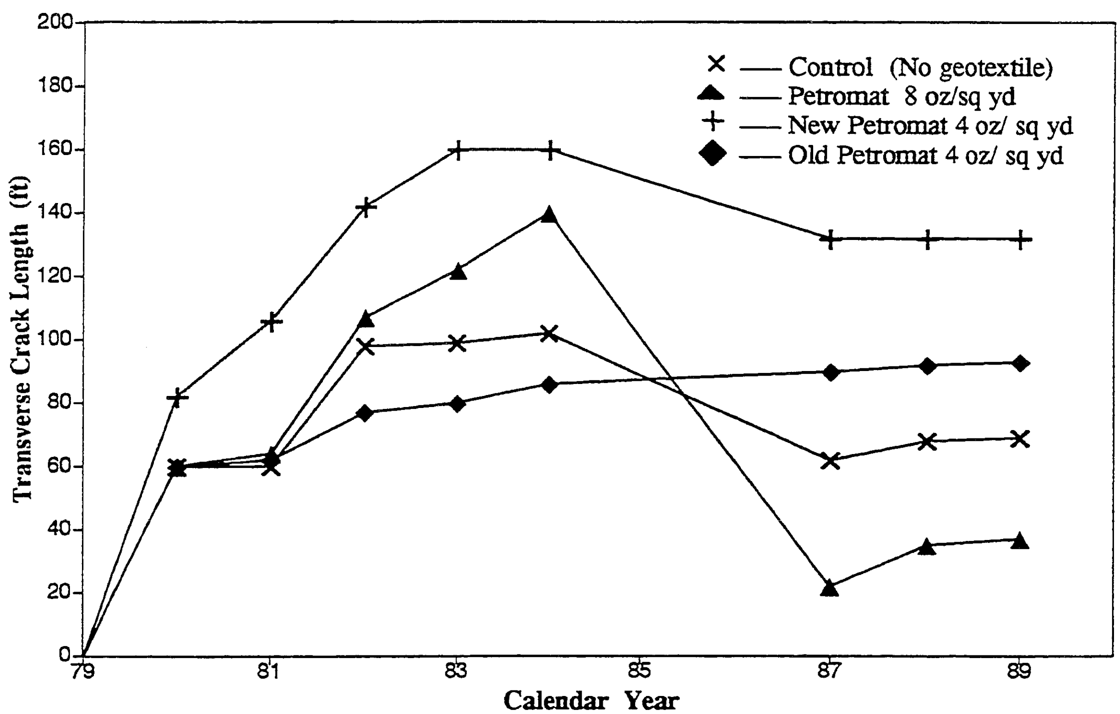

Figure 26: Transverse Crack Length Vs Overlay Life
I H– 40 Near Amarillo Westbound, Texas (Ref 7)

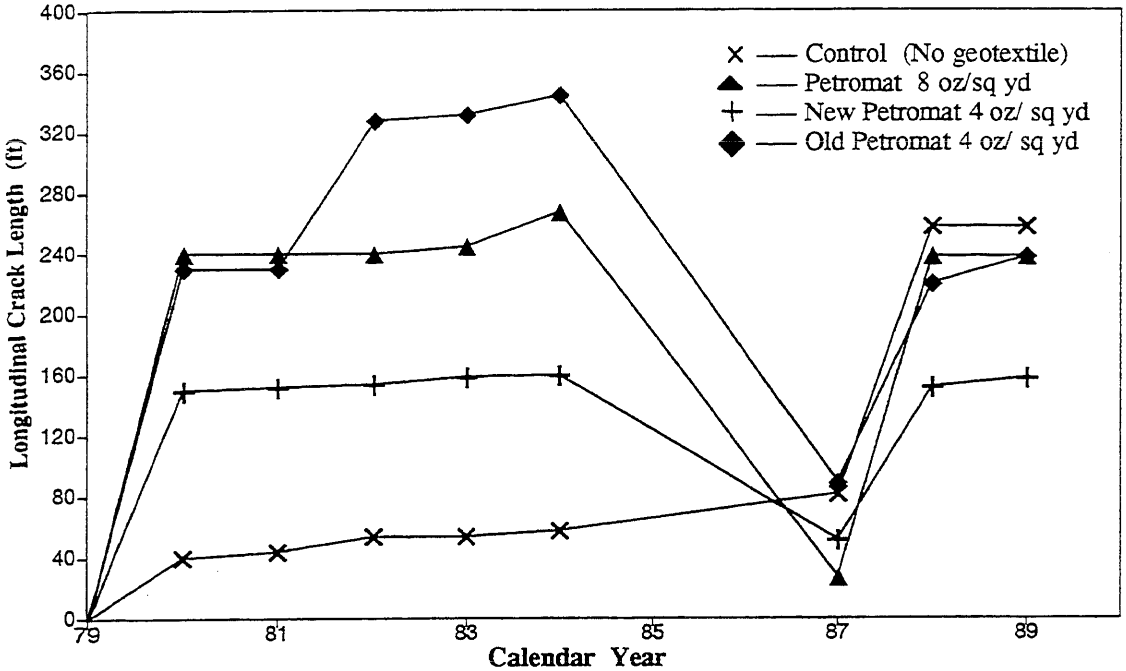

Figure 27: Longitudinal Crack Length Vs Overlay Life I H- 40 Near Amarillo Westbound, Texas (Ref 7)

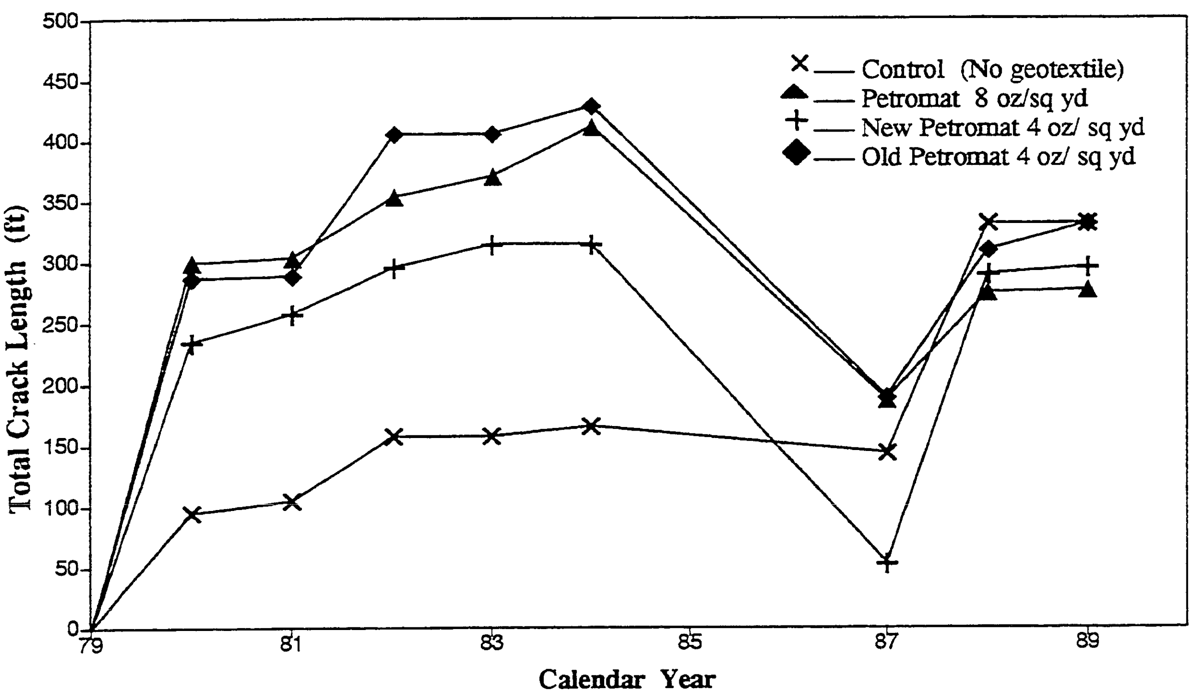

Figure 28: Total Crack Length Vs Overlay Life I H- 40 Near Amarillo Westbound, Texas (Ref 7)

The following conclusions were developed from this study:

a) Geotextiles may significantly retarded the reflection cracking, particularly in the first three to four years.

b) Very thin overlays (less than 1.5 in. thick) placed over Geotextiles on high volume roads resulted in premature failure of the roads.

c) Asphalt impregnated Geotextiles remained intact even after moderate cracking. This will reduce the flow of surface water into the base and reduce pumping.

3.2.9.5. US Army Corps of Engineers Study

In 1977, the US Corps of Engineer's Cold Regional Research and Engineering Lab (CRREL) (27) conducted a study on the performance

Table 6: Performance of Overlay on Greenland Runway (Ref 27)

Overlay Thickness	% Of Cracking	
	After 1 Year	After 2 Years
Less than 2 in.	71 %	100 %
More than 3 in.	46 %	57 %

of Phillips Fibers Corporation 4 oz/ sq yd to 6 oz/sq yd Petromat and the Monsanto 6 oz/ sq yd to 8 oz/ sq yd Bidim Geotextiles. Three Geotextiles were used on a severely cracked runway with varying AC overlay thicknesses constructed with AC-2.5. The runway was located in Greenland and was subjected to extremely cold climatic conditions. The results of this study are shown in Table 6. The pavements were severely cracked due to thermal contraction and it was considered that this study would be a confirmatory test for the performance of geotextiles in cold climates. The results of the study indicated the following:

a) Thick overlays (more than 3 in.) showed better performance than 2 in. overlays. It took longer for cracks to propagate in the thicker overlays.

b) Some difference was noticed in the performance of different types of geotextiles. A small pavement area study (20 ft by 40 ft) showed that 4 oz/sq yd geotextile had 34 % more cracking than the 8 oz/sq yd geotextile.

c) After cracking developed in the overlay, the geotextile still remained intact and served as a water proofing membrane.

3.2.9.6 NEEP–10 Study

In 1970 the Federal Highway Administration initiated the National Experimental and Evaluation Program Project # 10, NEEP–10 (1) for reducing reflection cracking in AC overlays. Fourteen states participated in this program. In addition to many other treatments, performance of six different types of geotextiles was also evaluated. According to the NEEP–10 report the geotextiles showed promising results on some projects and poor results on some the others. Their performance was better for fatigue cracking as compared to thermal cracking.

3.2.10 Major Variables Affecting Geotextile Performance

Geotextiles have produced poor to excellent results on various projects. The discrepancies in their performance can be attributed to such variables as joint/crack displacement, joint/crack width, and displacement rate.

3.2.10.1 Effect of Horizontal Movement at the Joint/Crack

3.2.10.1.1 Total displacement at the Joint/Crack

It has been observed in the past that performance of geotextiles has been poor in regions having extremely cold climate and on those pavements having longer slab lengths. Lower temperatures and longer slabs result in higher thermal contraction, thereby resulting in greater horizontal displacement at the joint/crack. It can be inferred that geotextiles have shown poor performance for greater horizontal displacement at the joint/crack. Various trials were performed to see the effect of horizontal joint movement.

Joseph and Haas (10) studied the performance of different geotextiles against reflection cracking in the laboratory. They designed their equipment to simulate conditions as close as possible to the field. They studied the following conditions:

a) Cooled the specimen to –30 C ± 2 C, until the temperature gradient reached a steady state.

b) Subjected the specimen to a uniform cyclic load at a pre determined displacement level, under controlled strain, until fracture propagated through the full depth. They used two displacement levels for the experiment called, "low level displacement (0.21 mm)" and "high level displacement (0.26 mm)".

c) Used 0.0399 mm/min displacement rate.

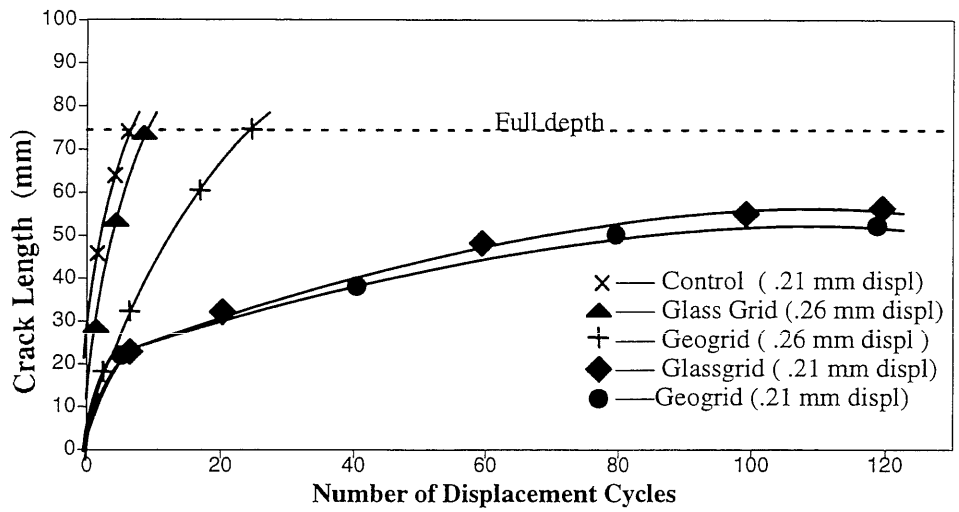

Figure 29: Crack Length Vs Number of Displacement Cycles (Ref 10)

The results from the study of Joseph and Haas (10) are shown in Figure 29. It is seen that both Geogrid and Glass Grid show much better performance at low level displacement (0.21 mm) than at high level displacement (0.26 mm). The performance of Glass Grid was not very different from the control section and the performance of Geogrid was slightly better.

McGhee (6) concluded that horizontal joint movements greater than 0.04 in. have significant effect on reflection cracking. He further said that AC specimens could not withstand deformation greater than 0.05 in. without cracking. Bone et al (28) agreed with his findings.

Based on his lab overlay studies, Lytton (5) defined three ranges of thermal openings as follows:

a) From 0 in. to 0.03 in. – No geotextile is needed.

b) From 0.03 in. to 0.07 in. – An effective range for geotextiles.

c) Greater than 0.07 in. – An opening movement, which geotextiles normally can not withstand.

3.2.10.1.2 Rate of Horizontal Displacement

The rate of horizontal movement is also very important for overlay performance. It is generally observed that an AC overlay subjected to slow pulse load can offer more resistance to cracking than the one subjected to a fast pulse load (5, 34).

3.2.10.2 Effect of Initial Joint/Crack Width

Geotextiles have performed very well on pavements having load related fatigue distress such as AC pavements with closely spaced alligator cracking. Geotextiles used on fatigue cracks, less than 1/8 in. wide, have given the best results. Fatigue cracks more than 3/8 in. wide require a rigid filler.

Pourkhosrow (29) concluded that paving geotextiles could not bridge over cracks more than 3/8 in. wide.

3.2.10.3 Effect of Vertical Deflection Across the Joint/Crack

As discussed in Section 2, vertical deflection at a joint is a function of traffic volume, amount of load transfer across the joint/crack, and differential subgrade support under the existing pavement. Geotextiles have performed reasonably well for horizontal joint/crack movement, but their performance for vertical deflection has been questionable. Numerous studies have been conducted to evaluate the effectiveness of geotextiles against such distress.

Results from a study conducted by McGhee (6) in Virginia are shown in

Table 7.

McGhee (6) concluded that paving geotextile delayed reflection cracking better than the control section if Bankleman beam vertical deflection across the joint/crack is less than 0.002 in.

Table 7: Effect of Vertical Deflection on Overlay Performance in Virginia (Ref 6)

Vertical Deflection Across the Joint (in.)	% of Joints Reflected Through	
	Control Joints	Geotextile Treated Joints
0	44	0
0.002	54	29
> 0.008	100	100

Predoehl (4) concluded that overlays on pavements having less than 0.003 in vertical deflection gave crack free service for 10 years even when no geotextile was used. The effective range of pavement geotextiles is for vertical deflection between 0.003 in. and 0.008 in. For vertical deflections more than 0.008 in. a geotextile interlayer has been found ineffective and a minimum of 4 in. of overlay is needed to retard significant cracking within the first 10 years. The Asphalt Institute (13) recommended that for good performance of an overlay differential deflection should not exceed 0.002 in.

Smith (8) developed an apparatus to simulate a moving wheel load on an AC beam. On top of a plate he applied a tack coat and then placed an AC beam which simulated an overlay. He made a 0.125 in. wide and 1.25 in.

deep cut at the bottom of the beam. The magnitude of moving load was adjusted so as to apply a radius of curvature of 125 ft, which induced a realistic strain level in the beam. He then monitored the propagation of cracking against number of moving load passes and concluded the following:

a) Paving geotextiles did not reduce beam deflection and were not effective as structural reinforcement in flexible pavements.

b) Paving geotextiles generally delay reflection cracking due to their presence as a soft layer.

3.2.10.4 Effect of Overlay Thickness

The performance of an overlay is directly related to its thickness. A thick overlay alone can effectively retard reflection cracking. This

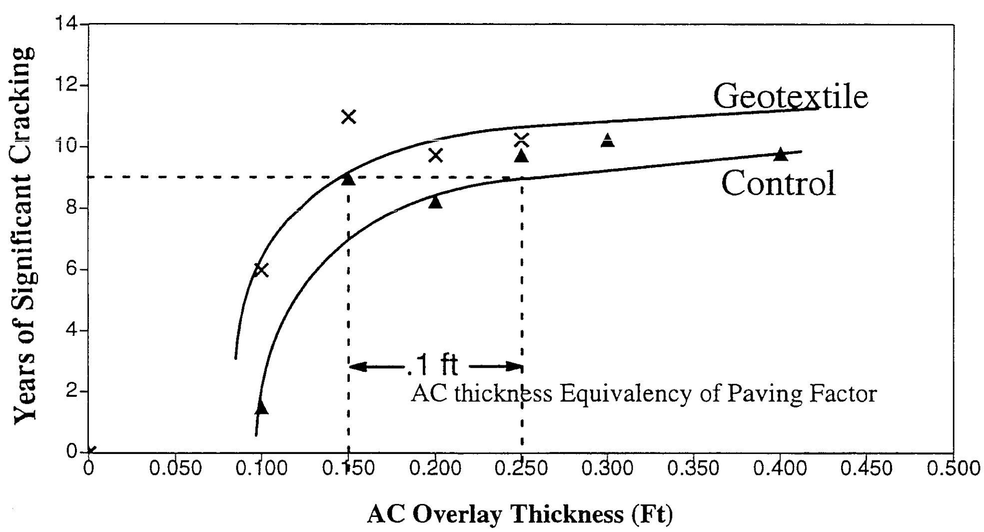

Figure 30: Estimated Geotextile Equivalency as a Function of AC Pavement Thickness, California (Ref 4)

alternative, however, is not always cost effective. To decrease cost, geotextiles are often placed under the overlay and the required thickness of overlay is reduced. Predoehl (4) conducted a study to find equivalency factors between the paving geotextile and the overlay thickness, Figure 30 (also see Table 3 and Table 4). For the control section, the benefit of increasing the overlay thickness reduces rapidly for overlay thicknesses greater than 3 in. Once a geotextile is used, the advantage of increasing overlay thickness significantly reduces after 2 in. to 2.5 in. In Figure 30 it is observed that 1.2 in. to 1.8 in. overlay thickness gave the greatest change in reflection cracking control. Predoehl (4) found that the geotextile interlayer is equivalent to about 1 in. of asphalt concrete.

Sherman (30) observed the performance of Petromat geotextile under AC overlays on three projects and concluded that the geotextile was equivalent to 1.25 in. to 1.5 in. of asphalt concrete.

3.2.10.5 Effect of Tack Coat Quantity

A vehicle while turning at high speed, changing speed on curves, accelerating (while starting), or decelerating (while applying brakes) transfers horizontal shear stress to the overlay. Ultimately this stress is to be transferred to the underlying pavement and finally to the subgrade. Any interlayer introduced at the bottom of the overlay should provide sufficient shear resistance in order to effectively transfer the shear stress to the underlying pavement. Application of too much tack coat reduces the shear resistance at the interface and may result in slippage and tearing at critical locations. On the other hand too little tack coat will result in poor bond between a geotextile, overlay, and PCC pavement and will reduce the stress relieving ability. The correct amount of tack coat is important for best results. Smith (8) recommended the following relationship to estimate the amount of tack coat needed:

$$RTC = 0.05(TW)^{0.30} \qquad \text{Equation 1}$$

Where:

RTC=Recommended tack coat rate (gal/sq yd)

T=Geotextile thickness (mils)

W=Geotextile weight (oz/sq yd)

The recommended tack coat in Equation 1 includes an allowance of 0.05 gal/sq yd for absorption by the underlying pavement (surface hunger). Smith (8) recommends rounding up the calculated quantity to the next

Table 8: Recommended Tack Coat Rates For Different Paving Geotextiles (Ref 8)

Serial	Type of Geotextile	Minimum Tack Coat Required (gal/sq yd)
1	Amoco 4545	0.30
2	Bidim C–22	0.25
3	Bidim C–34	0.35.
4	True Tex MG75	0.30
5	True Tex MG100	0.35
6	Trevira T1115	0.30
7	Nicolon 50	0.30
8	Petromat	0.25
9	Dupont T376	0.15
10	Q–Trans–50	0.35
11	Fibretex 200	0.30

higher 0.05 gal/sq yd. Using Equation 1 the tack coat application rates have been calculated for different geotextiles as shown in Table 8. Dykes (31)

recommended that the quantity of tack coat should be reduced by 20 % if used on steep grades, in speed changing zones, and on relatively impervious surfaces. On highly porous surfaces, the quantity should be increased by 20 %.

3.2.10.6 Geotextile Stiffness

To act as reinforcement the geotextiles must have sufficient thickness and its modulus of elasticity should be greater than that of the AC overlay. Barksdale et al (32) classified geotextiles based on their stiffness as shown

Table 9:Tentative Stiffness Classification Of Geosynthetics (Ref 32)

Stiffness Descrip–tion	Secant Stiffness @ 5% Strain, Sc (lbs/in.)	Elastic Limit (lbs/in.)	Tensile Strength (lbs/in.)	Failure Elongation (% Initial Length)	Typical Cost Range ($/sq yd)
Very Low	<800	10–30	50–150	10–100	0.30–0.50
Low	800–1500	15–50	60–200	10–60	0.40–0.50
Stiff	1500–4000	20–400	85–1000	10–35	0.50–3.00
Very Stiff	4000–6500	≥ 300	350–5000	5–15	3.00–7.00

in the Table 9. A geotextile with a high modulus of elasticity does not ensure that it will act as a reinforcement. To act as a reinforcement, a geotextile must have high stiffness, which is defined as its modulus of elasticity times thickness. In his study, Barksdale (32) concluded that for an AC overlay, a geotextile stiffness of at least 4000 lbs/in. is required before a geotextile starts acting as reinforcement, i.e., it has to be "very stiff" according to the classification given in Table 9. Only "Polygrid", "Glassgrid" and "very heavy weight geotextiles" provide the required stiffness at present. Geo grids, due to large opening between its reinforcing members, provides good aggregate interlock. The performance of Geogrid is therefore comparable with the woven geotextiles although the stiffness of woven geotextiles is usually 2 to 2.5 times greater than the stiffness of Geogrid. Some very stiff, high modulus, heavy duty membranes have been used under overlays and it has been observed that the crack moved from immediately above the joint to away from the joint. (5).

Most of the geotextiles used in the past had stiffness, less than 4000 lbs/in. and yet many of them retarded reflection cracking to some degree. Geotextile with low stiffness probably acted as a stress relieving interlayer (like SAMI) and reduced the stress at the tip of the joint/crack. The following geotextile properties are important to perform as a stress relieving interlayer:

a) Sufficiently soft and thick geotextile. Non woven geotextile is more suitable for this purpose because of low stiffness properties. Needle punched, spun bonded or woven geotextile can also be used.

b) Polypropylene or Polyester geotextiles are the most common. Glass, Nylon, or combination of Nylon and Polyester/Polypropylene have also been used.

c) In recent years, asphalt impregnated low stiffness geotextiles have also been used as a stress absorbing membrane interlayer (SAMI). These geotextiles are usually from 0.05 in. to 0.15 in. thick.

3.2.10.7 Climatic Conditions

Geotextiles have performed best for load associated distress (alligator cracking) and have been found generally ineffective against thermal cracking. It can therefore be said that their performance in cold climates has been less favorable. Ahlrich (33) summarized geotextile performance for various pavement locations and plotted a performance map. He found that generally the performance of geotextiles in northern states (having colder

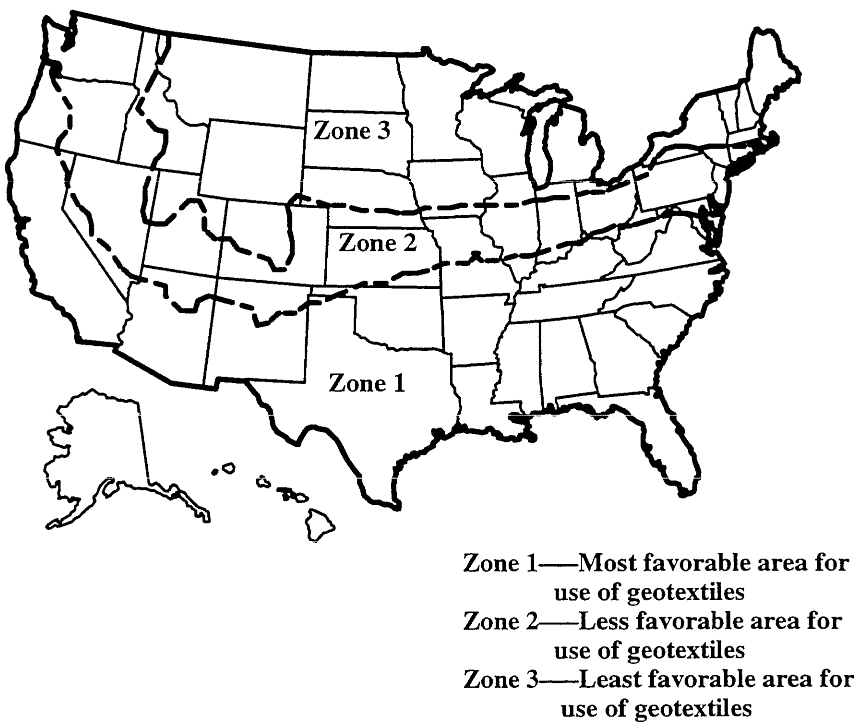

Figure 31: Climatic Zones as a Guidance To Geotextile Performance With AC Pavements (Ref 9)

climate) was poor. He then divided the United States into three climatic zones, shown in the Figure 31. He classified Zone 1 to be the most favorable area for geotextiles, Zone 2 a little less favorable, and zone 3 being the least favorable area. Ahlrich (33) recommended that geotextiles should not be used in areas where the freezing index is more than 500 Degree Days (Zone 3). Acceptable performance has been observed in cold climates on two projects in Pennsylvania and one project in Michigan (33).

3.2.11 Possible Modes of Failure of An AC Overlay With SAMI/ Geotextile Interlayer

Lytton (5) and Button and Lytton (34) observed three modes of failure in an AC overlay with SAMI/geotextile interlayer. In mode 1 failure the crack propagates rapidly upward from the old crack and after reaching the interlayer it stalls for a while before it propagates from the top of the interlayer and moves upward towards the surface of the overlay. The presence of an asphalt rubber interlayer or soft geotextile impregnated with asphalt results in large amount of deformation and alters the energy balance at the tip of the joint/ crack. Due to low stiffness of the stress relieving interlayer large strain occurs at low stress level. This does not prevent the crack but definitely retards it. This mechanism of crack stalling is called, "crack blunting" by some authors.

Mode 2 failure was observed by Lytton (5) in the laboratory, when he placed a 0.75 in thick leveling course on a PCC slab. A low stiffness paving geotextile was placed prior to the overlay. The stress relief mechanism was observed in this type of failure. The crack started from the bottom of the leveling course and after reaching the interlayer, it temporarily halted. The crack then began from the top of the overlay and propagated downward towards the geotextile interlayer.

Mode 3 failure occurred when a high stiffness geotextile (stiffer than surrounding material) was placed beneath the overlay. In this type of failure the reinforcement mechanism took place. The crack propagated upward towards the reinforcing interlayer. The crack then made a 90 degrees turn to the horizontal direction and moved along the interface between the reinforcement and the underlying material. This crack traveled laterally until insufficient energy was left to move any further. Majidzadeh et al (35) described this type of failure as a buffer zone concept. It has been noticed that this mode of failure only occurs in an asphalt concrete overlay if the stiffness of the geotextile is more than 4000 lbs/in.

3.3 Summary of Reflection Cracking Control Procedures

3.3.1 Mechanism

There are several reasons for the initiation and propagation of reflection cracking and the associated pavement damage. Past experience of various researchers leads to the following conclusions :

a) Horizontal movement in a concrete slab due to thermal contraction and resulting joint/crack opening is the major cause of reflection cracking. Such movement causes tensile stress in an AC overlay.

b) Daily temperature cycles occur more often but produce very little damage per cycle. Most of the damage caused by joint opening can be attributed to the seasonal temperature variation.

c) The factors that aggravate reflection cracking due to joint opening include:

1) Longer slab.

2) Low temperature in winter.

3) Rate of temperature decrease during the day.

4) Higher coefficient of thermal contraction of PCC slab.

5) Higher coefficient of thermal contraction of AC overlay.

6) Wider gap between the joint / crack.

7) Higher stiffness modulus of AC overlay.

d) The Asphalt Institute recommends that for the best performance of an overlay, the maximum opening resulting from low temperature should not exceed 0.02 in.

e) Differential vertical movement at a joint/crack due to traffic load causes shear stress in the overlay. Such movement contributes little towards initiation of reflection cracking if the vertical movement is less than 0.002 in. It can, however, cause further deterioration of asphalt along the existing crack in the overlay.

f) Traffic load causes considerable damage to the pavement if the vertical movement of slab across the joint/crack is more than 0.002 in.

g)Vertical movement of a pavement slab across the joint/crack depends upon the size of the void present under the slab and the load transfer efficiency at the joint/crack.

3.3.2 Summary of Design and Construction Methods To Retard Reflection Cracking

3.3.2.1 Pre–Overlay Repair

Pre–overlay repair used in conjunction with any other method/technique to retard reflection cracking, brings positive results and should be accomplished.

3.3.2.2 Increasing Overlay Thickness

Thick overlays constructed with a high quality dense graded asphalt mix and low viscosity asphalt considerably delays reflection cracking. It is the easiest but usually the most expensive alternative.

Usually an overlay more than 4 in. thick causes clearance and shoulder elevation problems. Expenditures incurred on all the related changes added to the cost of a thick AC overlay may make it an uneconomical option.

3.3.2.3 Cracking and Seating

A PCC slab broken into small sections (2 ft to 6 ft fragments) and properly seated with the help of a roller effectively reduces reflection cracking. To achieve the best results in Illinois the size of the broken sections should be 4 sq ft to 6 sq ft and the length of such fragments should be equal to or slightly longer than its width. In warmer regions length/width of a broken sections could be a little greater but should not exceed 6 ft in any case.

The cracking and seating procedure is not recommended for jointed reinforced concrete pavement which performs as a structural section. The cracking and seating operation reduces the structural integrity of the existing pavement and it requires a much thicker overlay. A thick overlay not only increases the cost but also creates problems of clearance and shoulder edge drop off. This method involves more money, more time, and heavy equipment and should only be used if the pavement is severely cracked/faulted and no longer behaves as a structural section.

3.3.2.4 Sawing and Sealing Joints in AC Overlay

Sawing and sealing joints in an AC overlay is an effective way to avoid further deterioration of a reflected crack. It only works well if the saw cut is accurate in relation to the underlying concrete joint. Mismatched joints may reflect as another crack adjacent to the saw cut joint. It is best suited for JRCP with longer slab length. On slabs with mid crack or slabs having small slab length, it becomes uneconomical due to the amount of saw cut work.

3.3.2.5 Crack Arresting Interlayer (Granular Layer)

Large aggregate size and large void space can result in rutting problems because of mix instability. Due to larger size of aggregate, total overlay thickness is usually 6 in. to 10 in. The thick overlay causes clearance and shoulder elevation problems.

3.3.2.6 Bond Breakers

A bond breaker in the immediate vicinity of the joint/crack and provides limited degree of stress relief in the overlay. It is not very effective because of the following reasons:

a) Use of Wax paper or aluminum foil may break the bond but do not transfer enough shear force to the underlying pavement. Slippage may occur under the wheels of an accelerating, decelerating, or sharply turning vehicle.

b) Stone dust does not remain an effective bond breaker for a long period of time. Usually some asphalt cement flows to create bond between the stone dust and the underlying pavement. It is also difficult to spread a uniform thickness of the stone dust around the joint/crack.

3.3.2.7 Stress Absorbing Membrane Interlayer (SAMI)

Cracks do propagate through the SAMI and the overlay but travel at comparatively slower rate than in control sections. The performance of SAMI under the overlays on flexible pavements with fatigue cracking has been better than those under overlays on rigid pavements with thermal cracking. A treatment applied to the full width of the old pavement has produced better results than the one only applied around the joint/crack.

A SAMI with lower stiffness is more effective than the one with higher stiffness. The stiffness should not be so low that slippage could occur under the wheels due to a suddenly stopping or sharply turning vehicle. Stiffness of the SAMI without aggregate varies from 6500 psi to 7500 psi at 70 F to 75 F.

Since stiffness of SAMI is inversely proportional to the thickness of the SAMI, a thicker SAMI will be more effective. Usually the thickness of

SAMI varies from 0.25 in. to 0.375 in.

3.3.2.8 Geogrid or Geotextile Reinforcement

Geotextiles have performed poor to excellent in the past. In most cases they effectively retarded the growth of reflection cracking. This is particularly true in the first three to four years. Use of such interlayers has enhanced the life of overlays and reduced their maintenance cost in some cases.

Geosynthetics can improve the overlay performance by the following mechanisms:

a) Act as reinforcement.

b) Act as stress relieving interlayer.

c) Reduce surface water infiltration.

To act as reinforcement, the geosynthetic must have a minimum of "Very Stiff" classification (Table 9) and it should have more than 4000 lbs/in. secant stiffness. (Stiffness is equal to modulus of elasticity times thickness of the geotextile.)

A reinforced interlayer only delays and does not completely stop the crack. It tries to dissipate the stored energy by changing the direction of the crack from vertical to horizontal along the interface between the reinforcement and the underlying material.

Geotextiles with lower stiffness will act as a stress relieving interlayer in the pavement and reduce the stress at the tip of the joint/crack. Most paving geotextiles used in the past fall into this category and display less than 4000 lbs/in. stiffness. They act as a stress relieving interlayer instead of a reinforcement. Softer and thicker geotextiles can perform best as stress relieving interlayers.

Asphalt impregnated geotextile interlayers will remain intact even after moderate cracking occurs in an overlay. Such interlayers also act as impermeable layers and do not let surface water flow into the base. This will eliminate pumping, reduce differential vertical settlement, and lower the moisture gradient which is a major cause of warping in the slab.

Geotextiles have performed better in the pavements with load associated distresses (alligator cracking), than those with thermal cracking in cold regions.

The performance of geotextiles has been greatly influenced by the amount of horizontal displacement at the joint/crack. It has been experienced that:

a) For less than 0.02 in. horizontal displacement, geotextiles are not required.

b) Geotextiles are most effective on the pavements with 0.02 in. to 0.07 in. of opening movement at the joint/crack.

c) Geotextiles normally can not withstand an opening movement more than 0.07 in. wide.

Geotextiles have performed very well on pavements with fatigue distress such as closely spaced alligator cracking. Their performance is affected by the initial crack width. Geotextiles used over fatigue cracks, less than 1/8 in. wide have produced the best results. Geotextiles placed on pavements with more than 3/8 in. wide fatigue cracks did not performed well. Cracks wider than 3/8 in. should be filled with rigid filler prior to geotextile placement.

Though geotextiles have performed fairly well in cases of horizontal joint/crack movement, their effectiveness against vertical joint/crack deflection has been questionable. Pavements with less than 0.002 in. vertical deflection usually don't require geotextiles. Geotextiles are partially effective in the range of 0.002 in. to 0.008 in. vertical joint/crack movement. For the pavements having more than 0.008 in. vertical joint deflection a geotextile interlayer is ineffective and a minimum of 4 in. thick overlay is needed to effectively retard the reflection cracking.

A thicker overlay quite effectively reduces crack propagation but it is not as cost effective as the geotextile interlayer. Use of geotextiles can reduce the required overlay thickness and decrease cost. From past experience it has been noted that most geotextiles are equivalent to 1 in. to 1.5 in. of AC in relation to reflection control.

The correct amount of tack coat is important for best performance of a geotextile interlayer. Application of too much tack coat reduces the shear resistance at the interface. This may result in slippage and tearing at critical locations where vehicles accelerate, decelerate, or make sharp turns. On the other hand too little tack coat will result in poor bond between the geotextile and overlay/PCC pavement and will reduce the stress relieving ability. The following relationship is recommended to estimate the correct amount of tack coat:

$$RTC = 0.05(TW)^{0.30} \qquad \text{Equation 1}$$

Where:

RTC=Recommended tack coat rate (gal/sq yd)

T=Geotextile thickness (mils)

W=Geotextile weight (oz/sq yd)

Equation 1 includes an allowance of 0.05 gal/sq yd for absorption by the underlying pavement (surface hunger).

Wrinkles in the paving geotextiles can be a source of premature cracking in an AC overlay. Heavier or thicker geotextiles (8 oz/sq yd or more) develop less wrinkling during construction as compared to thinner geotextiles (4 oz/sq yd or less). Stiffer geotextiles also develop less wrinkles than softer geotextiles of equal weight.

CHAPTER 4

PROPOSED ISAC SYSTEM

4.1 Introduction

After carrying out indepth study of the causes and phenomenon of reflection cracking and the behavior and performance of overlays with interlayers, it is felt that neither SAMI nor geotextile can completely stop the initiation of cracking. A stress relieving interlayer (rubber asphalt or thick geotextile with low stiffness) allows for some deformation and reduces stress at the crack tip but often some stress still remains undissipated and a crack will form in the overlay if the tensile strength of the asphalt concrete is exceeded. When a high stiffness interlayer is used, it provides reinforcement to the AC overlay and temporarily retards the movement of the crack. Since it does not allow any relative movement between the overlay and the underlying pavement, the upward moving crack changes direction and starts moving laterally along the interface between the reinforcement and the underlying material (failure mode–3, in Section 3.2.9.3). The crack movement can be effectively controlled if a composite layer consisting of geotextile and SAMI is provided in such a way that it relieves stress at the crack tip and at the same time provides reinforcement to the overlay. Such a composite layer could contain the upward propagation of a crack and dissipate the stress at the tip of the joint/crack. To take advantage of the observed performance characteristics of these applications a composite geotextile and rubber asphalt material named "Interlayer Stress Absorbing Composite (ISAC)" is suggested to be introduced between the overlay and the underlying pavement. ISAC will be designed to effectively stop the upward propagation of a crack in the AC overlay and to also adequately reinforce the AC overlay.

4.2 Interlayer Stress Absorbing Composite (ISAC)

The proposed ISAC system is shown in Figure 32a and Figure 32b. ISAC consists of a low stiffness geotextile a rubber asphalt membrane, and a high stiffness geotextile.

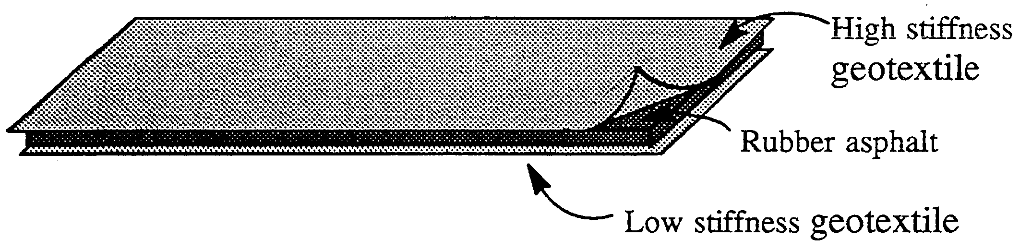

Figure 32 a: Interlayer Stress Absorbing Composite (ISAC)

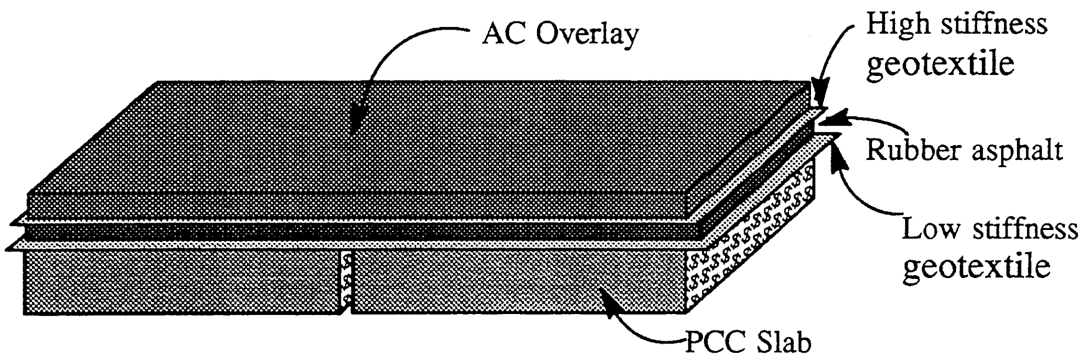

Figure 32 b: ISAC Placed Between PCC Slab & AC Overlay

4.2.1 Low Stiffness Geotextile

A low modulus, low stiffness geotextile will be provided at the bottom of the composite interlayer. This layer will serve the following three functions:

a) Contain the rubber asphalt membrane.

b) Fully bond with the existing pavement with the help of a tack coat.

c) Because of low stiffness, it will accommodate sufficiently large strain at the joint/crack so as to allow horizontal movement of the underlying pavement without breaking its bond with the slab.

4.2.2 Rubber Asphalt Membrane

A blend of vulcanized rubber (25 % to 30 %by weight) and appropriate viscosity asphalt (70 % to 75 % by weight) will be prepared at temperature of 300 F to 400 F to form a rubber asphalt core of desired viscosity and stiffness for ISAC. It will be cooled to a temperature range of 250 F to 300 F and then a 0.125 in. to 0.375 in. thick layer of this blend (rubber asphalt)will be placed between the two layers of geotextile. This sandwiched rubber asphalt membrane is intended to serve the following two functions:

a) Provide flexible bond between two geotextiles.

b) Act as a stress absorbing membrane interlayer (SAMI) and allow relative horizontal movement between the two geotextiles and between the overlay and the underlying pavement so as to reduce the stress at the tip of the joint/crack.

4.2.3 High Stiffness Geotextile

A high modulus, high stiffness geotextile will form the upper layer of ISAC. According to the classification given in Table 9, it will be a ‘‘very stiff’’ geotextile and it will have a stiffness greater than 4000 lbs/in. This layer is intended to serve the following three functions:

a) Contain the rubber asphalt membrane.

b) Fully bond with the overlay.

c) Provide high stiffness and reinforcement to the overlay. Even at high stress value, it should allow very little strain in the overlay and therefore prevent propagation of any crack.

4.3 Installation of ISAC

An appropriate quantity of tack coat (quantity recommended in Equation 1 Section 3.3.2.8) should be applied on the existing pavement surface prior to placement of ISAC. ISAC is placed with the low stiffness geotextile towards the bottom and the high stiffness geotextile towards the top, Figure 32 b. A tack coat is again applied on the upper surface of the ISAC layer and the overlay is then placed.

4.4 Anticipated Operating Mechanism

Once thermal contraction takes place in the underlying pavement as a result of seasonal/daily temperature drop, horizontal displacement of the underlying pavement takes place and the existing joint/crack spacing increases.

The low stiffness geotextile, which is fully bonded with the underlying pavement, except at the joint/crack (between points a and b, Figure 33 a) allows large strain in the unbounded portion. The increase in length is equal to the expansion taking place at the joint/crack caused by the thermal contraction taking place in the slab, Figure 33 b. Since the two geotextile layers are bonded with

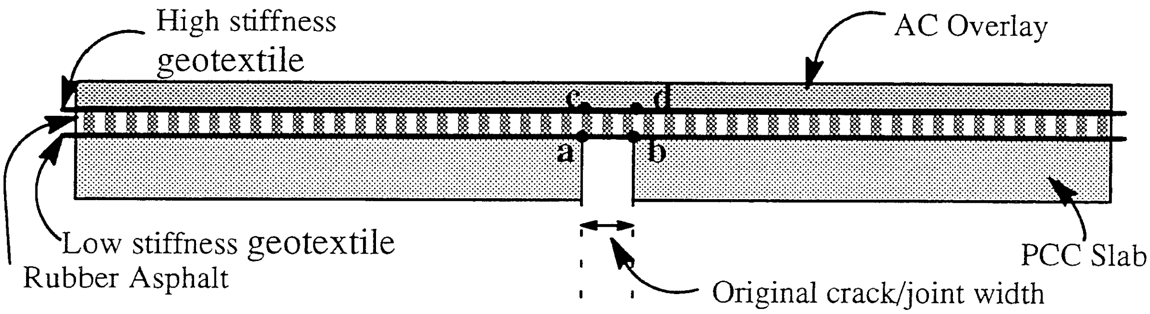

Figure 33 a: Pavement Condition At Normal Temperature

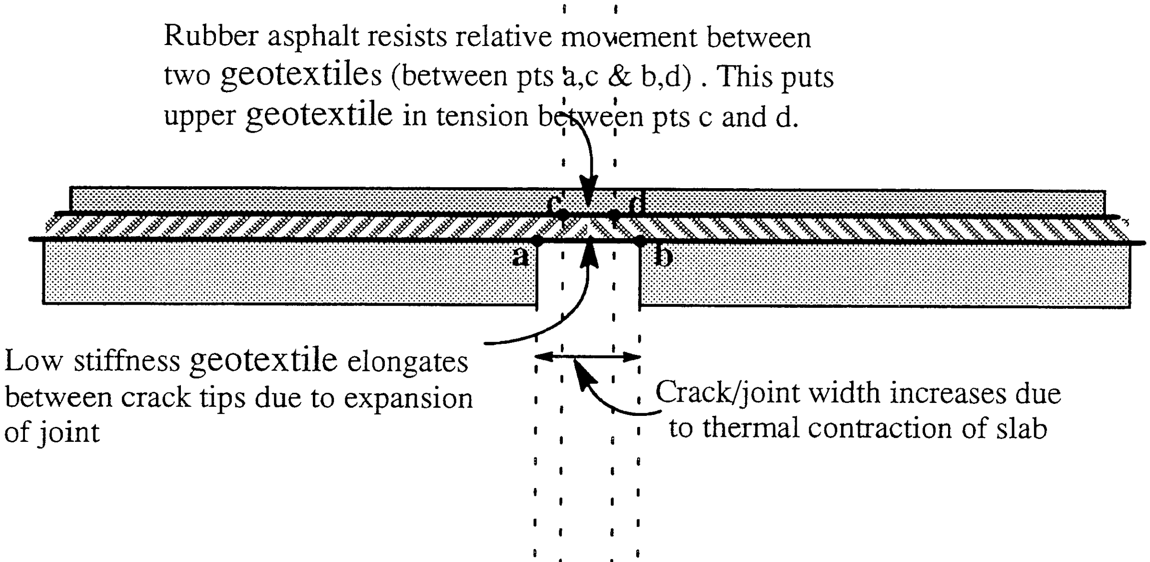

Figure 33 b: Pavement Condition At Low Temperature – Stage 1

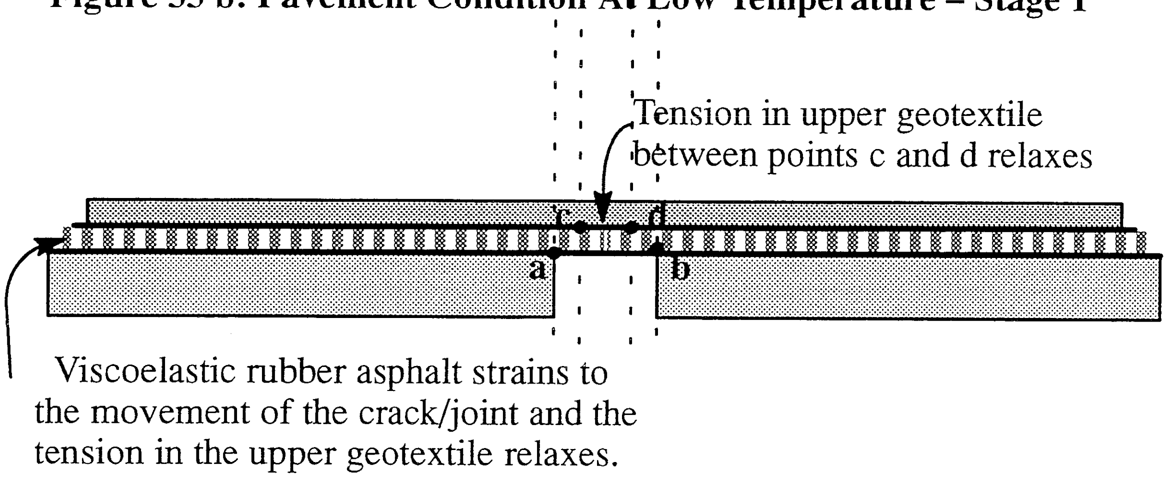

Figure 33 c: Pavement Condition At Low Temperature – Stage 2

each other through the rubber asphalt membrane, horizontal movement of the lower geotextile (low stiffness geotextile) will induce some tensile stress in the upper geotextile (high stiffness geotextile), in the area immediately above the joint/crack (Figure 33b). The upper geotextile due to its high stiffness will experience very little strain and will limit the stress in the overlay which is bonded to it. The two geotextile layers are bonded with each other with the help of a rubber asphalt membrane, which is a viscoelastic material. Due to its viscoelastic properties the rubber asphalt will gradually relax and consequently the tensile stress in the upper geotextile (high stiffness geotextile) will be minimal, Figure 33 c.

CHAPTER 5

ISAC DEVELOPMENT AND EVALUATION PROCEDURES

5.1 Introduction

The goal of this study is to design an "Interlayer Stress Absorbing Composite (ISAC)"which can effectively alleviate/mitigate the problem of reflection cracking in AC overlays. This involves development, fabrication, and finally the evaluation of ISAC. Techniques used in the past to mitigate reflection cracking have shown positive results under certain conditions but have given poor performance once subjected to the range of field conditions. ISAC will be tested and evaluated in the laboratory by keeping in mind the findings in Chapter 3 and by simulating field conditions as close as possible.

Although in the literature review it is observed that reflection cracking is attributed to both vertical and horizontal movement of the slab at the joint/ crack it has been noticed that major damage to the overlay occurs from the horizontal movement of the slab with temperature variance. To achieve simplicity the effect of traffic load has not been considered in this study.

5.2 ISAC Development and Evaluation Procedures

The following procedures have been used to develop and evaluate the ISAC system:

a) Through the use of various thermal/structural models and laboratory equipment, determine the properties of materials needed for an "Interlayer Stress Absorbing Composite (ISAC) system."

b) Fabricate one or more ISAC systems which will mitigate reflection cracking in AC overlays.

c) Conduct laboratory testing and evaluate the performance of one or more ISAC systems by comparing them with a control section.

5.3 Research Approach

In order to develop and evaluate the ISAC system the following research approach was taken:

5.3.1 Phase 1 – Preparation Testing and Classification of Materials

The Climate–Materials–Structural (CMS) pavement model (model developed at the University of Illinois) (14) was used to establish the operating temperature range in multilayered pavement systems for typical Northern Illinois climatic conditions.

Several samples of rubber asphalt were prepared by mixing the crumb rubber with different type of asphalt cements at different asphalt to rubber ratios at a particular temperature. Properties of the materials intended to be used in the ISAC system were established by carrying out various tests. Materials were then selected based on their properties.

5.3.2 Phase 2 – Fabrication of Prototype ISAC System

After all the materials intended to be used in the ISAC system have been selected based on their properties, several prototype ISAC systems will be fabricated. these ISAC systems will consist of different type of materials with varying rubber asphalt thickness.

5.3.3 Phase 3 – Laboratory Testing and Evaluation of ISAC System

ISAC will be placed over a cracked or jointed PCC slab, prior to placing an AC overlay. Field conditions will be simulated in the laboratory to evaluate the behavior of an AC overlay placed on a cracked or jointed PCC slab treated with an ISAC layer. Thermal strain in the slab will be simulated by use of a mechanical device and the overlay will be monitored for reflection cracking. The performance of ISAC will be evaluated in relation to simulated thermal cycles. The performance of the ISAC system will be compared with a control pavement without ISAC.

5.4 Assumptions

Testing will be carried out with the following assumptions:

a) Slab length =15 ft.

b) Coefficient of thermal contraction of concrete/
asphalt concrete = 6 E – 6 in. /in. / F.

c) ISAC is fully bonded with the underlying pavement
as well as with the overlay.

d) Northern Illinois climatic conditions.

e) No moisture gradient exists in the pavement.

f) Pre overlay repair has been carried out and all the slabs with voids underneath and with poor load transfer, showing Benkleman Beam vertical deflection across the joint/crack more than 0.002 in., have been either repaired or replaced. Since the vertical deflection across the joint/crack is very low (less than 0.002 in.) contribution of traffic towards the initiation of reflection cracking is very small. The effects of traffic load is neglected in this study to achieve simplicity. However traffic loads will be considered at a later time during field evaluation.

CHAPTER 6

MATERIALS SELECTION AND PREPARATION OF ISAC

6.1 Introduction

To effectively approach the design problem of an ISAC system it is considered necessary to identify the properties of the materials intended to be used in the system. Woven and non woven geotextile samples need to be tested for their engineering properties and their behavior needs to be studied under simulated field conditions. Several samples of rubber asphalt have to be prepared by blending various ratios of crumb rubber with different types and ratios of asphalt cements and its behavior has to be studied at varying temperatures and rates of deformation. Use of various thermal/structural models has been made to determine the extreme temperatures likely to be encountered in the field and various laboratory testing procedures have been developed to duplicate field conditions in the laboratory.

6.2 Temperature Effects

A major cause of reflection cracking is seasonal/daily temperature variation in the pavement. It is thus imperative to know the range of temperatures which influence pavement behavior. This temperature range will not only provide the maximum seasonal/daily thermal variation required to calculate movement in the PCC slab, but will also give the average maximum and minimum temperatures to which ISAC will be exposed. Durability and performance of the materials intended to be used in ISAC can thus be tested within this range of temperature.

6.2.1 Maximum Seasonal/Daily Temperature Variations in the Pavement

The Climate–Materials–Structural (CMS) pavement model (14) was used to find the maximum and minimum daily temperatures in the pavement for an average year. The CMS model was used to provide the temperature in a pavement at a particular depth and at a particular time of the year in Northern Illinois area. A pavement section consisting of a 10 in. thick PCC slab, 0.25 in. thick ISAC layer, and 2.5 in. thick AC overlay was assumed in the CMS model. Maximum and minimum daily temperatures at four different points in the pavement including at the surface, mid depth of AC overlay, interface (center of ISAC), and at mid depth of the PCC slab as shown in Figure 34 were computed for a typical year. Details of these results are shown in Appendix A. The results are presented in Figures 35,36, 37, and 38. The maximum seasonal and daily temperature variations are also shown in Appendix A as well as in Figures 35 through 38

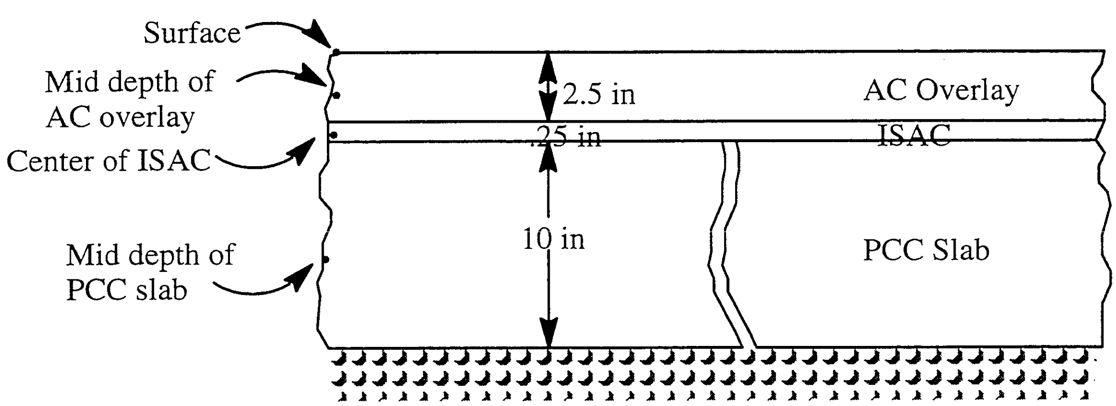

Figure 34: Pavement Cross Section Used For Thermal Evaluation

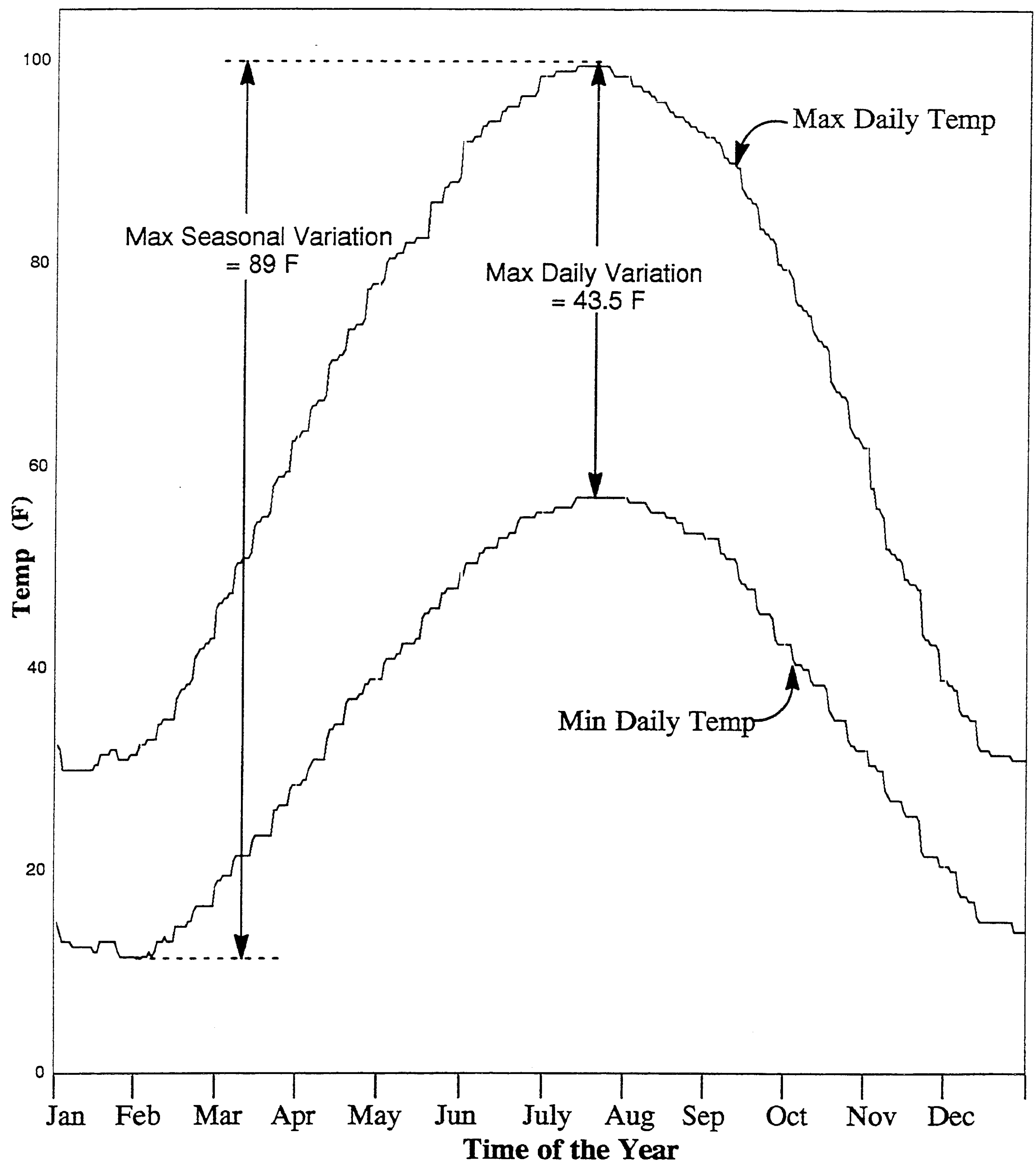

Figure 35: Yearly Temperature Variation At the Overlay Surface

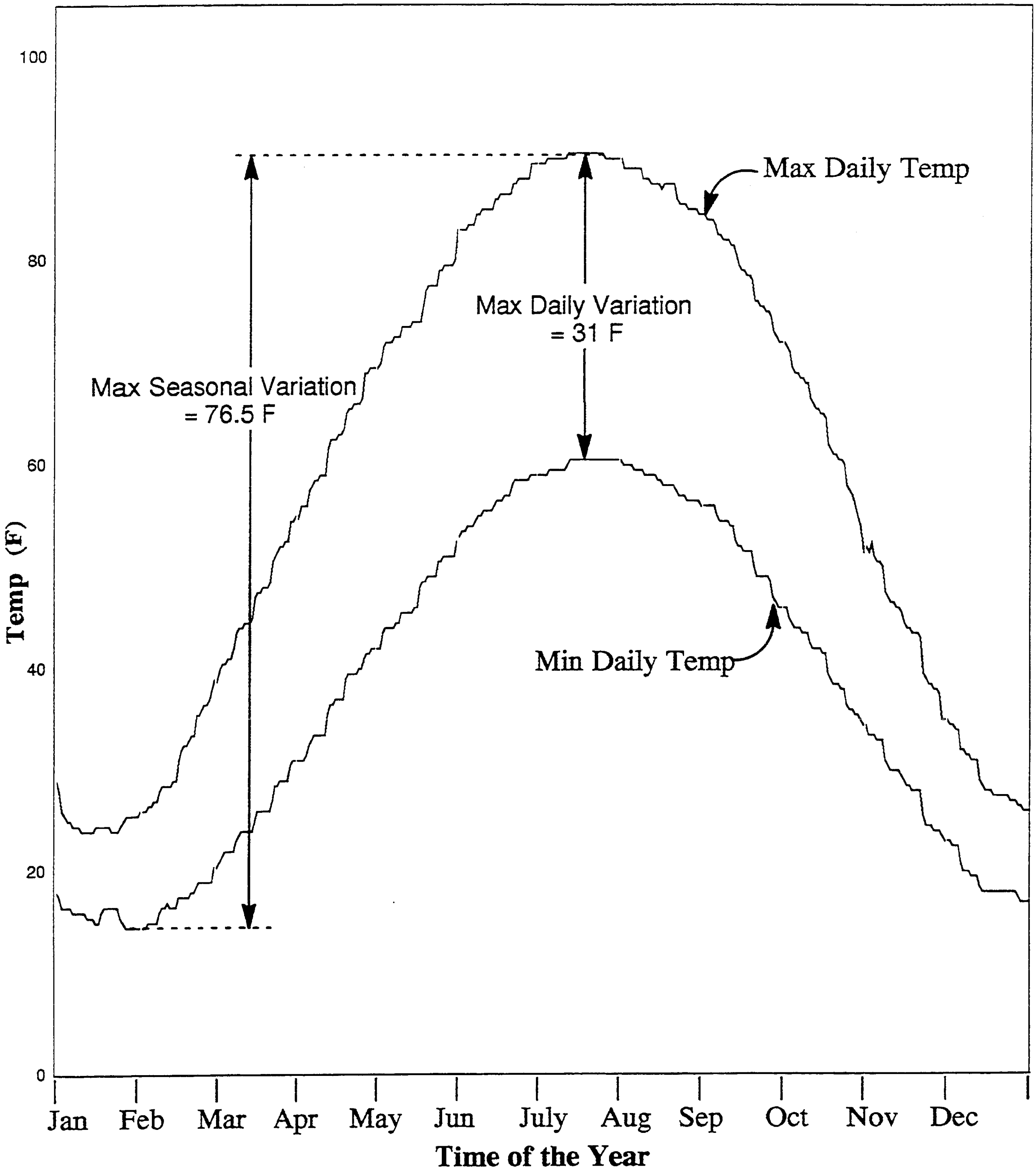

Figure 36: Yearly Temperature Variation At Mid Depth of the AC Overlay

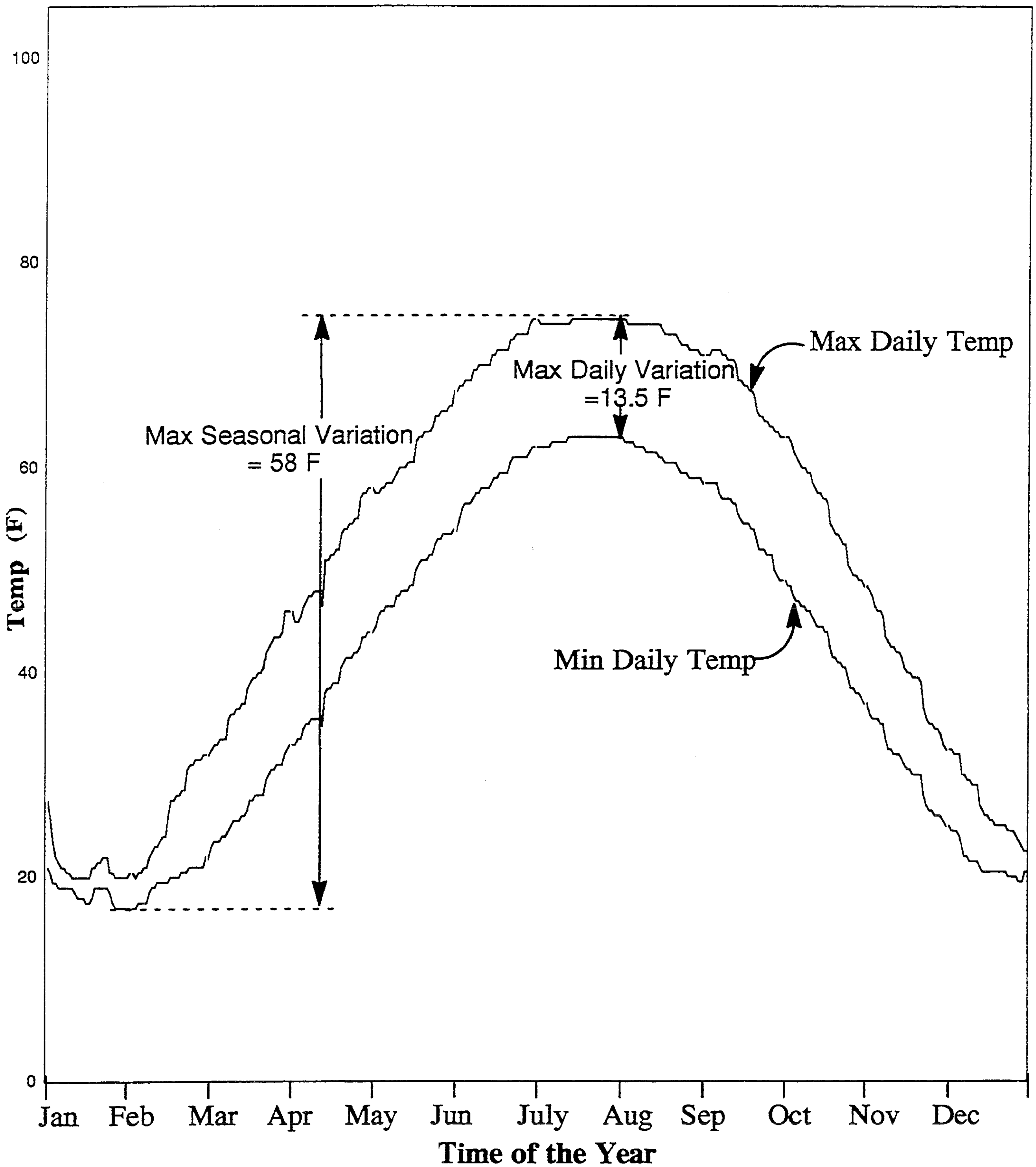

Figure 37: Yearly Temperature Variation At Interface (Center of ISAC)

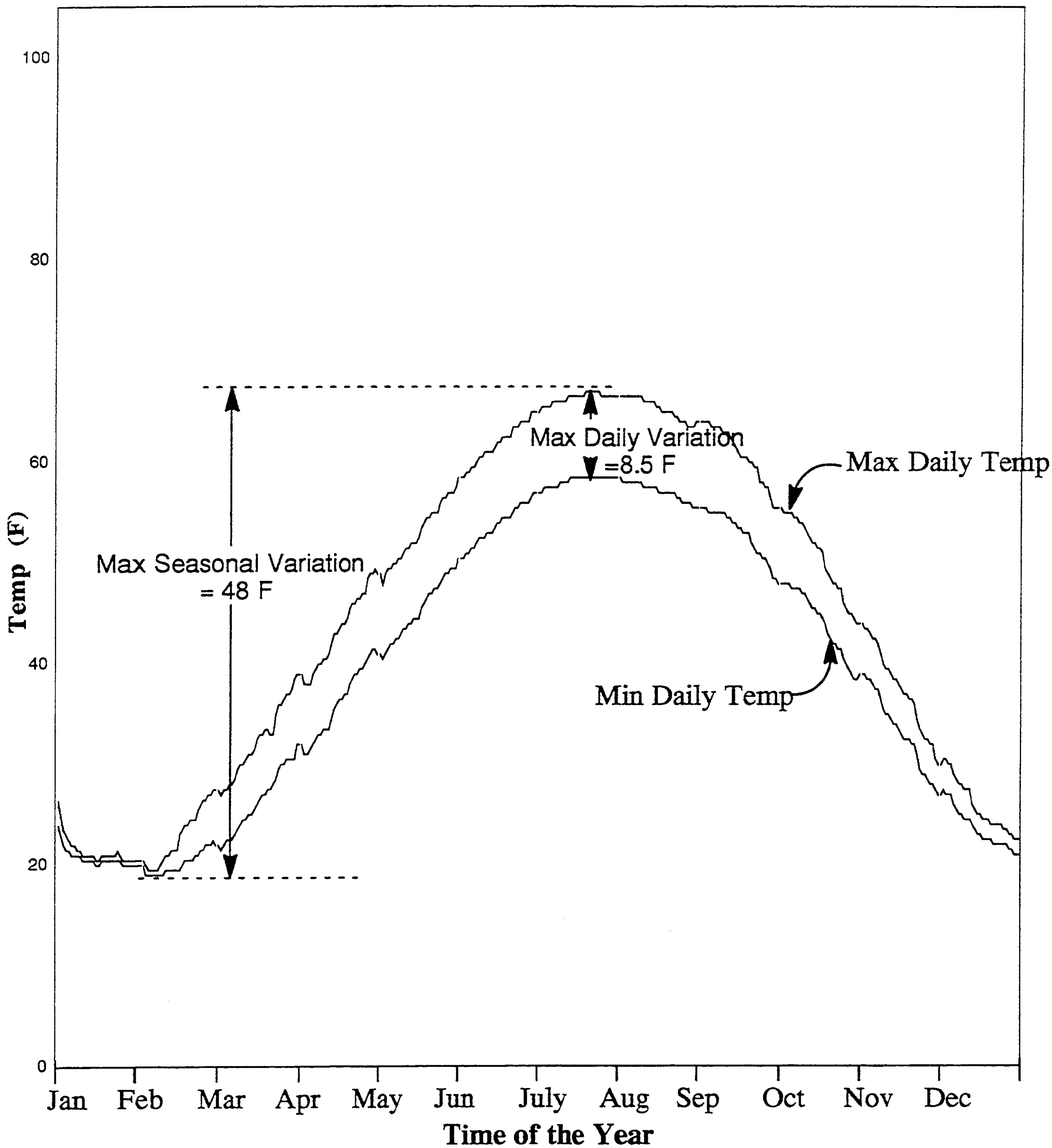

Figure 38: Yearly Temperature Variation At Mid Depth of The PCC Slab

Some of the important climatic parameters from Figure 35 through Figure 38 are presented in Table 10.

Table 10: Temperature Range and Temperature Variation in the Pavement

S/No	Point of Interest in The Pavement	Maximum Seasonal Variation (F)			Maximum Daily Variation (F)
		Min Temp During The Year	Max Temp During The Year	Max Seasonal Variation	
1.	At the surface (Top of the overlay)	10	99	89	43.5
2.	At mid depth in the overlay	13.5	90	76.5	31
3.	At Interface (Center of ISAC)	16.5	74.5	58	13.5
4.	Mid Depth in PCC slab	19	67	48	8.5

6.2.2 Temperature Study Results

Based on the summary of important climatic parameters in Table 10 the following temperature variations are observed:

a) The joint/crack opening due to slab contraction could be calculated, based on maximum seasonal variation of 58 F for slab contraction and 76.5 F for AC overlay contraction in Northern Illinois.

b) The maximum daily temperature variation at the center of the slab is 8.5 F which is relatively insignificant for joint/crack opening calculations.

c) The ISAC materials will be exposed to extreme temperatures in the range of 16.5 F to 74.5 F.

6.2.3 Joint/Crack Opening Calculations

Low temperatures in winter causes a PCC slab to contract and open the existing joints/cracks, Figure 39 a. Since the AC overlay is fully bonded with the underlying pavement, tensile stress is created in the overlay directly above the joint/crack. Overlay material on the other hand also contracts in response to low temperature. Reduced length of the overlay, in the area

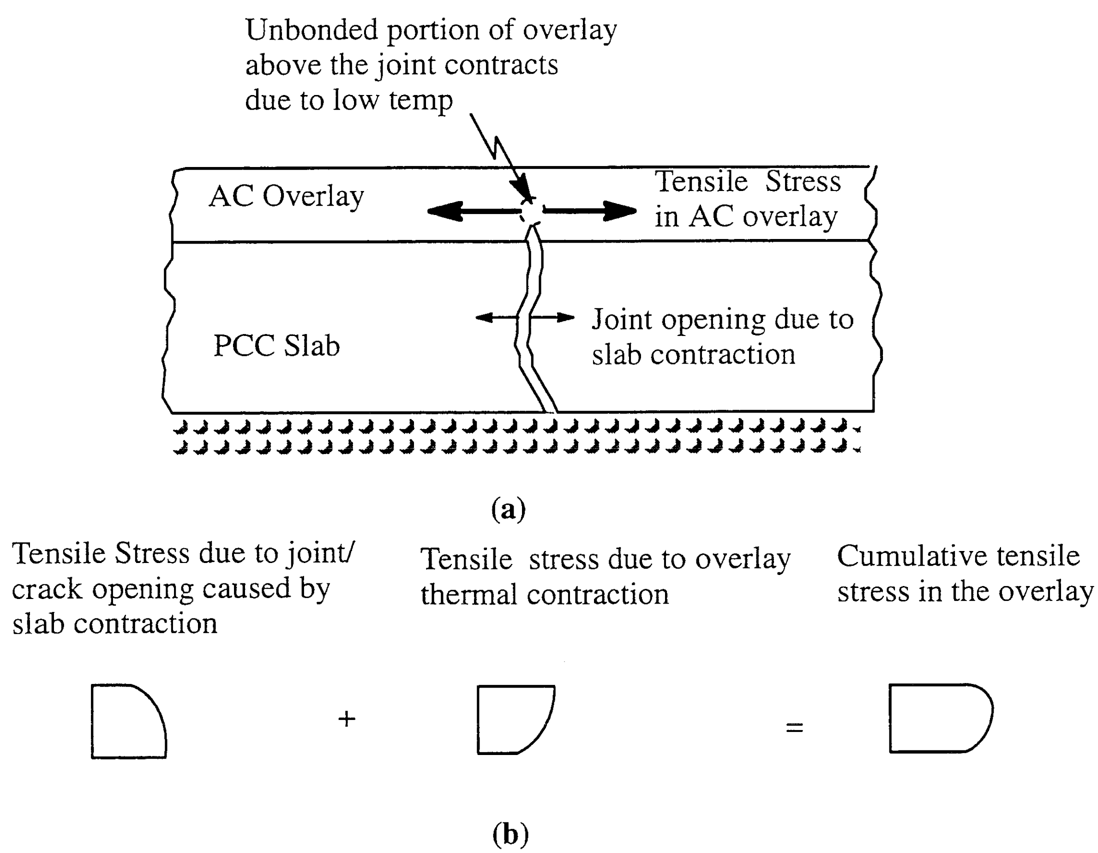

Figure 39: Joint/Crack Opening

directly above the joint/crack, provides further resistance to the joint opening and induces additional tensile stress in the overlay. The total stress in the AC overlay is proportional to the net relative movement being resisted by the overlay, Figure 39 b.

6.2.3.1 Net Relative Movement Resisted by The Overlay

The net resisted movement between the overlay and the slab can be calculated from Figure 39 b.

Net resisted movement=Thermal contraction in the PCC Slab
+Thermal contraction in the AC overlay
directly above the joint/crack.

Net resisted movement={Slab Length * Seasonal temp variation of the slab
* Coefficient of thermal contraction of PCC slab}
+ {Crack/joint opening * Seasonal temp variation of
AC overlay * Coefficient of thermal contraction of AC}

$$= \{ (15*12) * (58) * (6E\text{–}6) \} + \{ (0.375) * (76.5) * (6E\text{–}6) \}$$

$$= 0.06264 + 0.00017$$

$$= 0.0628 \text{ in.}$$

$$\simeq 0.063 \text{ in.}$$

Note: Assuming coefficient of thermal contraction
for PCC slab and AC = 6E–6 (Ref 2)

In the above calculations viscoelastic properties of the AC overlay have not been considered.

6.3 Geotextile Testing

6.3.1 Engineering Properties

Eight types of woven geotextiles and two non woven geotextiles were tested for their engineering properties. A total of seven geotextile properties were measured in the laboratory. Initially tests were performed on control samples (i.e., without heating the geotextile samples). The effect of heat due to impregnation with hot rubber asphalt and laying a hot overlay was then evaluated to determine how these factors would influence geotextile properties. The measured properties are summarized in Table 11 and Table 12. Standard ASTM procedures were selected to reasonably simulate the in service conditions. Weight of geotextiles was measured according to ASTM D3776 and the thickness was measured using ASTM D1777. The wide width tensile strength test (ASTM D4595) was performed on non woven geotextiles. Eight inch wide non woven geotextile specimens were tested with 4 in.

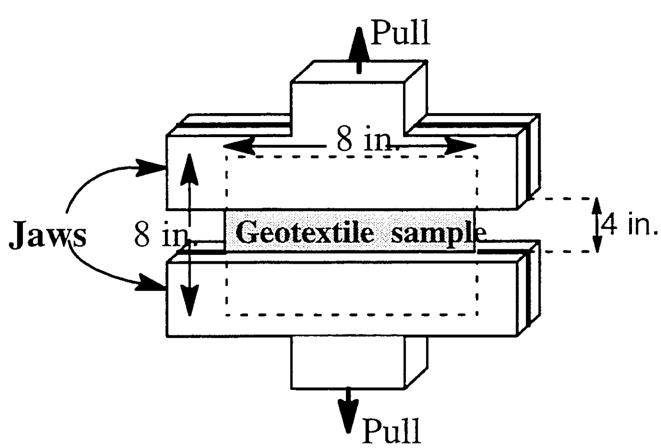

Figure 40: Tensile Strength Test on Non Woven Geotextiles

gauge length, Figure 40, giving an aspect ratio (specimen width/specimen length ratio) of 2. An aspect ratio of 2 was considered high enough to ensure that 'necking" and "roping" of the geotextile does not occur and laterally restrained field conditions are maintained. For woven geotextiles, a narrow strip test with specimen 1 in. wide and 4 in. gauge length, Figure 41, was

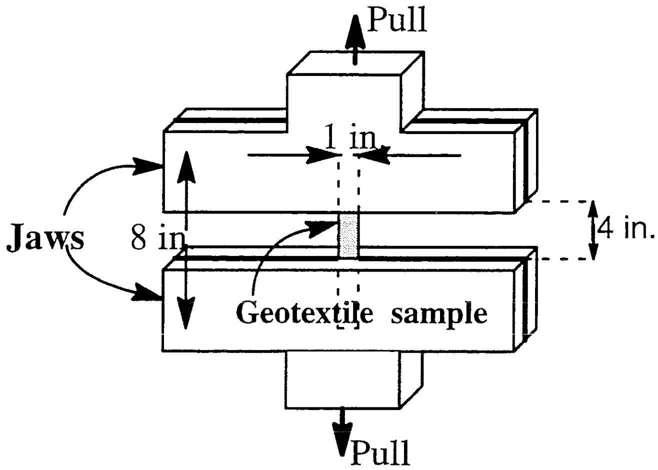

Figure 41: Tensile Strength Test on Woven Geotextiles

carried out, since an uneven stress distribution was observed in the wider specimens (more than 1 in. wide) of woven geotextiles at the time of failure. Also the wide strip tensile strength of the woven specimens would have exceeded the capacity of the standard geotextiles grips due to their high tensile strength. No problem of "necking" and "roping" was observed in case of narrow strip test. Tests were performed at room temperature and loading rate of 0.5 in./min was used.

The tensile force per in. width of Geotextile was defined as tensile stress. The tensile stress vs strain relations for the selected geotextiles are shown in Figures 42 through 51. From Figures 42 through 51 and Table 11 the modulus at 5% and 10% strain and modulus at failure were computed. The modulus at failure is defined as "The ratio of stress to strain at failure". Failure was considered when any of the following conditions occurred:

a) Tearing of the geotextile took place.

b) Tensile load reached a peak value and then reduced with further increase in strain.

c) An elongation of 50 % of the original length occurred.

The computed moduli are shown graphically in Figure 52.

A heat transfer model developed in the University of Illinois (36) was used to evaluate the influence of temperature on different geotextiles strength properties. A 3 in. thick overlay at initial temperature of 300 F was assumed to be placed on the geotextile and a heat dissipation curve was developed, Figure 53. Influence of 3 in. thick AC overlay at initial temperature of 300 F on the geotextiles was simulated by placing the geotextile samples in an oven with the temperature gradient similar to the one shown in Figure 53. The change in geotextile length was then measured and percent shrinkage for each geotextile was computed. The samples were also tested for tensile strength and moduli at 5 % and 10 % strain and at failure. The tensile strength and moduli of the geotextiles before and after placing a 3 in. thick, 300 F hot overlay are also shown in Figures 42 through 51 and Figure 54 respectively.

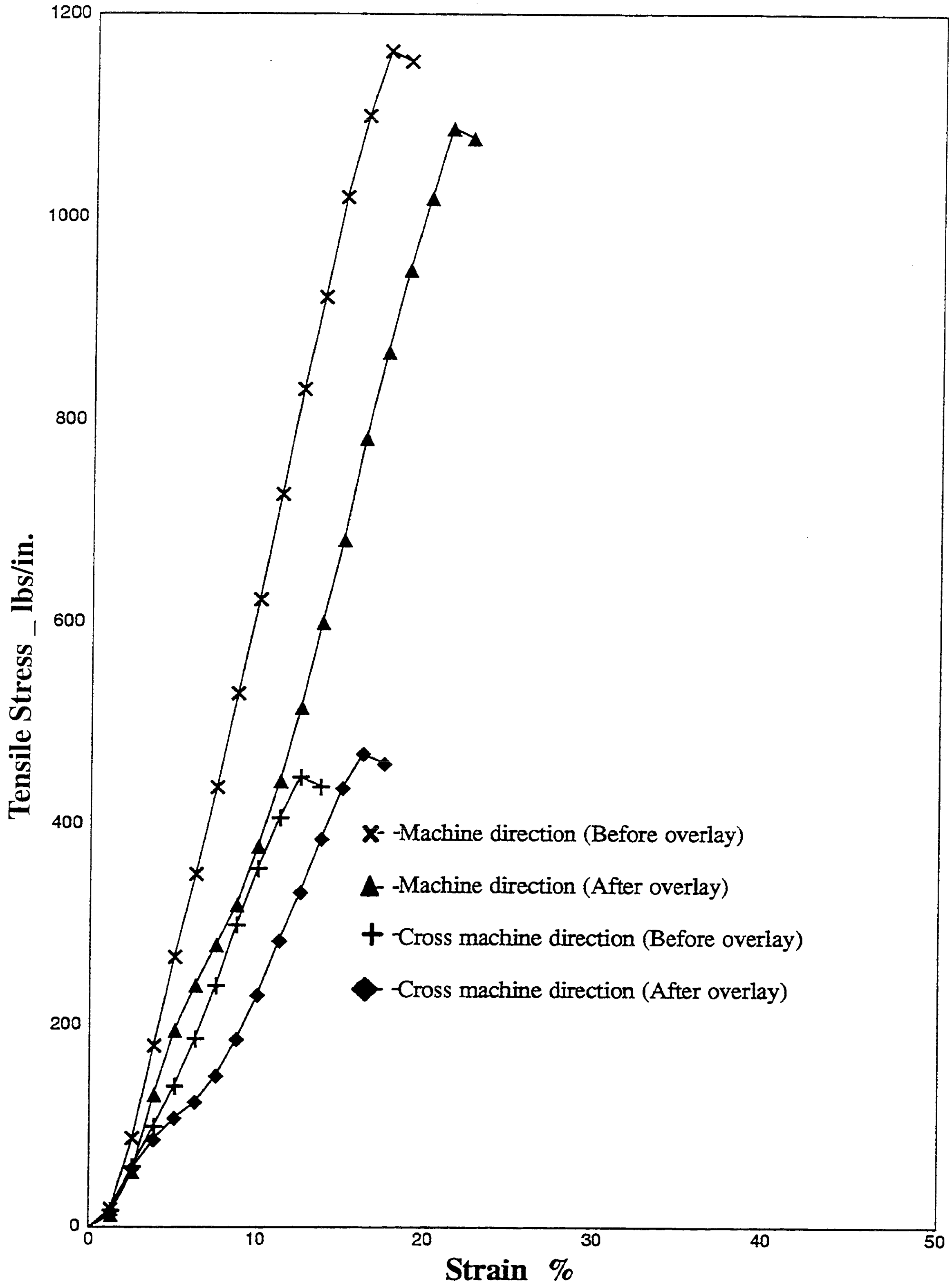

Figure 42: Woven Geotextile – TT 200/50 (Bidim Rock)

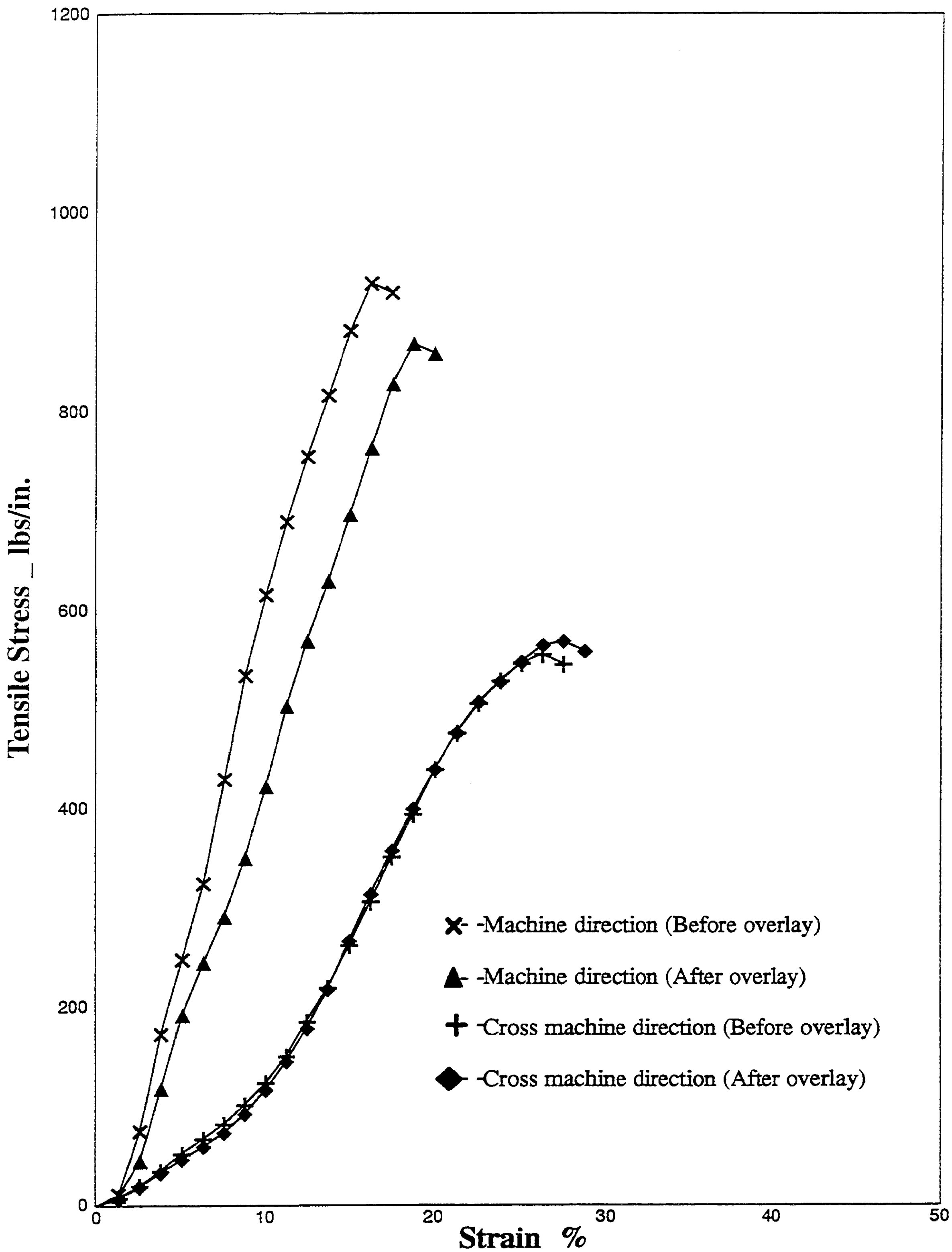

Figure 43: Woven Geotextile – Huesker–200/100

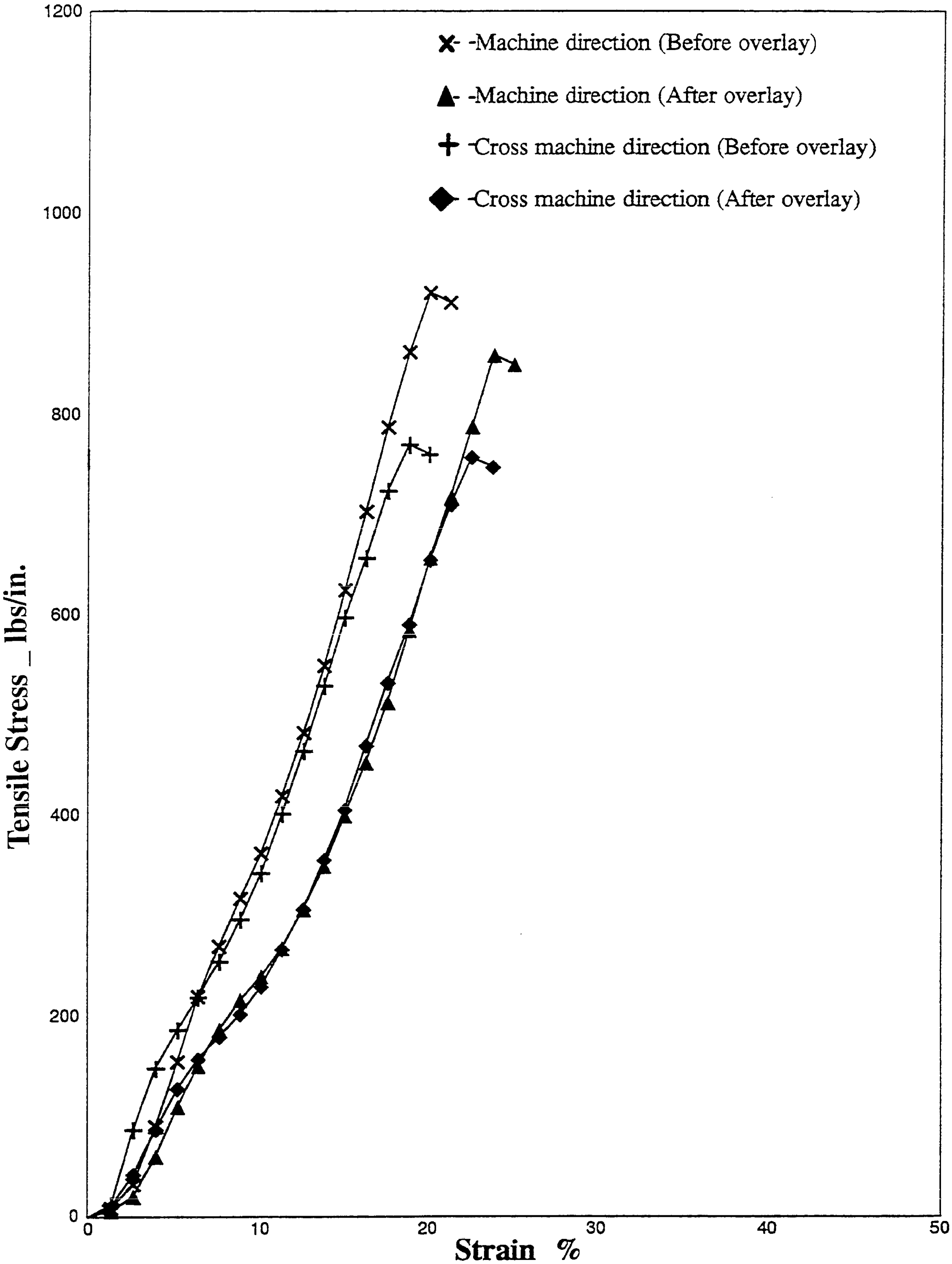

Figure 44: Woven Geotextile – GTF 1000T (EXXON)

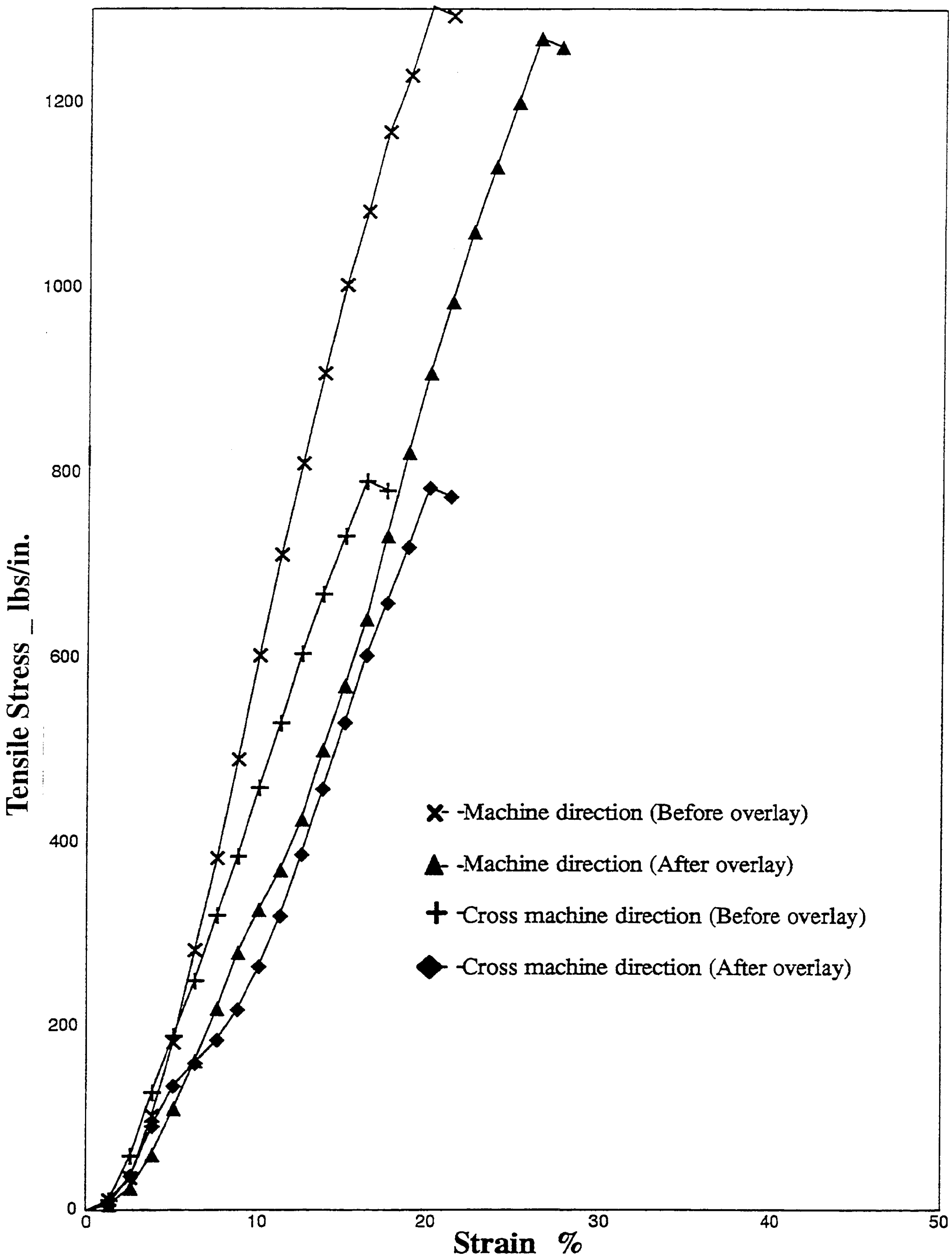

Figure 45: Woven Geotextile – GTF 1500T (EXXON)

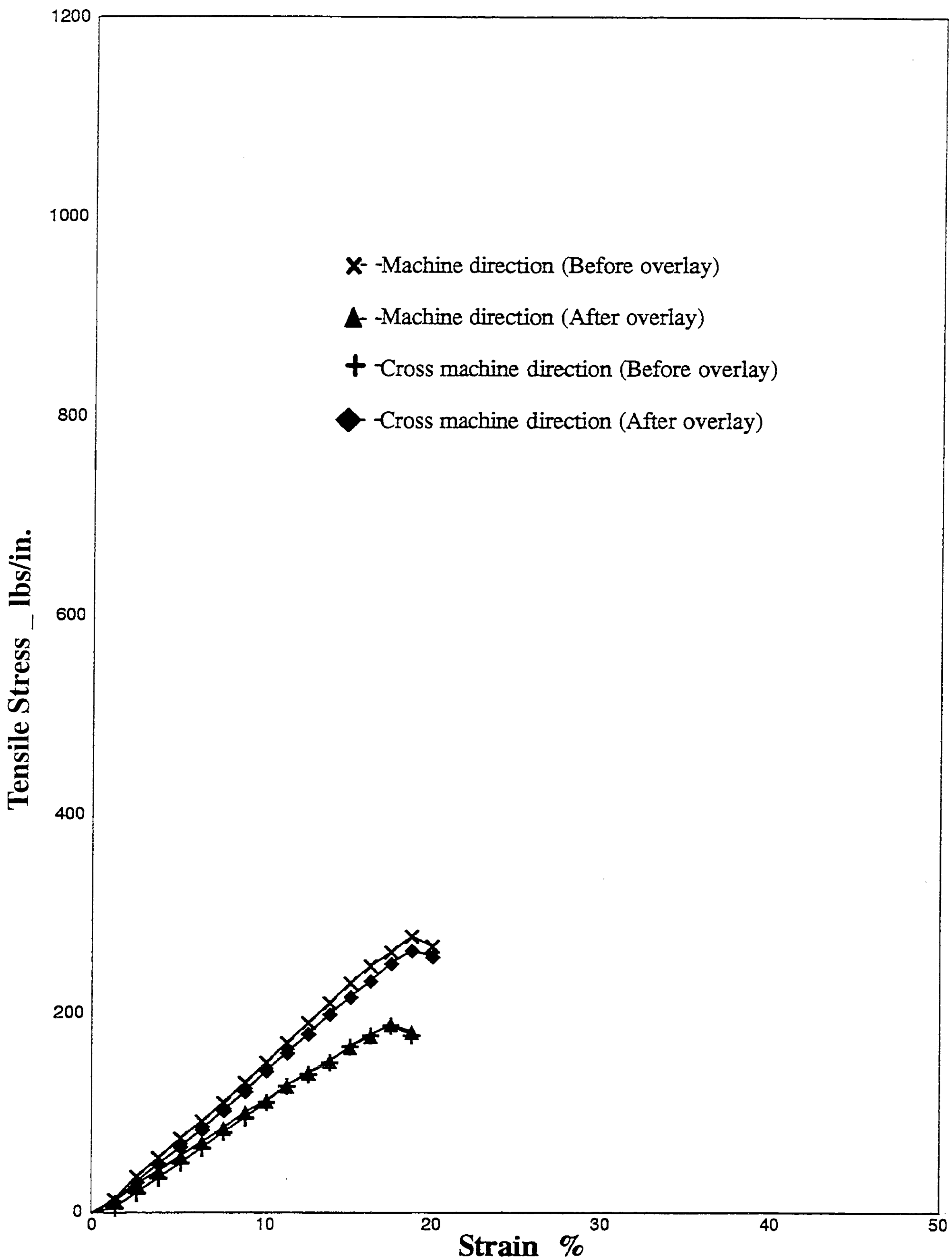

Figure 46: Woven Geotextile – GTF–400E (EXXON)

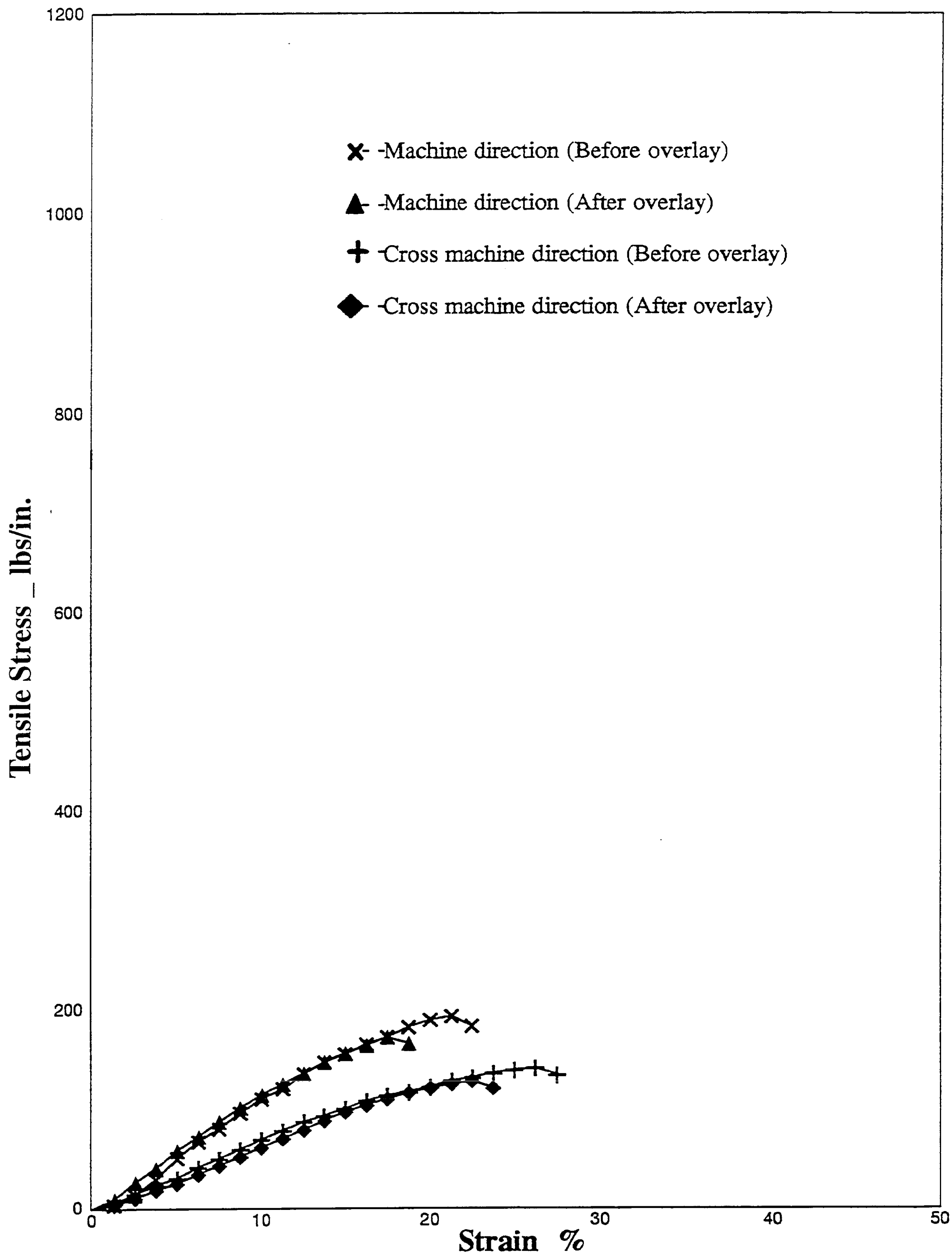

Figure 47: Woven Geotextile – GTF–200S (EXXON)

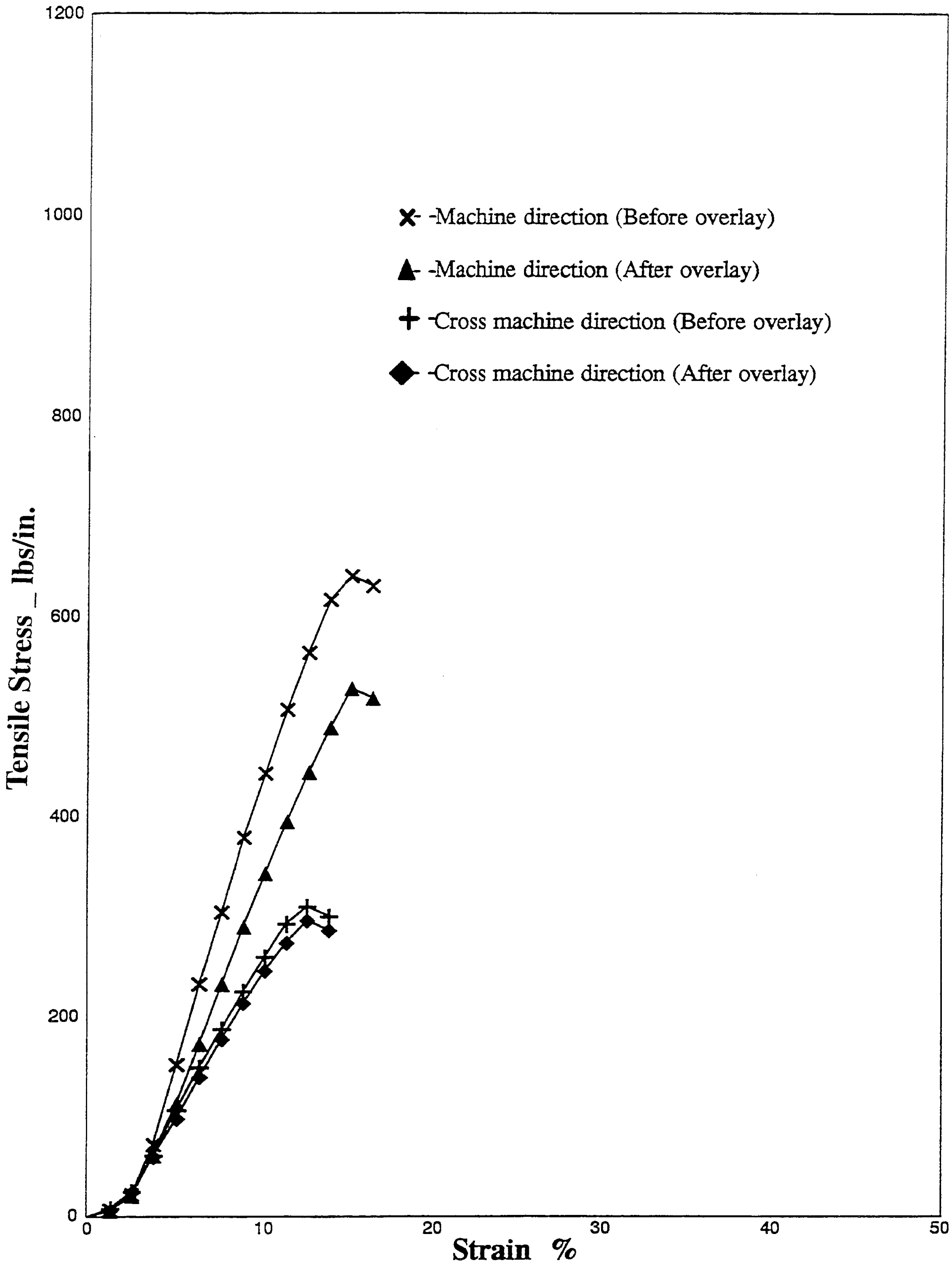

Figure 48: Woven Geotextile – Robusta

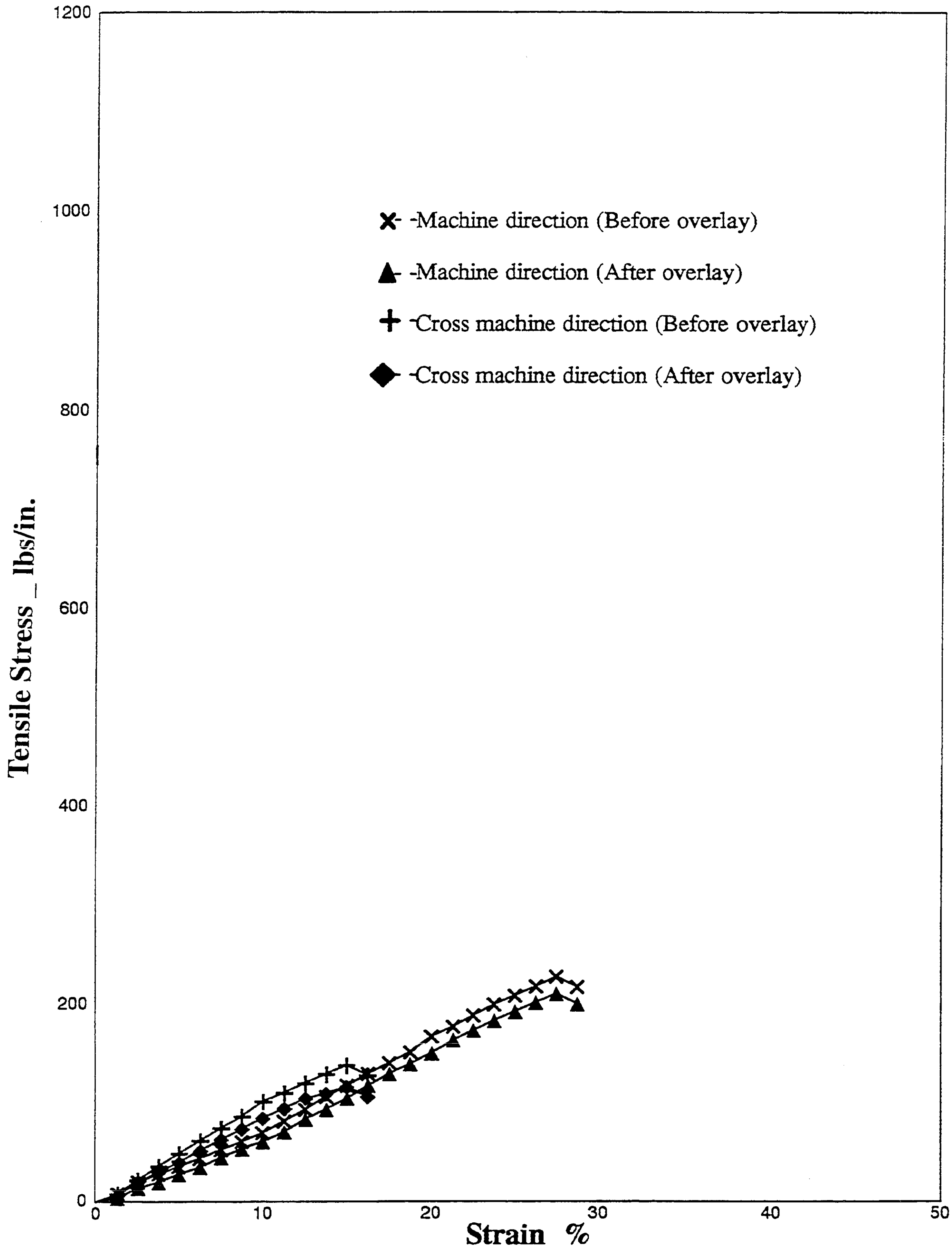

Figure 49: Woven Geotextile – Nicolon

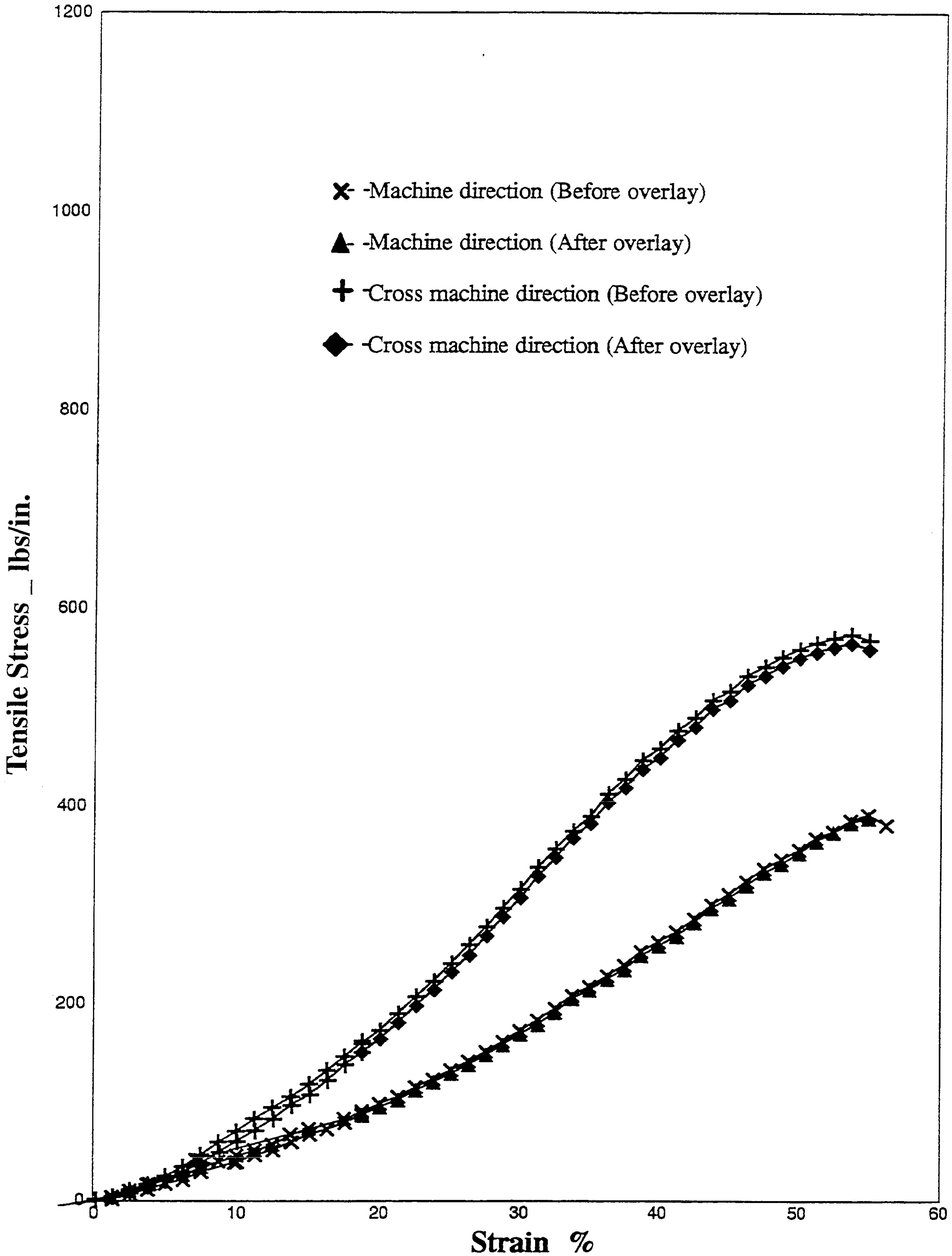

Figure 50: Non Woven Geotextile – AMOCO 4545

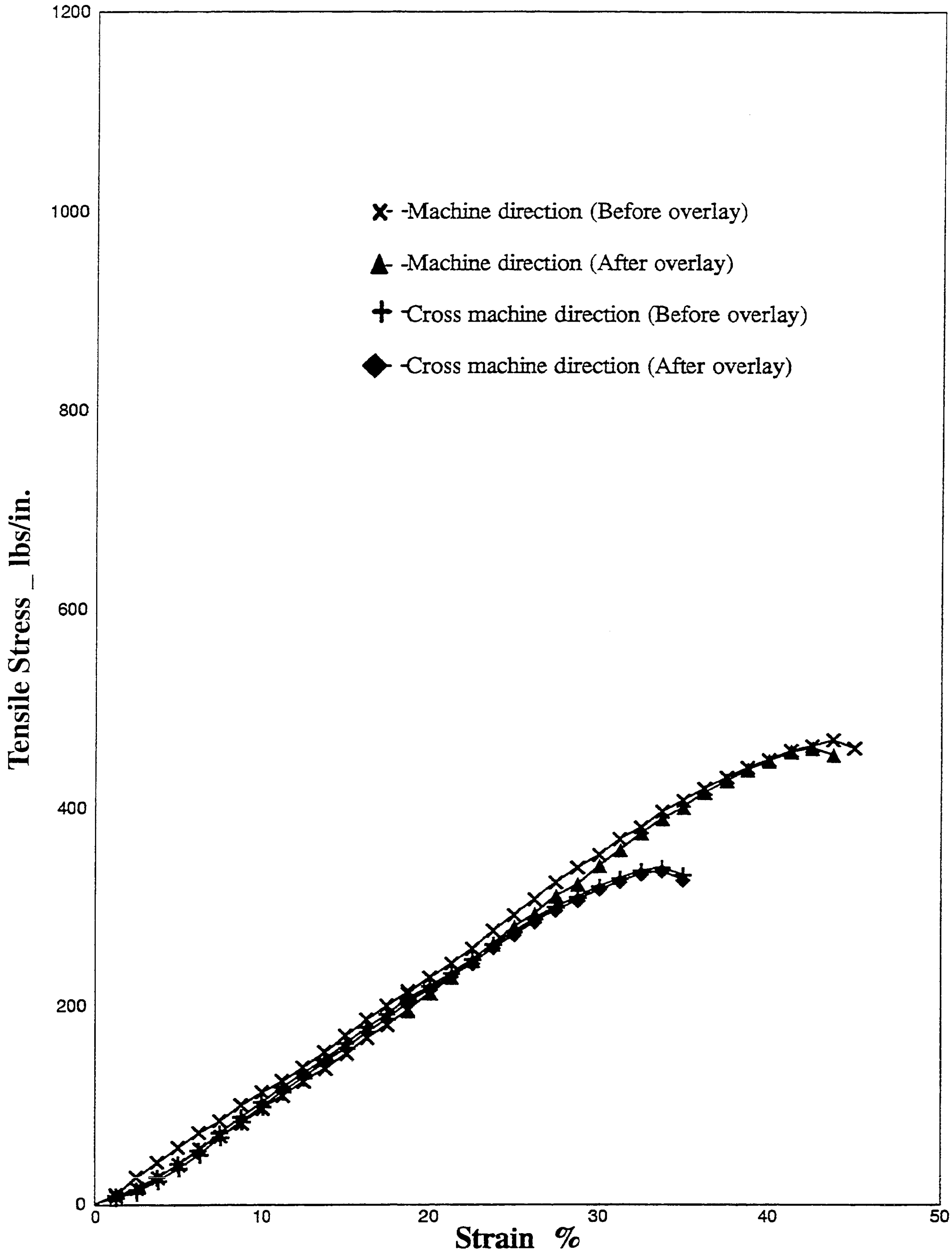

Figure 51: Non Woven Geotextile – GTF–125EX (EXXON)

Table 11: Modulus Values for Various Geotextiles

S/No	Geotextile Type	Direction of Test		Modulus @ 5 % Strain (M_5)			Modulus @ 10 % Strain (M_{10})			Modulus/0– at Failure (M_f)		
				Applied Stress (f) (lbs/in.)	Strain (e) (in./in.)	Modulus @ 5 % Strain $=M_5=f/e$ (lbs/in.)	Applied Stress (f) (lbs/in.)	Strain (e) (in./in.)	Modulus @ 10 % Strain $=M_{10}=f/e$ (lbs/in.)	Ultimate Tensile Stress (f) (lbs/in.)	Strain at Failure (e) (in./in.)	Modulus at Failure $=M_f=f/e$ (lbs/in.)
A	TT 200/50	Mach	A	268	0.05	5360	623	0.1	6230	1165	0.175	6657
	Woven Polye–		B	195	0.05	3900	378	0.1	3780	1089	0.2125	5124
	ster Fabric	Cross	A	140	0.05	2800	356	0.1	3560	448	0.125	3584
	(Bidim Rock)		B	108	0.05	2160	230	0.1	2300	471	0.1625	2898
B	200/100	Mach	A	248	0.05	4960	616	0.1	6160	930	0.1625	5723
	Woven Polye–		B	192	0.05	3840	423	0.1	4230	869	0.1875	4634
	ster Geotextile	Cross	A	53	0.05	1060	124	0.1	1240	557	0.2625	2122
	(Huesker)		B	47	0.05	940	117	0.1	1170	570	0.275	2073
C	GTF–1000T	Mach	A	155	0.05	3100	363	0.1	3630	922	0.2	4610
	(EXXON)		B	110	0.05	2200	240	0.1	2400	860	0.2375	3621
	(Woven)	Cross	A	187	0.05	3740	343	0.1	3430	771	0.1875	4112
			B	128	0.05	2560	230	0.1	2300	758	0.225	3369
D	GTF–1500T	Mach	A	182	0.05	3640	603	0.1	6030	1304	0.2	6520
	(EXXON)		B	110	0.05	2200	327	0.1	3270	1270	0.2625	4838
	(Woven)	Cross	A	189	0.05	3780	460	0.1	4600	792	0.1625	4873
			B	135	0.05	2700	265	0.1	2650	785	0..2	3925
E	GTF–400E	Mach	A	75	0.05	1500	151	0.1	1510	278	0.1875	1482
	(EXXON)		B	57	0.05	1140	113	0.1	1130	190	0.175	1085
	(Woven)	Cross	A	50	0.05	1000	112	0.1	1120	189	0.175	1080
			B	66	0.05	1320	143	0.1	1430	264	0.1875	1408

Note:– A –Modulus values for geotextile before placing an AC overlay
B –Modulus values for geotextile after placing a 3 in. thick 300 F hot AC overlay

Table 11: Modulus Values for Various Geotextiles

S/No	Geotextile Type	Direction of Test	Modulus @ 5 % Strain (M_5): Applied Stress (f) (lbs/in.)	Strain (e) (in./in.)	Modulus @ 5 % Strain $=M_5=f/e$ (lbs/in.)	Modulus @ 10 % Strain (M_{10}): Applied Stress (f) (lbs/in.)	Strain (e) (in./in.)	Modulus @ 10 % Strain $=M_{10}=f/e$ (lbs/in.)	Modulus at Failure (M_f): Ultimate Tensile Stress (f) (lbs/in.)	Strain at Failure (e) (in./in.)	Modulus at Failure $=M_f=f/e$ (lbs/in.)
F	GTF–200S	Mach A	51	0.05	1020	111	0.1	1110	194	0.2125	913
	(EXXON)	B	59	0.05	1180	115	0.1	1150	173	0.175	989
	(Woven)	Cross A	31	0.05	620	70	0.1	700	142	0.2625	541
		B	26	0.05	520	62	0.1	620	129	0.225	573
G	Robusta	Mach A	152	0.05	3040	444	0.1	4440	642	0.15	4280
	(Woven)	B	113	0.05	2260	344	0.1	3440	530	0.15	3533
		Cross A	107	0.05	2140	261	0.1	2610	312	0.125	2496
		B	98	0.05	1960	247	0.1	2470	298	0.125	2384
H	Nicolon	Mach A	36	0.05	720	70	0.1	700	228	0.275	829
	(Woven)	B	28	0.05	560	61	0.1	610	211	0.275	767
		Cross A	49	0.05	980	102	0.1	1020	139	0.15	926
		B	40	0.05	800	85	0.1	850	117	0.15	780
I	AMMOCO	Mach A	20	0.05	400	45	0.1	450	387	0.5375	720
	4545	B	18	0.05	360	40	0.1	400	385	0.5375	716
	(Non Woven)	Cross A	24	0.05	480	70	0.1	700	576	0.5375	1071
		B	22	0.05	440	61	0.1	610	567	0.5375	1054
J	GTF–125EX	Mach A	57	0.05	1140	113	0.1	1130	470	0.4375	1074
	(EXXON)	B	41	0.05	820	98	0.1	980	462	0.4225	1093
	(Non Woven)	Cross A	40	0.05	800	103	0.1	1030	341	0.3375	1010
		B	37	0.05	740	100	0.1	1000	338	0.3375	1001

Note:– A –Modulus values for geotextile before placing an AC overlay
B –Modulus values for geotextile after placing a 3 in. thick 300 F hot AC overlay

Table 12: Engineering Properties of Geotextiles

S/No	Geotextile Type	Weight oz/sq yd	Thickness (Mils)	Direction of Test	Shrinkage Due to Simulated 3 in. thick & 300 F hot AC overlay (%)	Moduli: Modulus @ 5 % Strain (M_5) (lbs/in.)	Moduli: Modulus @ 10 % Strain (M_{10}) (lbs/in.)	Moduli: Modulus at Failure: Modulus (M_f) (lbs/in.)	Moduli: Modulus at Failure: Strain at Failure (%)	Ultimate Tensile Strength: Tensile Strength (lbs/in.)	Ultimate Tensile Strength: Strain at Failure (%)
A	TT 200/50	16.5	51	Mach A	1.5	5360	6230	6657	17.5	1165	17.5
	Woven Polye–			B		3900	3780	5124	21.25	1089	21.25
	ster Fabric			Cross A	2.25	2800	3560	3584	12.5	448	12.5
	(Bidim Rock)			B		2160	2300	2898	16.25	471	16.25
B	200/100	15.5	28	Mach A	3	4960	6160	5723	16.25	930	16.25
	Woven Polye–			B		3840	4230	4634	18.75	869	18.75
	ster Geotextile			Cross A	1.5	1060	1240	2122	26.25	557	26.25
	(Huesker)			B		940	1170	2073	27.5	570	27.5
C	GTF–1000T	17.5	30	Mach A	3	3100	3630	4610	20	922	20
	(EXXON)			B		2200	2400	3621	23.75	860	23.75
				Cross A	2.25	3740	3430	4112	18.75	771	18.75
				B		2560	2300	3369	22.5	758	22.5
D	GTF–1500T	22.5	40	Mach A	3	3640	6030	6520	20	1304	20
	(EXXON)			B		2200	3270	4838	26.25	1270	26.25
	(Woven)			Cross A	3	3780	4600	4873	16.25	792	16.25
				B		2700	2650	3925	20	785	20
E	GTF–400E	6	28	Mach A	3	1500	1510	1482	18.75	278	18.75
	(EXXON)			B		1140	1130	1085	17.5	190	17.5
	(Woven)			Cross A	2.75	1000	1120	1080	17.5	189	17.5
				B		1320	1430	1408	18.75	264	18.75

Note:– A – Values for geotextile before placing an AC overlay
B – Values for geotextile after placing a 3 in. thick & 300 F hot AC overlay

Table 12: Engineering Properties of Geotextiles

S/No	Geotextile Type	Engineering Properties of Geotextile									
		Weight	Thick-ness	Dire-ction of Test	Shrinkage Due to Simulated 3 in. thick & 300 F hot AC overlay	Moduli				Ultimate Tensile Strength	
						Modulus @ 5 % Strain	Modulus @ 10 % Strain	Modulus at Failure			
		oz/sq yd	(Mils)		(%)	(M_5) (lbs/in.)	(M_{10}) (lbs/in.)	Modulus (M_f) (lbs/in.)	Strain at Failure (%)	Tensile Strength (lbs/in)	Strain at Failure (%)
F	GTF–200S	4.25	26	Mach A	2	1020	1110	913	21.25	194	21.25
	(EXXON)			B		1180	1150	989	17.5	173	17.5
	(Woven)			Cross A	3	620	700	541	26.25	142	26.25
				B		520	620	573	22.5	129	22.5
G	Robusta	12.5	40	Mach A	4.75	3040	4440	4280	15	642	15
	(Woven)			B		2260	3440	3535	15	530	15
				Cross A	4.75	2140	2610	2496	12.5	312	12.5
				B		1960	2470	2384	12.5	298	12.5
H	Nicolon	5.75	27	Mach A	3	720	700	829	27.5	228	27.5
	(Woven)			B		560	610	767	27.5	211	27.5
				Cross A	2.25	980	1020	926	15	139	15
				B		800	850	780	15	117	15
I	AMOCO	4.5	45	Mach A	.75	400	450	720	53.75	387	53.75
	4545			B		360	400	716	53.75	385	53.75
	(Non Woven)			Cross A	1.25	480	700	1071	53.75	576	53.75
				B		440	610	1054	53.75	567	53.75
J	GTF–125EX	4	40	Mach A	.5	1140	1130	1074	43.75	470	43.75
	(EXXON)			B		820	980	1093	42.25	462	42.25
	(Non Woven)			Cross A	.75	800	1030	1010	33.75	341	33.75
				B		740	1000	1001	33.75	338	33.75

Note:– A – Values for geotextile before placing an AC overlay
B – Values for geotextile after placing a 3 in. thick & 300 F hot AC overlay

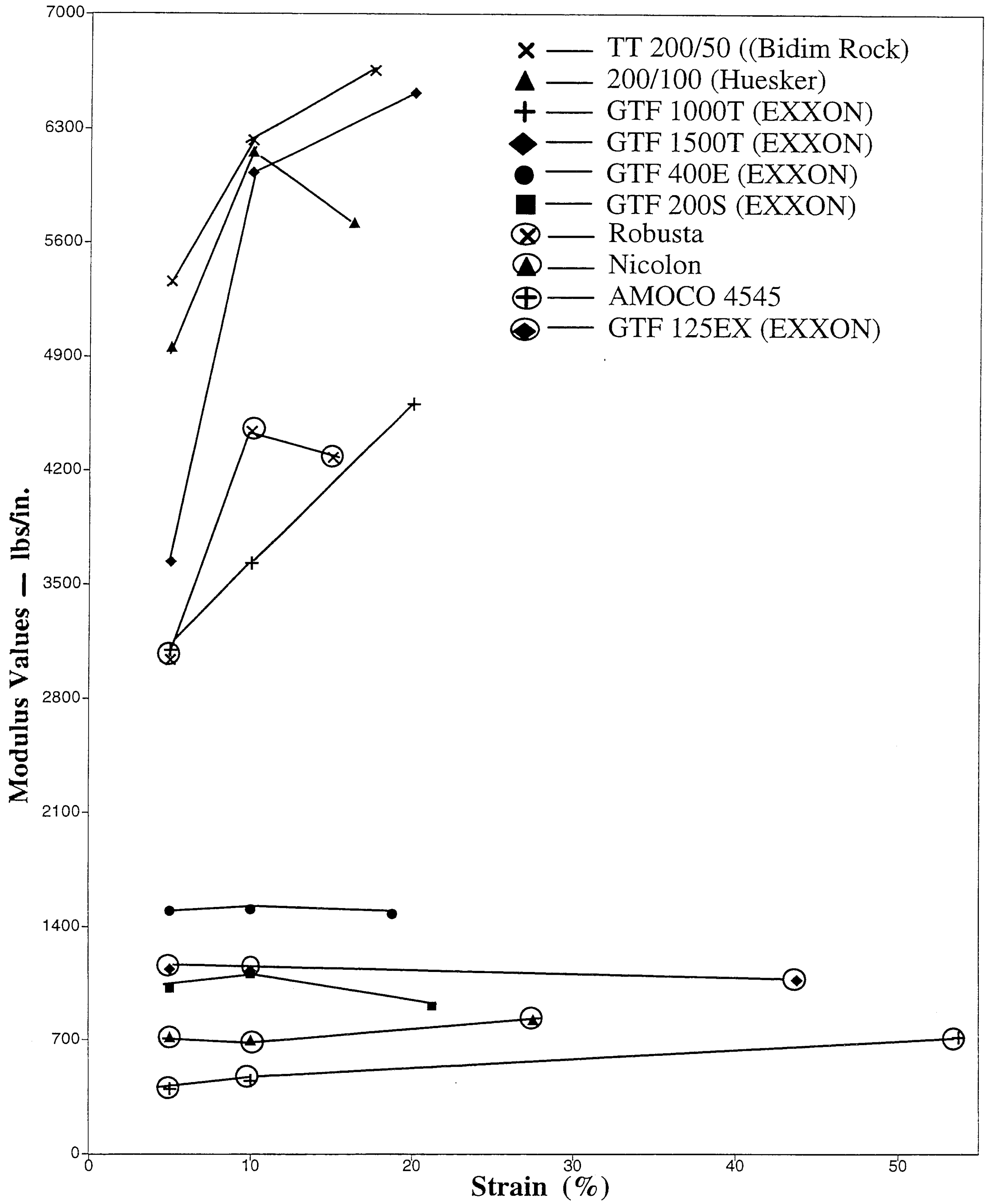

Figure 52: Comparison of Moduli at 5 %, 10 % and Failure Strain (Machine Direction Only)

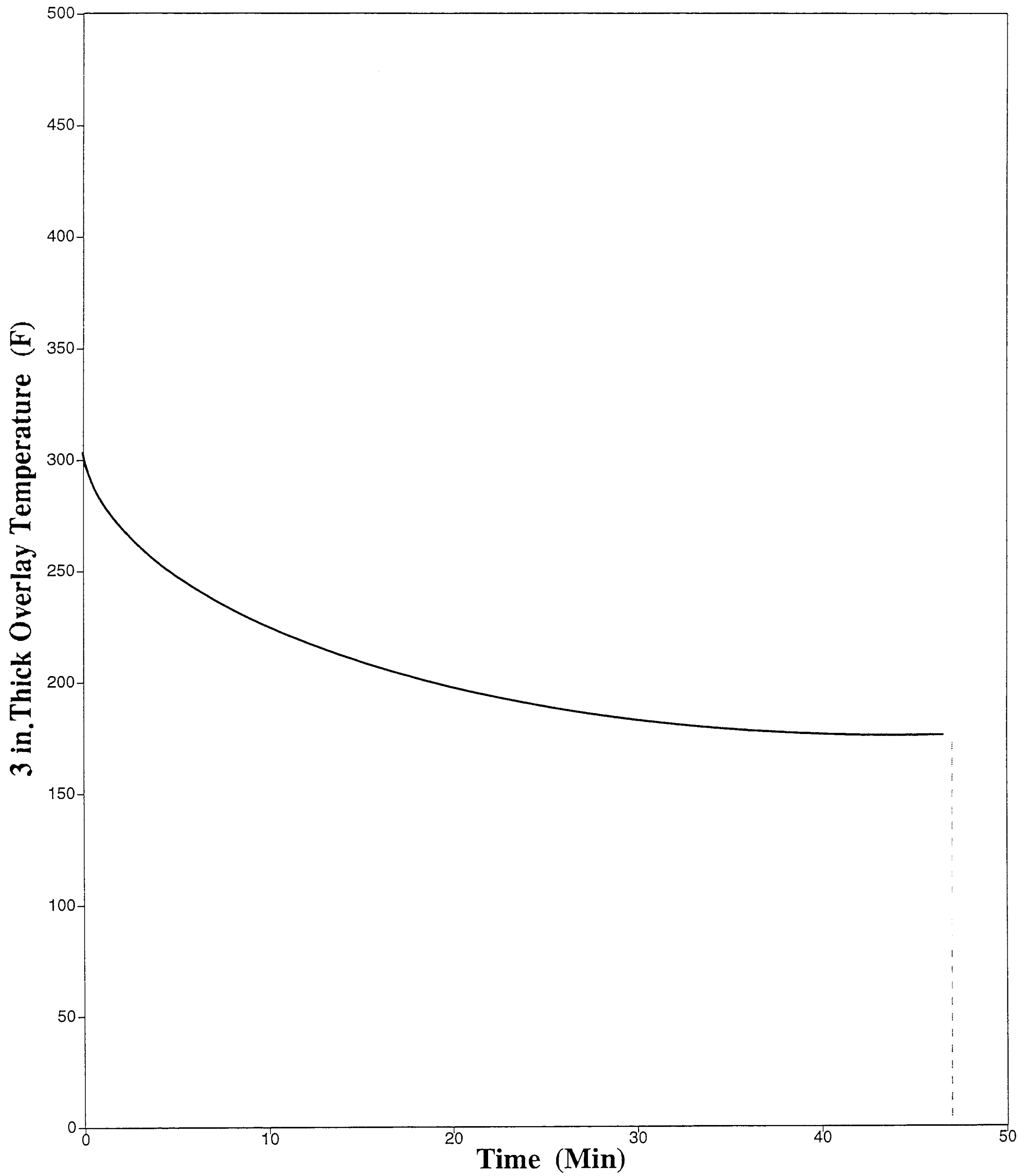

Figure 53: Heat Dissipation Curve for a Geotextile After Placing 3 in. Thick 300 F AC Overlay

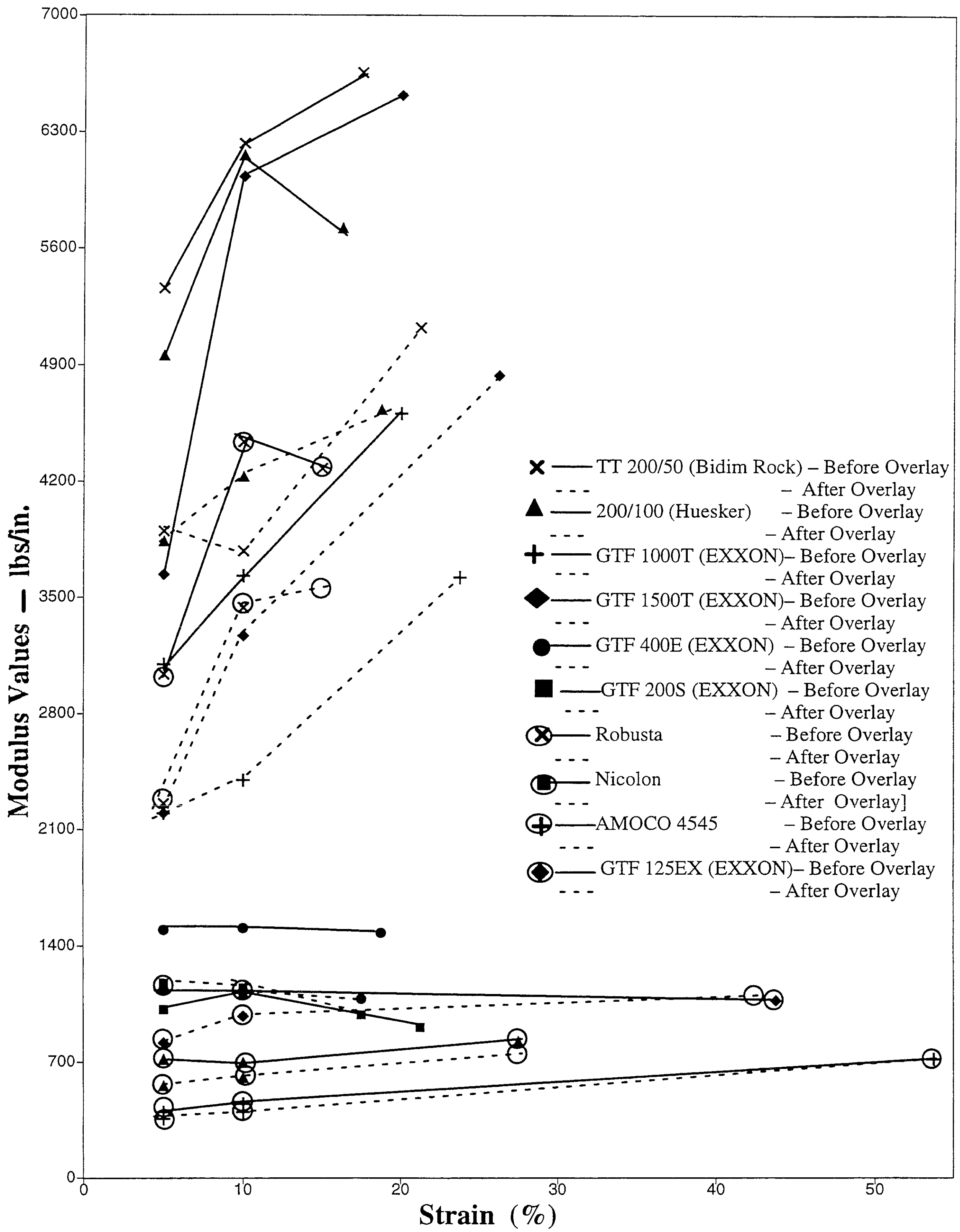

Figure 54: Comparison of Moduli for Different Geotextiles Before and After Placing an Overlay

6.3.2 Summary From Test Results

The following conclusions can be drawn from the geotextile testing program:

a) All the geotextiles exhibited different characteristics in machine and cross machine direction.

b) All geotextiles except AMOCO 4545 were stronger in the machine direction and weaker in cross machine direction.

c) For all geotextiles, the modulus at 10 % strain was higher than modulus at 5 % strain. Most of the geotextiles, except Huesker 200/100, Robusta and GTF 200S (EXXON) had modulus at failure higher than that at 10 % strain.

d) Influence of 3 in. thick AC overlay at initial temperature of 300 F on the geotextiles was simulated by placing the geotextile samples in an oven with the temperature gradient similar to that shown in Figure 53. Shrinkage in most of the geotextiles due to contact with hot AC varied from 1.5 % to 3 %. Maximum shrinkage took place in Robusta which was 4.75%.

e) Significant reduction in moduli of most of the geotextiles took place due to the AC temperatures. The reduction in moduli was more significant in woven geotextiles than in non woven geotextiles.

f) Bidim Rock TT 200/50 showed highest moduli and highest ultimate strength. It also displayed the lowest shrinkage and minimum reduction in moduli due to an AC overlay.

6.4 Preparation and Testing of Rubber Asphalt

6.4.1 Preparation of Rubber Asphalt

Three samples of rubber asphalt were prepared using asphalt cements AC–5, AC–10, and AC–20. Each sample was prepared by blending crumb rubber (25 % by weight) with an appropriate type of asphalt cement (75 % by weight) in a container and heating at a temperature of 400 F for 20 min. The mixture was then cooled to a temperature of 300 F and used to fabricate the test specimens. The properties of the three asphalt cements utilized in this testing program are shown in Table 13. Vulcanized rubber in crumb form was used in the rubber asphalt mix. The specific gravity of the rubber in crumb form was measured as 0.408.

Table 13: Asphalt Cement Test Results

S/No	Properties of Asphalt	Asphalt Type		
		AC–5	AC–10	AC–20
1	Viscosity @ 140 F (Poise)	700	1378	2437
2	Viscosity @ 275 F (c St)	239	326	440
3	Penetration @ 39.2 F (dmm)	41	32	17
4	Penetration @ 77 F (dmm)	119	96	60
5	R & B Softening point (F)	43	47	51
6	Specific Gravity @ 60 F	1.0226	1.0219	1.0293

6.4.2 Specimen Fabrication and Test Description

Testing procedures were developed to study the behavior of rubber asphalt when exposed to different field conditions. The effects of temperatures and rates of loading on the shear strength and stiffness of a 3/8 in. thick rubber asphalt interlayer were studied. In order to study the properties of the rubber asphalt layer shear properties PCC blocks were formed. Two in. by 2 in. by 1 in. concrete blocks, Figure 55 a, were prepared and cured for 28 days. A 3/8 in. thick spacer was placed between the 2 in. by 2 in. faces of the concrete blocks and they were firmly clamped together as arrangement shown in Figure 55b. The spacer was then removed and the 2 in. by 2 in. by 1 in. space between the two concrete blocks was filled with rubber asphalt at 300 F. The rubber asphalt sandwiched between the two concrete blocks was allowed to cool and then the specimens were removed from the clamp, Figure 55c. Shear tests on the specimens were carried out with the apparatus shown in Figure 56. One of the concrete blocks (bottom one) was clamped as shown and a horizontal force was applied on the side of the upper block so that a shear force was created in the rubber asphalt interlayer. No load normal to the shear plane was applied. A plot of head movement versus load was determined for each specimen using a load cell and an X–Y plotter. The shear tests were performed at temperatures 0 F, 20 F, 40 F, 60 F, 80 F and 100 F. The specimens were conditioned at the desired test temperature in an environmental chamber for four hours prior to the testing. At each temperature the specimens were sheared using six different loading rates of 0.05 in./min, 0.2 in./min, 0.5 in./min, 1 in./min, 2 in./min, and 3 in./min. The recorded shear load was divided by the interlayer cross sectional area, 4 in. sq, to obtain the shear strength in psi.

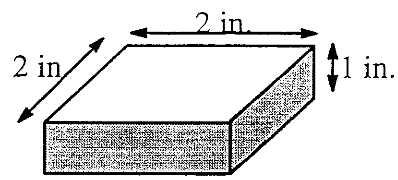

Figure 55 a: Concrete Block

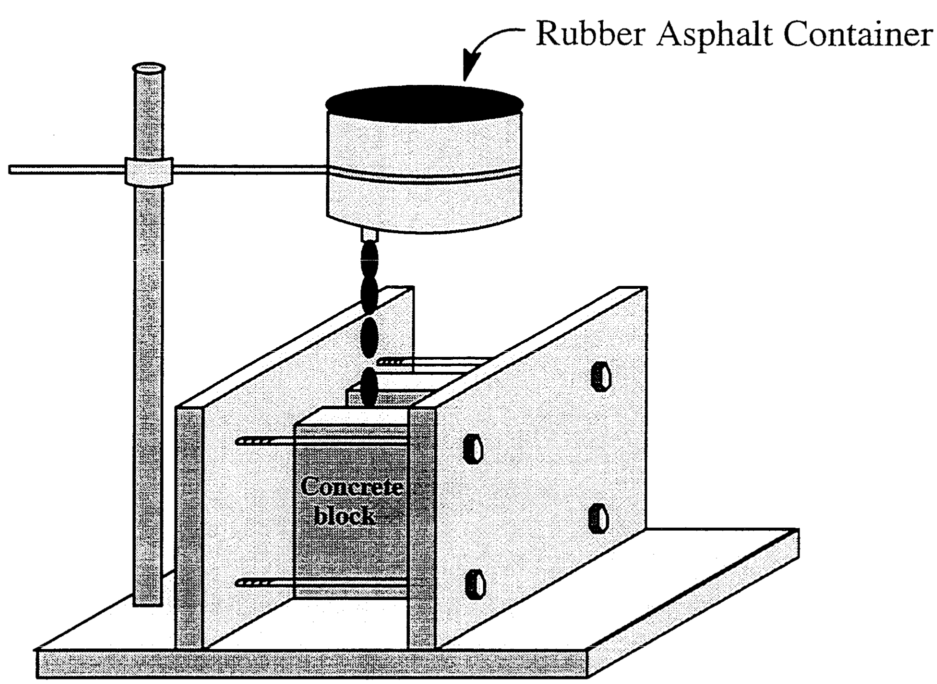

Figure 55 b: Arrangement to Tightly Grip the Two Concrete Blocks and Pour 3/8 in. Thick Rubber Asphalt Interlayer

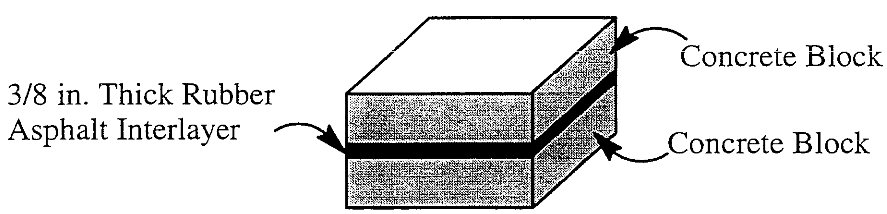

Figure 55 c: Test Specimen

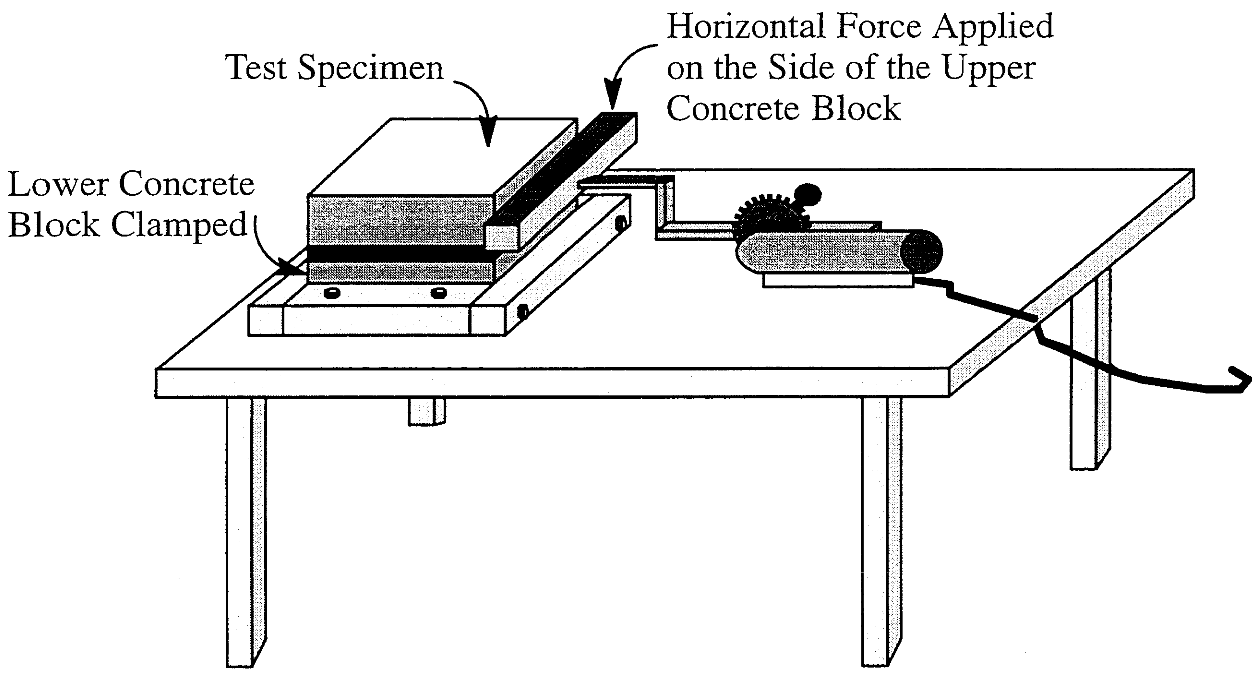

Figure 56: Shear Testing Device

6.4.3 Test Results

The shear strength vs shear displacement of various rubber asphalts at different temperatures and rates of shear are shown in Appendix B as well as in Figures 57 through 74.

The stiffness of various rubber asphalts at different temperatures and rates of shear at 0.05 in. shear displacement are shown in Table 14.

The effect of temperature on stiffness of various rubber asphalts at different deformation rates are shown in Figures 75 through 77.

The effect of rate of deformation on stiffness of various rubber asphalts at different temperatures are shown in Figures 78 through 80.

From the test results the following rubber asphalt properties were observed:

a) Rubber asphalt with AC–20 exhibited the highest shear strength/stiffness. The mix with AC–5 showed the lowest shear strength/stiffness.

b) Shear strength/stiffness decreased with increase in temperature.

c) Shear strength/stiffness increased with increase in rate of deformation.

d) All three rubber asphalts showed lower shear strength/stiffness in the range of 60 F to 100 F. The rate of increase in stiffness was, however, much higher below 60 F at temperatures of 40 F, 20 F and 0 F.

e) At temperatures of 60 F and above the stress strain diagram was non linear and the rubber asphalt behaved like a viscoelastic material.

f) At low shear rate (0.05 in./min) and at low temperatures (40 F, 20 F and 0 F) the stress strain diagram was non linear. As the shear rate increased, the stress displacement diagram became closer to linear and the behavior of rubber asphalt gradually became more elastic.

g) At low shear displacement (less than 0.05 in) the stress displacement diagram was fairly linear in all the cases.

h) At low temperatures (below 40 F) and high rates of deformation (more than 2 in./min), the material became brittle and failed between 0.04 to 0.06 in. displacement.

i) Significant increase in stiffness was noticed between 0.05 in./min to 0.5in./min shear rate. Above 0.5 in./min shear rate, the increase in stiffness was generally less.

j) In this study the thickness of the rubber asphalt interlayer was kept constant (3/8 in.). The effect of rubber asphalt thickness on stiffness was not evaluated.

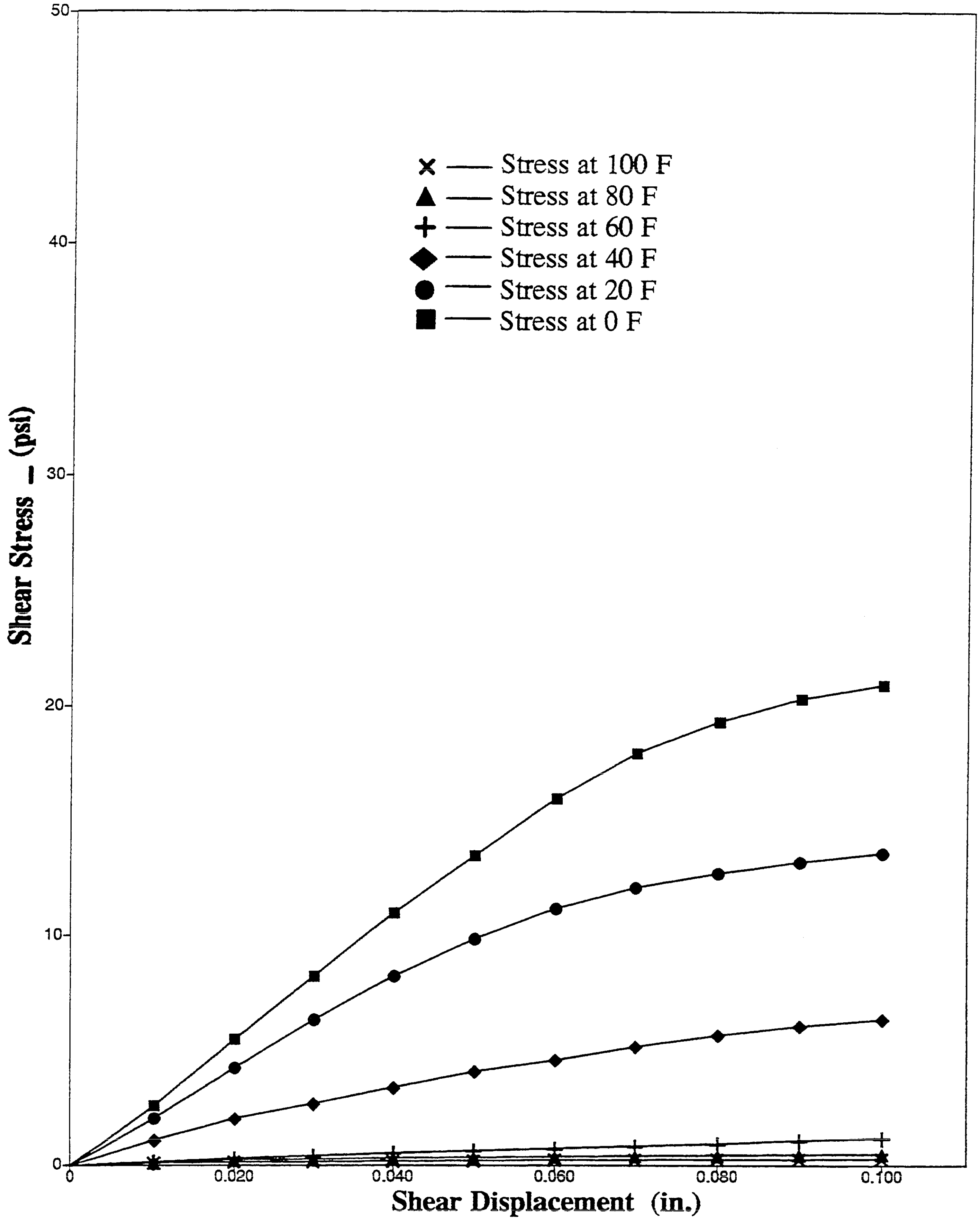

Figure 57: Shear Stress vs Displacement For Rubber Asphalt With 25 % Crumb Rubber & 75 % AC–5 @ Shear Rate of 0.05 in./min

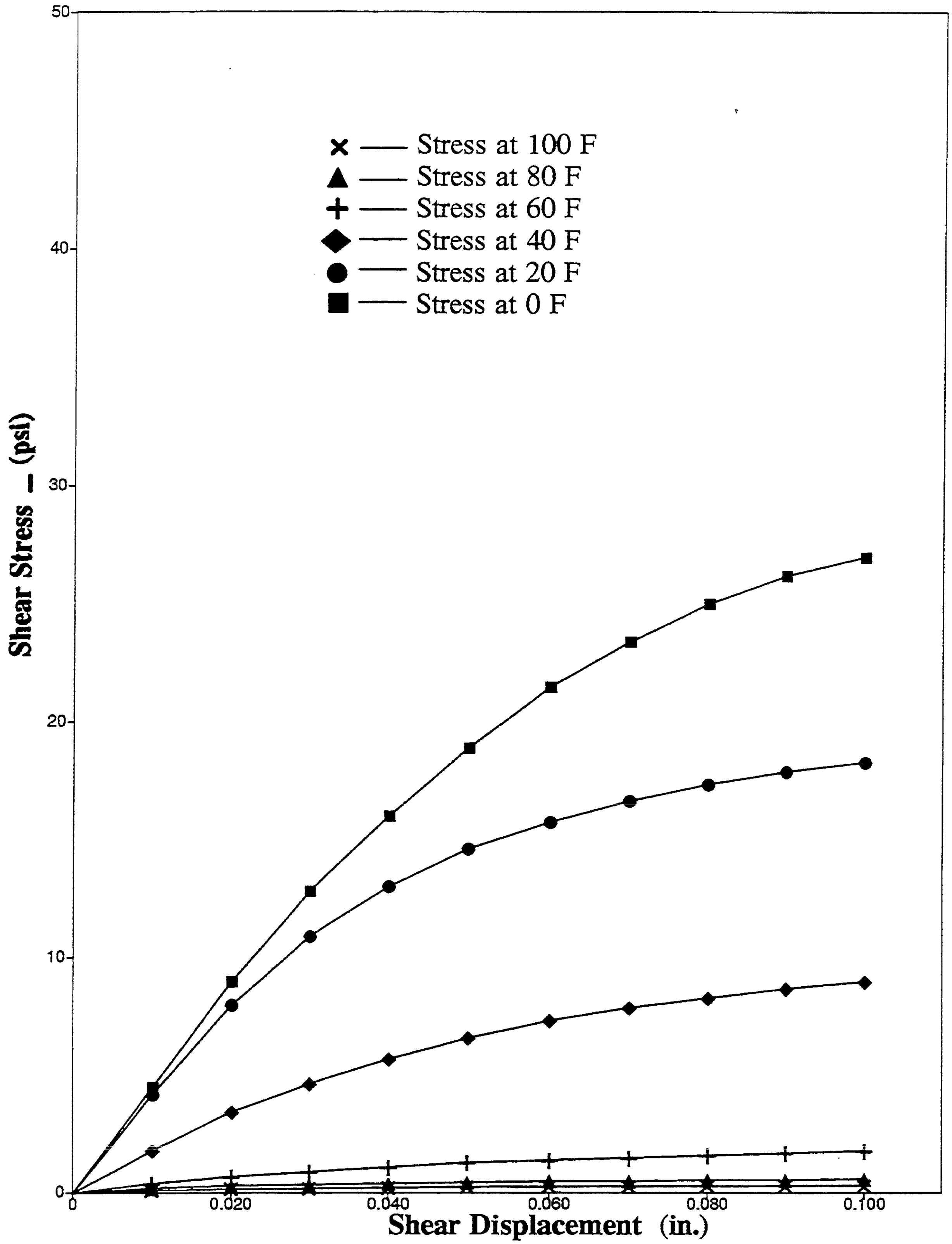

Figure 58: Shear Stress vs Displacement For Rubber Asphalt With 25 % Crumb Rubber & 75 % AC–10 @ Shear Rate of 0.05 in./min

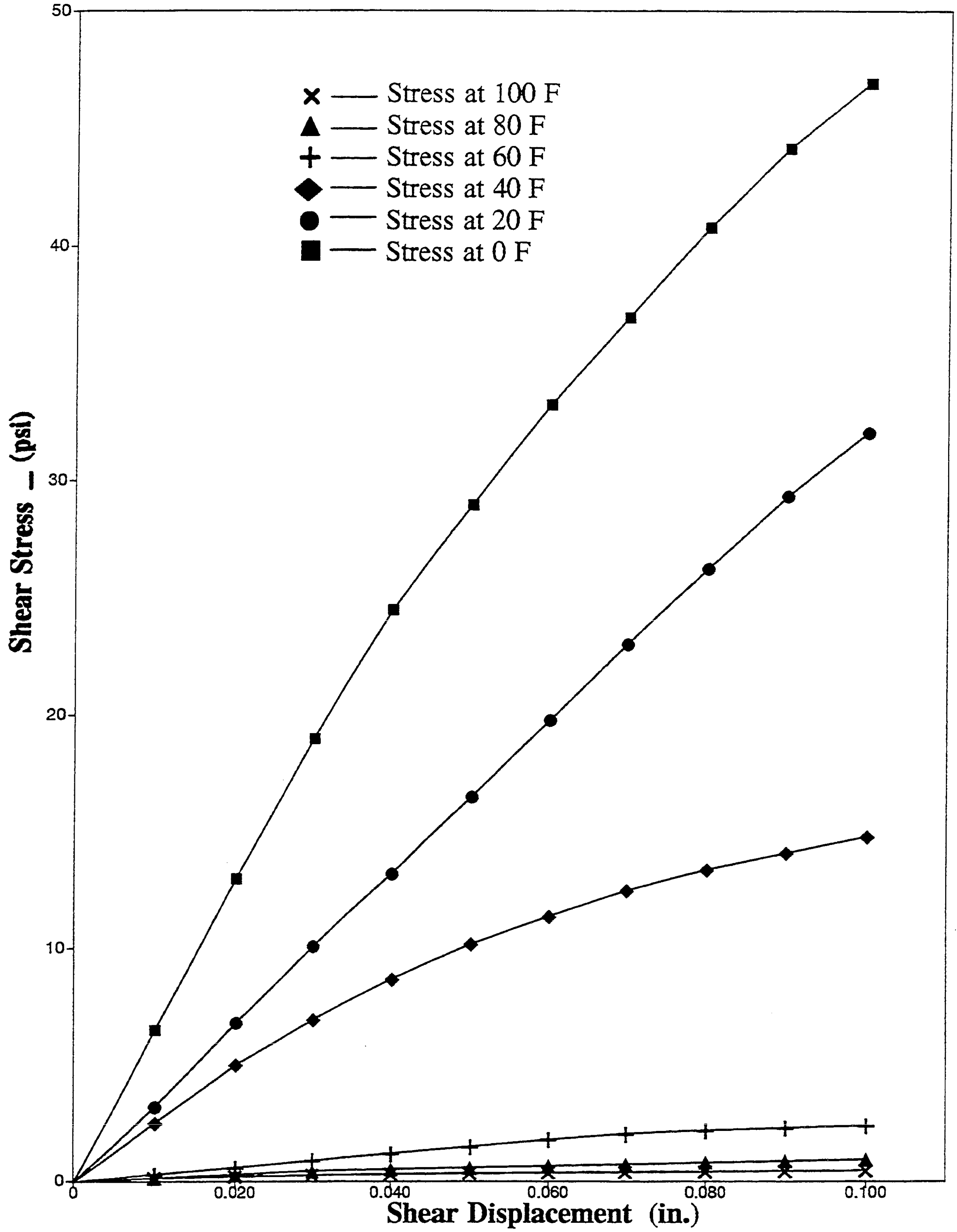

Figure 59: Shear Stress vs Displacement For Rubber Asphalt With 25 % Crumb Rubber & 75 % AC–20 @ Shear Rate of 0.05 in./min

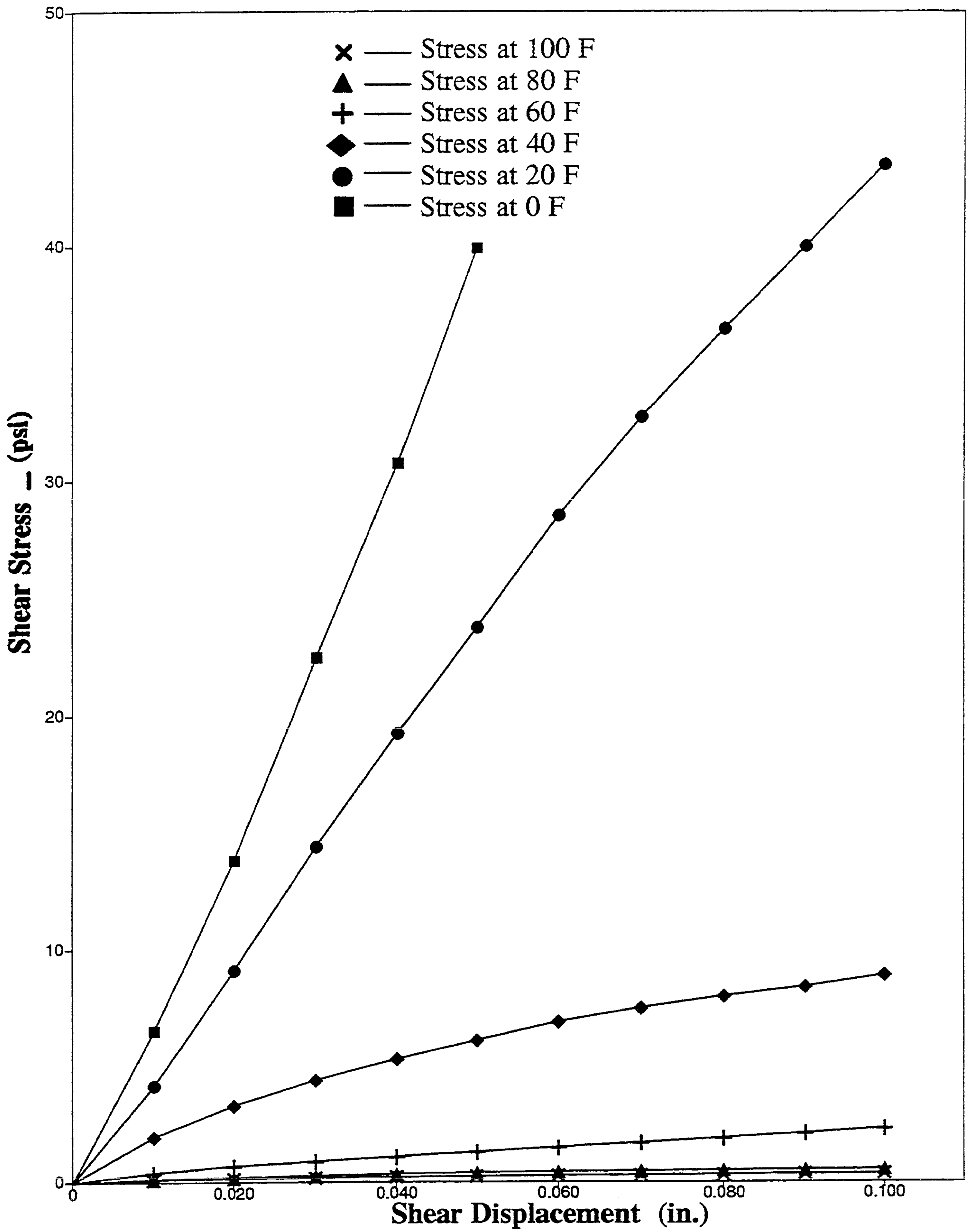

Figure 60: Shear Stress vs Displacement For Rubber Asphalt With 25 % Crumb Rubber & 75 % AC–5 @ Shear Rate of 0.2 in./min

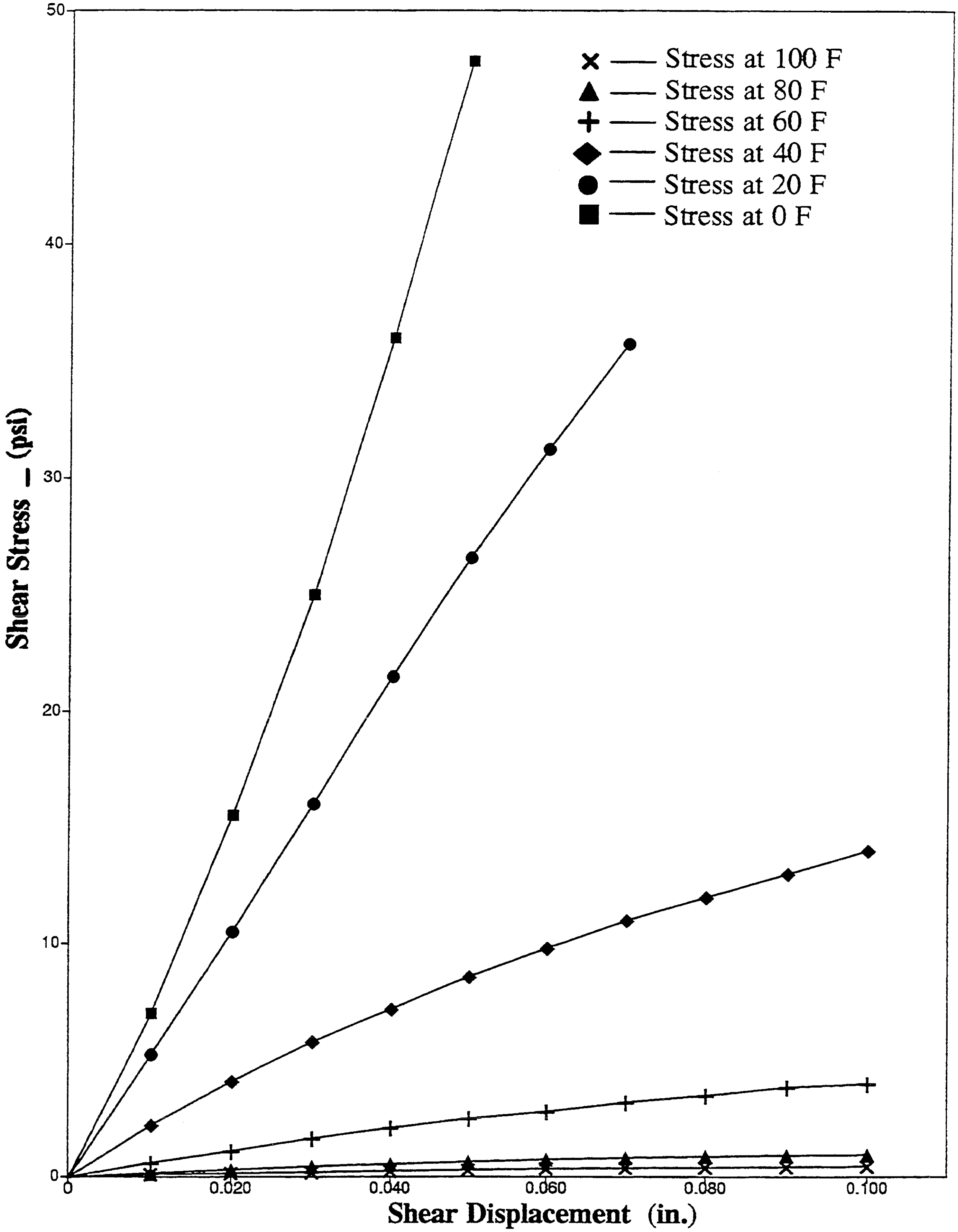

Figure 61: Shear Stress vs Displacement For Rubber Asphalt With 25 % Crumb Rubber & 75 % AC-10 @ Shear Rate of 0.2 in./min

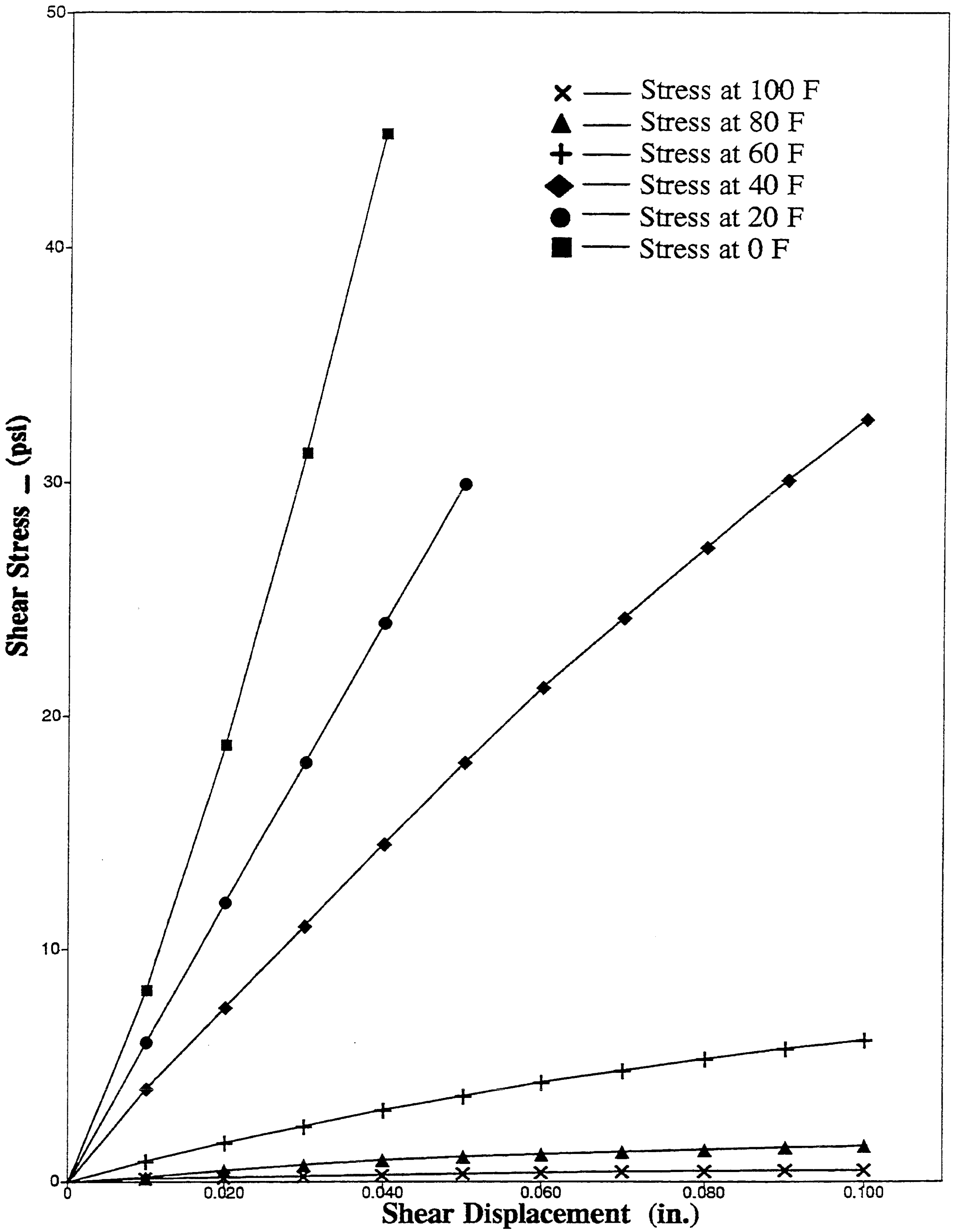

Figure 62: Shear Stress vs Displacement For Rubber Asphalt With 25 % Crumb Rubber & 75 % AC–20 @ Shear Rate of 0.2 in./min

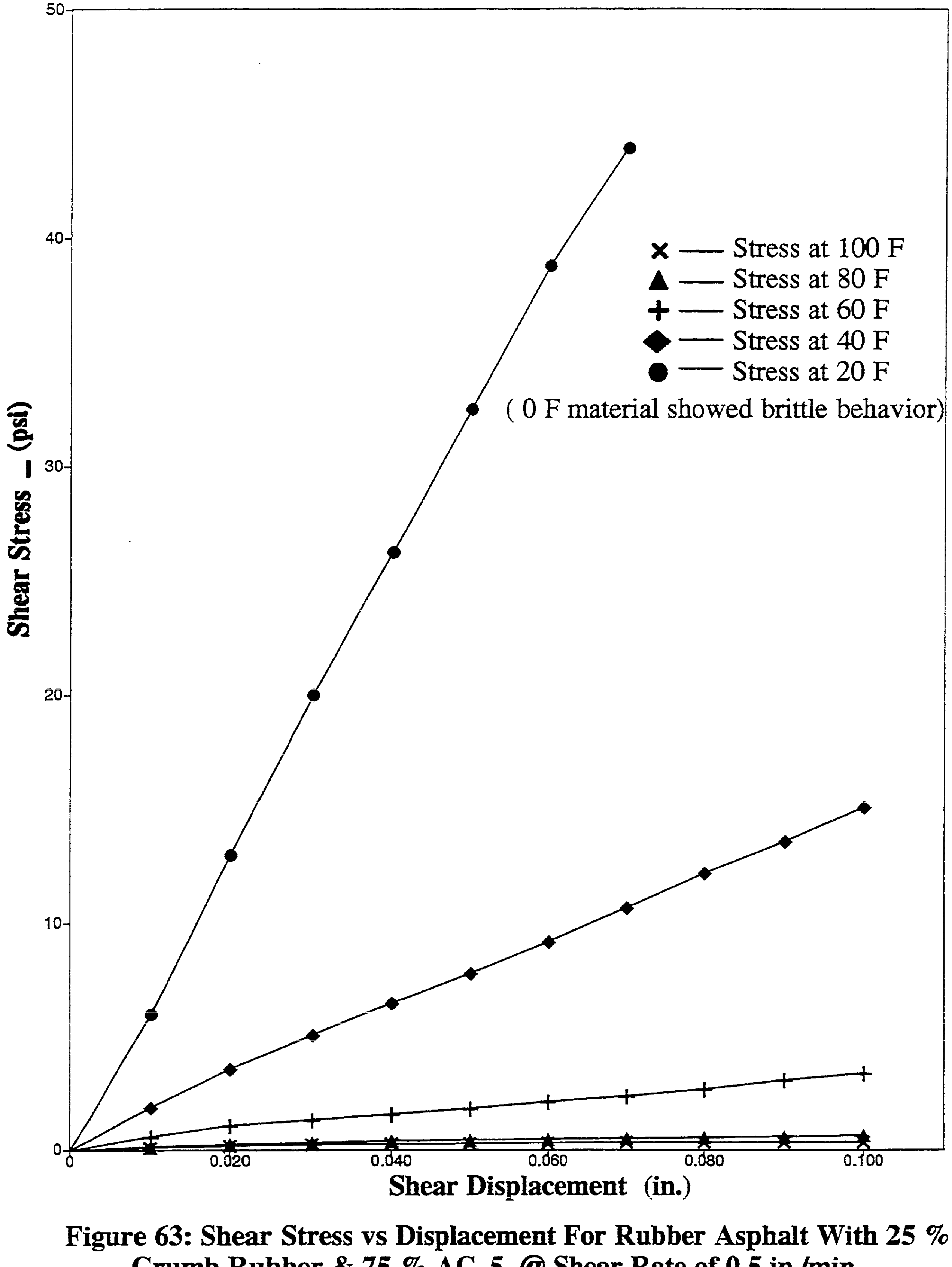

Figure 63: Shear Stress vs Displacement For Rubber Asphalt With 25 % Crumb Rubber & 75 % AC–5 @ Shear Rate of 0.5 in./min

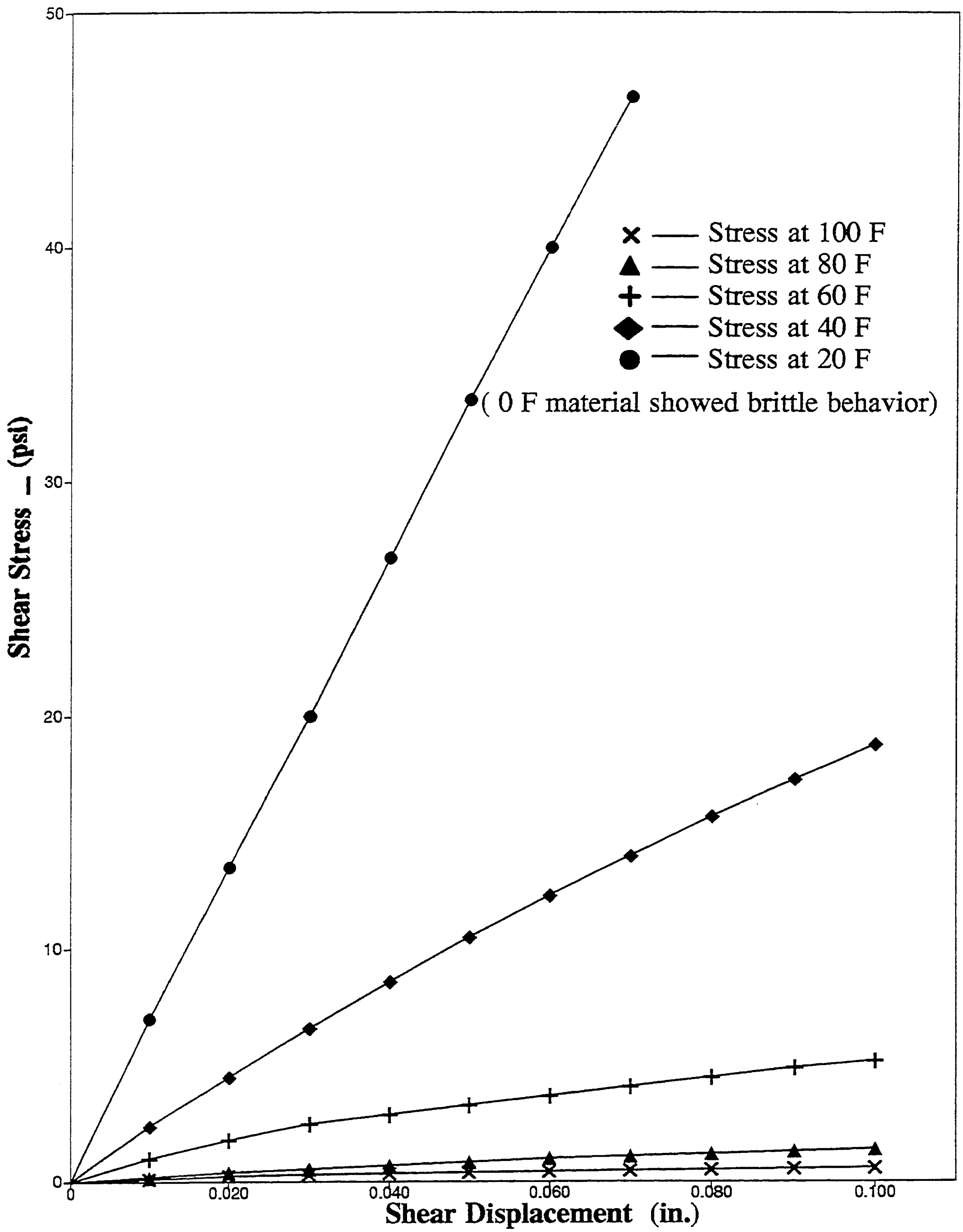

Figure 64: Shear Stress vs Displacement For Rubber Asphalt With 25 % Crumb Rubber & 75 % AC–10 @ Shear Rate of 0.5 in./min

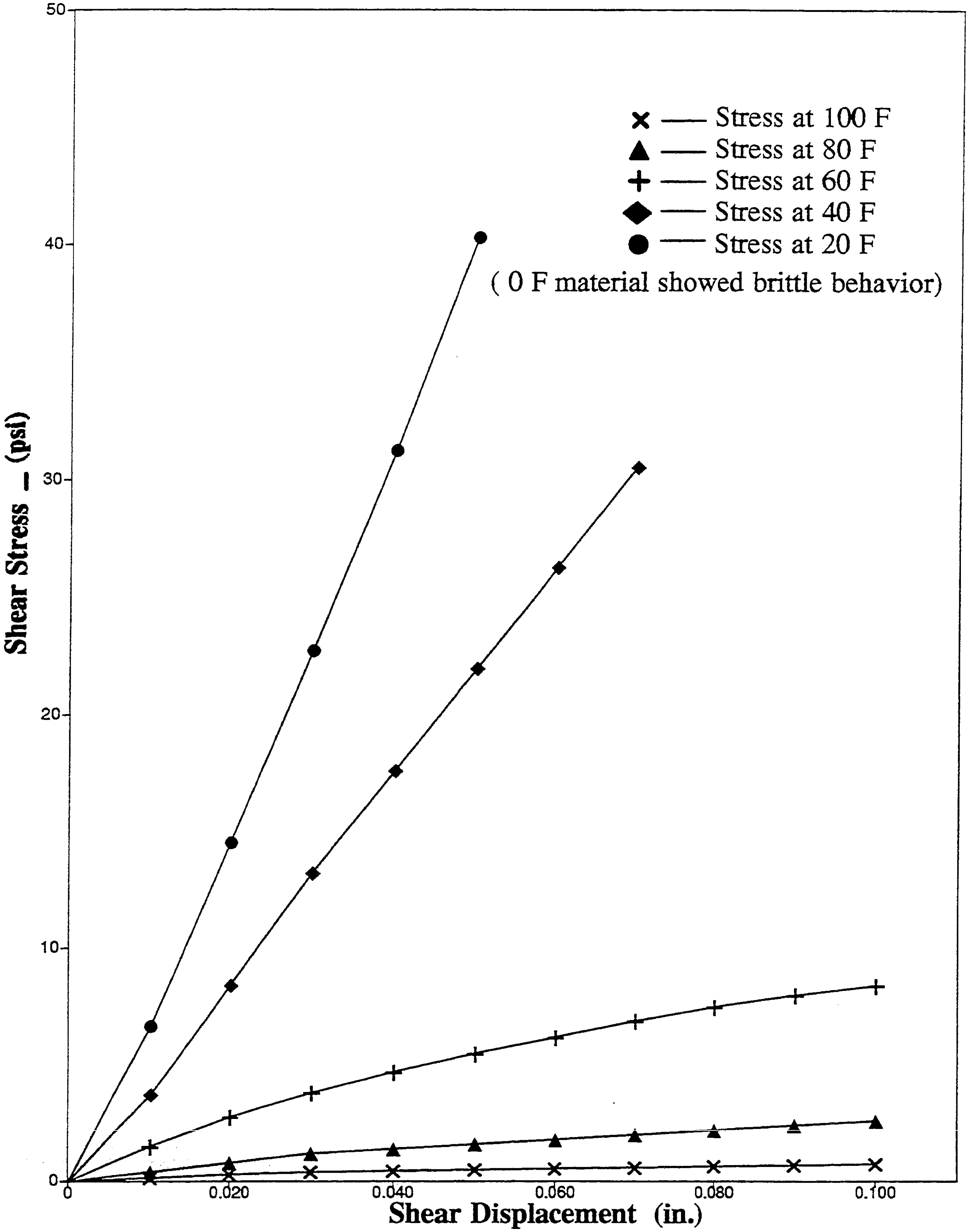

Figure 65: Shear Stress vs Displacement For Rubber Asphalt With 25 % Crumb Rubber & 75 % AC–20 @ Shear Rate of 0.5 in./min

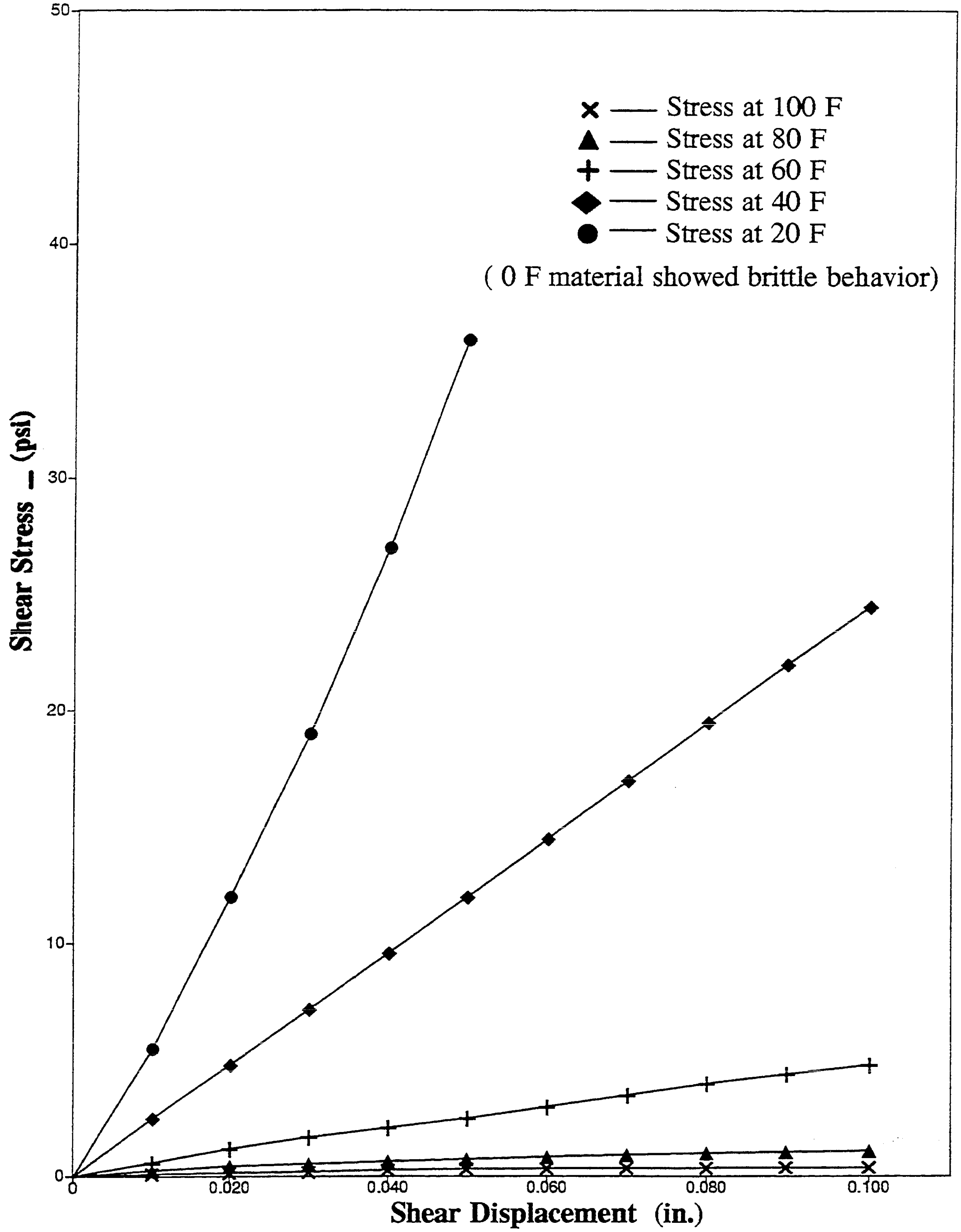

Figure 66: Shear Stress vs Displacement For Rubber Asphalt With 25 % Crumb Rubber & 75 % AC–5 @ Shear Rate of 1 in./min

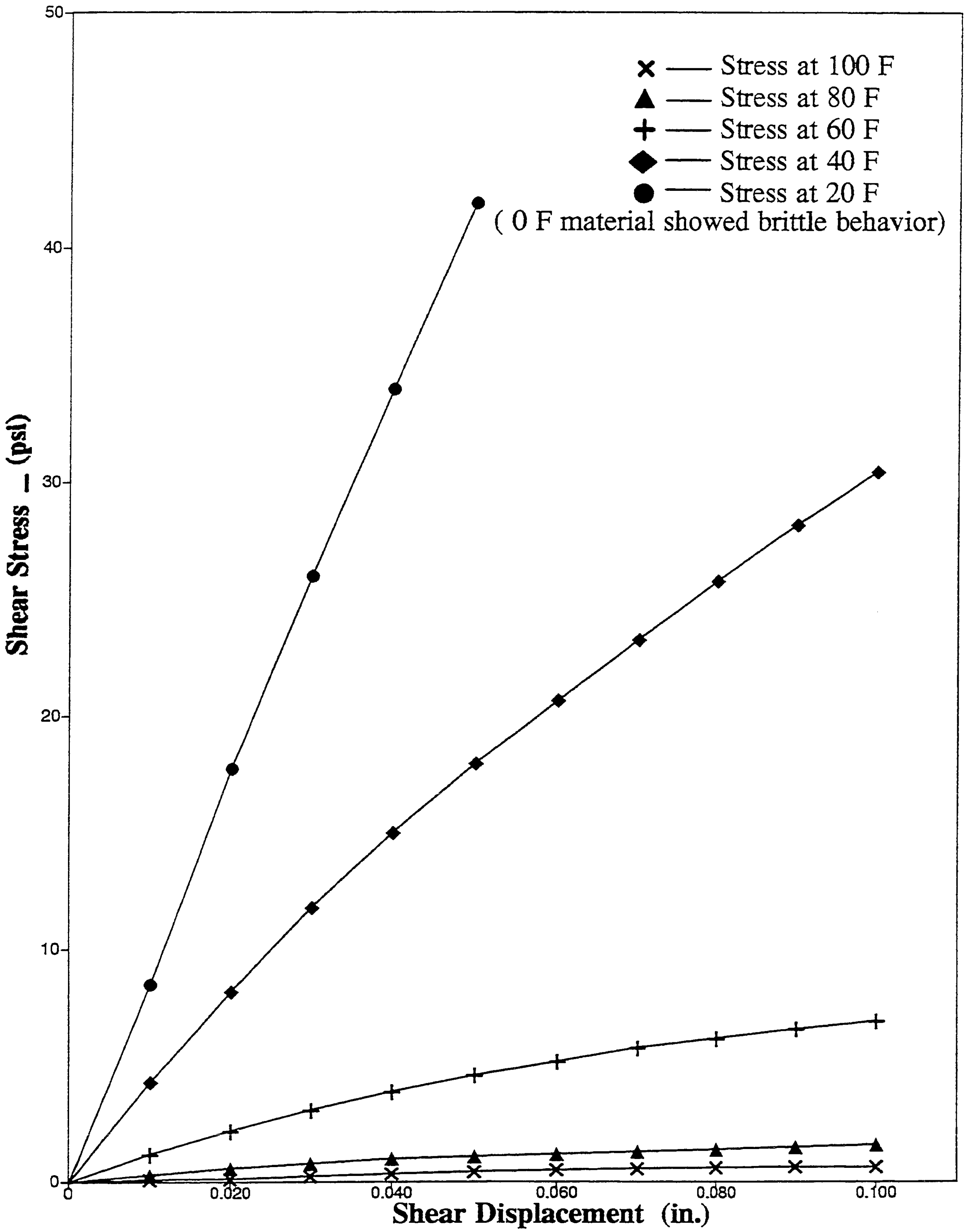

Figure 67: Shear Stress vs Displacement For Rubber Asphalt With 25 % Crumb Rubber & 75 % AC–10 @ Shear Rate of 1 in./min

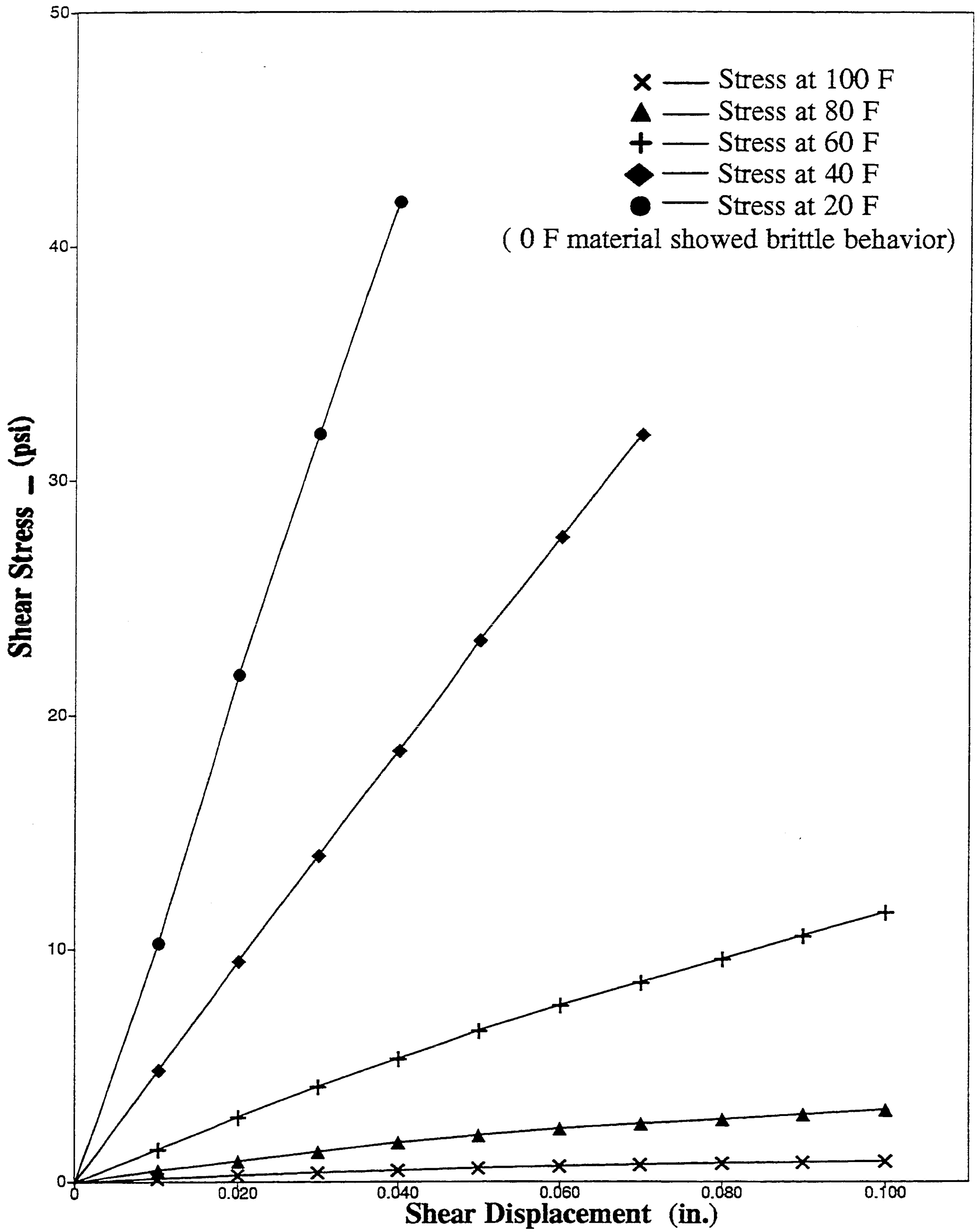

Figure 68: Shear Stress vs Displacement For Rubber Asphalt With 25 % Crumb Rubber & 75 % AC–20 @ Shear Rate of 1 in./min

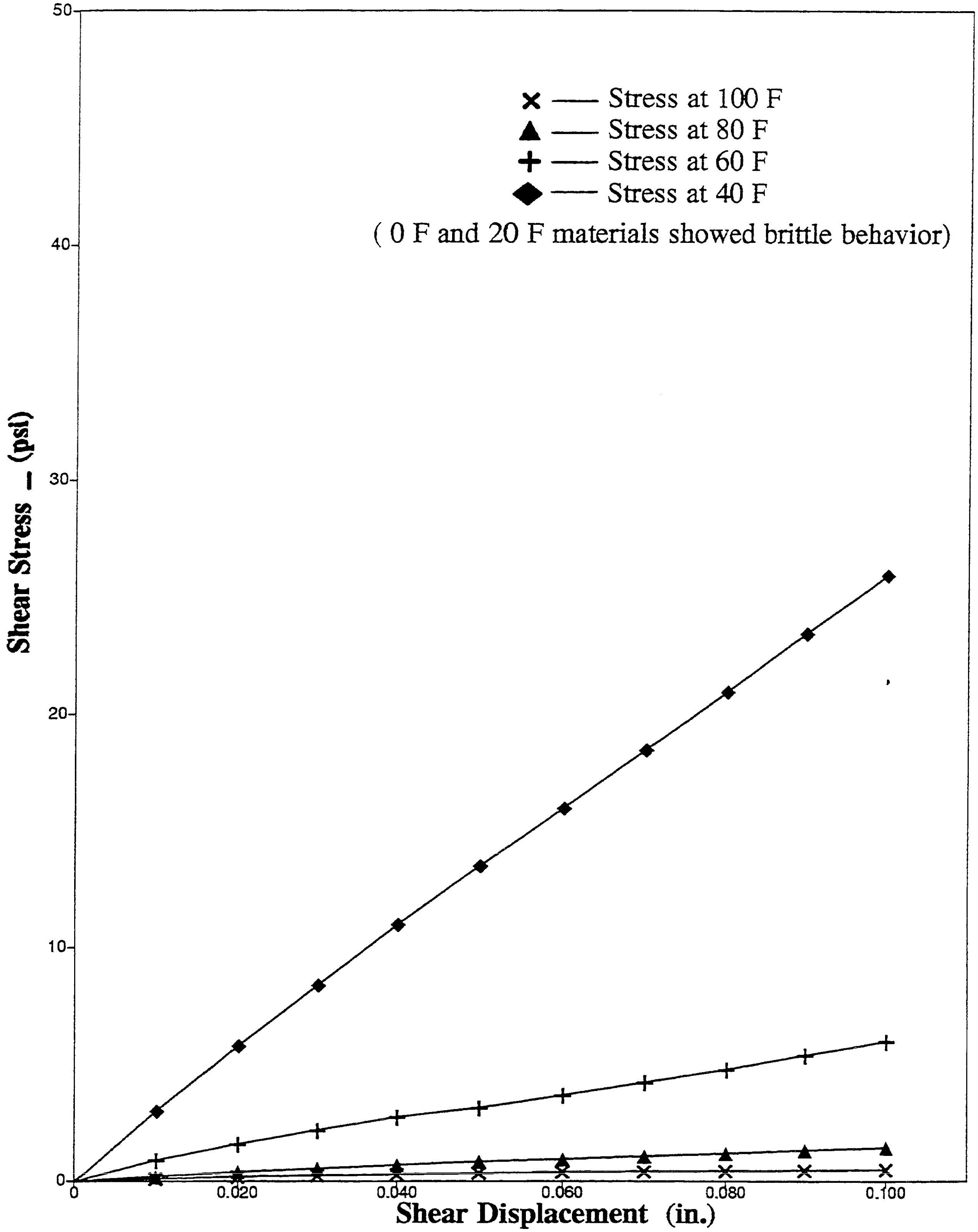

Figure 69: Shear Stress vs Displacement For Rubber Asphalt With 25 % Crumb Rubber & 75 % AC–5 @ Shear Rate of 2 in./min

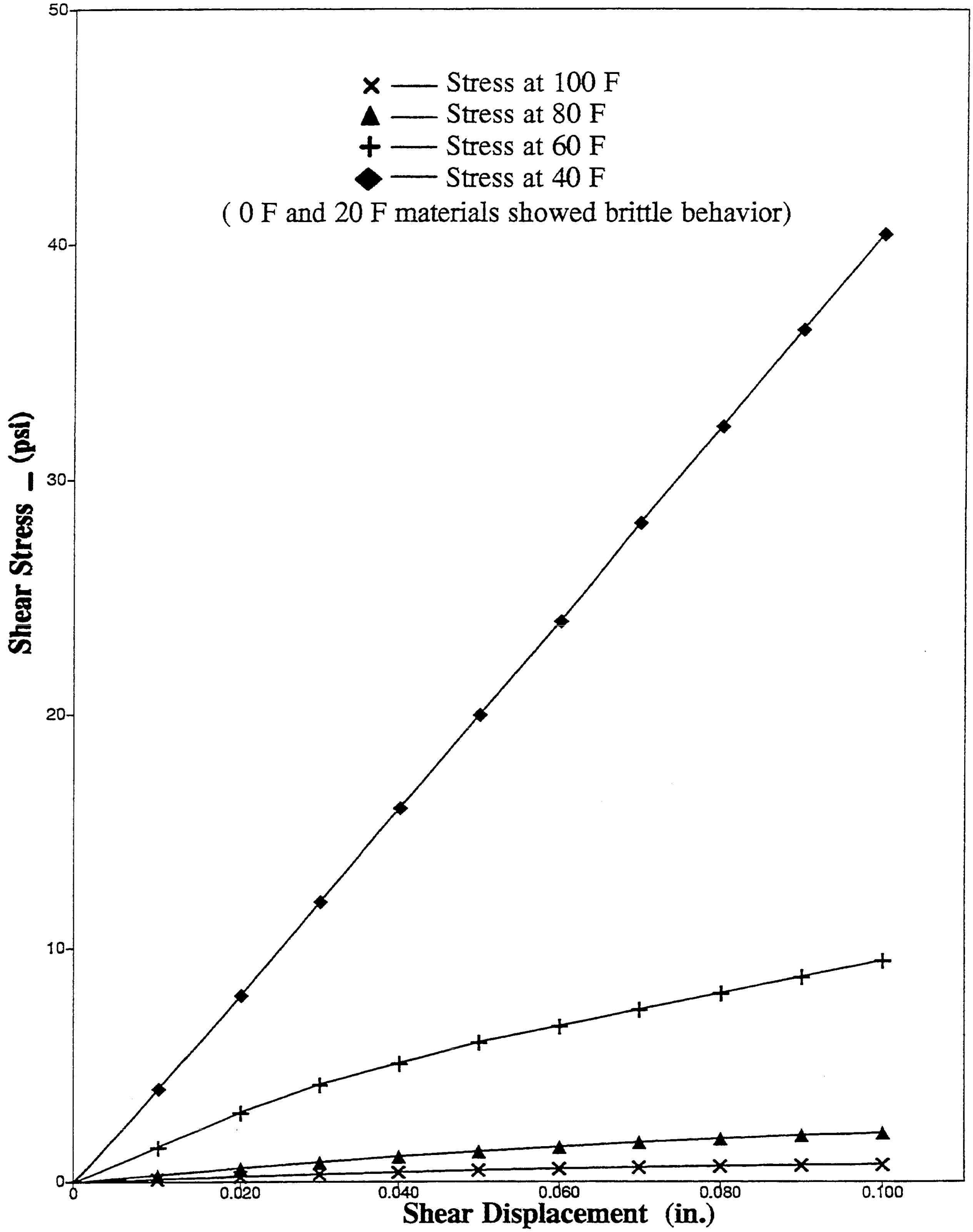

Figure 70: Shear Stress vs Displacement For Rubber Asphalt With 25 % Crumb Rubber & 75 % AC–10 @ Shear Rate of 2 in./min

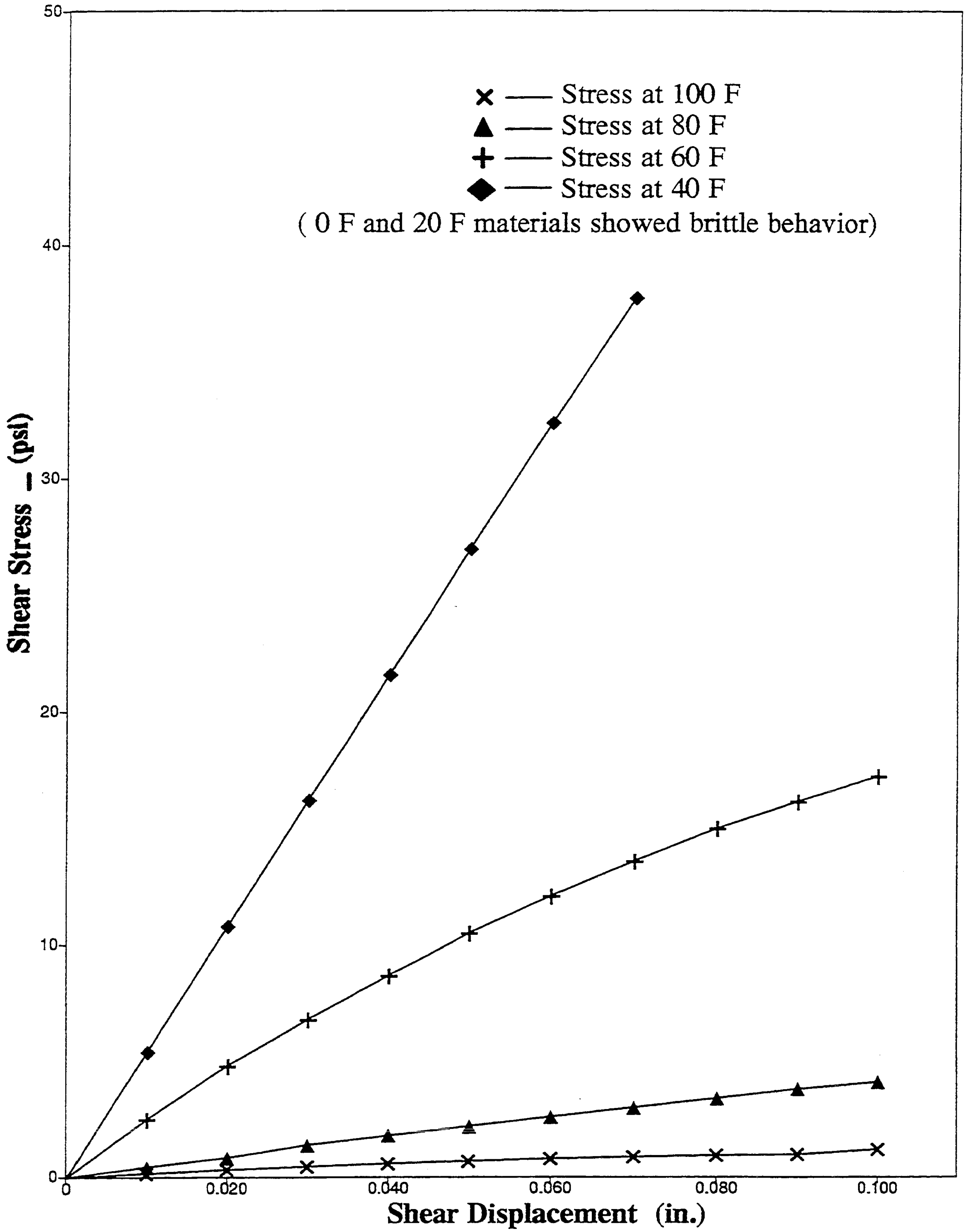

Figure 71: Shear Stress vs Displacement For Rubber Asphalt With 25 % Crumb Rubber & 75 % AC–20 @ Shear Rate of 2 in./min

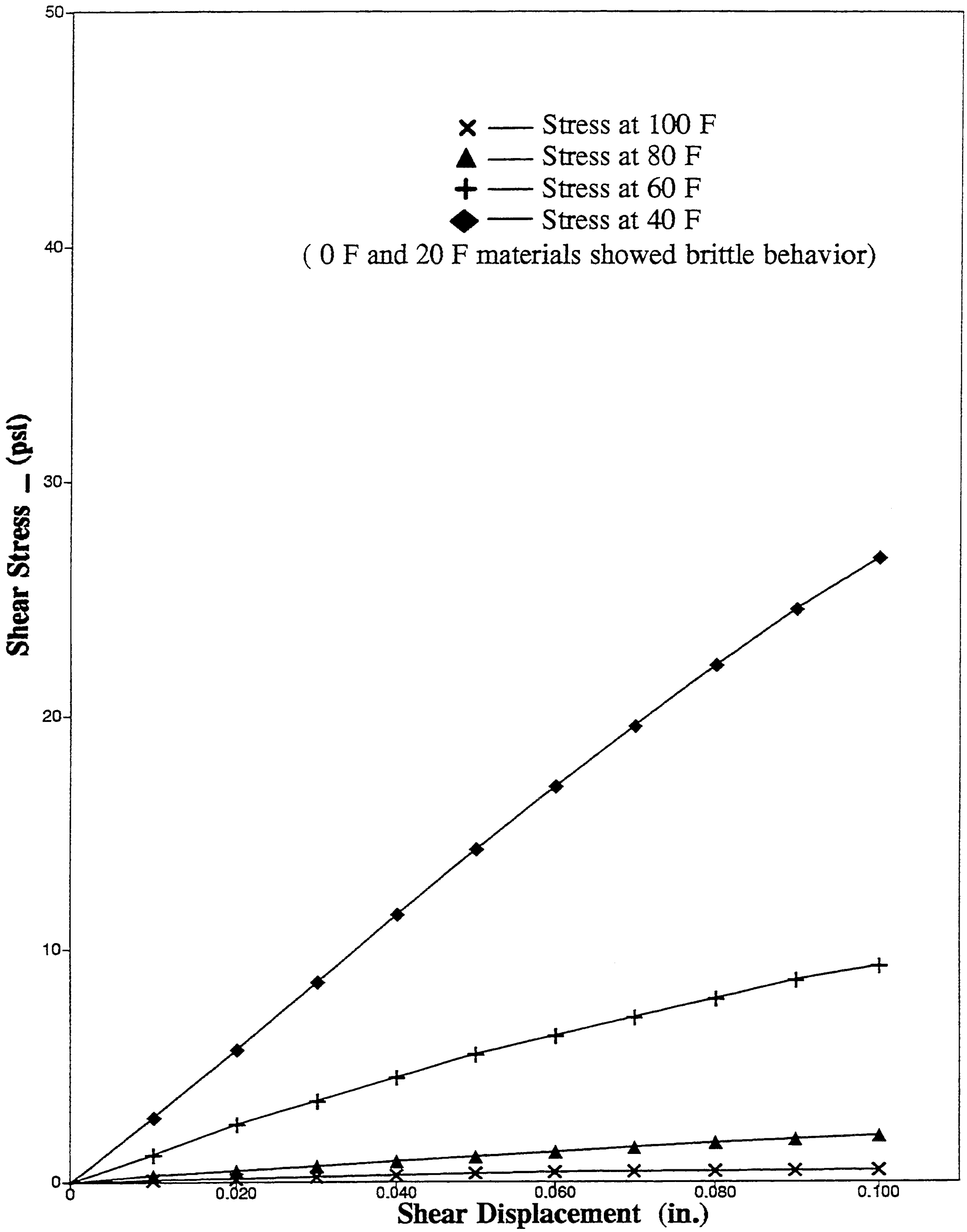

Figure 72: Shear Stress vs Displacement For Rubber Asphalt With 25 % Crumb Rubber & 75 % AC–5 @ Shear Rate of 3 in./min

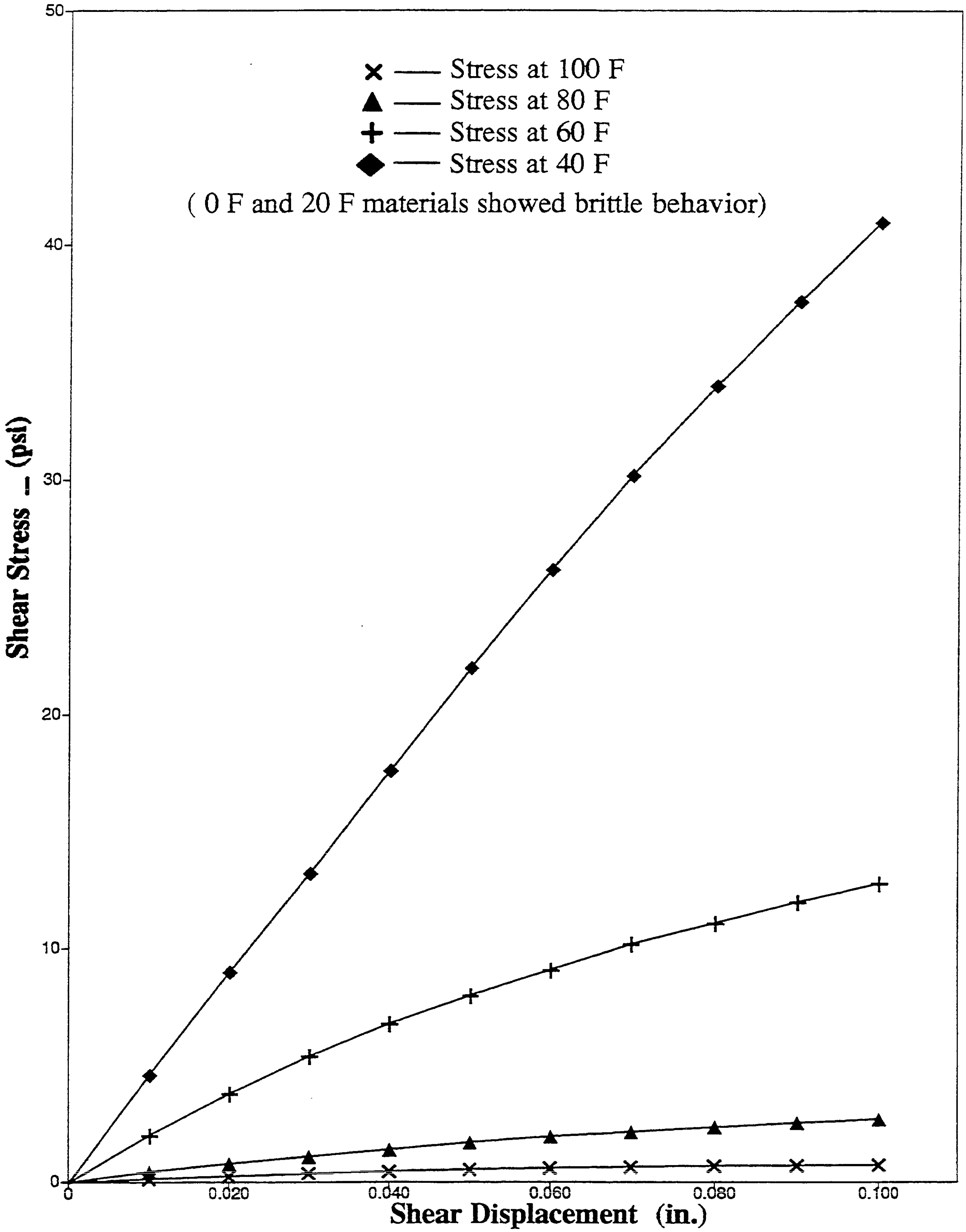

igure 73: Shear Stress vs Displacement For Rubber Asphalt With 25 % Crumb Rubber & 75 % AC–10 @ Shear Rate of 3 in./min

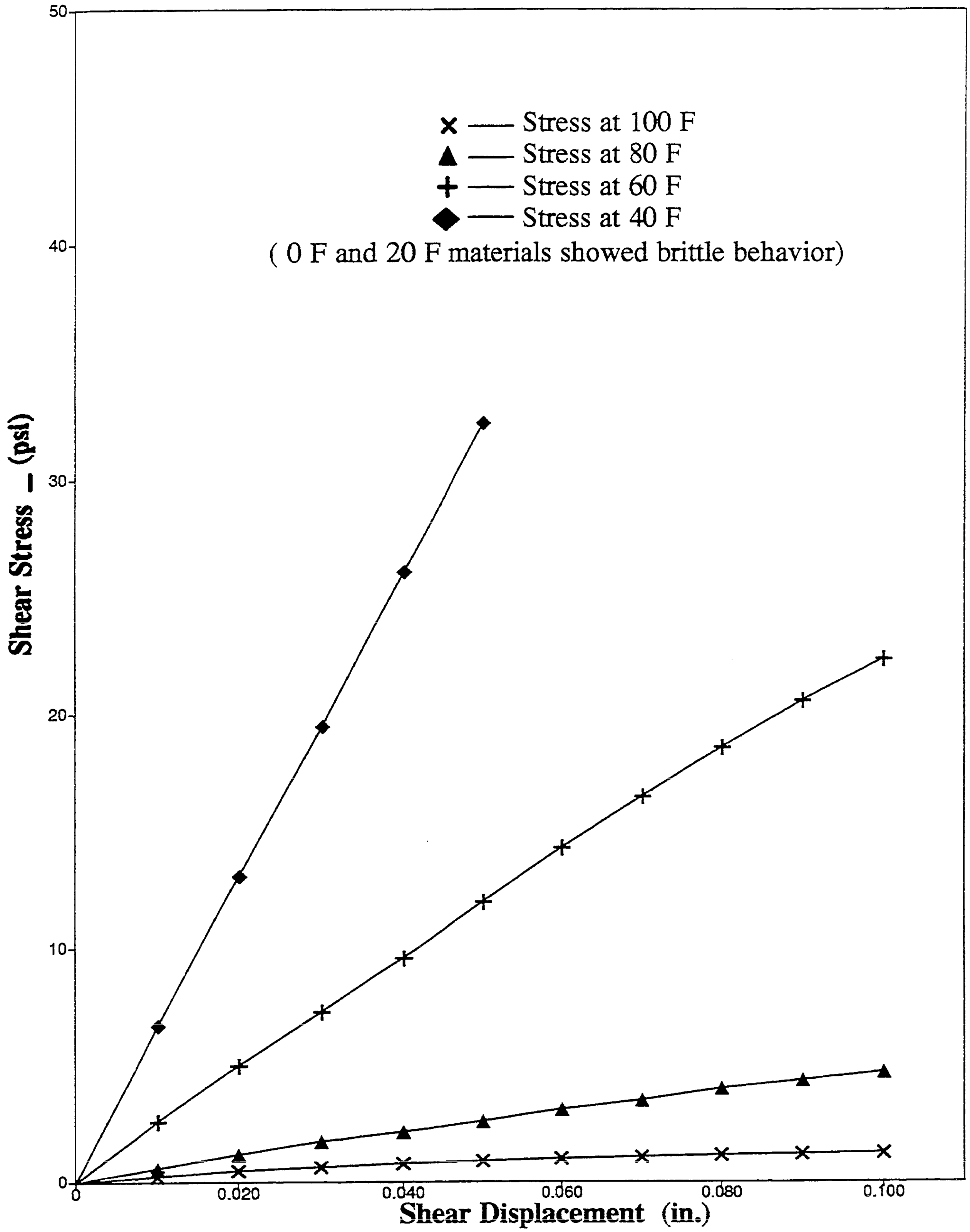

Figure 74: Shear Stress vs Displacement For Rubber Asphalt With 25 % Crumb Rubber & 75 % AC–20 @ Shear Rate of 3 in./min

Table 14 : Stiffness Of Various Rubber Asphalts at 0.05 in. Shear Displacement at Various Temperatures and Rates of Deformation

Type of Rubber Asphalt	Temp (F	Stiffness Of AC at Various Rates of Shear											
		0.05 in./min		0.2 in./min		0.5 in./min		1 in./min		2 in./min		3 in./min	
		Stress psi	Stiff–ness pci	Stress psi	Stiff–ness pci	Stress psi	Stiff–ness pci	Stress psi	Stiff–ness pci	Stress psi	Stiff ness pci	Stress psi	Stiff–ness pci
25 % crumb	100	0.22	4.4	0.25	5	0.3	6+	0.32	6.4	0.35	7	0.37	7.4
rubber + 75 %	80	0.35	7	0.4	8	0.45	9	0.75	15	0.85	17	1.1	22
AC–5	60	0.65	13	1.3	26	1.85	37	2.5	50	3.15	63	5.5	110
	40	4.1	82	6.1	122	7.8	156	12	240	13.5	270	14.3	278
	20	9.88	197.6	23.8	476	32.5	650	36	720				
	0	13.5	270	40	800								
25 % crumb	100	0.25	5	0.3	6	0.4	8	0.45	9	0.5	10	0.55	11
rubber + 75 %	80	0.45	9	0.65	13	0.85	17	1.1	22	1.3	26	1.7	34
AC–10	60	1.3	26	2.5	50	3.3	66	4.6	92	6	120	8	160
	40	6.6	132	8.6	172	10.5	210	18	360	20	400	22	440
	20	14.6	292	26.6	532	33.5	670	42	840				
	0	18.9	378	48	960								
25 % crumb	100	0.35	7	0.4	8	0.5	10	0.6	12	0.7	14	0.9	18
rubber + 75 %	80	0.6	12	1.1	22	1.6	32	2	40	2.2	44	2.6	52
AC–20	60	1.5	30	3.7	74	5.5	110	6.5	130	10.5	210	12	240
	40	10.2	204	18	360	22	440	23.2	464	27	540	32.5	650
	20	16.5	330	30	600	40.4	808	51.75	1035				
	0	29	580	58	1160								

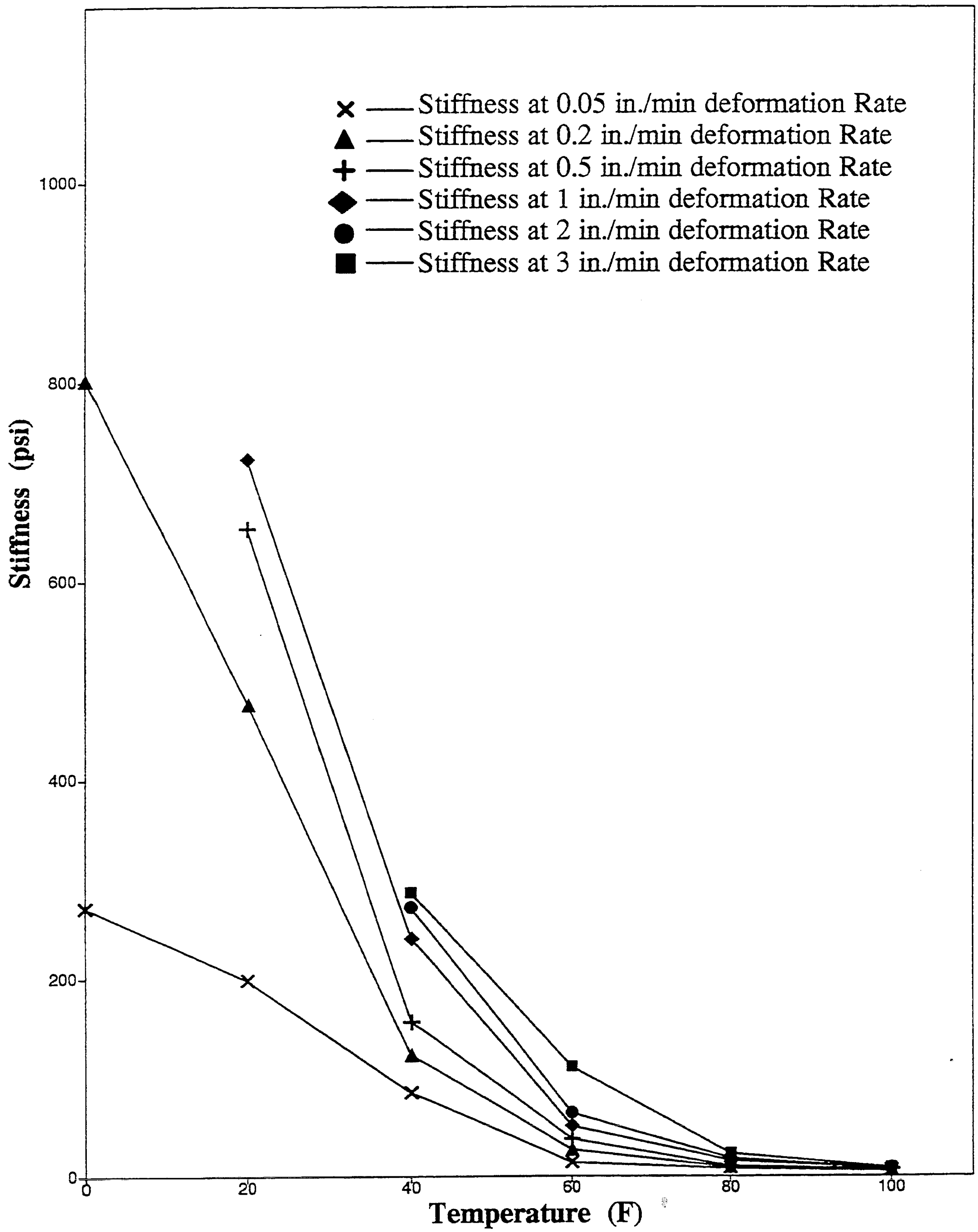

Figure 75: Stiffness vs Temperature at Various Deformation Rates For Rubber Asphalt With 25 % Crumb Rubber & 75 % AC–5

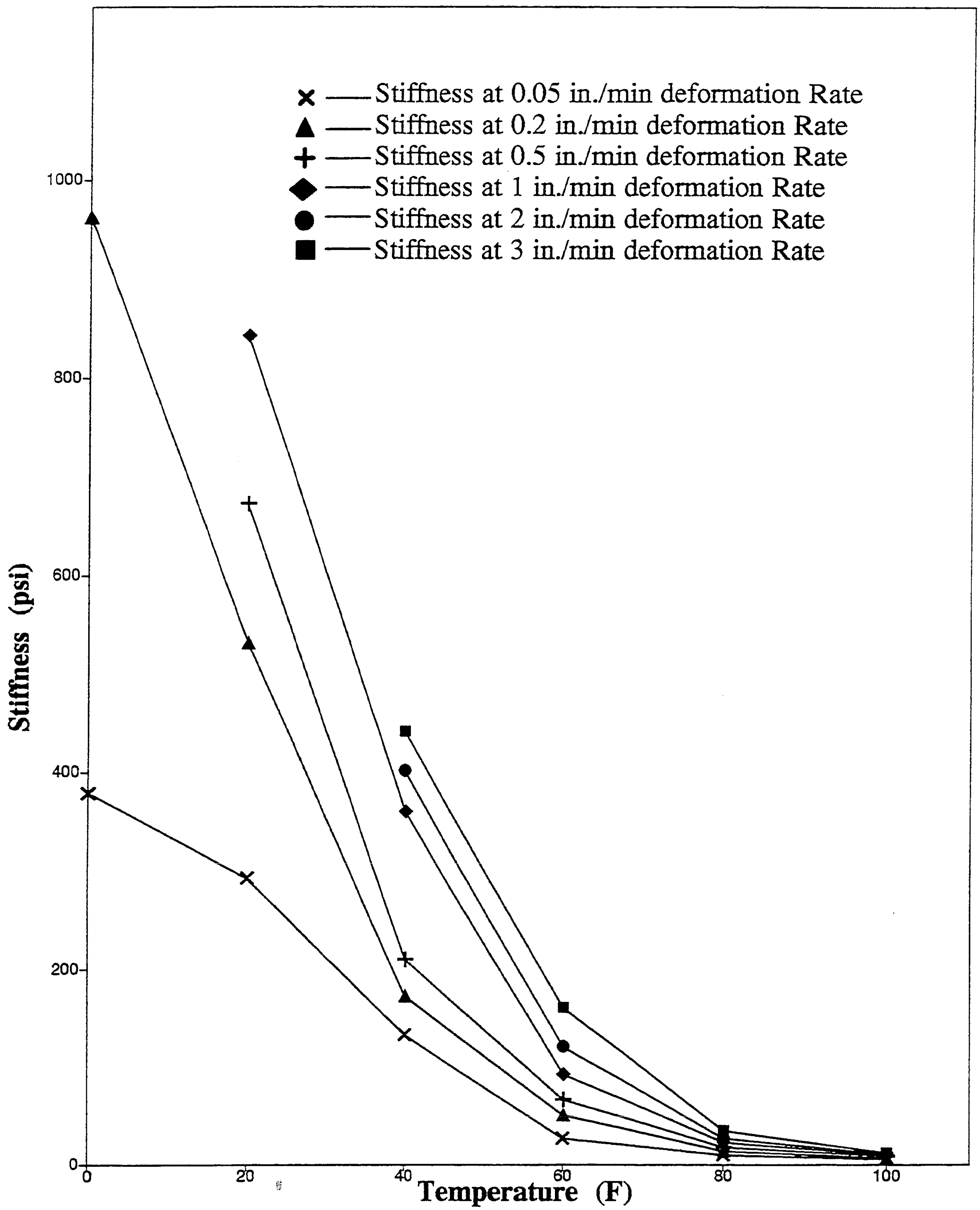

Figure 76: Stiffness vs Temperature at Various Deformation Rates For Rubber Asphalt With 25 % Crumb Rubber & 75 % AC–10

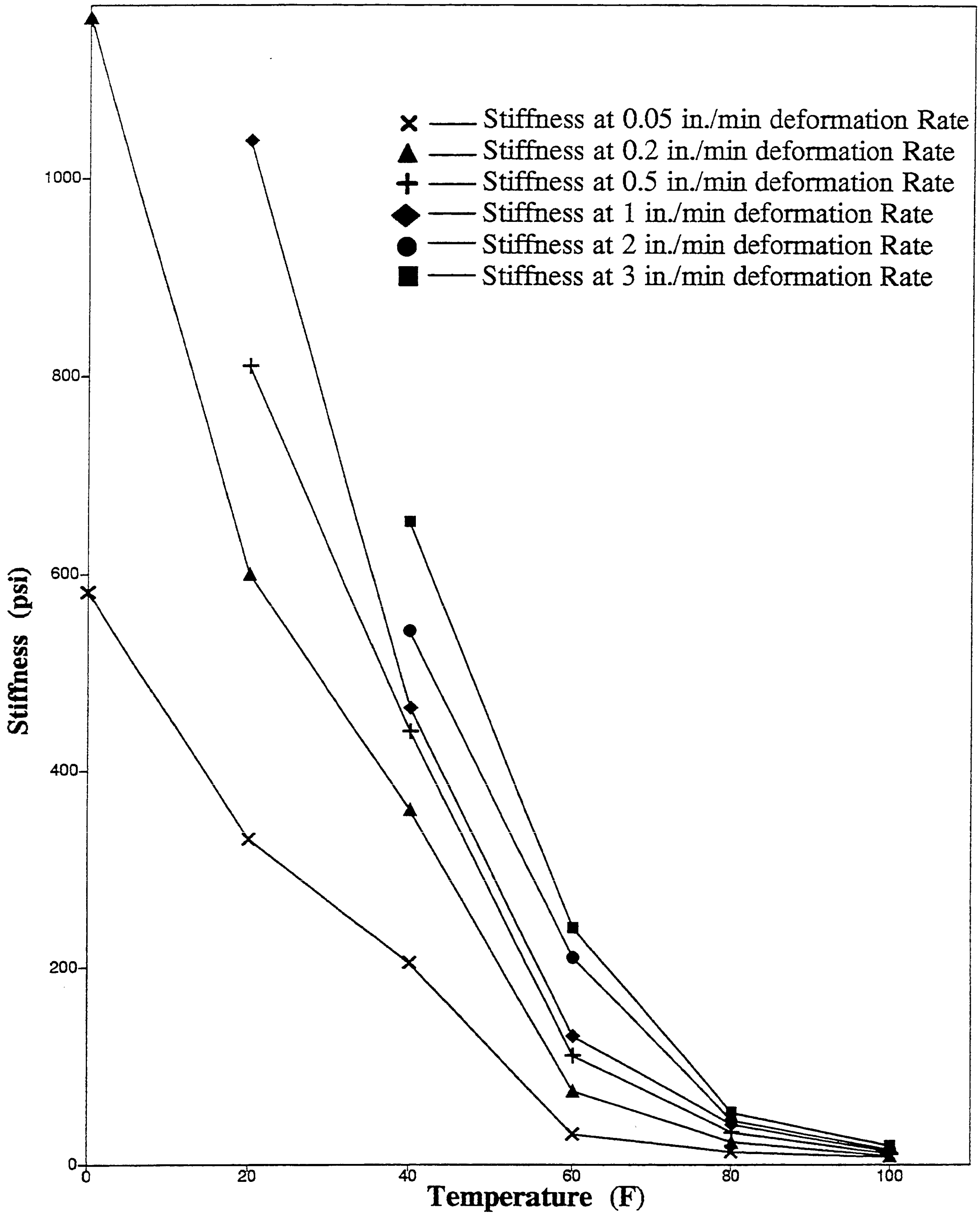

Figure 77: Stiffness vs Temperature at Various Deformation Rates For Rubber Asphalt With 25 % Crumb Rubber & 75 % AC–20

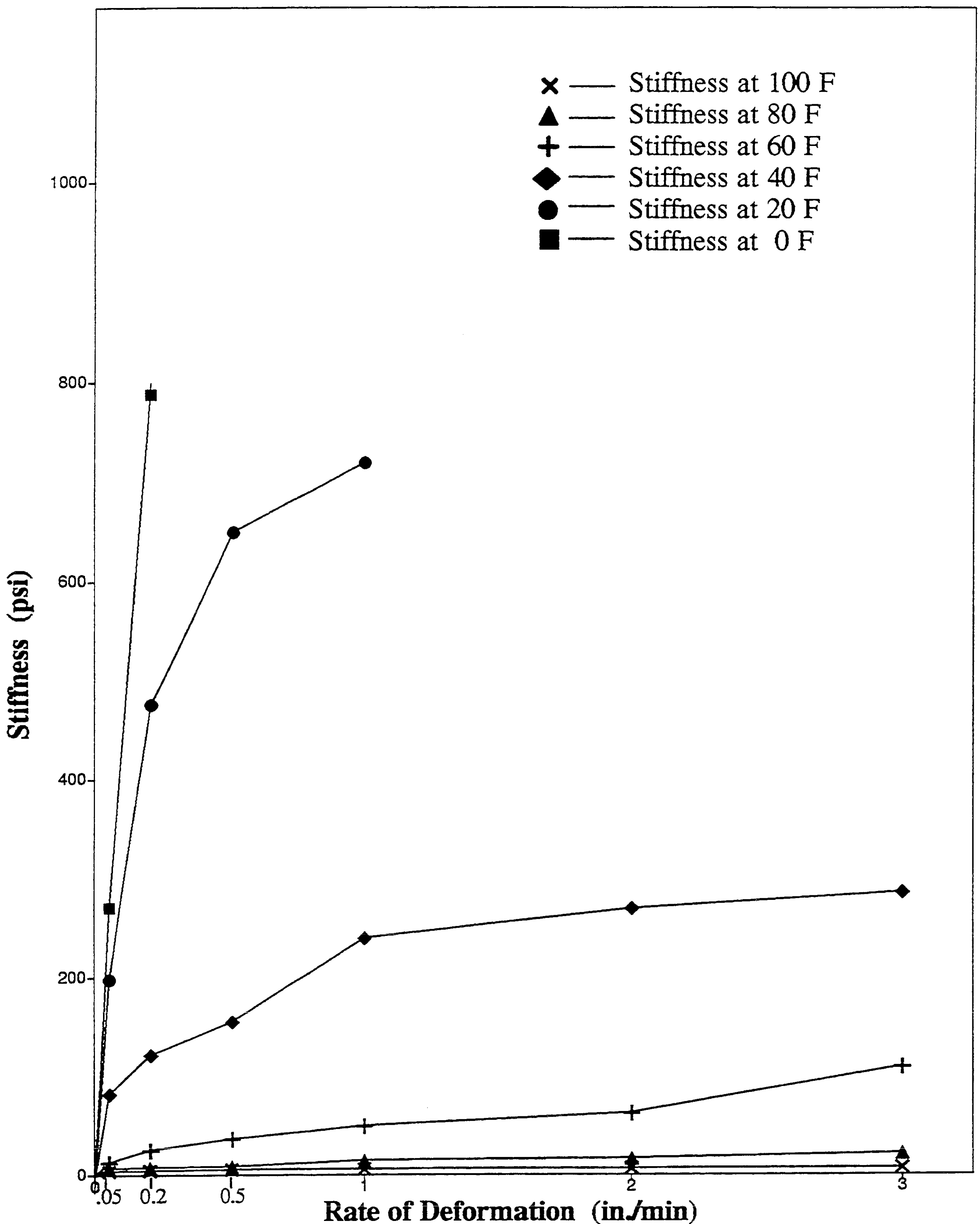

Figure 78: Stiffness vs Rate of Deformation at Various Temperatures For Rubber Asphalt With 25 % Crumb Rubber & 75 % AC–5

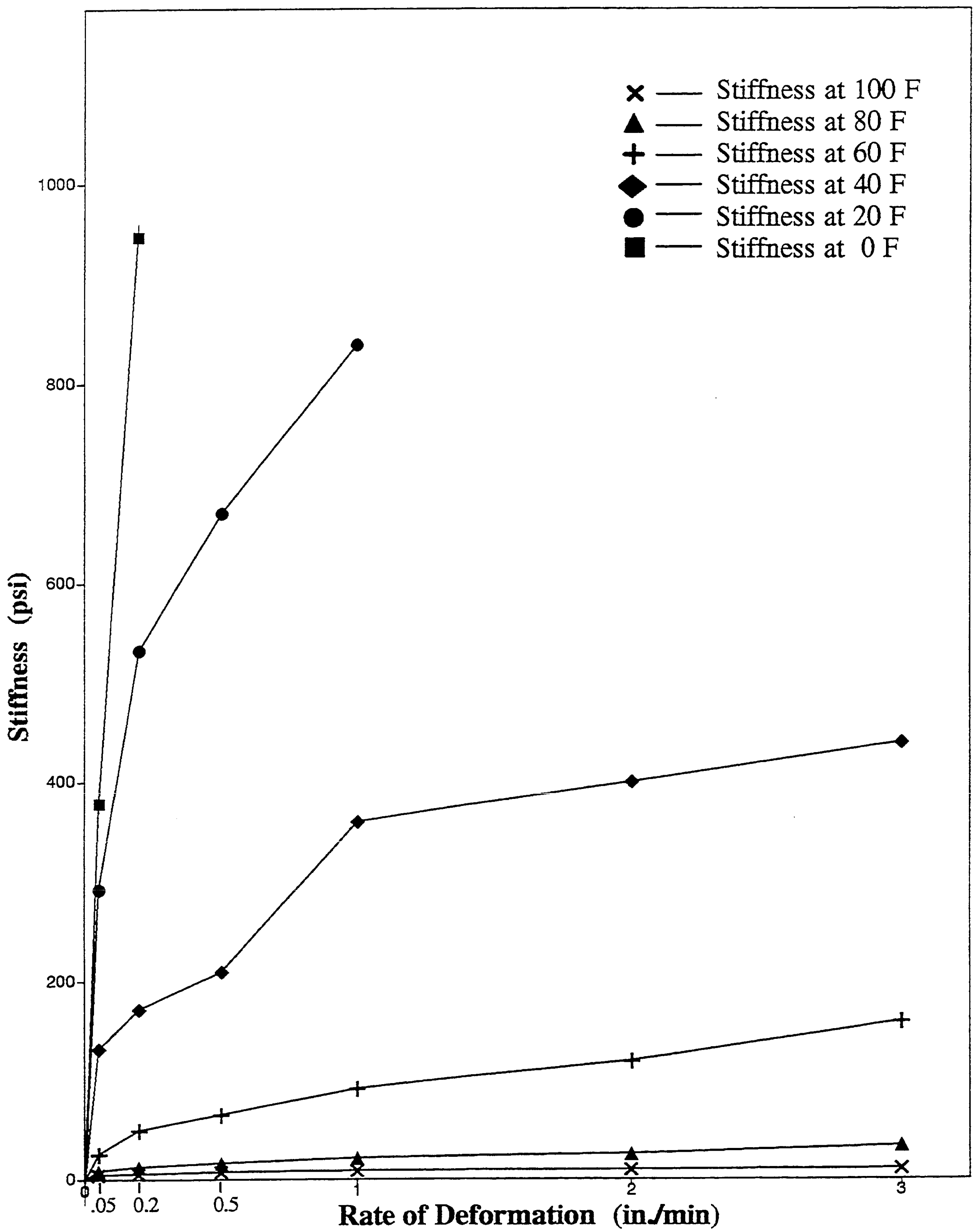

Figure 79: Stiffness vs Rate of Deformation at Various Temperatures For Rubber Asphalt With 25 % Crumb Rubber & 75 % AC–10

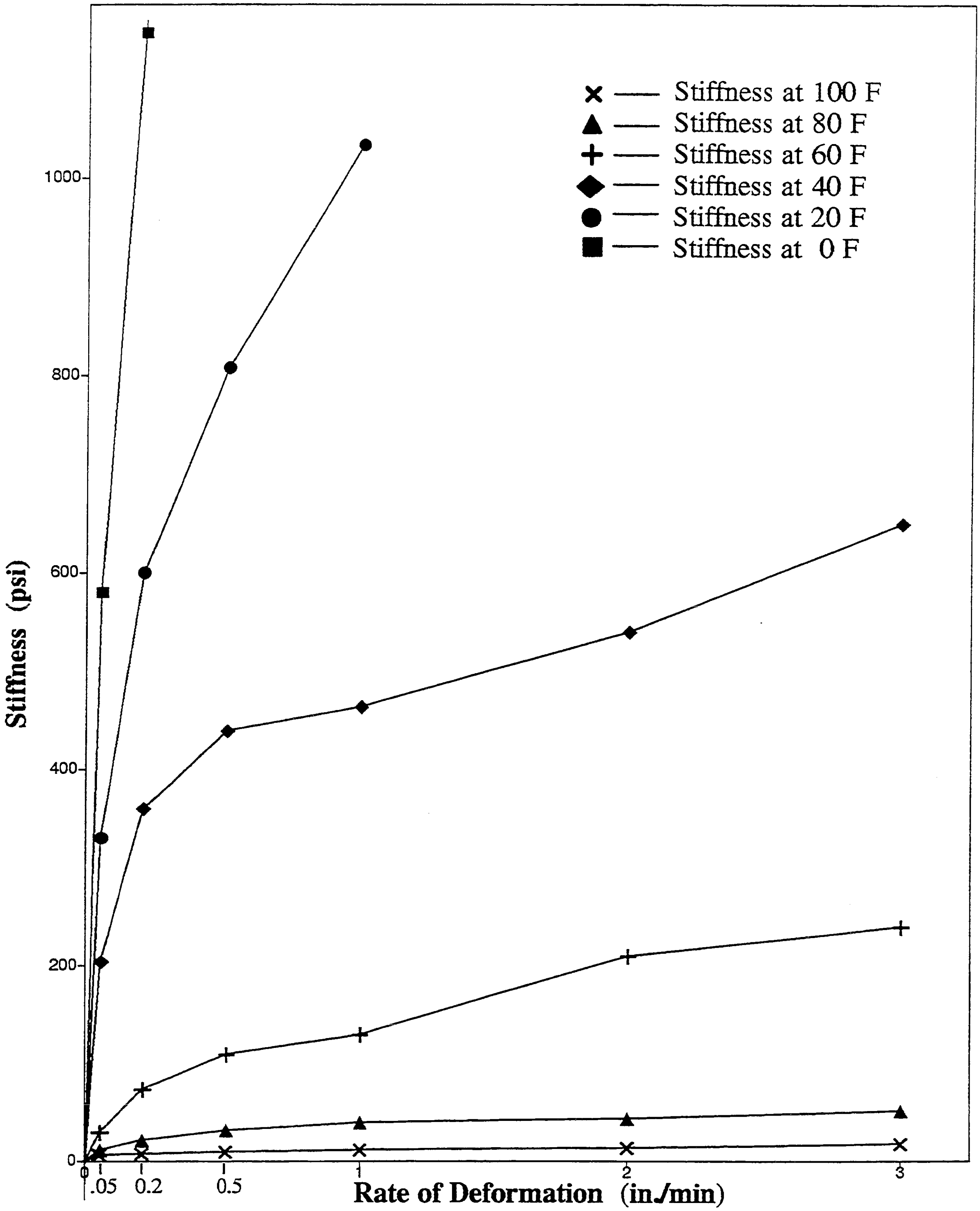

Figure 80: Stiffness vs Rate of Deformation at Various Temperatures For Rubber Asphalt With 25 % Crumb Rubber & 75 % AC–20

6.5 Asphalt Concrete Mixture – Preparation and Testing

6.5.1 Materials

An AC–20 was used to prepare the asphalt concrete mix for the overlay. Standardized tests were performed on the asphalt. A summary of the test results is given in Table 13.

Crushed limestone was obtained from the Fairmont Quarry in Illinois. The aggregate gradation is shown in Table 15 and Figure 81. Standard tests were performed to determine various physical properties of the aggregate. The results of these tests are summarized in Table 16.

6.5.2 Mixture

The Marshall Mix Method was used to select the appropriate blend, gradation, and optimum asphalt content for the AC overlay. The following mix formula was selected:

Coarse aggregate — 71.4 %

Fine aggregate — 18.5 %

Mineral Filler — 4.8 %

AC–20 — 5.2 %

6.5.3 Testing

ASTM procedures were followed to evaluate the Marshall mix specimens. In addition a split tensile test was performed on specimens at 20 F with a loading rate of 2 in./min. and tensile strength of AC mix at 20 F was calculated. The summary of test results is shown in Table 17.

Table 15: Sieve Analysis of Aggregate

Sieve No	% Passing Coarse Aggregate	% Passing Fine Aggregate	% Passing Mineral Filler	% Passing IDOT SPEC.
1/2 in	100	100	100	90–100
3/8 in	86.4	100	100	66–100
#4	28.9	97	100	24–65
#8	3.2	87.3	100	16–48
#16	1.9	76.5	100	10–32
#50	1.8	18.4	100	4–15
#100	1.7	2.6	97.4	3–10
#200	1.6	1	76.8	2–6

Table 16: Aggregate Properties

S/No	Aggregate Type and it's Properties	
1.	**Coarse Aggregate** (Material retained on # 4 sieve)	
	Apparent Specific Gravity (Gsa)	2.71
	Bulk Specific Gravity (Gsb)	2.59
	Bulk Specific Gravity SSD (GsbSSD)	2.64
	Absorption Percent	1.75
2.	**Fine Aggregate** (Material passing # 4 sieve)	
	Apparent Specific Gravity (Gsa)	2.70
	Bulk Specific Gravity (Gsb)	2.51
	Bulk Specific Gravity SSD (GsbSSD)	2.56
	Absorption Percent	2.75
3.	**Mineral Filler**	
	Apparent Specific Gravity (Gsa)	2.65

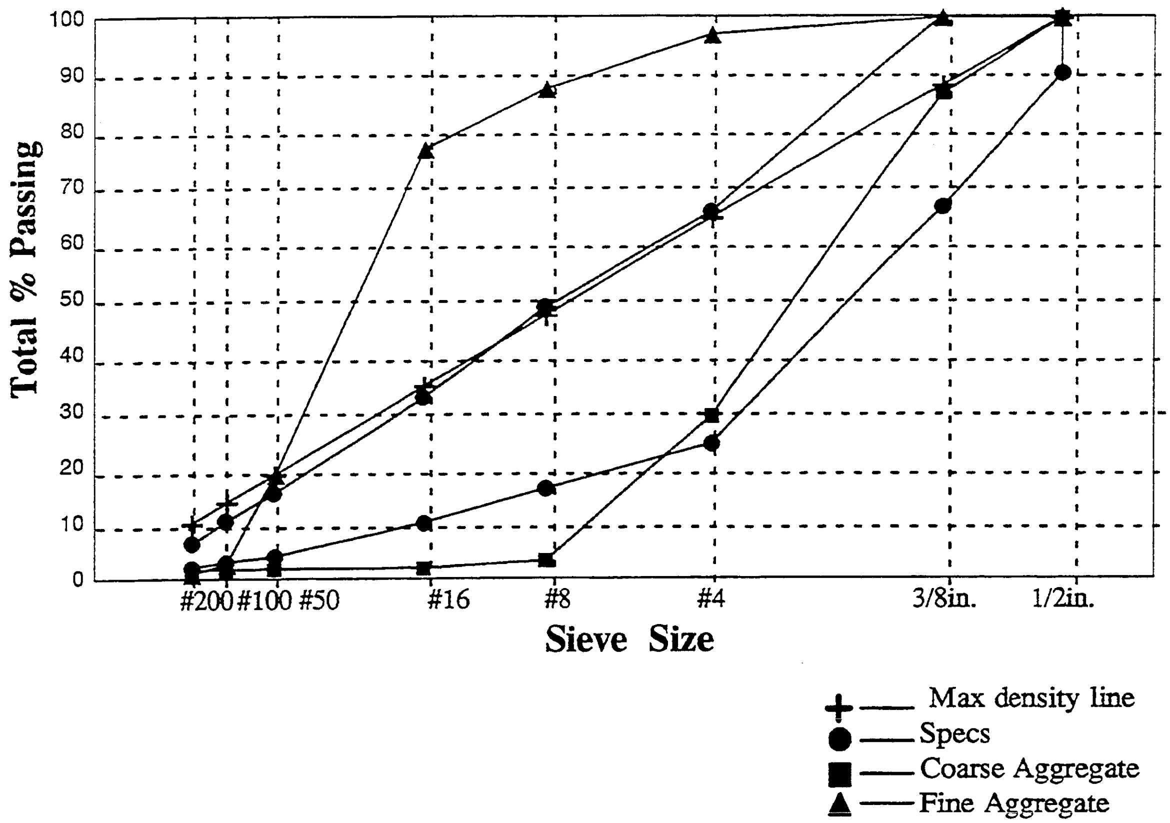

Figure 81: Aggregate Gradation

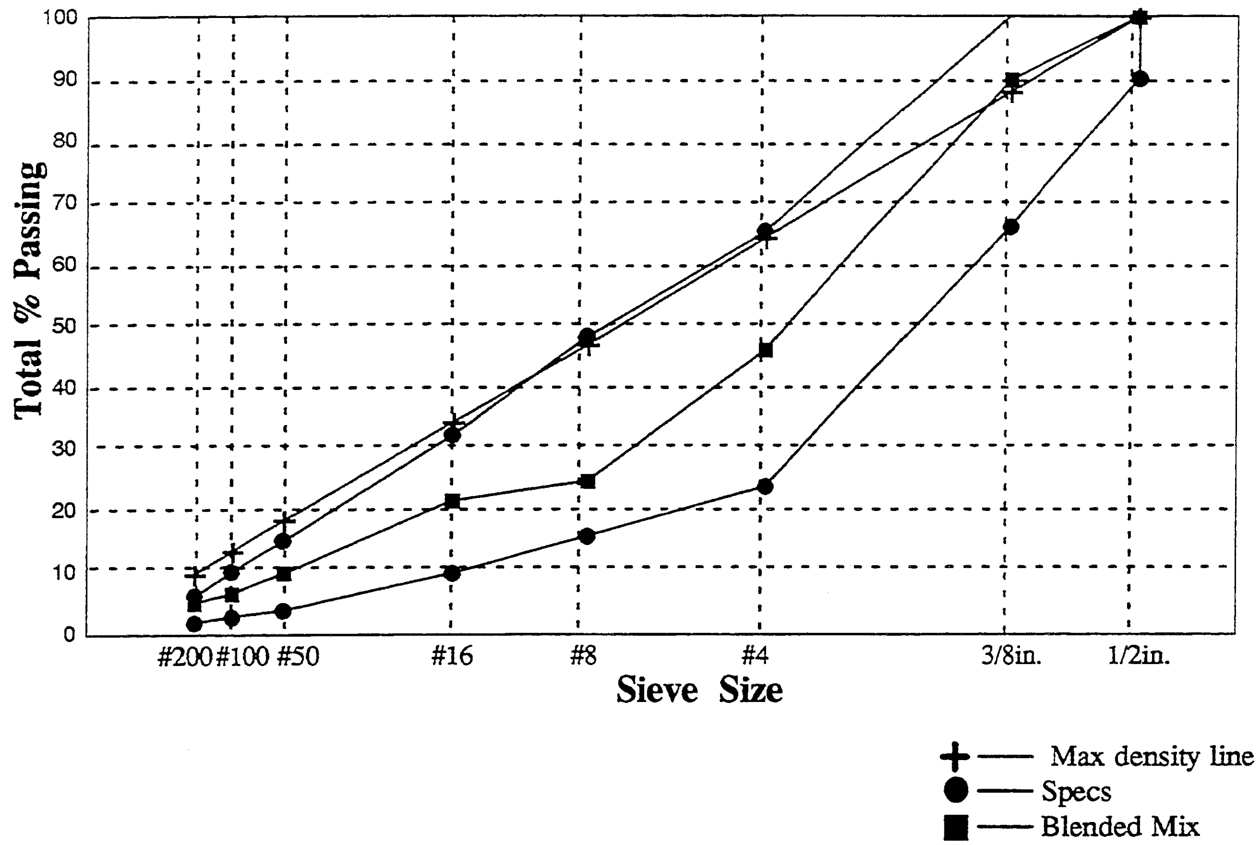

Figure 82: Blend Gradation

Table 17: Average Mixture Properties of Marshall Specimens at Optimum Asphalt Content

S/No	Mixture Properties at 5.2 % Asphalt Content (By Weight of Mix)		IDOT Specs
1	Unit Weight (PCF)	148.8	—
2	Air Void Content %	4	3–5
3	VMA %	12.25	14
4	VFA percent filled with asphalt %	75	—
5	Marshall Stability (lbs)	2100	2000
6	Marshall Flow 0.01 in.	11.5	8–16
7	Tensile Strength @ 20 F (psi)	454	—

CHAPTER 7

PREPARATION OF PROTOTYPE ISAC SYSTEM

7.1 Introduction

An extensive study of the properties and behavior of different types of geotextiles and rubber asphalts was conducted in Chapter 6 so that a more knowledgeable selection of the materials for the ISAC System could be made. From Table 12, Figure 52 and Figure 54 it is noticed that Bidim Rock TT 200/50 will provide the best engineering properties in terms of a high strength geotextile on the top side of the ISAC layer. From the same table and figures it is found that AMOCO 4.5 oz could serve as the low strength geotextile at the bottom of the ISAC system. Test results/behavior of rubber asphalt,Table 14, Figures 75, 76, and 77, however show that rubber asphalt made with 75 % AC–20 and 25 % rubber has very low stiffness at high temperatures and may not satisfy the ISAC system requirements. It is felt that ISAC, when placed under an AC overlay, will be exposed to variable temperature conditions and all types of traffic, including vehicles making sharp turns and applying sudden brakes.Therefore, there is possibility of slippage between the PCC slab and the AC overlay at the rubber asphalt interface in the ISAC system. The rubber asphalt must be tested against slippage and if necessary the quality of rubber asphalt (its stiffness and temperature susceptibility) should be improved by use of strength modifiers.

7.2. Fabrication Of ISAC Sample

A device shown in Figure 83 was developed to fabricate a 94 in. long and 8 in. wide ISAC sample. The device consisted of a 95 in. by 12 in. by 7/8 in. steel plate with two parallel slots (8 in. apart) designed to accommodate side rails. Side rails of various heights can be inserted into these slots so as to give net height of 1/8 in., 3/16 in., and 1/4 in. above the plate. End rails of the similar height can be fixed with the help of screws at the ends of the 8 in. wide space bounded by the two side rails. As a first attempt 1/8 in. side/end rails were evaluated. After inserting the side rails in the slots, a layer of heavy duty foil was placed between them to prevent the rubber asphalt from bonding to the plate. A 95 in. long and 6 in. wide section of Bidim Rock TT 200/50 geotextile was cut

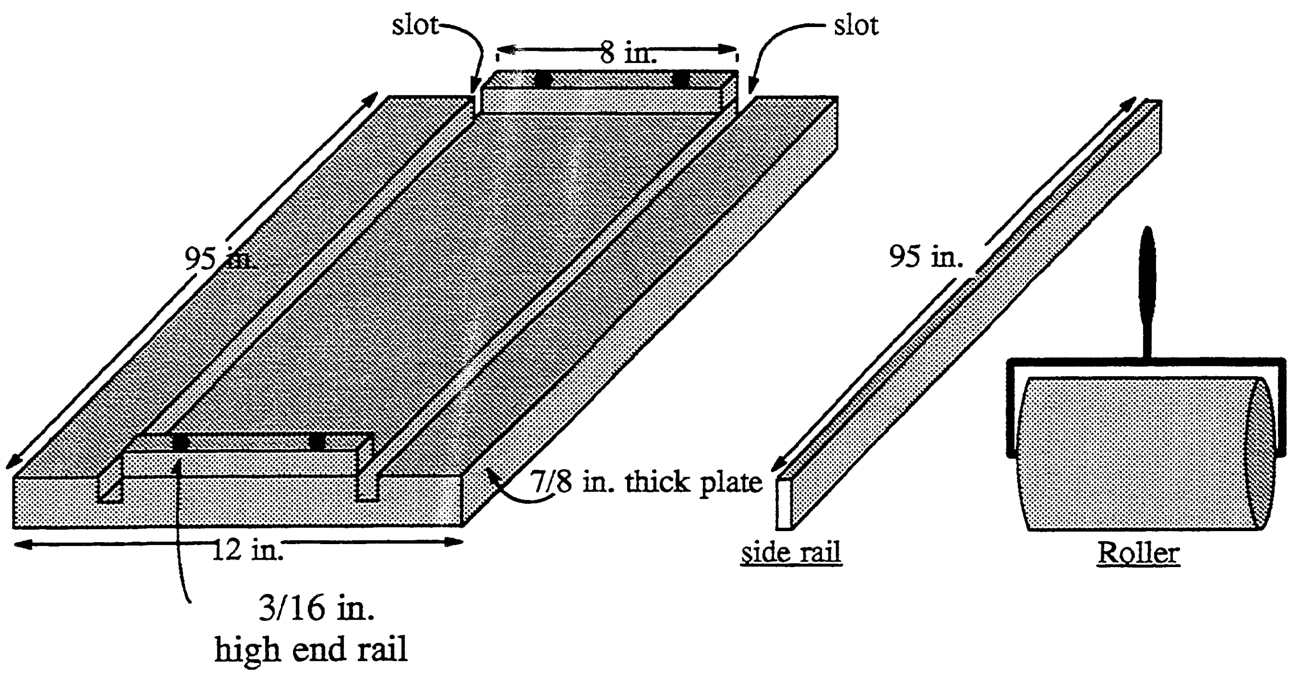

Figure 83: Device to Fabricate an ISAC Layer

and placed between the two side rails. The geotextile was then stretched and fixed under the end rails with the help of screws. The fabrication device was put into an environmental chamber at 100 F temperature. Rubber asphalt was prepared by blending 75 % AC–20 and 25 % crumb rubber at 400 F for 30 min., cooled down to 300 F, and then placed over the high strength woven geotextile in the fabrication mold. The rubber asphalt was spread in the space bounded by the side rails and end rails of the mold, and leveled off by removing the excess material. In an attempt to remove the excess material, most of the rubber asphalt came off with the scoop. It was realized that the height of the side and end rails was too little and a such a thin and uniform layer of rubber asphalt could not be achieved. Above procedure was repeated with 3/16 in. high side and end rails and fairly good results were obtained. A 94 in. long and 6 in. wide section of AMOCO 4545 geotextile was then cut and placed on top of hot rubber asphalt. A 35 lb steel roller was placed with its sides resting on the side rails and manually rolled back and forth in order to achieve a uniform ISAC layer thickness. The temperature of the environmental chamber was then lowered to 40 F and ISAC was allowed to cool. The end and side rails were then taken off, and the ISAC layer along with the foil was removed. The foil was peeled off and a 3/16 in. thick 6 in. wide, and 7.5 ft long piece of ISAC layer was ready to be used.

7.3 Check Against Slippage

7.3.1 General

The movement of an asphalt concrete overlay with respect to the underlying pavement has been observed on some highways. Such failure, though not

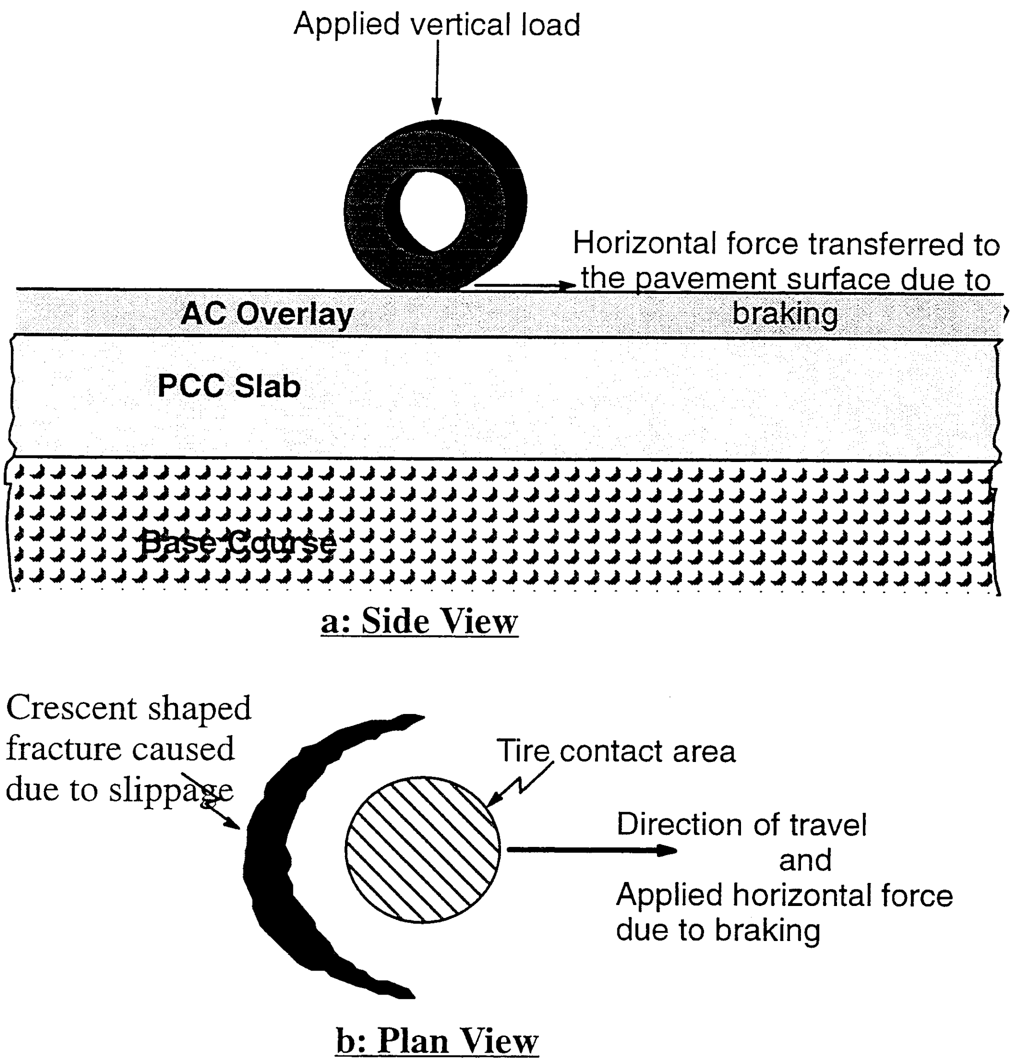

Figure 84: Typical Slippage Failure (Ref 44)

very common, has usually occurred in the wheel path and in the areas where the vehicles make sharp turns or apply sudden brakes. Typically a slippage crack is crescent shaped with its arched end pointing in the direction opposite to that of the vehicle motion, Figure 84.

The crescent shape indicates that such cracks could occur when all of the following conditions have been met (44):

a) Shear stress in the vertical plane of the overlay exceeded the shear strength of the overlay and a crack developed along the side of the braking tire.

b) Tensile stress in the overlay behind the tire exceeded the tensile strength of the material, causing a crack behind the braking tire.

c) Compressive strength of the overlay was exceeded, causing shoving in front of the braking tire.

d) Shear stress at the interface produced by the braking tire exceeded the shear strength of the interface, causing a relative movement between the overlay and the underlying pavement.

To be conservative in this study the tensile strength, compressive strength, and shear strength of AC overlay in its vertical plane were not taken into account while considering the slippage failure at the interface. It was assumed that the first three conditions ((a), (b) and (c)) had occurred in the AC mix and the slippage between the AC overlay and the underlying pavement was only resisted by the shear strength at the ISAC interface. It will thus be ensured that the last condition (d) does not occur.

Slippage between the AC overlay and the underlying pavement can be prevented by:

a) Reducing the shear stress at the interface which can be achieved by increasing the overlay thickness.

b) Increasing the shear strength between the overlay and the underlying pavement at the interface.

The first solution of Increasing the overlay thickness was determined to be less economical than the second solution. Adequate shear strength at the interface will therefore be used to prevent slippage.

In a controlled section of the pavement (without any treatment) shear strength at the interface is developed both by adhesion and mechanical interlock. Once the layer of ISAC is introduced between the AC overlay and the PCC slab, mechanical interlock will significantly decrease and what is left is predominantly the adhesion component of rubber asphalt contributing towards shear strength at the interface. It is necessary to determine the magnitude of shear stress developing at the interface due to a braking vehicle, quantify the shear strength of the ISAC layer, and if the former exceeds later then the properties of rubber asphalt will have to be improved.

7.3.2 Shear Stress Developed at the Interface

The computer program "CIRCLY" (15) was used to compute the stresses at the interface in a multi layered pavement system caused by vertical and horizontal load inputs at the surface. The following features of the pavement and traffic were used as input values in the program:

a) Subgrade of infinite depth with an elastic modulus of 5000 psi and poison's ratio of 0.45.

b) A 10 in. thick PCC slab with an elastic modulus of 4,000,000 psi and poison's ratio of 0.15.

c) Asphalt concrete overlay of varying depth to include 2.5 in., 3 in., 3.5 in. and 4 in. with an elastic modulus of 500,000 psi and poison's ratio of 0.35.

d) A tire pressure of 90 psi was assumed.

7.3.3 Horizontal Stress at Pavement Surface

Data relating to the braking effect of a vehicle on the pavement including the coefficient of friction has been taken from the 1986 AASHTO Guide For Pavement Design (37) and has been shown in Figure 85 and Table 18. The force transferred to the pavement due to skid resistance is shown in Table 18. for various vehicle speeds. In the table it may be noted that the maximum horizontal force (6120 lbs) is transferred to the pavement surface at 30 MPH vehicle speed. The horizontal stress at the pavement surface can now be calculated as follows:

Total vertical load on the tire = 9000 lbs

Assuming tire foot print to be circular and tire pressure =90 psi

$90 * (3.14159 * R^2) = 9000$ (R being the radius of the footprint)

R = 5.64 in.

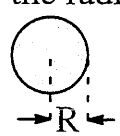

Horizontal force transferred to the surface of the pavement by one tire = 6120 lbs

Horizontal stress transferred to the pavement surface = $6120/(3.14159 * (5.64)^2)$

=61.25 psi

The computer program "CIRCLY" was run using the above input values and the stresses at the interface were computed for each thickness of overlay. The results are shown in Appendix C and graphically plotted in Figures 86 through 90. Maximum shear stress at the interface occurred directly under the wheel. Maximum shear stress transferred to the interface for various overlay thicknesses is summarized in Table 19.

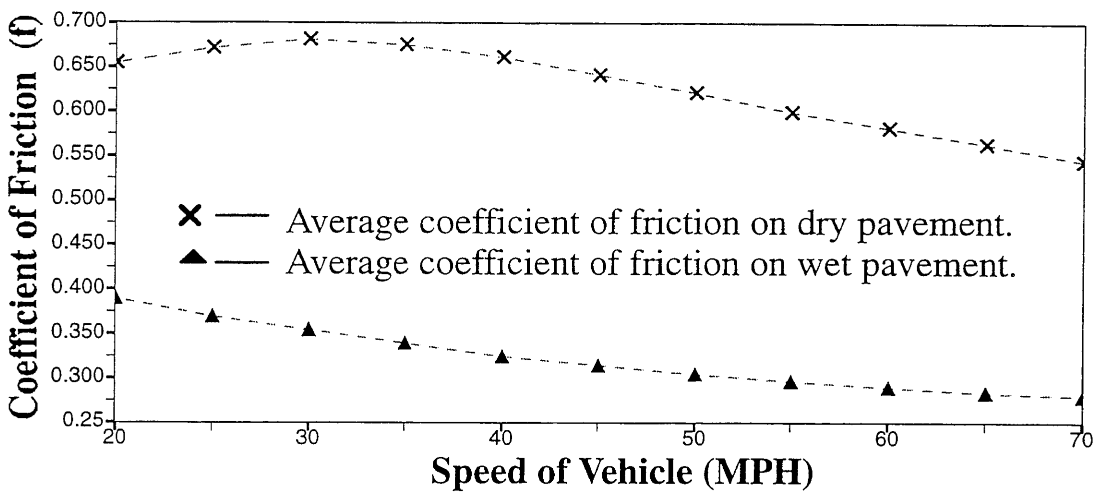

Figure 85: Variation in Coefficient of Friction With Vehicular Speed (Ref 37)

Table 18: Braking Effect and Force Transferred To The Pavement Due To Skid Resistance (Ref 37)

Speed of Vehicle (V) (MPH)	Coefficient of Friction (f)		Braking Distance $D = V^2/30f$ (ft)		Braking Time $t = 1.3636 * D/V$ (Sec)		Deceleration $a = -1.075 * V^2/D$ (ft/sec/sec)		Horizontal Force Transferred From Wheel To The Pavement On Applying Brakes $H = f * WeightOnOneWheel = f * 9000$ (lbs)	
	Dry Pave-ment	Wet Pave-ment	Dry Pave-ment	Wet Pave-ment	Dry Pave-ment	Wet Pave-ment	Dry Pave-ment	Wet Pave-ment	Dry Pavement	Wet Pavement
20	0.66	0.4	20	33	1.364	2.25	21.5	13.04	5940	3600
25	0.675	0.38	31	55	1.691	3	21.7	12.2	6075	3420
30	0.68	0.35	44	86	2	3.91	22	11.25	6120	3150
35	0.675	0.34	60	127	2.34	4.95	21.9	10.37	6075	3060
40	0.66	0.32	81	167	2.76	5.69	21.2	10.3	5940	2880
45	0.64	0.31	105	218	3.182	6.61	20.7	9.99	5760	2790
50	0.62	0.30	134	278	3.65	7.58	20.1	9.67	5580	2700
55	0.60	0.30	168	336	4.16	8.33	19.37	9.68	5400	2700
60	0.58	0.29	207	414	4.7	9.41	18.7	9.35	5220	2610
65	0.56	0.29	251	486	5.26	10.2	18.1	9.35	5040	2610
70	0.54	0.28	302	583	5.88	11.4	17.5	9.04	4860	2520

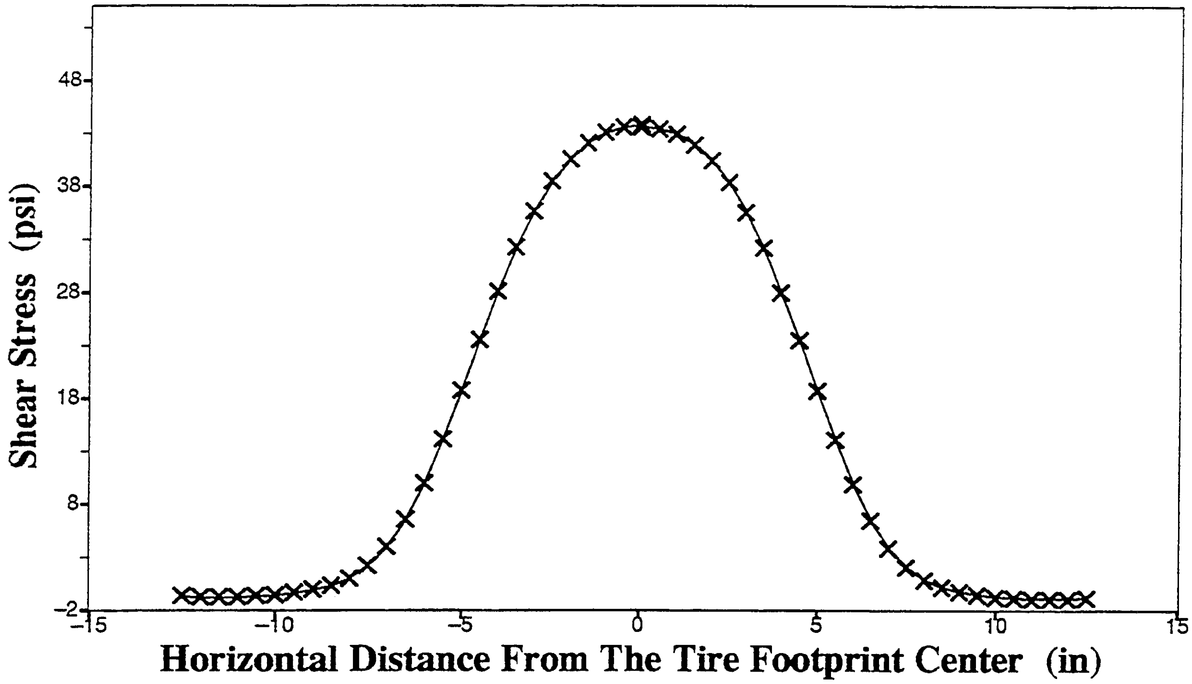

Figure 86: Shear Stress On Horizontal Plane at Interface For 2.5 in. Thick Overlay

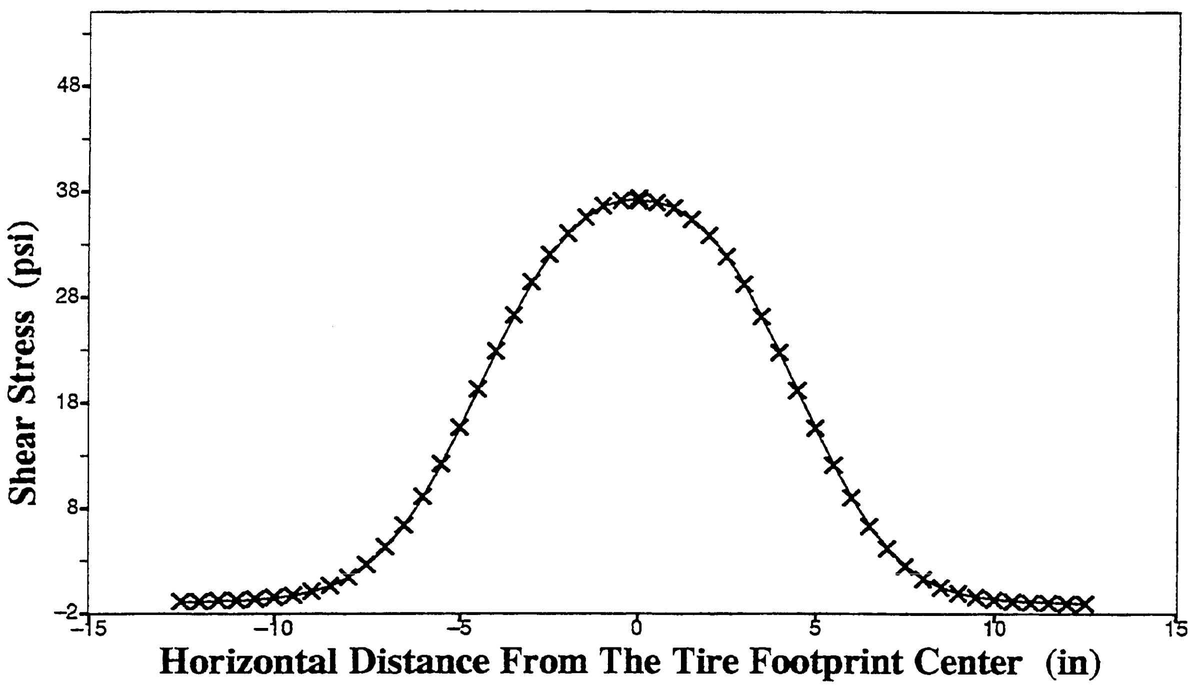

Figure 87: Shear Stress On Horizontal Plane at Interface For 3 in. Thick Overlay

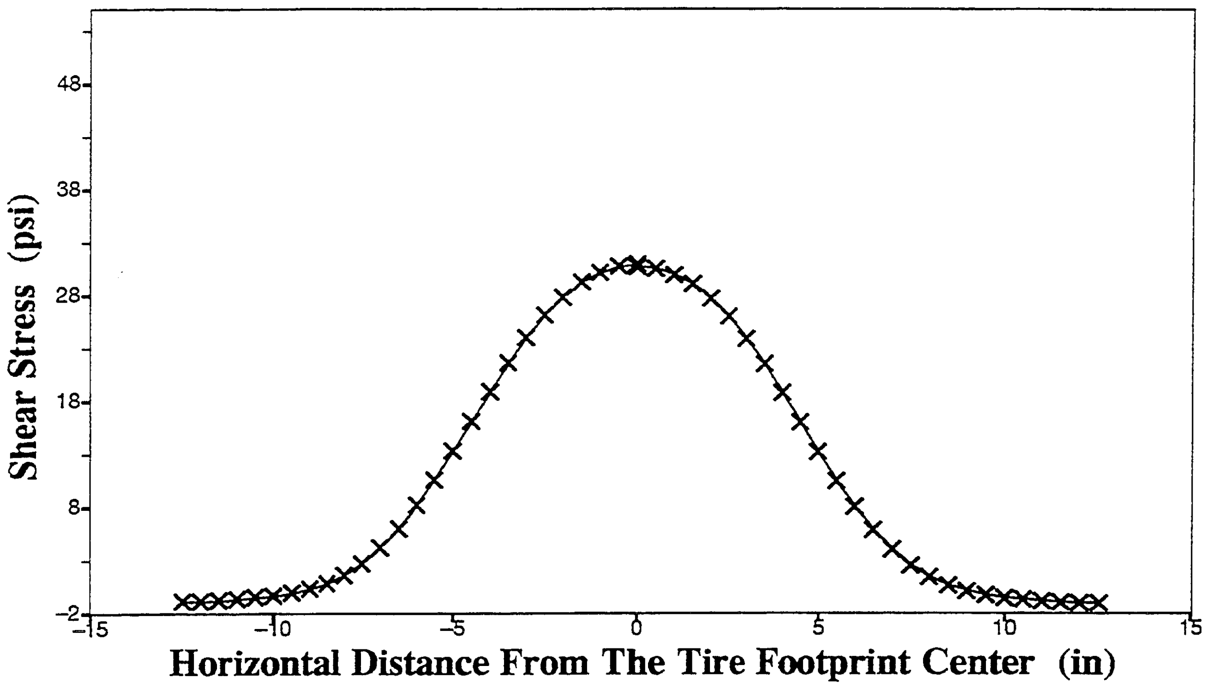

Figure 88: Shear Stress On Horizontal Plane at Interface For 3.5 in. Thick Overlay

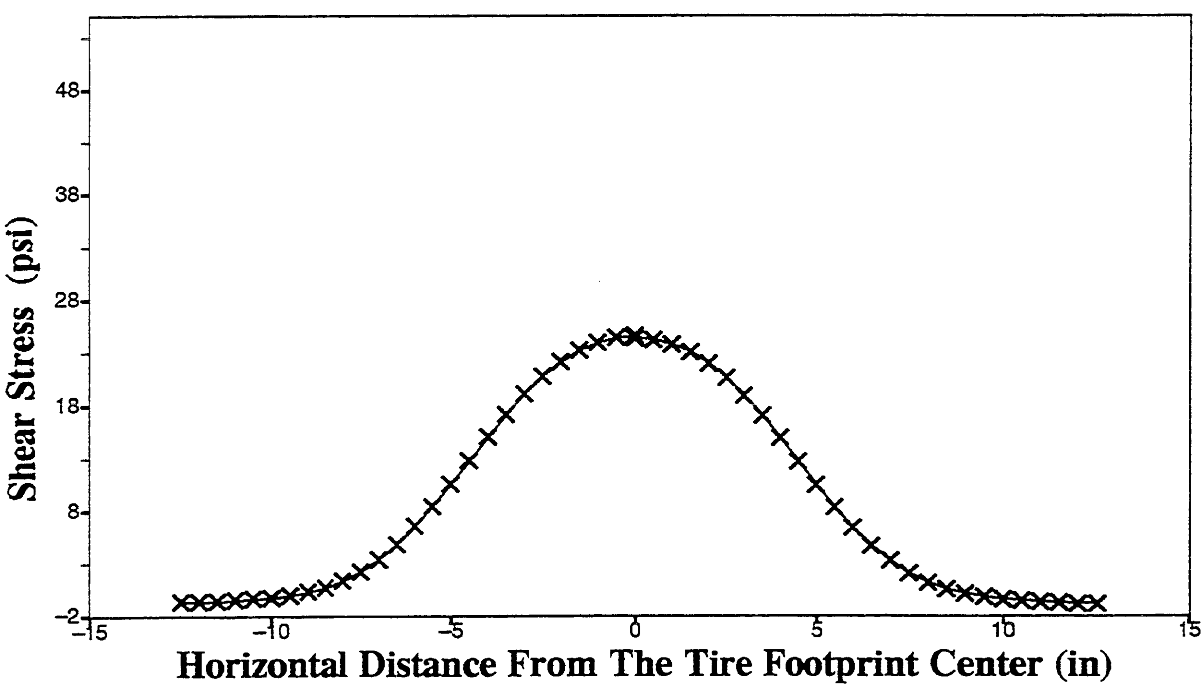

Figure 89: Shear Stress On Horizontal Plane at Interface For 4 in. Thick Overlay

Table 19: Maximum Shear Stress at Interface For Various Overlay Thicknesses

Overlay Thickness (in.)	Maximum Shear Stress at Interface (psi)
2.5	43.7
3	37.2
3.5	30.8
4	24.5

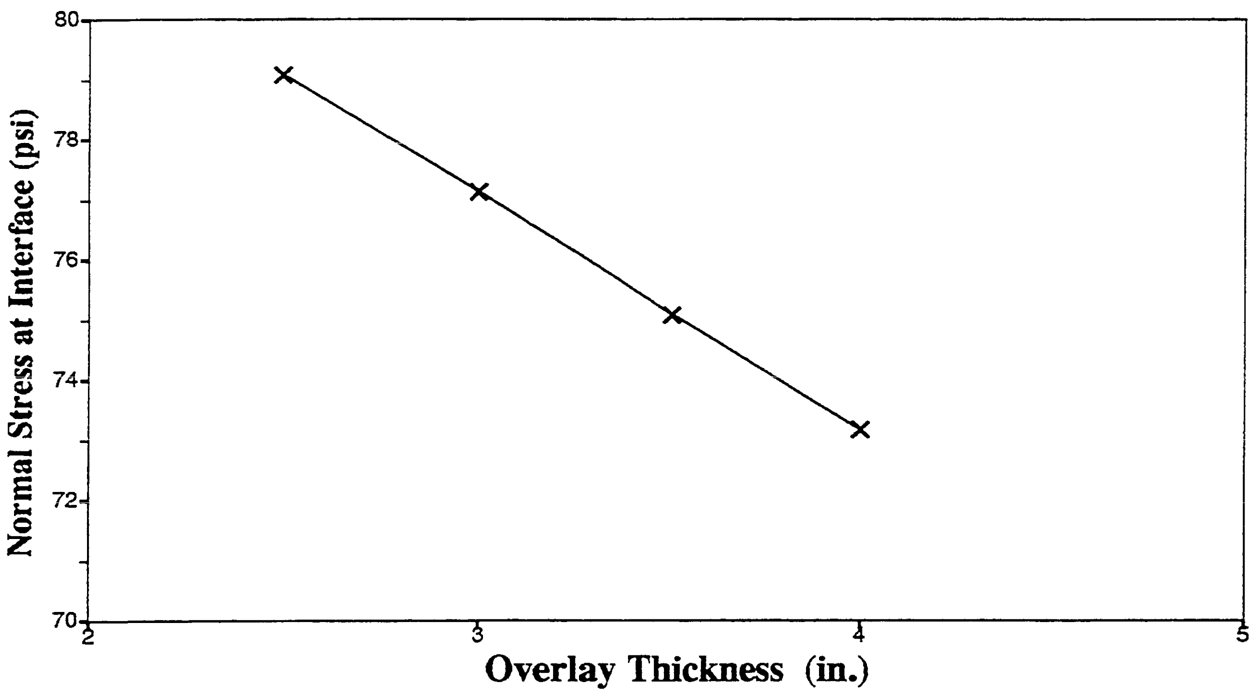

Figure 90: Variation In Normal Stress at Interface Due to Moving Vehicle With Change in Overlay Thickness

7.3.4 Laboratory Evaluation of Interface Shear Strength

Laboratory testing was performed to determine the shear strength at the overlay interface. Three types of test specimens were fabricated as follows:

a) AC section with no interface.

b) An AC overlay placed on a PCC pavement with tack coat at the interface.

c) An AC overlay placed on a PCC pavement with ISAC layer at the interface.

Testing equipment was developed and used to find out the interfacial shear strength of the test specimens. During testing, effort was made to duplicate the field conditions affecting the shear strength at the interface between an AC overlay and PCC pavement such as temperature, confining pressure, and rate of shear.

7.3.4.1 Fabrication of Test Specimens

An AC mixture was prepared using the mix formula determined previously in Section 6.4.1. This material was used to fabricate AC cylinders with 2 in. diameter and 3 in. height, Figure 91. The cylinders were compacted at 300 F by using a 2 in. diameter tamping foot vibrator so as to achieve an average AC density of 147 PCF.

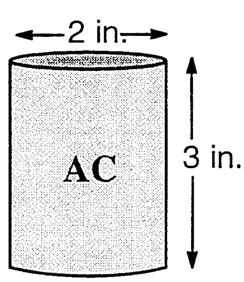

Figure 91: Asphalt Concrete Control Specimen

PCC cylinders with 2 in. diameter and 2 in. height were prepared and cured for 28 days. The specimens were dried and the appropriate quantity of tack coat was applied to them. The cylinders were then put into a 2 in. diameter mold and 3 in. of AC was compacted on to the tack coated concrete surface in three equal layers using the foot vibrator so as to achieve an average AC density of 147 PCF, Figure 92.

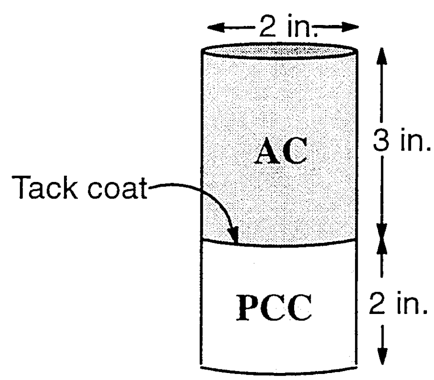

Figure 92: Specimen With Tack Coat at Interface

Small PCC cylinders with 2 in. diameter and 2 in. height were prepared and cured for 28 days. They were dried and an appropriate quantity of tack coat was applied. A circular 2 in. diameter section was cut from the ISAC layer and placed on the tack coated concrete surface. Another layer of tack coat was applied to the top of the ISAC layer. The concrete cylinder along with the ISAC layer were placed into a 2 in. diameter mold, and 3 in. of AC was compacted above the tack coated ISAC surface in three equal layers as described previously so as to achieve an average AC density of 147 PCF, Figure 93.

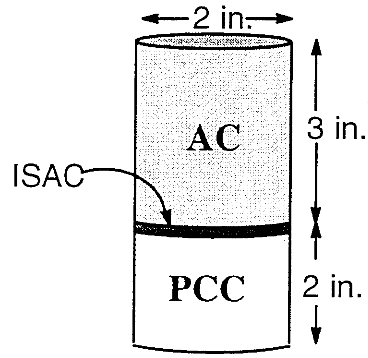

Figure 93: Specimen With ISAC at Interface

7.3.4.2 Laboratory Testing

The shear testing equipment shown in Figure 94 which was developed at University of Illinois was used to evaluate the shear resistance of AC and the interlayer (tack coat or ISAC) at the interface. While performing the tests, factors influencing shear strength of the AC/interlayer such as temperature, confining load, and rate of shear were considered.

Tests were performed at six different temperatures of 0 F, 20 F, 40 F, 60 F, 80 F and 100 F. The specimens were put in an environmental room at

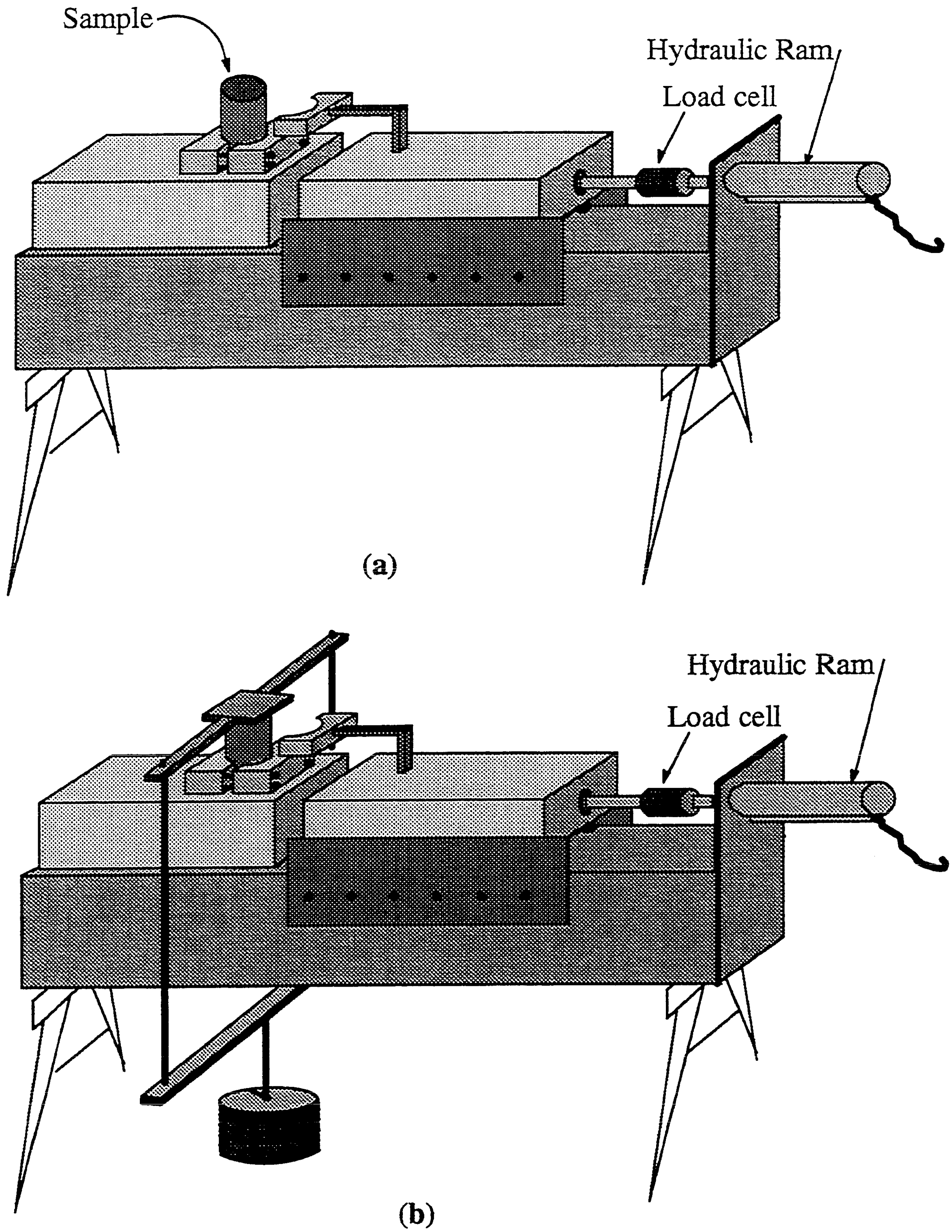

Figure 94: Device to Determine Shear Strength of Pavement Samples

the desired temperature for at least three hours prior to testing.

The bottom half of the specimen was tightly clamped and a vertical confining pressure of 79 psi was applied normal to the intended shear plane, Figure 94. The applied confining pressure represents the vertical stress at the interface of a PCC slab with a 2.5 in. thick AC overlay caused by a moving vehicle. The stress (79 psi) was computed by using the ‘‘BISAR”Computer program (38).

A horizontal force was applied to the upper half of the sample so as to create a shear force in the intended shear plane. Three rates of shear which included 1 in./min, 30 in./min, and 300 in./min were used. A plot of head movement vs load was developed for each specimen using an X–Y plotter. The ultimate shear load was recorded and divided by the cross sectional area of the shear plane to obtain the ultimate shear strength. A summary of the results is presented in Table 20 and the shear strength vs temperature for each type of specimen has been plotted to facilitate direct comparison in Figure 95, Figure 96, and Figure 97.

Table 20: Shear Strength of Asphalt Concrete, Interface With Tack coat and Interface With ISAC layer at at Various temperatures

Temp (F)	Type of sample	Shear strength (psi)		
		@ 1 in./min	@ 30 in./min	@ 300 in./min
0	AC Tack coat ISAC	359 128 80	388 117 76	426 102 66
20	AC Tack coat ISAC	386 179 113	442 185 117	529 184 108
40	AC Tack coat ISAC	317 176 99	426 191 127	605 232 136
60	AC Tack coat ISAC	230 123 58	414 175 119	557 267 178
80	AC Tack coat ISAC	160 88 33	282 144 103	487 215 181
100	AC Tack coat ISAC	108 67 26	165 98 68	266 131 116

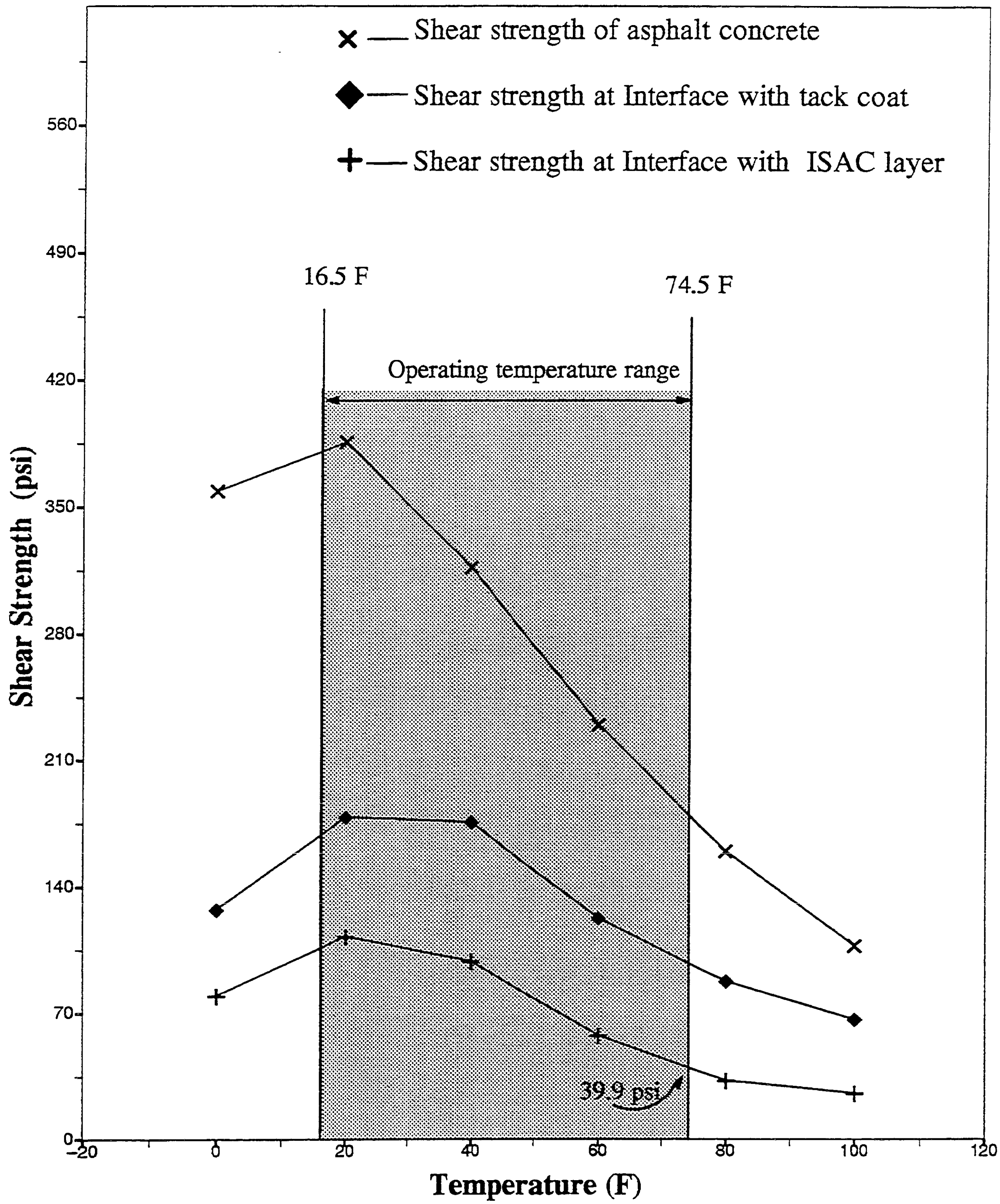

Figure 95: Shear Strength vs Temperature at 1 in./min Rate of Shear

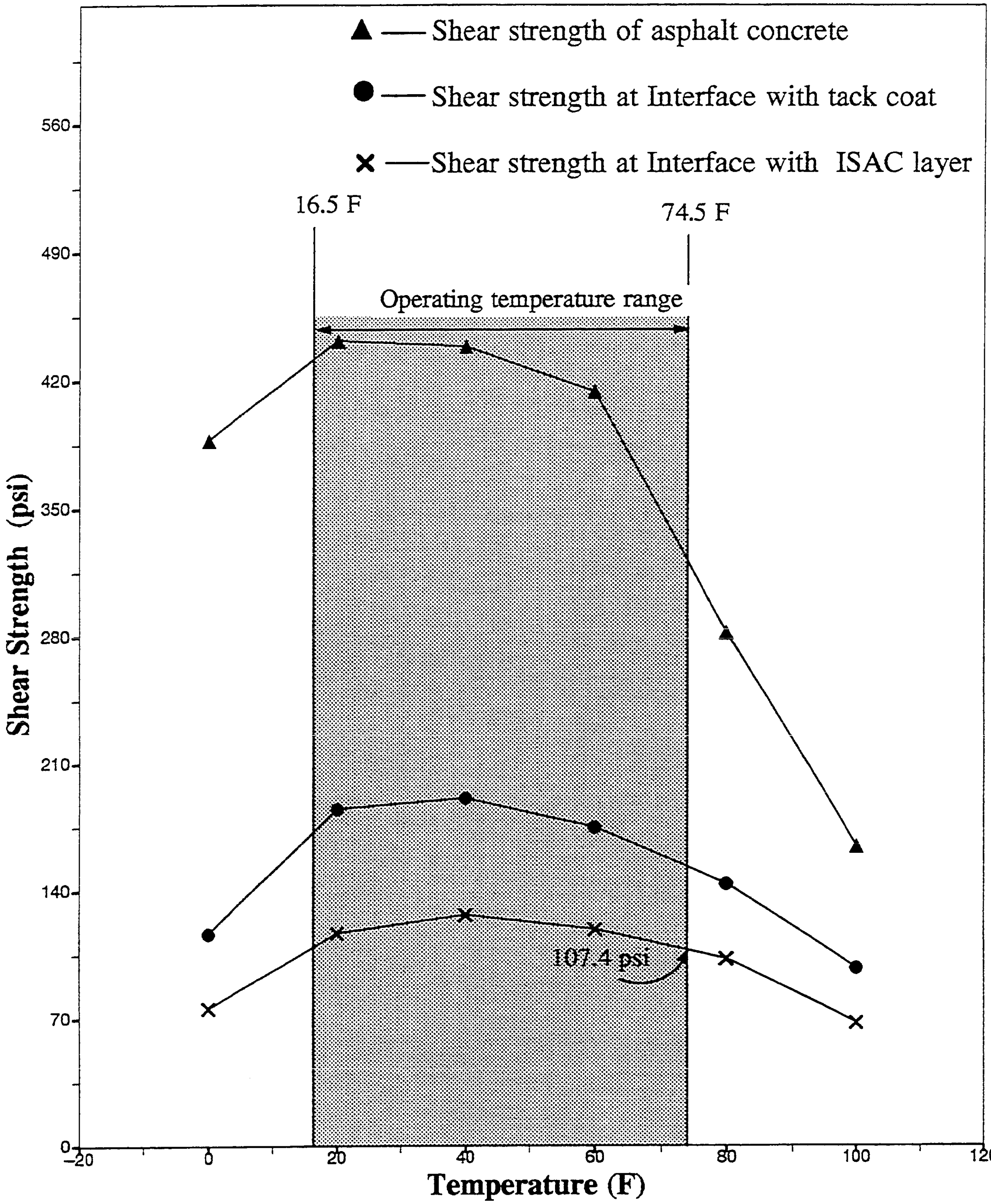

Figure 96: Shear Strength vs Temperature at 30 in./min Rate of Shear

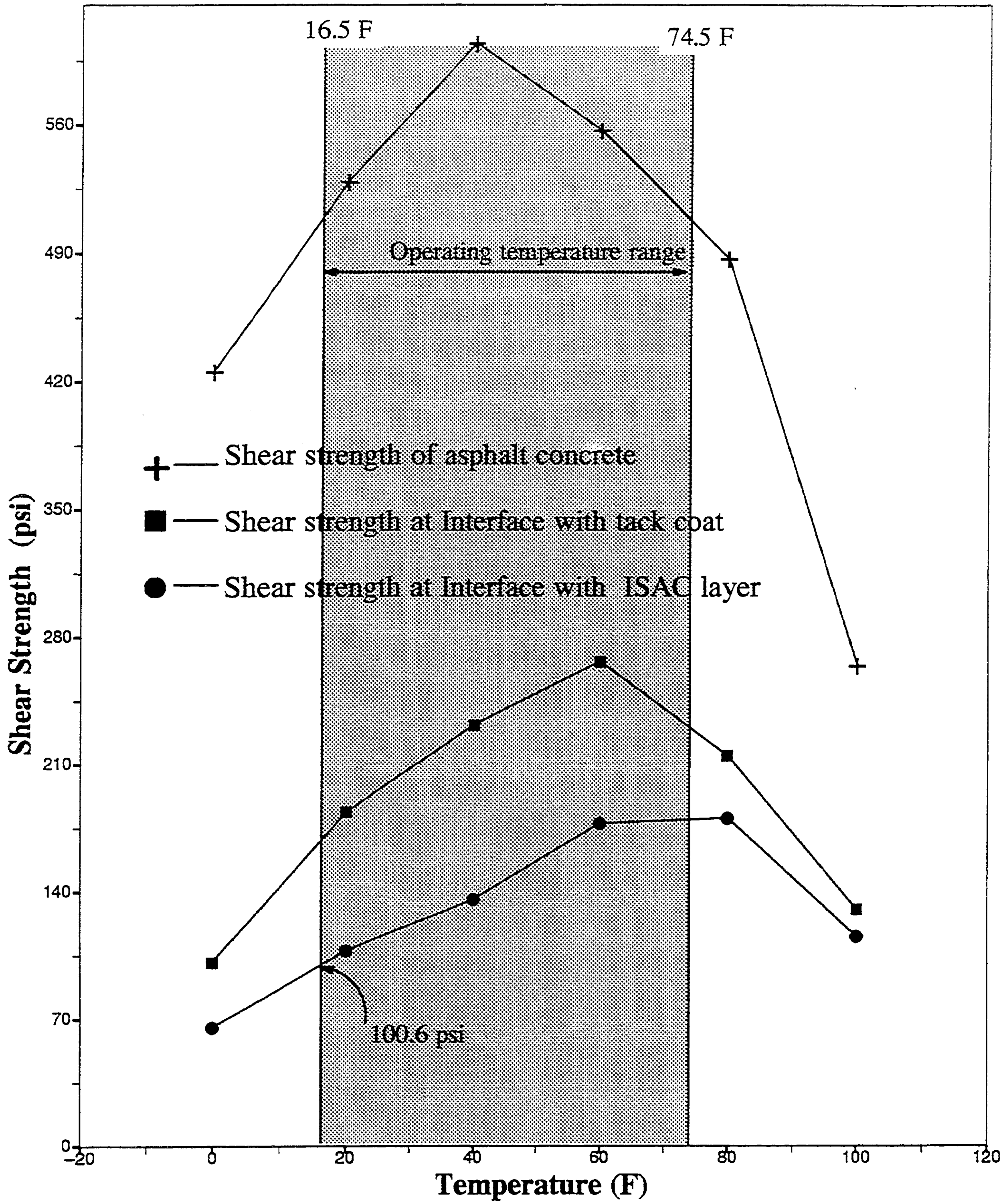

Figure 97: Shear Strength vs Temperature at 300 in./min Rate of Shear

7.3.5 Discussion on the Shear Strength of Fabricated ISAC Sample

Figures 86 through 89, Figures 95 through 97, and Table 19 and Table 20 were evaluated to relate the shear strength of ISAC with the shear stresses developing at the interface without ISAC. Based on this evaluation the following observations were made:

a) For a 2.5 in. thick overlay a shear stress of 43.7 psi developed in the horizontal plane at the interface, Table 19. For the no slippage conditions, shear strength of the ISAC layer placed at the interface should not be less than 43.7 psi for an operating temperature range of 16.5 F to 74.5 F, Table 10.

b) All the samples with the ISAC layer at the interface sheared along the rubber asphalt interface.

c) For all shear rates (1 in./min, 30 in./min and 300 in./min) in the operating temperature range, the shear strength of the sample with the ISAC layer at the interface was considerably less than the shear strength of the samples with the tack coat interface, Figures 95 through 97.

d) At high shear rate (300 in/min) within the operating temperature range, 16.5 F is the most critical temperature for shear strength of the ISAC interface, Figure 97. A 100.6 psi shear strength was developed in the ISAC interface at 16.5 F (Interpolating from Figure 97 and Table 20), which is considerably higher than the shear stress being developed at the interface without ISAC (43.7 psi). The ISAC sample was determined to be acceptable against slippage for high rate of shear.

e) At medium rate of shear (30 in/min) within the operating temperature range, 74.5 F is the most critical temperature for the shear strength of the ISAC layer interface, Figure 96. A 107.4 psi shear strength was developed in the ISAC interface at 74.5 F (Interpolating from Figure 96 and Table 20), which is far more than the shear stress being developed at the interface (43.7 psi). The ISAC sample was determined to be acceptable against slippage for medium rate of shear.

f) At slow rate of shear (1 in/min) within the operating temperature range, 74.5 F is the most critical temperature for shear strength of the ISAC layer interface, Figure 95. A shear strength of 39.9 psi was developed in the ISAC interface at 74.5 F (Interpolating from Figure 95 and Table 20), which is less than the shear stress being developed at the interface (43.7 psi). The ISAC layer was determined to be inadequate to resist slippage for slow rate of shear.

g) Based on this evaluation, the present ISAC core material was determined to be inadequate against slippage at slow rate of shear. The shear strength of the ISAC layer needed to be improved by modifying the properties of the rubber asphalt (its stiffness and temperature susceptibility) by adding a modifier.

7.4 Modified ISAC Layer

To ensure that the ISAC layer interface is resistant to slippage even at low rate of shear, the properties of the rubber asphalt (stiffness and temperature susceptibility)were improved by adding hydrated lime as a modifier. Hydrated lime will also serve as a mineral filler. To determine the most appropriate quantity of hydrated lime, a number of ISAC samples were prepared with different percentages of hydrated lime in the rubber asphalt mix. Samples were prepared with each type of ISAC core material in the same way as explained in Section 8.3.4.1 and tested for shear at 74.5 F. The samples were sheared at slow rate of shear (1in./min) on the shear device shown in Figure 92 since slow shear was a critical value. In Figure 98 the shear strength of these samples have been plotted against percentages of hydrated lime used in the rubber asphalt mix. Figure 98 can now be used to determine the percentages of hydrated lime in the rubber asphalt mix

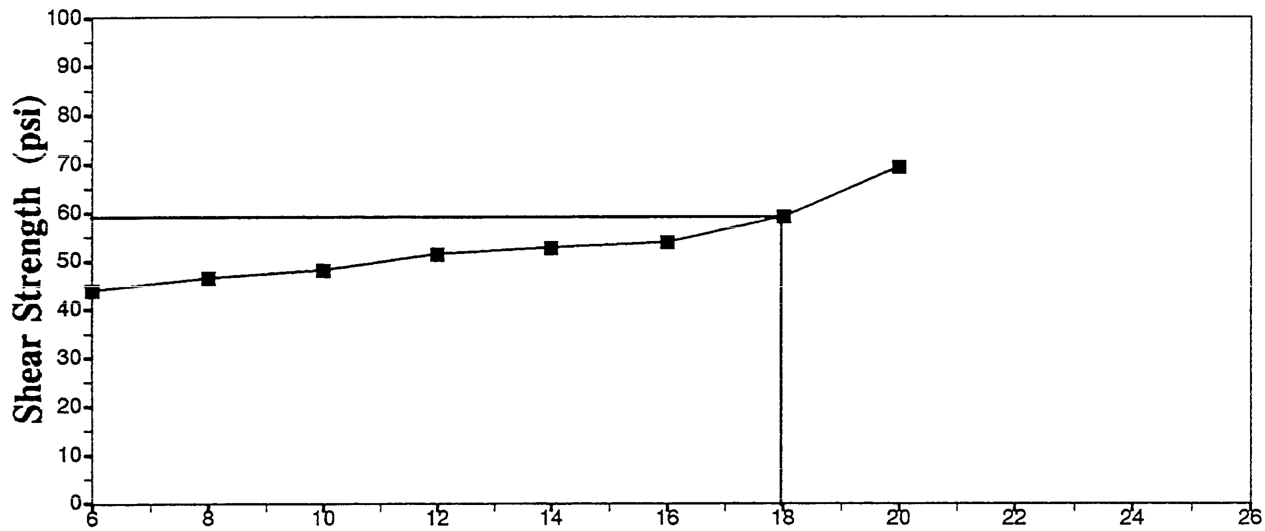

Figure 98: Shear Strength of various ISAC samples with different Percentages of Lime in The Rubber Asphalt mix (Rubber–25% of the total weight) Measured at 74.5 F and 1 in./min Rate of Shear

corresponding to the desired level of shear strength required in the ISAC interface. An ISAC with 18 % lime in the rubber asphalt provided 59.2 psi shear strength, which is roughly 36 % more than the shear stress developed at the interface (Taking 36 % as safety factor). Based on these findings the following mix formula was determined for the rubber asphalt used in the ISAC layer:

AC–20 ——— 57 % of total weight.

Crumb rubber— 25 % of total weight.

Hydrated lime— 18 % of total weight.

7.4.1 Temperature Stiffness Effects

A new ISAC sample was fabricated using the above mix formula and was checked for brittleness at low temperature. To check the temperature effect on brittleness of the modified ISAC layer laboratory testing was performed to determine the shear strength at the overlay interface. Pavement test specimens with different material at interface were prepared and testing was performed as in Section 7.3.4. Four types of test specimens were fabricated as follows:

a) AC section with no interface.

b) An AC overlay placed on a PCC pavement with tack coat at the interface.

c) An AC overlay placed on a PCC pavement having an ISAC core material with 75 % AC–20 and 25 % crumb rubber at the interface.

d) An AC overlay placed on a PCC pavement having an ISAC core material with 57 % AC–20, 25 % crumb rubber, and 18 % hydrated lime at the interface.

The samples were sheared at 0.05 in./min and at six different temperatures of 0 F, 20 F, 40 F, 60 F, 80 F and 100 F. The results are shown in Table 21 and Figure 99. From these results it may be noticed that shear strength of the modified ISAC significantly improved throughout the operating temperature range. The ISAC layer provided adequate performance properties and did not seem too brittle at low temperature. It is however felt that at lower temperatures (below 20 F) the rubber asphalt may become too stiff to allow any movement within the layer and absorb the induced stresses due to daily temperature variations during winter.

7.4.2 Stiffness Evaluation at Low Temperature

The stiffness of the rubber asphalt lime mix at low temperature was quantified and evaluated in order to optimize the design of the ISAC layer.Samples of the modified ISAC layer were prepared and sheared at 20 F and at an extremely slow rate of shear, 0.0016 in./min, which is a typically accepted as the rate of PCC slab movement during daily temperature variation. The shear strength vs horizontal displacement is shown in Figure 100.

The slope of the initial part of the curve in Figure 100 ie. ''Shear stress/ Displacement" was computed and defined as ''Initial Shear Displacement Modulus". In this case the available initial shear displacement modulus was $S_{aval} = 2210$ pci Figure 100.

Table 21: Shear Strength of Samples With Different Materials at Interface Sheared at Various Temperatures at 0.05 in./min Rate of Shear

Temp (F)	Shear strength (psi)			
	AC	Tack coat	ISAC	ISAC (Modified)
0	338	136	83	108.7
20	347	173	110	157
40	241	168	80	134.6
60	119	89	25	48
80	77	50	6	13
100	72	48	2	6.5

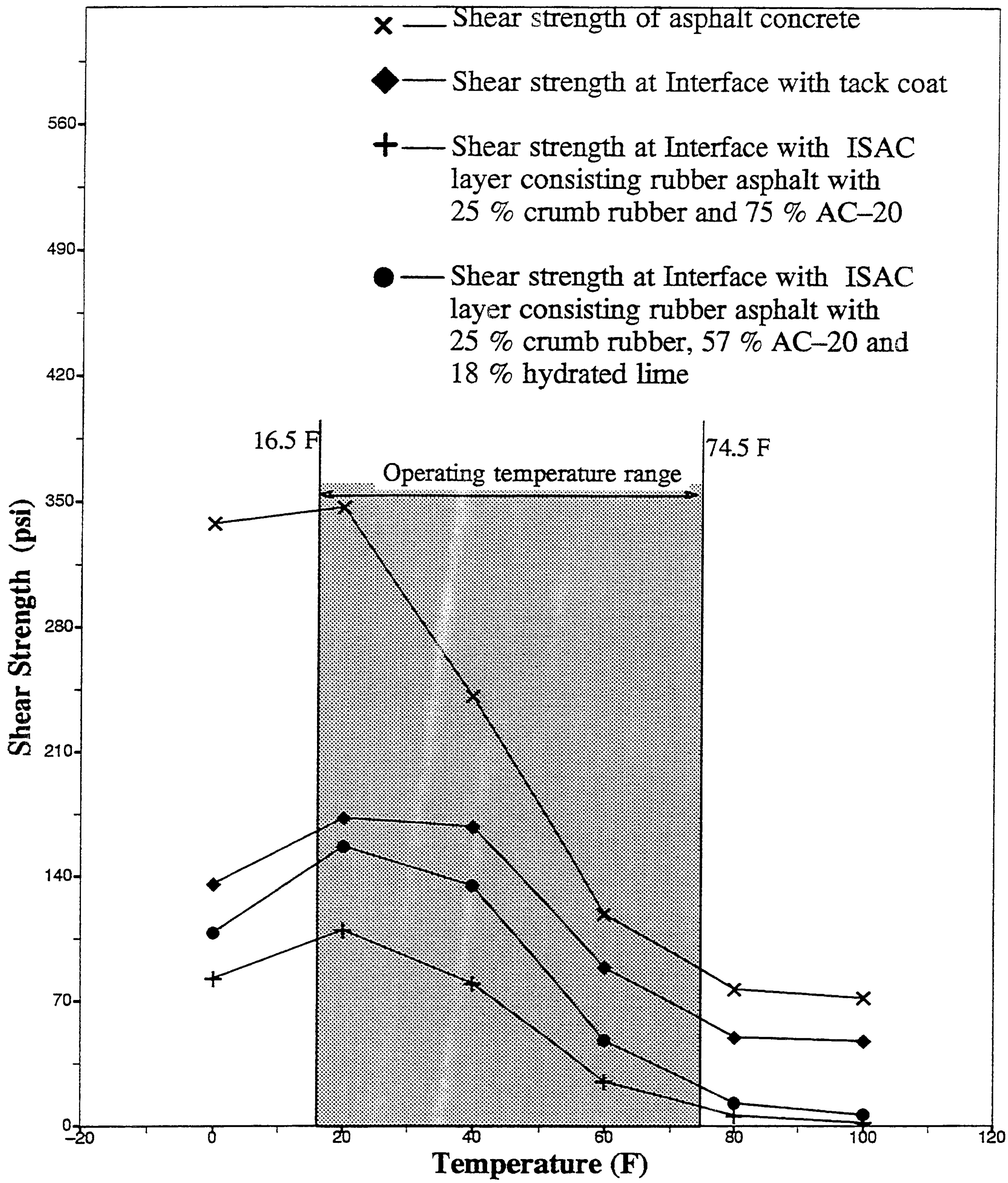

Figure 99: Shear Strength vs Temperature at 0.05 in./min Rate of Shear

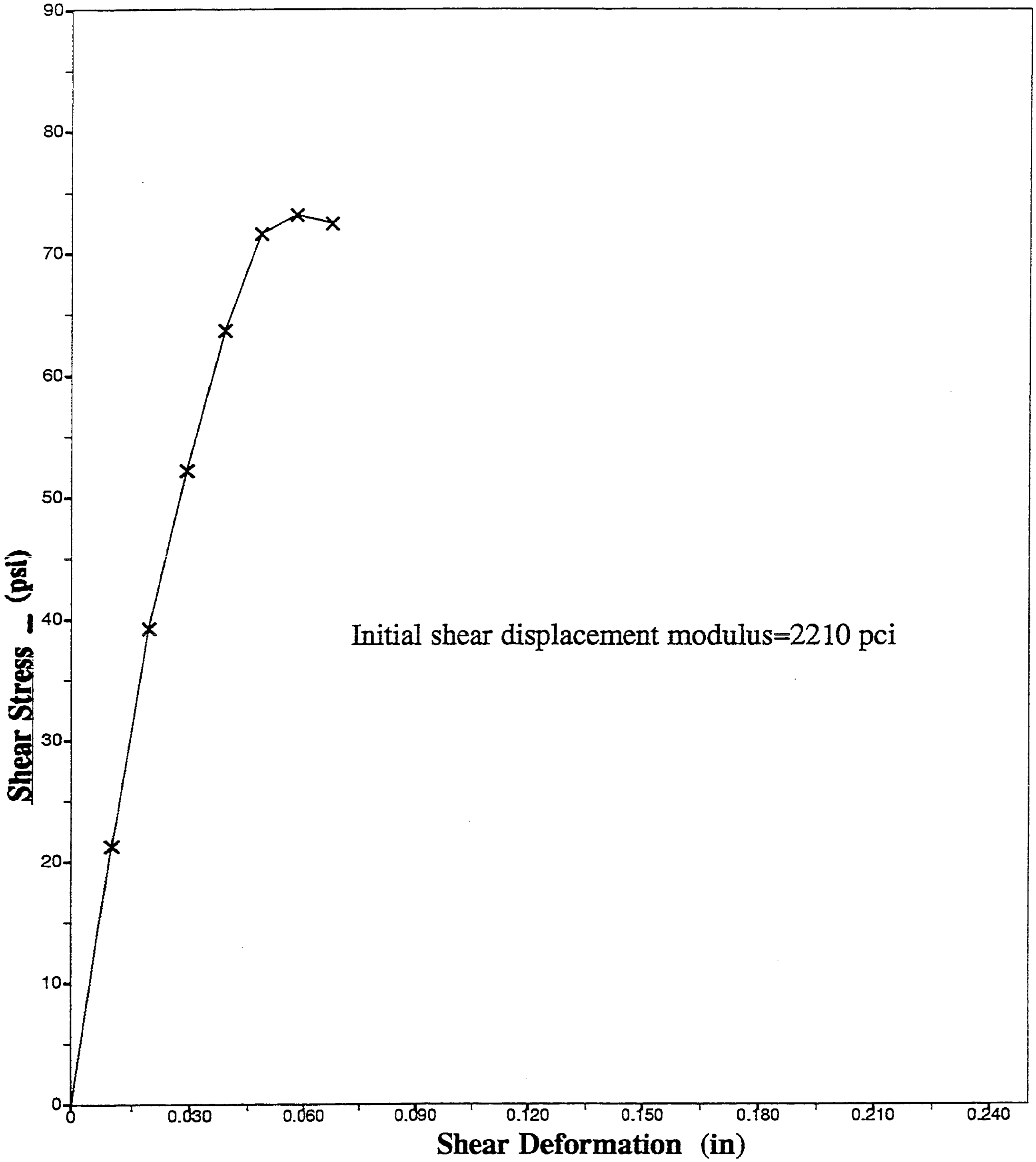

Figure 100: Shear Stress vs Shear Displacement For ISAC Layer With 18 % Lime 25 %Rubber and 57 % AC–20 at 20 F at 0.0016 in./min Rate of Shear

In order to understand the concept "of initial shear displacement modulus" consider a typical pavement section consisting of a 15 ft long PCC slab, an ISAC layer, and a 3 in. thick AC overlay, Figure 101.

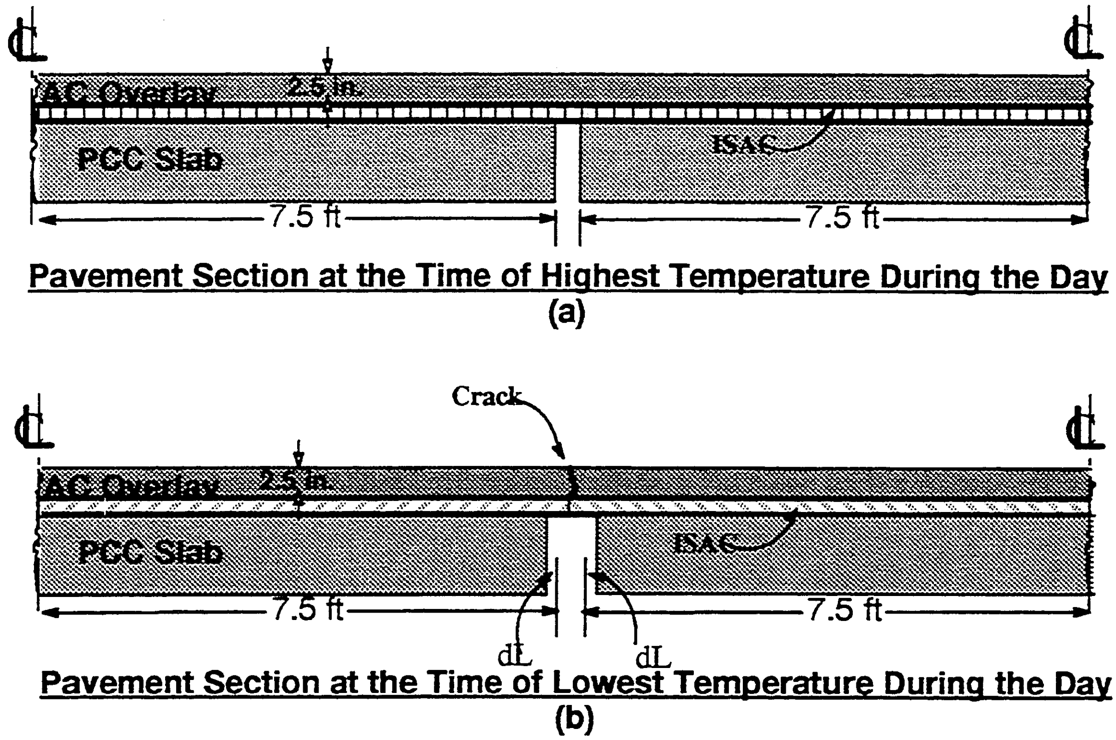

Figure 101: Transfer of Stresses to the ISAC Layer and the AC Overlay Through Shrinkage of PCC Slab Due to Daily Temperature Variation

From Figure 101:

Let dL be the length change in one half of the slab length .

dL =(Slab Length / 2) * Coefficient of thermal contraction

* Daily temperature variation

dL = {(15/2)*12} * (6E–6) * (13.5)

dL=0.00729 in.

Since the movement at the center of the slab will be zero, average displacement of the slab with respect to the AC overlay = 0.00729/2=0.003645 in. For each 1 in. width of pavement, the shear resistance presented by the ISAC layer to yield an average displacement of 0.003645 in. must be

=Average displacement * (Initial shear displacement modulus) * (Length of displacement)

=0.003645 * S * (7.5 * 12)

=0.32805 S lbs............................(1)

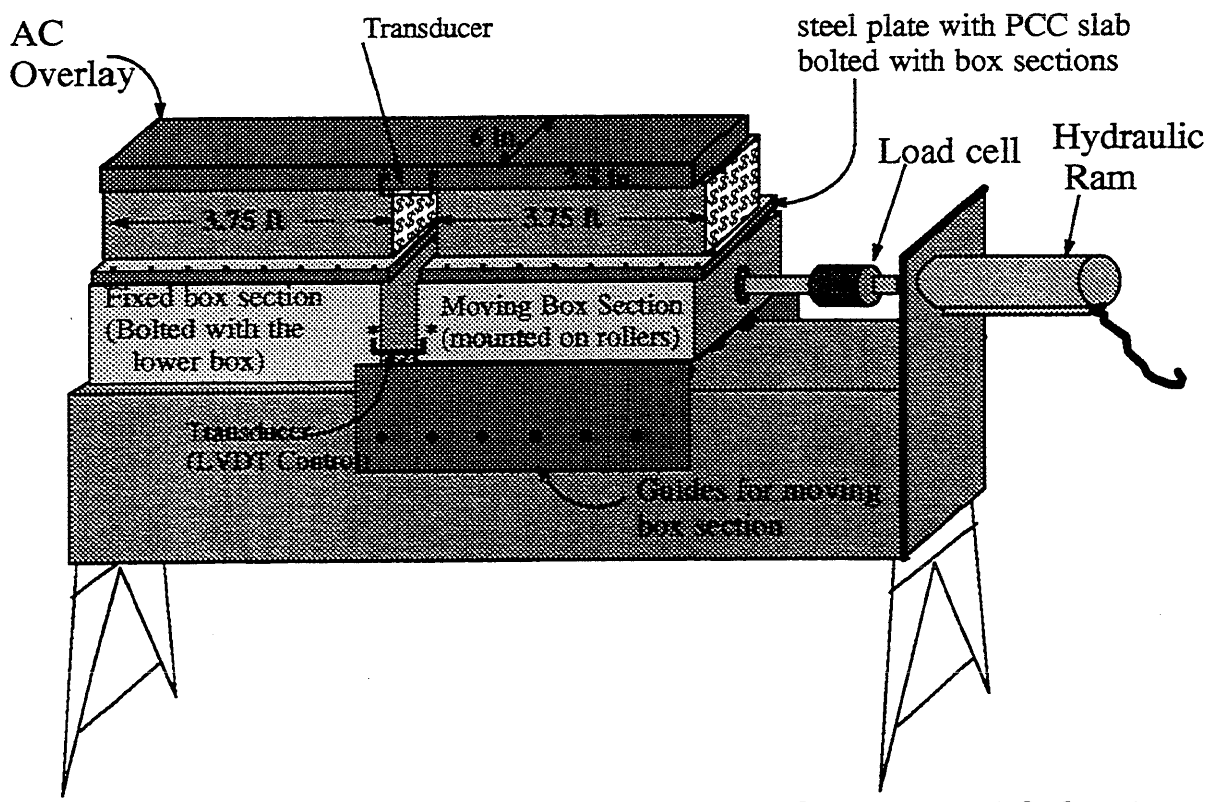

Figure 102: Device Used For Evaluating the Tensile Strength of AC Overlay at 20 F and With 0.0016 in./min. Rate of Pull

Assuming that no load is taken by the geotextile and all the stresses are transferred to the AC overlay, tensile stress transferred to the AC overlay at the time of cracking = Tensile strength in AC overlay at 20 F and at 0.0016 in./min rate of pull * cross sectional area of the AC overlay

= 275 * (2.5*1)

(An AC overlay at 20 F was pulled at 0.0016 in./min rate using equipment shown in Figure 102 and tensile strength of the AC overlay was evaluated as 275 psi in the laboratory. The operating mechanism of the testing equipment has been more elaborately explained in section 8.2 and Figure 106.)

= 687.5 lbs ....(2)

For limiting conditions, equating (1) and (2) above

0.32805 S = 687.5

S=2095 pci

Thus the maximum permissible initial shear displacement modulus of

ISAC = $S_{permissible}$ = ***2095 pci***

Whereas S_{aval} = 2210 pci

Since $S_{aval} > S_{permissible}$, ISAC is believed to be too stiff to function properly at cold temperature and needs to be improved.

7.5 Modified ISAC Layer With Lower Stiffness

To develop ISAC with appropriate stiffness, 30 % crumb rubber was used instead of 25 % and three types of ISAC layers were developed using 10 %, 12.5 % and 15 % lime in the rubber asphalt lime mix. Samples were prepared

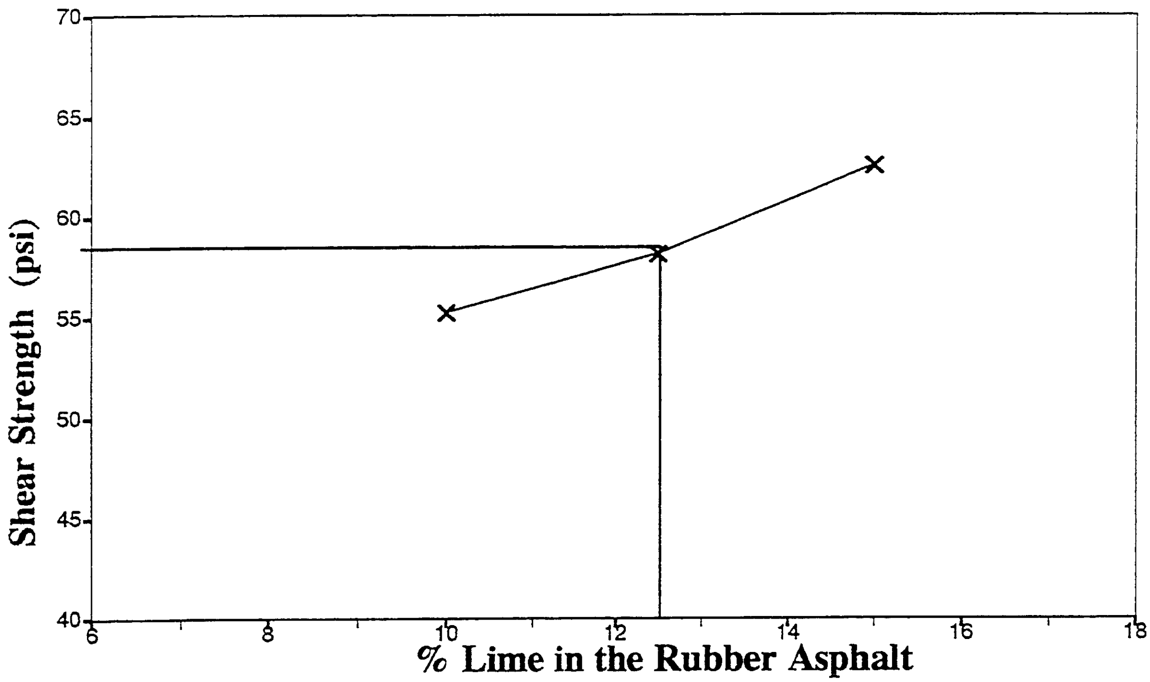

Figure 103: Shear Strength of various ISAC samples with different Percentages of Lime in The Rubber Asphalt mix (30 % Rubber) measured at 74.5 F and 1 in./min Rate of Shear

and sheared at 74.5 F and 1 in./min rate of shear. Shear strength vs percentage of lime has been presented in Figure 103. From the Figure 103 it is observed that a mix with 12.5 % hydrated lime, 30 % rubber, and 57.5 % AC–20 provides 58.2 psi shear strength which is 33 % more than the 43.7 psi shear stress required at the tack coat interface (33 % safety factor in this case).

7.5.1 Check For Temperature Stiffness Effects

An ISAC layer with rubber asphalt having 57.5 % AC–20 (of total weight), 30 % crumb rubber (of total weight), and 12.5 % hydrated lime (of total weight)was fabricated and samples were prepared and tested as described in Section 7.4. The results from these tests are shown in Table 22 and

Figure 104. From these results it is seen that the shear strength of this ISAC layer also improved throughout the operating temperature range. It appears

Table – 22: Shear Strength of Samples With Different Materials at Interface sheared at Various temperatures at 0.05 in/min rate of shear

Temp (F)	Shear strength (psi)				
	ISAC	AC	Tack coat {75% AC 25% rubber}	ISAC {57.5% AC 30% rubber 12.5 % lime}	ISAC {57% AC 25% rubber 18% lime}
0	338	136	83	103.8	108.7
20	347	173	110	124	157
40	241	168	80	97.2	134.6
60	119	89	25	44.2	48
80	77	50	6	11.5	13
100	72	48	2	6.7	6.5

to be safe against brittleness. It may also be noted in Figure 104 that this ISAC had shear strength almost equal to that of the ISAC with 18 % lime in its core material but its stiffness at lower temperature was considerably reduced.

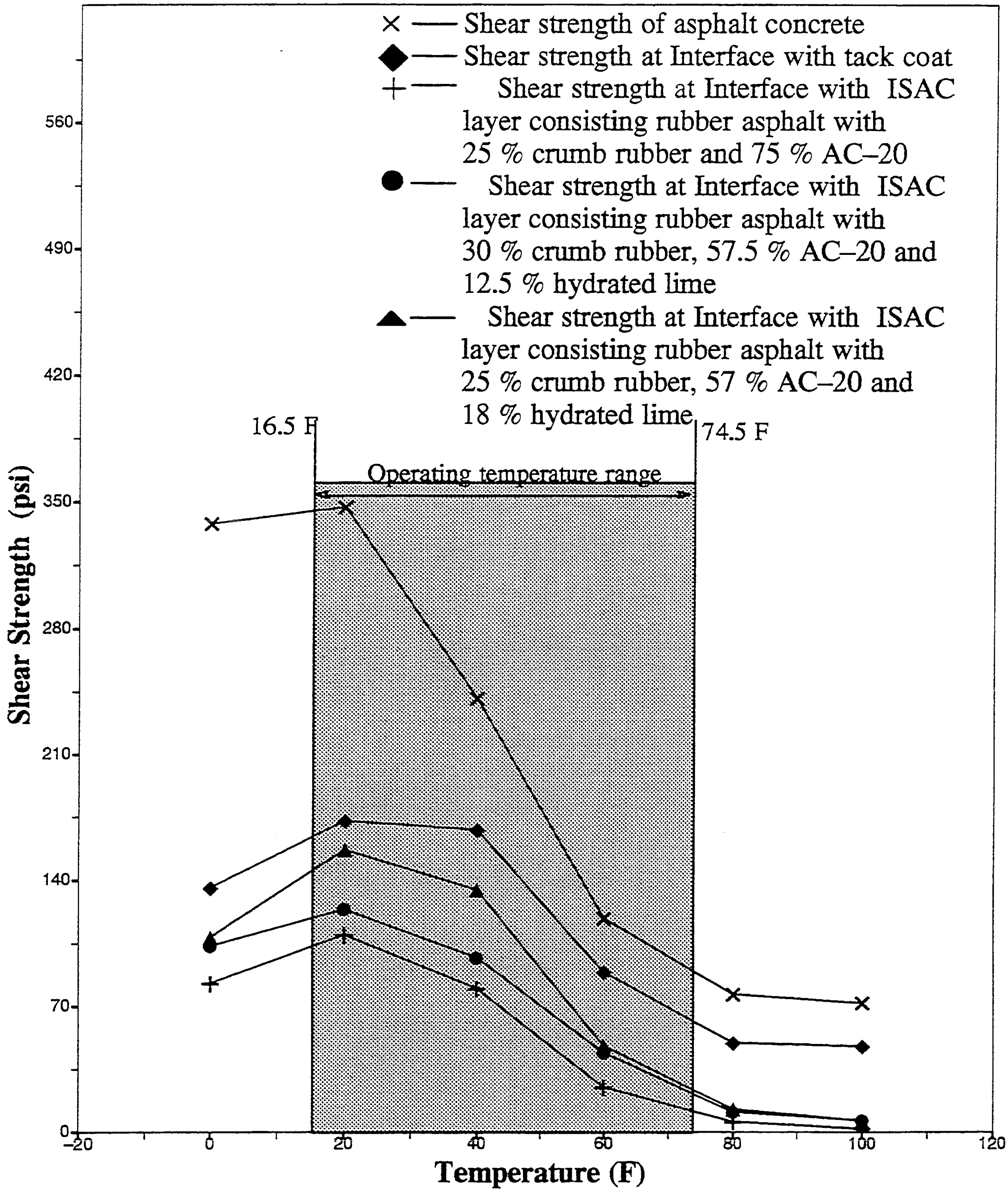

Figure 104: Shear Strength vs Temperature at 0.05 in./min Rate of Shear

7.5.2 Check For Stiffness at Low Temperature

A check for stiffness in the new ISAC was carried out by the same procedure as discussed in Section 7.4.2 for the ISAC with 18 % lime in the core material. Samples were prepared and sheared at 20 F and 0.0016 in./min shear rate. The shear strength vs horizontal displacement for the new ISAC is

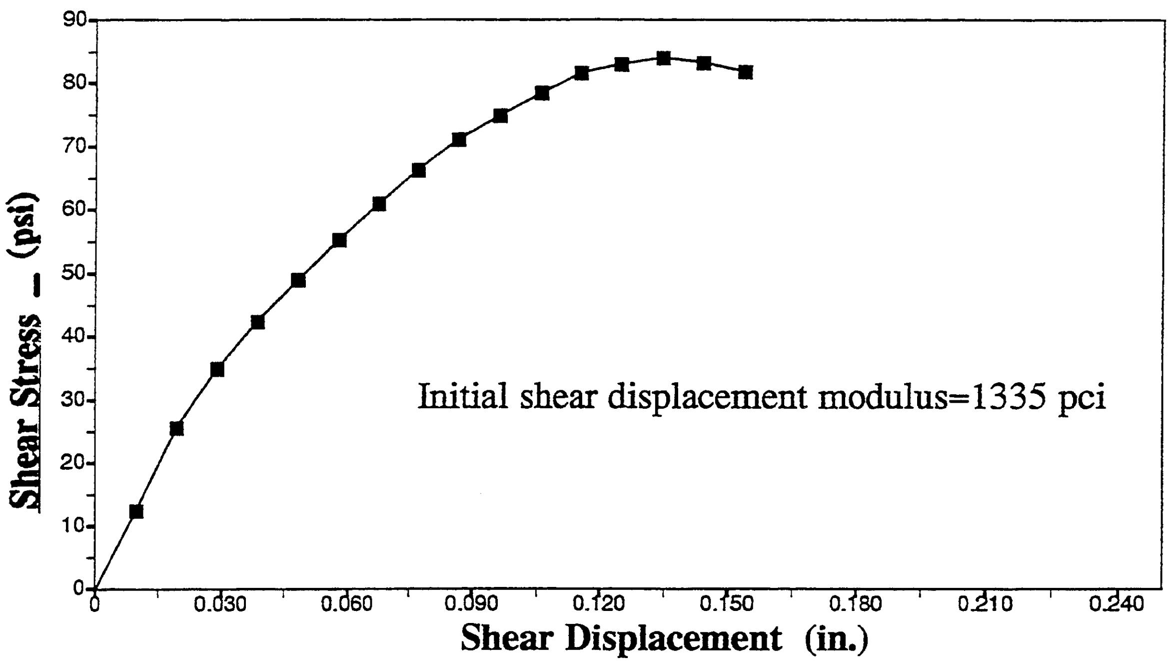

Figure 105: Shear Stress vs Shear Displacement For ISAC Layer With 12.5 % Lime 30 %Rubber and 57.5 % AC–20 At 20 F @ 0.0016 in./min Rate of Shear

shown in Figure 105. From Figure 105 "the initial shear displacement modulus" for the new ISAC layer = S_{aval} = 1335 pci.

From Section 7.4.2 the maximum permissible "Initial shear displacement modulus" = $S_{permissible}$ = 2095 pci.

Since $S_{aval} < S_{permissible}$, this ISAC should perform well at low temperature. Thus a rubber asphalt lime mix with the following formula was finally selected for use in the ISAC layer:

AC–20 ——— 57.5 % of total weight.

Crumb Rubber — 30 % of total weight.

Hydrated Lime — 12.5 % of total weight.

CHAPTER 8

LABORATORY TESTING AND EVALUATION OF ISAC

8.1 Introduction

After having satisfied the design parameters and developed the individual components of the ISAC system, its effectiveness for mitigating reflection cracking in an AC overlay was evaluated. Prior to testing ISAC in the field, it is important to evaluate its performance under simulated field conditions in the laboratory. A model pavement section with an AC overlay placed on a jointed PCC slab was constructed and placed in an environmental chamber. A mechanical device was used to simulate thermal strain in the slab and the joint was opened and closed at an extremely slow rate. Propagation of cracking in the overlay was monitored and performance of ISAC was evaluated by comparing the cycles to failure of an ISAC treated overlay with a control section without ISAC. The effect of joint expansion (which is a function of slab length and the seasonal temperature variation) was also evaluated for the ISAC system.

8.2 Testing Equipment and Methods

The components of the testing equipment and the materials arrangement are shown in Figure 106 a through Figure 106 e. The testing equipment, Figure 106 a, consists of one fixed section and a second horizontally movable section on rollers. A 6 in. wide and 7.5 ft long pavement section consisting of a 5 in. thick PCC slab, ISAC layer, and 2.5 in. of AC was placed on top of the two box

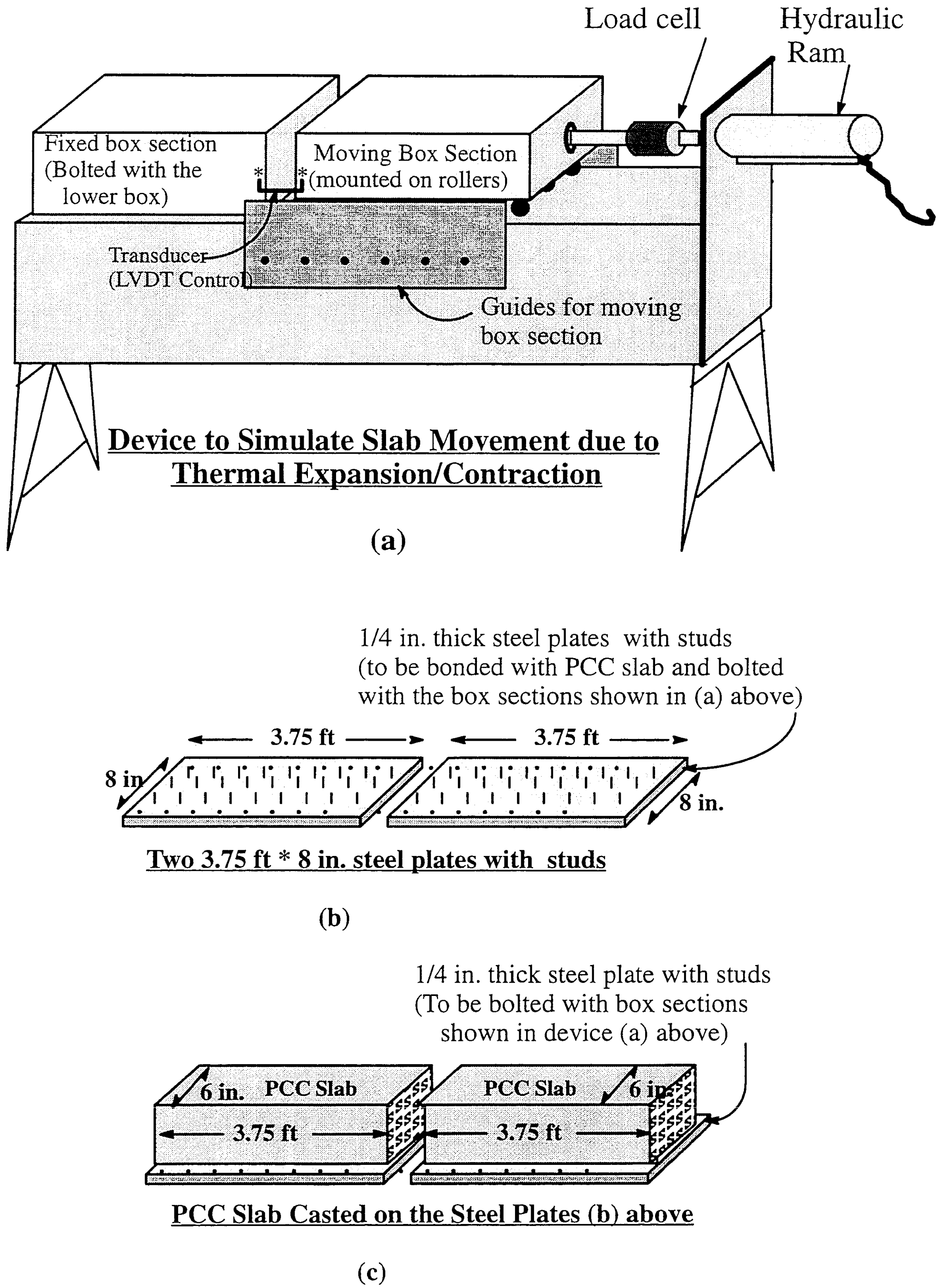

Figure 106: Diagrammatic Layout of Device for Testing the Overlay Against Thermal Cracking

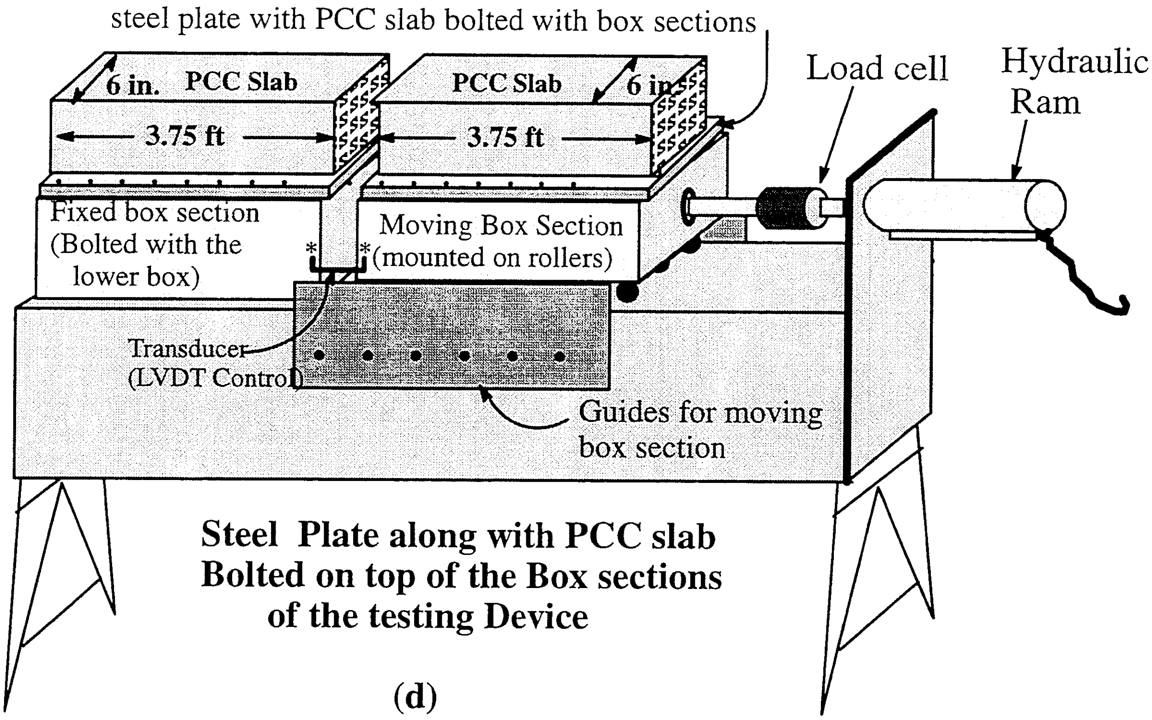

Steel Plate along with PCC slab Bolted on top of the Box sections of the testing Device

(d)

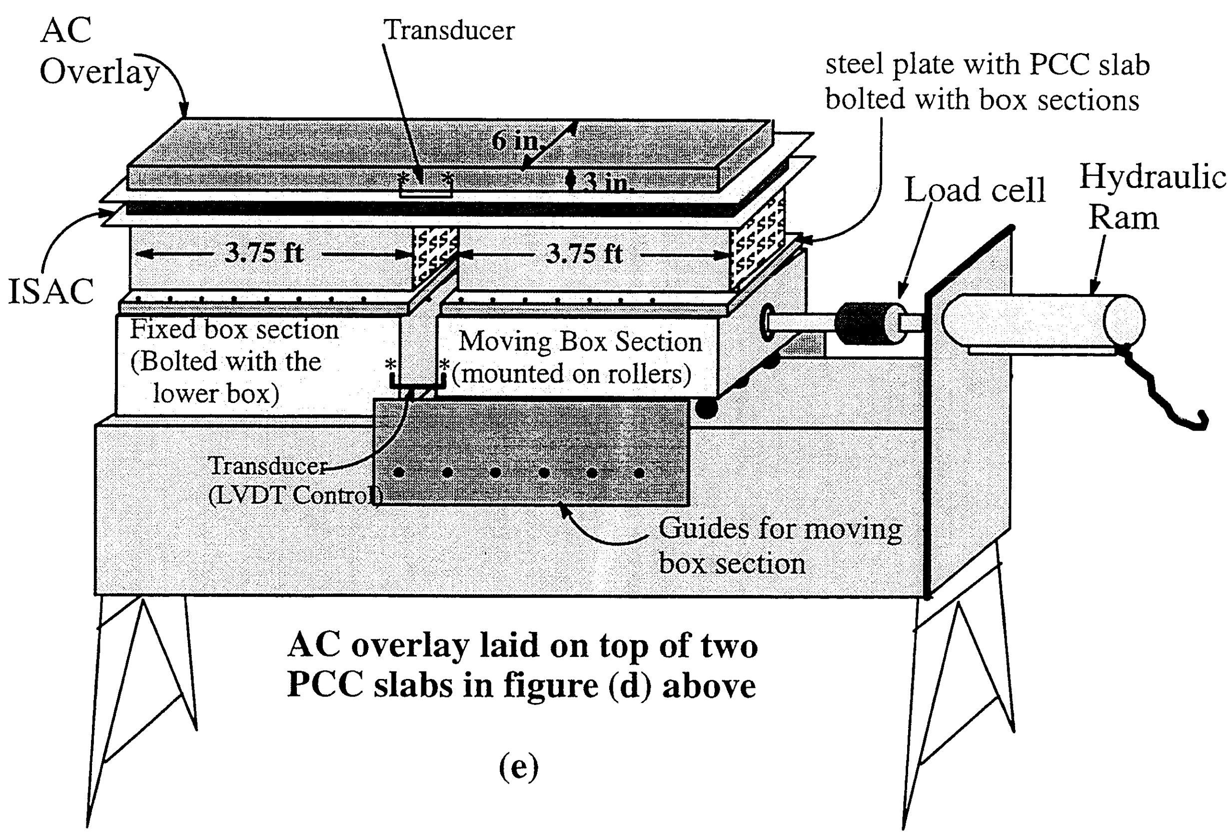

AC overlay laid on top of two PCC slabs in figure (d) above

(e)

Figure 106: Diagrammatic Layout of Device for Testing the Overlay Against Thermal Cracking

sections, Figure 106 b through Figure 106 e. The movable box section is attached to a hydraulic ram which opens and closes the PCC slab joint very slowly at 0.0016 in./min. A load cell placed between the movable box section and the hydraulic ramp indicates the force exerted by the hydraulic ram as it opens and closes the PCC slab joint. An LVDT device was located across the fixed and movable box sections to indicate relative movement of the two box sections. The testing device was placed into an environmental chamber which was held at 30 F during testing.

For attaching the pavement section on top of the two steel box sections, two 3.75 ft by 8 in. by 1/4 in. steel plates with steel studs were used, Figure 106 b. The PCC slab was caste on the studded side of the plates, Figure 106c, and after curing the plates were bolted on top of the two box sections, Figure 106 d. An initial joint opening between the two slabs of 1/4 in. was set by adjusting the hydraulic ram.

A pavement control section without ISAC and a pavement section with ISAC were prepared for evaluation. To prepare the pavement control section, an appropriate amount of tack coat was applied on the two PCC slabs and a 6 in. wide and 2.5 in. thick AC overlay was placed on top. To prepare an ISAC treated pavement section, tack coat was applied on the two PCC slabs, a 6 in. wide and 7.5 ft long section of ISAC was placed over the tack coated surface with the low strength geotextile towards bottom, and a 6 in. wide and 2.5 in. thick AC overlay was placed on top, Figure 106e.

An LVDT device was attached on the side of the overlay across the joint to

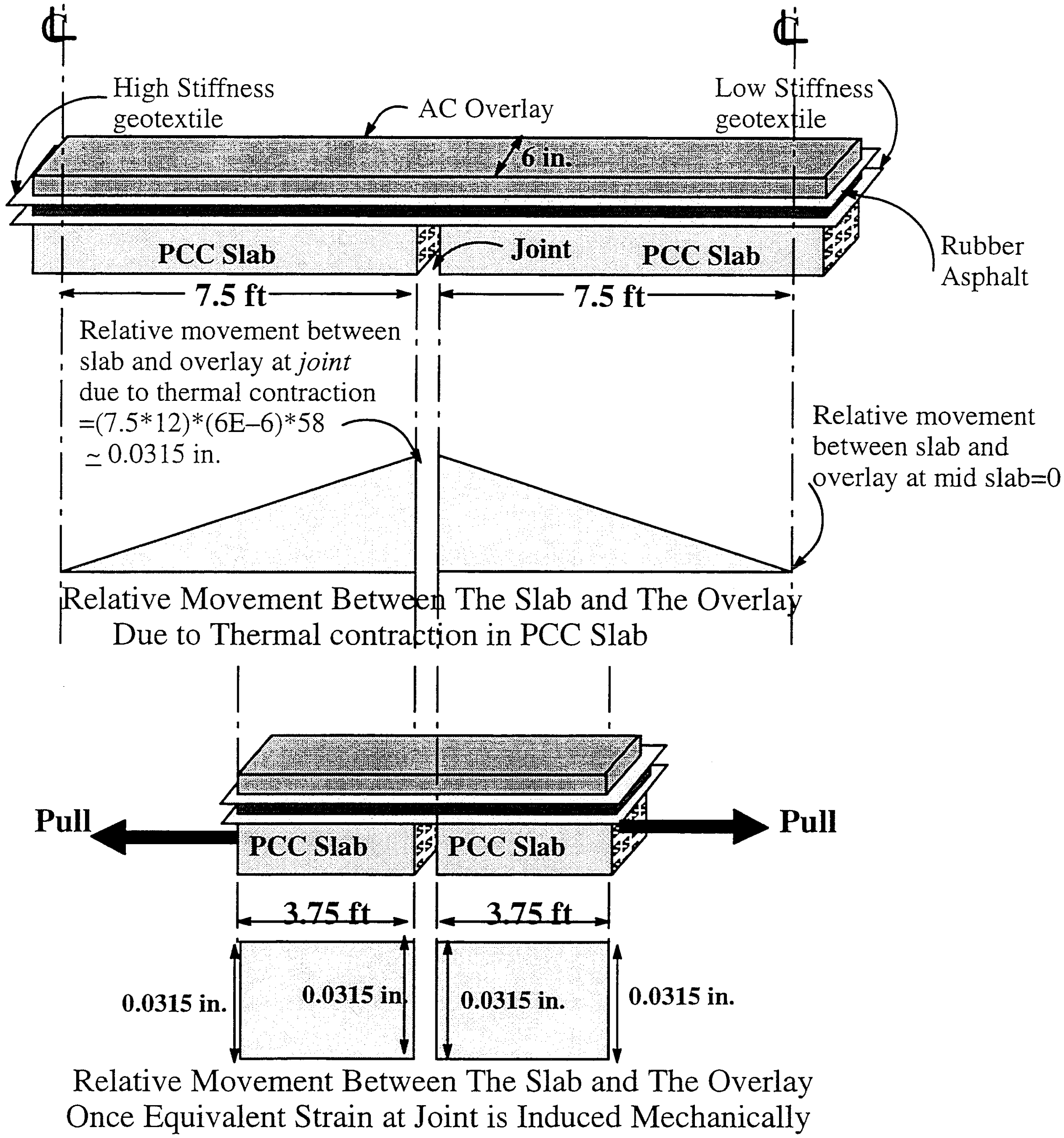

3.75 ft long PCC slab once pulled mechanically by 0.0315 in. will induce the same amount of shear resistance in the tack coat/ISAC at interface as the one developed at interface once 0.0315 in. expansion takes place at the joint due to thermal contraction in 7.5 ft long slab.

Figure 107: Effect of Mechanically Induced Thermal Strain on the Slab Length For Laboratory Testing

monitor any strain or cracking in the overlay above the joint. The LVDT and the load cell were connected to two separate plotters which plotted the strain/crack opening in the overlay above the joint and the force in the load cell against time.

The overlay was allowed to cool to 30 F before the movable box section was cycled back and forth by the hydraulic ram over a distance of 0.063 in. at a rate of 0.0016 in./min. In order to duplicate a worse case solution it would be advantageous to test ISAC at 16.5 F which is the minimum average field temperature, but the servo electronic system used in the testing device will not function properly below 30 F. The test was therefore conducted at 30 F. The shear strength of the rubber asphalt (core material of the ISAC) at 30 F was, however, similar to that at 16.5 F (Figure 104). Generally 0.0016 in./min was determined as the rate of PCC slab movement caused by seasonal or daily temperature variation and 0.063 in. is equivalent to the joint expansion which will occur due to seasonal temperature variation of 58 F, Table 10, in a pavement with 15 ft long PCC slabs (see Section 7.1.4).

It may be noted that a 7.5 ft long PCC slab moved mechanically through a distance of 0.063 in. will induce the same amount of shear force in the tack coat/ ISAC interface as 0.063 in. of expansion at the joint caused by thermal contraction of a 15 ft long slab. The mechanics for this procedure are explained in Figure 107.

8.3 Test Results

A pavement control section without ISAC and a pavement section with ISAC were evaluated to make performance comparisons.

8.3.1 Control Section

This test was performed using the equipment described in Section 8.2. The test pavement section had the following configuration:

a) Overlay thickness=2.5 in.

b) Joint crack width at start =1/4 in.

c) Total joint expansion=0.063 in. (Assuming 15 ft long slab)

Prior to placing the AC overlay an appropriate quantity of AC–10 tack coat (using formula mentioned in Section 3.3.2.8) was applied to the surface of the PCC slab. The LVDT device attached on the side of the overlay across the joint had a gauge length of 1 in. in this case. The PCC slab and AC overlay was allowed to cool to 30 F and the PCC slab was then subjected to 0.063 in. of cyclic movement at the rate of 0.0016 in./min. One cycle consisted of pulling the movable slab by 0.063 in. and then pushing it back to its original position at a rate of 0.0016 in./min which took 79 min and simulated seasonal temperature changes over one year. Forces in the load cell and strains in the AC overlay above the joint (obtained from LVDT device on overlay) were plotted against time in cycles, Figure 108. Plaster of paris was applied on the side of the overlay above the joint so that the crack growth could be monitored visually. The crack growth was plotted against number of cycles as shown in Figure 109. In Figure 108 it is observed that as the number of cycles increased, the maximum force in the load cell decreased and the maximum strain in the overlay above the joint increased. During the 7th cycle the AC overlay split apart as indicated by a highly visible wide crack. From Figure 109 it may be

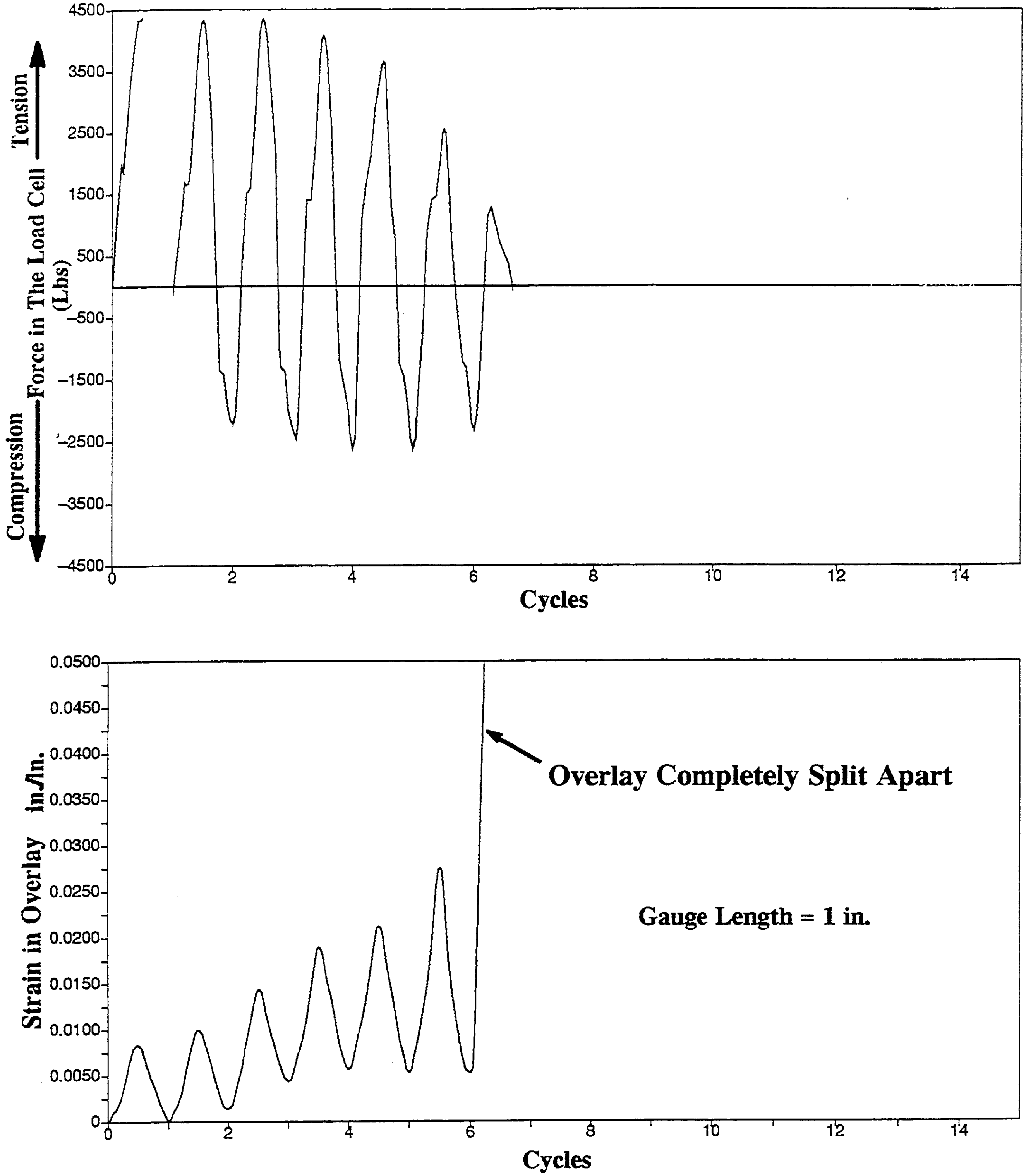

Figure 108: Force in Load Cell and Strain in Overlay as a Function of Test Cycles For a Pavement Control Section

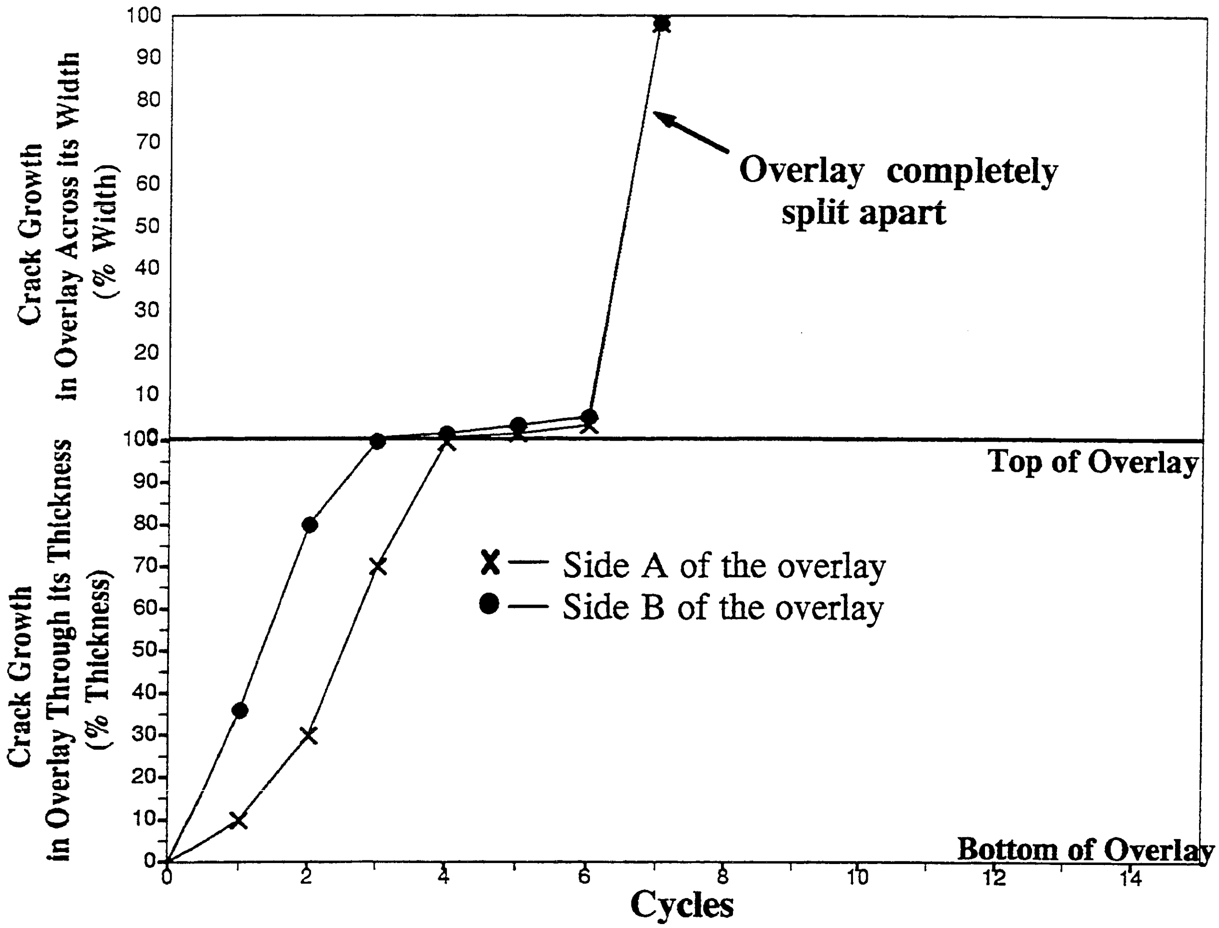

Figure 109: Crack Growth in Overlay vs Number of Cycles of Slab Movement For a Pavement Control Section

noticed that on one side of the AC overlay the crack propagated from the bottom and traveled through the depth in 3 cycles. On the other side of the overlay the crack traveled from bottom to top in 4 cycles. Both the cracks then traveled across the top of the overlay and joined with each other during the 7th cycle.

8.3.2 ISAC System Test No. 1

This pavement test section had a configuration similar to the control section and was treated with an ISAC layer as designed in Section 8.5. After applying the the tack coat on the PCC slab, ISAC was placed with its low strength geotextile towards bottom. A tack coat was applied over the ISAC layer and a 2.5 in. thick AC overlay was then placed on top. The LVDT device attached on the side of the AC overlay across the joint had a gauge length of 5 in. in this case. The test was performed using the same procedures as those for the control pavement. It must be added that the total displacement set on the signal generator (programmable equipment) for the PCC slab was 0.063 in. but once the test was being conducted it was observed from a dial gauge that the slab moved by 0.072 in. instead of 0.063 in. This test was allowed to run for 100 cycles since no signs of cracking in the overlay were observed. After 100 cycles the test with 0.072 in. movement was discontinued. The results from the test are shown in Figure 110. From the figure it may be noted that the maximum force in the load cell and the maximum strain in the overlay above the joint was substantially less than those in the control section. It may also be noted that unlike the control section the increasing number of cycles in this test had little effect on the maximum stain in the overlay. Even after 100 cycles maximum strain in the overlay was just 0.006 in./in. The slight increase in strain that was observed in the overlay could be caused by the elongation which took place in geotextile due to repeated load.

8.3.3 ISAC System Test No. 2

The test specimen which was used in Test No. 1 was evaluated further in Test No 2 and was subjected to 0.11 in. movement instead of 0.072 in. The test was conducted for 25 cycles and was discontinued after no signs of cracking

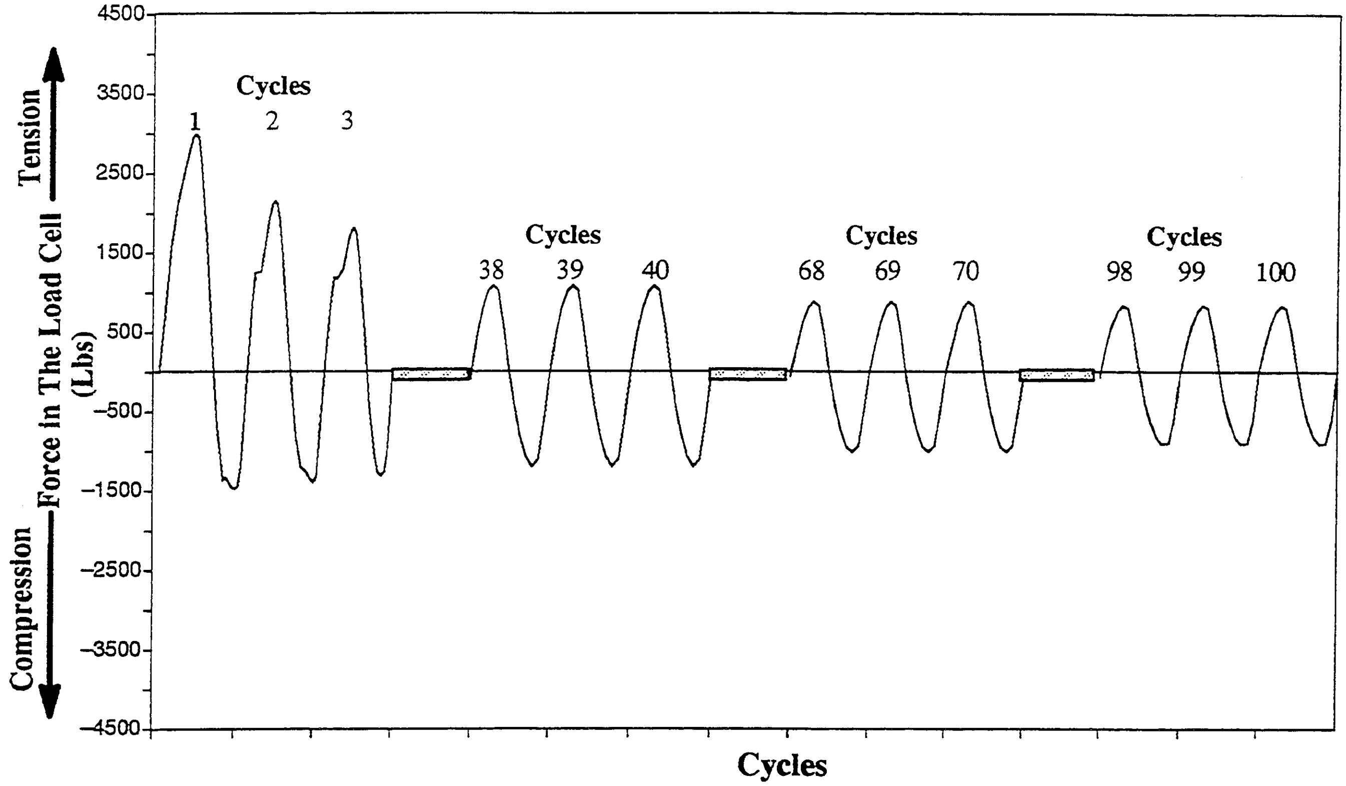

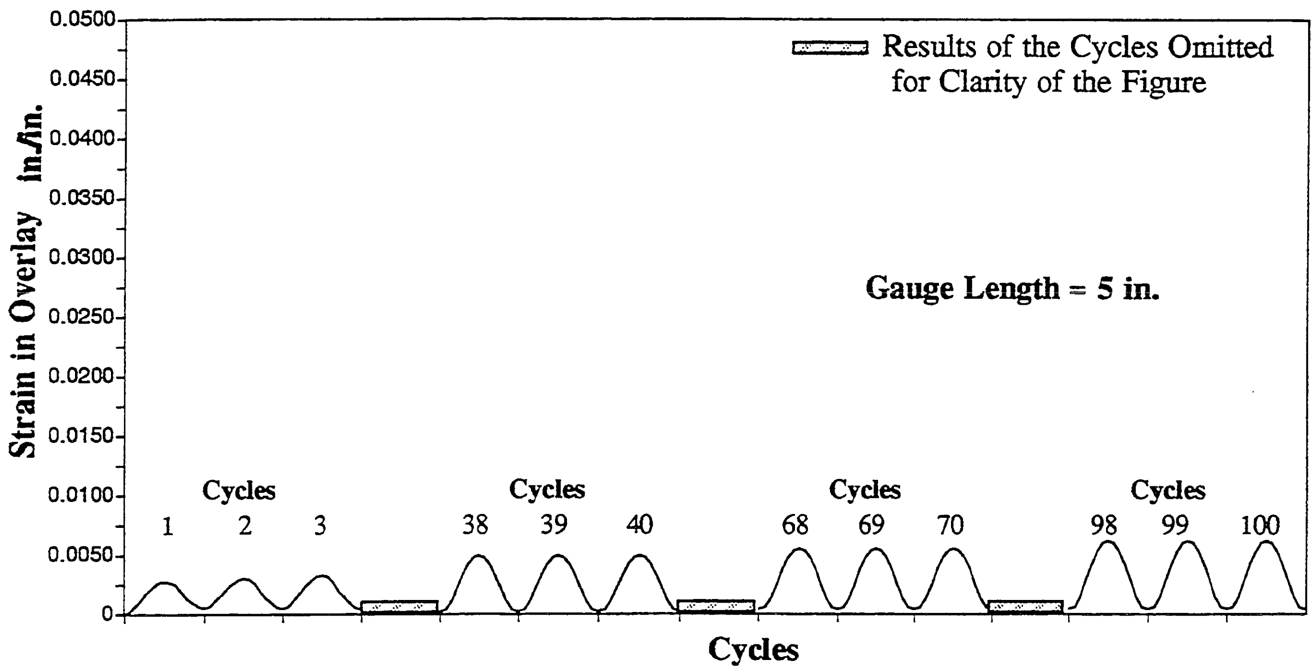

Figure 110: Force in Load Cell and Strain in Overlay as a Function of Test Cycles For a Pavement Section Treated With ISAC (Joint Expanded by 0.072 in. For 100 Cycles)

occurred. The results from this test are shown in Figure 111.

8.3.4 ISAC System Test No. 3

The original ISAC test specimen was now subjected to 0.135 in. movement in Test No.3. The test was conducted for 10 cycles before it was discontinued without any sign of cracking. A number of vertical hair line cracks however appeared on the plaster of paris when the slab joint was fully expanded during a cycle. The cracks were spread over a distance of about 1.5 ft on either side of the joint and were more closely spaced near the joint than away from the joint. These cracks were only visible in the plaster of paris and not visible in the asphalt concrete material. The brittle behavior of the plaster of paris as compared to the asphalt concrete material helped to make the cracks distinguishable in the plaster of paris. The results are shown in Figure 112.

8.3.5 ISAC System Test No. 4

The ISAC system test was continued with 0.16 in. joint expansion. The test was conducted for 10 cycles before it was discontinued without any sign of cracking. There was a slight indication of aggregate raveling on the top surface of the overlay above the joint once the joint was fully expanded during the slab movement in the last two or three cycles of this test. The results are shown in Figure 113.

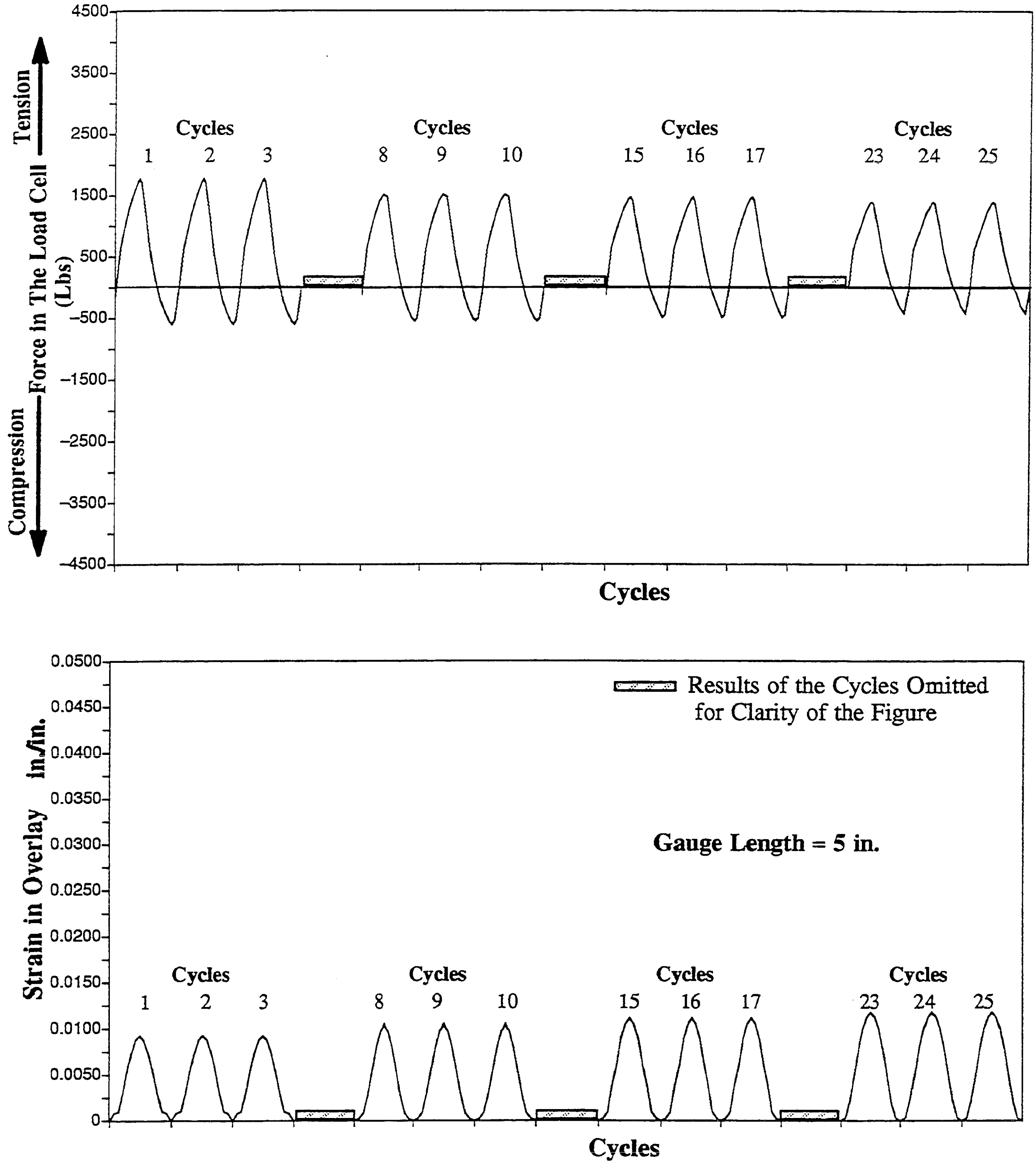

Figure 111: Force in Load Cell and Strain in Overlay as a Function of Test Cycles For a Pavement Section Treated With ISAC (Joint Expanded by 0.11 in. For 25 Cycles)

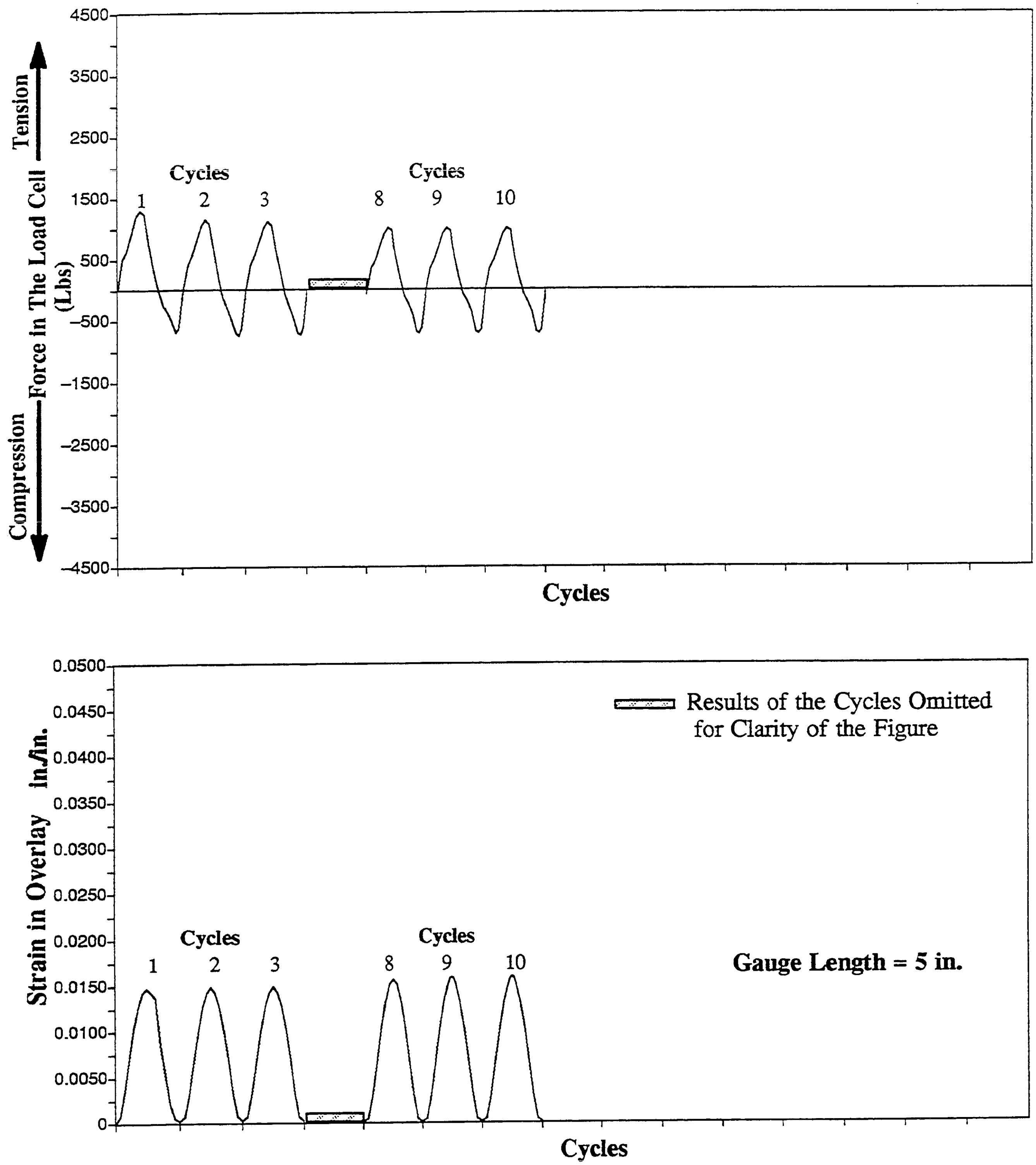

Figure 112: Force in Load Cell and Strain in Overlay as a Function of Test Cycles For a Pavement Section Treated With ISAC (Joint Expanded by 0.135 in. For 10 Cycles)

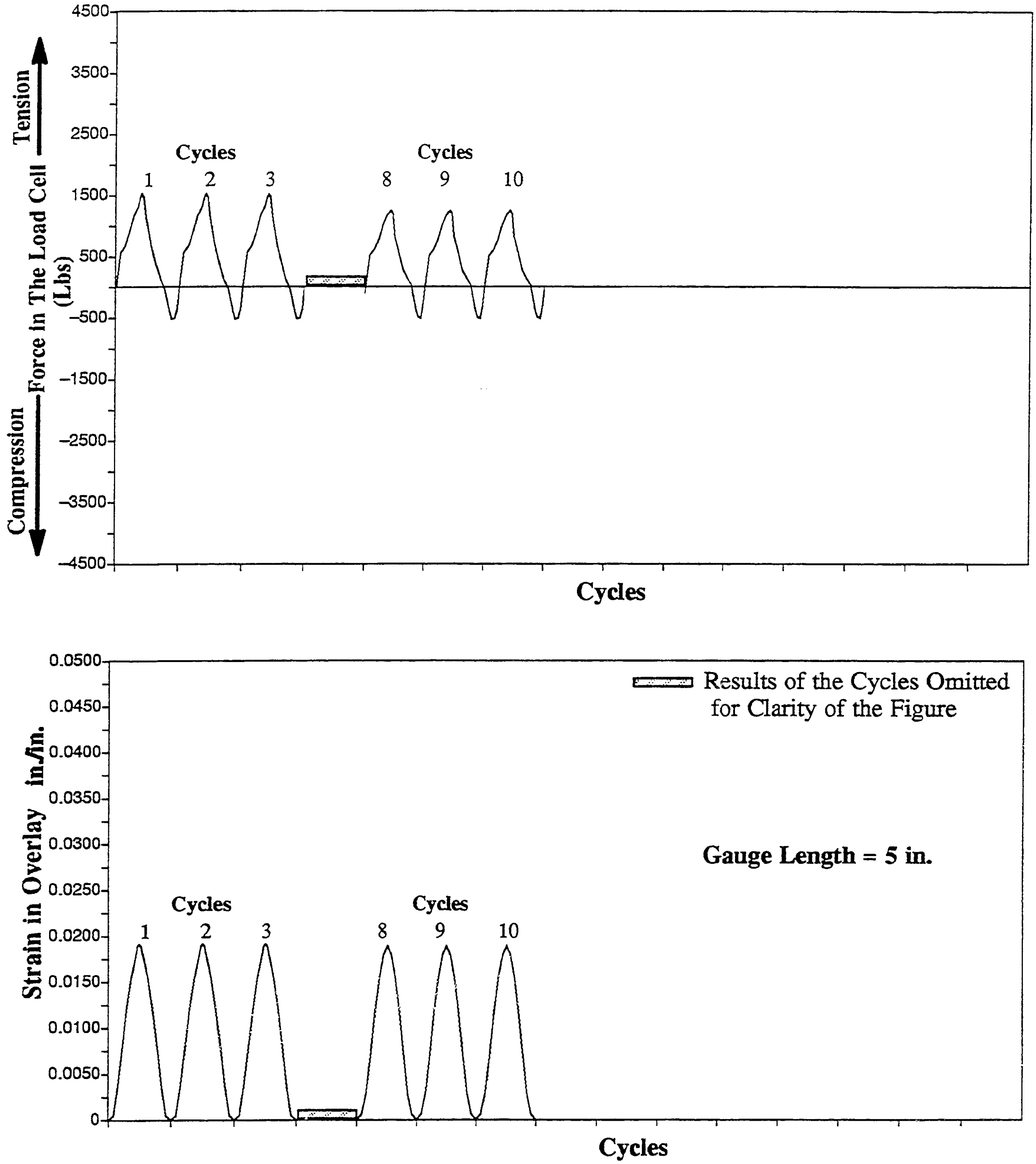

Figure 113: Force in Load Cell and Strain in Overlay as a Function of Test Cycles For a Pavement Section Treated With ISAC (Joint Expanded by 0.16 in. For 10 Cycles)

8.3.6 ISAC System Test No. 5

This test subjected the slab joint to 0.2 in. movement instead of 0.16 in. The test was conducted for 13 cycles and was discontinued after a very thin crack through the top of the overlay became visible when the joint was at 0.2 in. of movement. The high stress results shown in Figure 114 are created by the high strength geotextile in ISAC and not by the tensile strength of the AC. It should be noted that the strains are still substantially less than those induced during the 6th cycle in the control section.

8.4 COMPARATIVE TEST RESULTS

Figure 115 shows comparative laboratory test results between the ISAC system, control section, and a commercially available reflection cracking control material identified as "PROGUARD." The full length ISAC system was 7.50 ft. long and extended 3.75 ft. on either side of the overlay testing device joint shown in Figure 106. The 48 in. long ISAC test section extended 24 in. on either side of the testing device joint. The "PROGUARD" test section was also 7.50 ft. long and extended 3.75 ft. on either side of the joint. The AC overlays on all of the test sections were 2.5 in. thick.

Figure 115 indicates that both the control test section and "PROGUARD" test section displayed crack propagation completely through the AC overlay in less than 10 cycles of joint displacement of 0.072 in. per cycle. Neither the 48 in. long or full length ISAC sections experienced crack propagation in the AC overlay at joint displacement of 0.072 in. per cycle. The 48 in. long ISAC

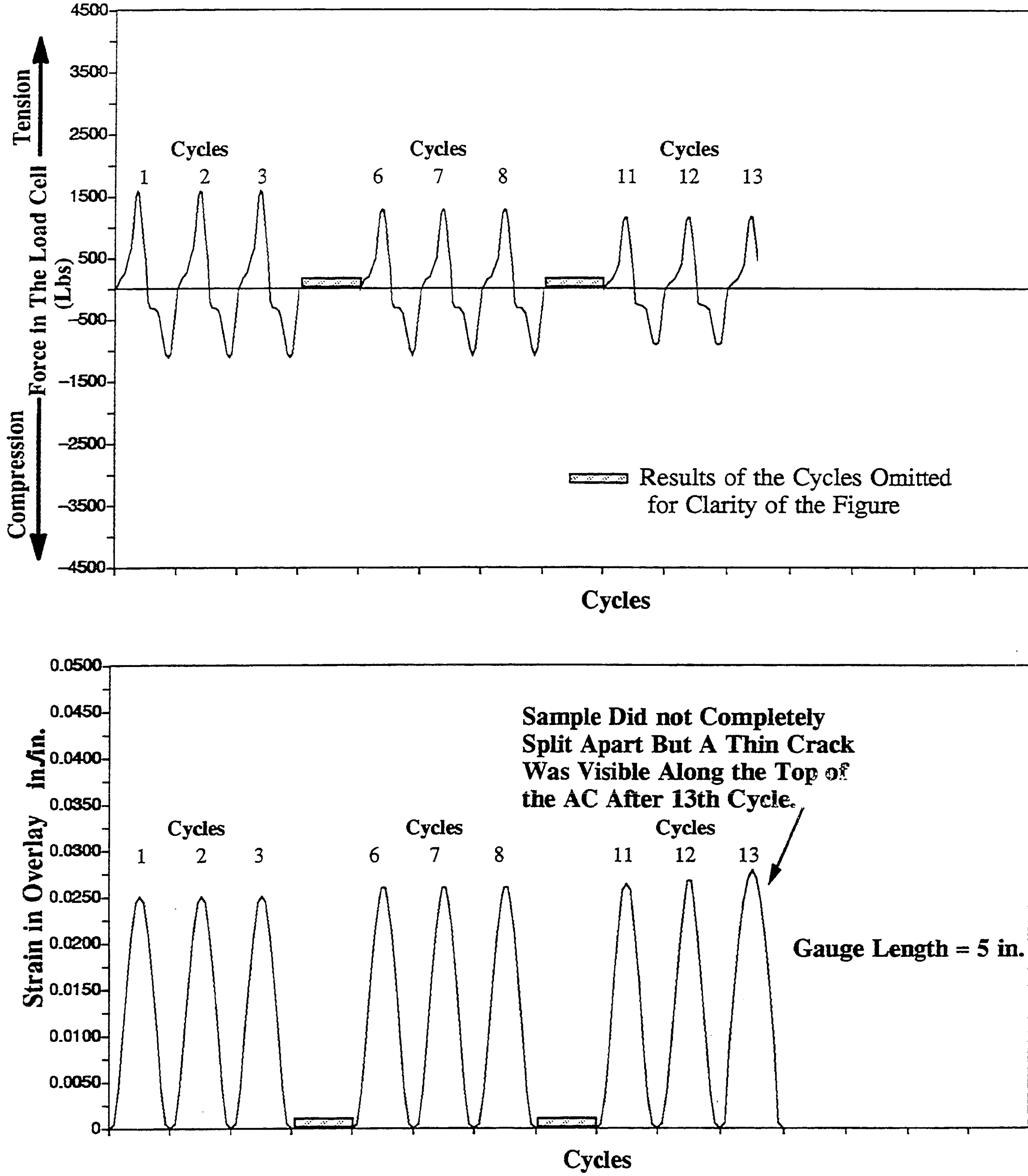

Figure 114: Force in Load Cell and Strain in Overlay as a Function of Test Cycles For a Pavement Section Treated With ISAC (Joint Expanded by 0.2 in. For 13 Cycles)

section was then subjected to additional joint displacement of 0.135 in. and 0.2 in. and a reflective crack in the AC overlay occurred at about 67 total cycles. The full length ISAC section was subjected to cycles of joint displacement of 0.11 in., 0.135 in., 0.16 in., and 0.20 in. for a total of 158 cycles before a very small reflective crack appeared in the 2.5 in. AC overlay.

It is quite evident that the ISAC system greatly outperformed the control test section and the "PROGUARD" test section in the laboratory. There is also an indication that the distance the ISAC material extends beyond the joint opening has an influence on the number of cycles to reflective crack formation in the AC overlay. The full length ISAC section performed better than the 48 in. long section. This may indicate that there is an advantage to the use of wider ISAC sections over pavement joints and cracks which experience large displacements.

8.5 Summary of The Test Results

The laboratory tests provided the following results:

a) A crack appeared in the overlay of the control pavement section in the very first cycle and the AC overlay completely split apart over the joint during the seventh cycle.

b) The AC overlay performed exceedingly well when it was treated with the ISAC system and tested under the test conditions similar to the control pavement. The strain in the overlay substantially decreased and the number of cycles to failure dramatically increased when ISAC was used. Even in the later tests (Test No. 2 to Test No. 5) when the slab movement was progressively increased, the overlay remained intact until the thirteenth cycle of Test No. 5 when the slab movement had been increased to 0.2 in. (more than three times the joint expansion of the control section) and the overlay and the ISAC geotextile had been subjected to 158 cycles. A thin crack appeared in the overlay at this time but the

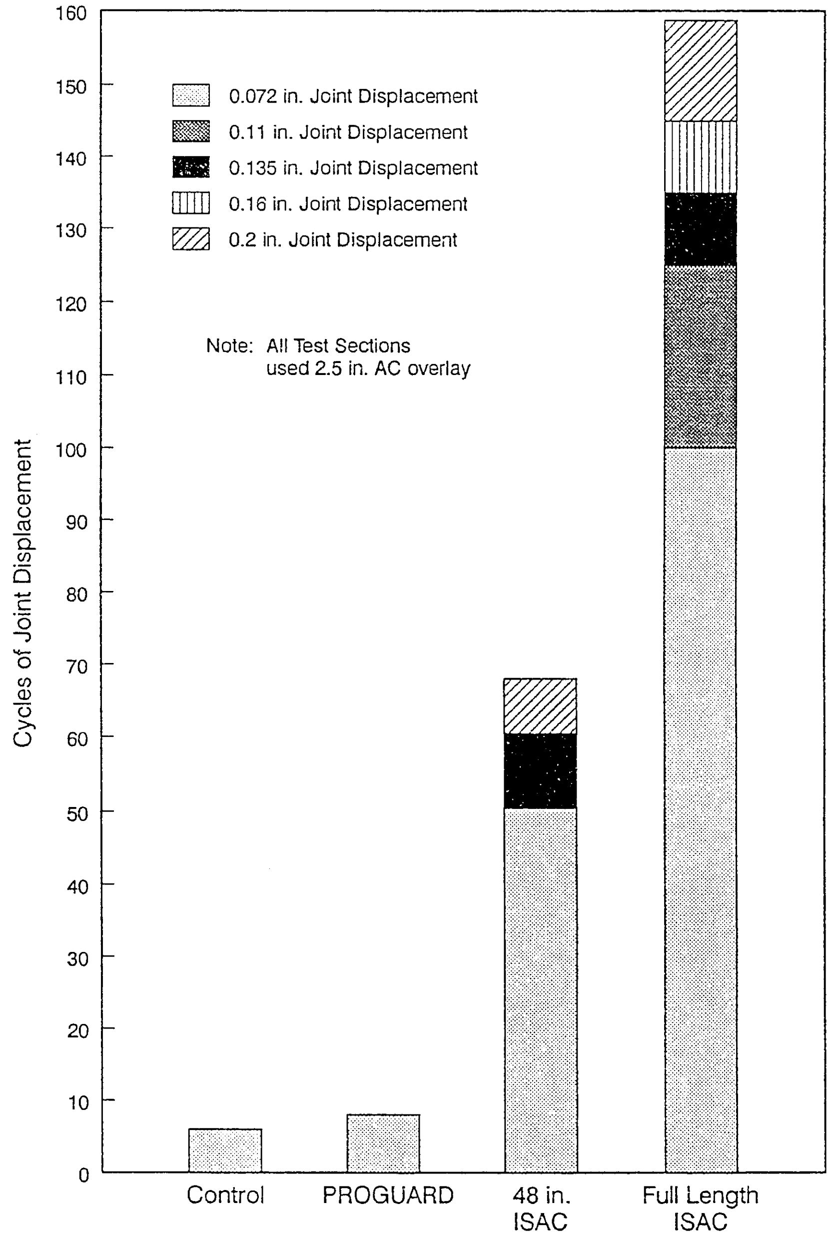

Figure 115: Comparative Laboratory Test Results

ISAC geotextile was still intact, holding the overlay together with a force of about 1180 lbs.

c) Maximum strain in the overlay above the joint increased as the number of cycles increased. The rate of increase in maximum strain in the overlay above the joint was substantially higher for the control pavement section than that treated with an ISAC layer.

d) A small increase in maximum strain noticed in the AC overlay above the joint when ISAC was used only occurred when the joint movement was increased and the cycles were increased.

e) During Test No. 3 at 0.135 in. joint movement and at about 120 cycles, a number of vertical cracks appeared in the plaster of paris which was spread over a distance of 1.5 feet on either side of the joint. The cracks were more closely spaced near the joint than away from the joint. These cracks were only visible in the plaster of paris and not visible in the asphalt concrete material. This indicated that the stress was spread more evenly over a larger area around the joint, with comparatively more stress near the joint and decreasing gradually farther away from the joint. Even at very high strain in the overlay (Test No. 4 and 5) the geotextile kept holding the overlay together and did not allow any crack to develop. Only a small area of raveling on the top surface of the overlay provided an indication that a possible crack had formed. This situation was evident only when the joint expansion was at a maximum opening of 0.2 in.

f) The ISAC test sections far outperformed the control test section and a test section using a commercial product "PROGUARD". The wider ISAC material performed better than a narrower 48–in. wide ISAC material. The ISAC material was able to accommodate pavement joint displacements up to and including 0.2 in. before any indication of reflection cracking occurred in the 2.5 in. AC overlay.

CHAPTER 9

ISAC FIELD TEST SECTION

9.1 Field Test Site

The field test site for the ISAC system was a jointed 9 in. PCC pavement designated as FA Route 567 (IL 38) in Lee and Ogle Counties near Rochelle, Illinois.

The pavement construction section which extended from sta 782+70 to sta 1197+27 (7.85 miles long) was completed during the Summer 1994. The construction project consisted of a rubblized section from sta 782+70 to sta 908+00, open graded base course section from sta 908+10 to sta 1022+75, 3 1/2 in. resurfacing from sta 1023+15 to sta 1125+00, and 2 ½ in. resurfacing from sta 1125+20 to sta 1148+19 and sta 1151+43 to sta 1196+82. All sections were overlaid with bituminous concrete binder (Type 2) and bituminous concrete surface course material (class I). The ISAC system was placed at transverse cracks and joints on the pavement section from sta 1125+00 to sta 1130+00.

9.2 Fabrication of ISAC Field Layers

The ISAC layers for field installation were fabricated in a steel mold so as to be 25 ft long and 36 in. wide. Thin 2 in. wide by 3/8 in. thick steel strips along both sides of the steel mold were used to maintain the ISAC material thickness to about 3/8 in.

The material properties and fabrication process for the ISAC layers were similar to those used in the laboratory except on a larger scale. The rubber asphalt in the ISAC layers was placed by use of a CRAFCO joint sealant dispenser provided and operated by Illinois Department of Transportation District 5 maintenance personnel. A contact releasing agent was used on the steel mold to prevent the ISAC layer from adhering to the mold when being fabricated. Twenty ISAC layers 25 ft long by 36 in. wide were fabricated for the field test site.

9.3 ISAC Pavement Installation

The 25 ft long by 36 in. wide ISAC layers were placed across 17 of the 20 transverse joints and cracks in the pavement section from sta 1125+00 to sta 1130+00 on August 5, 1994. The layers were placed just ahead of the asphalt concrete paving operations. The ISAC layers were placed so that one half of the layer width extended on either side of the pavement joint or crack. An RC–70 was used as the tack coat to bond the ISAC layer of the pavement. The ISAC layers were overlaid with 2 1/2 in. of asphalt concrete.

The RC–70 did a reasonably good job of bonding the ISAC layers to the underlying pavement and the ISAC layers remained in place when normal traffic passed over them. However, the RC–70 tack coat did not hold the ISAC layers well during the asphalt concrete paving operations and there were some problems with the ISAC layers sliding and wrinkling at this time. It is recommended that a stronger less temperature sensitive tact coat be used during future ISAC layer installations.

9.4 Field Observations

On February 8, 1995 a visual inspection of the reflective cracking in test sections on IL 38 was conducted. The air temperature at the time of inspection was about 4F with clear and windy conditions. On the 3 ½ in. AC resurfaced pavement section 15 full width reflective cracks were observed in the distance from sta 1120+00 to sta 1125+00. On the 2 ½ in. AC resurfaced pavement section from sta 1130+00 to sta 1135+00 a total of 16 full width reflective cracks was observed. On the ISAC test section from sta 1125+00 to sta 1130+00 with 2 ½ in. of AC overlay no reflective cracks were observed. The existing PCC pavement was 9 in. thick.

On November 17, 1995 inspection of IL 38 indicated 16 full width reflective cracks on the 3 ½ in. AC overlay section from sta 1120+00 to sta 1125+00 and 18 full width reflective cracks on the 2 ½ in. AC overlay section from sta 1130+00 to sta 1135+00. A partial transverse reflective crack about 6 ft. long was observed in the ISAC test section from sta 1125+00 to sta 1130+00 too. The air temperature was approximately 40F at time of observation. The long term field performance of the ISAC system will be periodically evaluated at the IL 38 test site over the next several years.

CHAPTER 10

SUMMARY AND CONCLUSIONS

10.1 Research Summary and Conclusions

The goal of this study was to develop a composite material which could effectively alleviate/mitigate the problem of reflection cracking in an AC overlay. The goal was achieved successfully through systematic, progressive, and analytical research work.

10.1.1 Summary of Developments

To approach the problem systematically the properties of the materials intended to be used in an ISAC system were first identified . Various thermal/structural models and laboratory equipment were used for this purpose. A Climate–Materials–Structural (CMS) pavement model (14) was used to establish the operating temperature range in Northern Illinois and then maximum daily variation and maximum seasonal variation to which the pavement and the ISAC will be exposed were computed. A number of woven and non woven geotextiles were selected and tested for their engineering properties such as tensile strength, initial modulus, modulus at failure, and percent shrinkage. Several samples of rubber asphalt were prepared by blending different ratios of crumb rubber with various types and ratios of asphalt cements at 400 F. These rubber asphalts were tested at different temperatures and the effects of temperature and rate of deformation on their stiffness were evaluated. Their performance and behavior in the field at critical temperatures were then predicted. An asphalt concrete mixture was prepared and tested using Marshall Mix Design procedures.

An ISAC layer was fabricated in the laboratory using the materials considered appropriate and was checked against slippage under an overlay with a vehicle making a sharp turn or applying sudden brakes. The computer program "CIRCLY" was used to compute shear stresses in a horizontal plane at the interface due to a vehicle applying sudden brakes on a multi layered pavement system. Testing equipment was developed to evaluate the interfacial shear strength and laboratory testing was performed to determine the shear strength of the fabricated ISAC layer under an AC overlay. While performing the tests, field conditions were simulated by duplicating the realistic values of temperature, confining load, and rate of shear. From the tests it was established that the initial fabricated ISAC layer was inadequate to resist slippage under slow rate of deformation. It was thus imperative to improve the shear strength of the rubber asphalt by using some asphalt modifier. Hydrated lime was used as an asphalt modifier and stiffness of the rubber asphalt in the ISAC system was improved to provide sufficient shear strength at the interface to resist the stresses developed under a slow moving vehicle.

ISAC was then evaluated for its effectiveness against reflection cracking. A laboratory pavement section with an AC overlay over a jointed PCC slab was constructed and placed in an environmental chamber. A mechanical device was used to simulate thermal strain in the slab and the joint was opened and closed at an extremely slow rate. The testing was conducted at 30 F and deterioration in the overlay was monitored using a sensitive LVDT device. The force required to pull and push the slab was also monitored using a load cell placed between the slab and the hydraulic ram. Performance of ISAC was evaluated by comparing the cycles to failure of an ISAC treated overlay with a control section without ISAC. The following was observed during the evaluation tests:

a) A crack appeared in the overlay of the control pavement section in the very first cycle and the AC overlay completely split apart over the joint during the seventh cycle.

b) The AC overlay performed exceedingly well when it was treated with the ISAC system and tested under the same test conditions similar to the control pavement. The strain in the overlay significantly decreased and the number of cycles to failure dramatically increased when ISAC was used.

c) Even in the later tests when the slab movement was progressively increased, the overlay remained intact and the crack appeared only when the slab movement had been increased to 0.2 in. and the overlay and the ISAC geotextile layer had been subjected to 158 cycles. Even after the crack appeared the ISAC layer was intact, holding the overlay together with a force of about 1180 lbs.

d) Maximum strain in the overlay above the joint increased as the number of cycles increased. The rate of increase in maximum strain in the overlay above the joint was considerably higher for the control pavement section than that treated with an ISAC layer.

e) At 0.135 in. joint movement at about 120 cycles, a number of vertical cracks appeared in the plaster of paris which was spread over a distance of 1.5

feet of the AC layer on either side of the joint. The cracks were more closely spaced near the joint than away from the joint. These cracks were only visible in the plaster of paris and not visible in the AC overlay.

f) Even at very high strain in the overlay (Test No. 4 and Test No. 5) the ISAC layer held the overlay together and did not allow any crack to develop. Only an indication of raveling on the top surface of the AC overlay was noticed.

g) The ISAC layer vastly outperformed one of the commercial products now available for reflection cracking control in AC overlays.

h) The field performance of the ISAC layer is encouraging.

10.1.2 Conclusions

Results of the evaluation tests conducted for the pavement control section and the ISAC treated section support several operating mechanisms.

The main idea that "The stress should not be stored indefinitely in the geotextile or the overlay and should be dissipated as it develops" was the key to success in this study. As the PCC slab moved due to thermal contraction and the joint opened, rubber asphalt being the softer material deformed and absorbed most of the stresses. During the process of deforming the rubber asphalt, the high strength geotextile was stretched to some extent. Since the high strength geotextile was bonded with the AC overlay on top, some stress did transfer to the AC overlay, but very little strain occurred. As the cycles increase, the strain in the geotextile increased due to repeated loads, and consequently the strain in the overlay also increased. Since the geotextile was fully bonded with the AC overlay, the geotextile held the AC together and did not allow a crack to develop even at considerably high joint movement (Test No. 5). Hair line cracks in the plaster of paris over a distance of 1.5 ft. on either side of the joint indicate that the strain was spread more evenly over a larger area around the joint, with comparatively more strain near the joint and decreasing gradually farther away from the joint.

The test results lead to following conclusions:

a) The ISAC system developed in this study should effectively alleviate/ mitigate the problem of reflection cracking in AC overlays on PCC pavement in the State of Illinois.

b) ISAC can be designed to suit the requirements of other states since every state has different slab length and different climatic conditions. It is felt that ISAC can be designed even for states where the slab length exceeds 75 ft.

While designing the ISAC layer for worse conditions several steps can be taken:

1) A softer ISAC core material will dissipate stress better and consequently less stress will be transferred to the overlay. This will allow more cycles to failure in the AC overlay. The core material should not however be so soft at high temperature during summer that it will allow slippage as a result of traffic. The proper core properties can be achieved by making the core material less temperature susceptible by the use of modifiers.

2) The use of a high strength geotextile with high initial modulus will allow less expansion in the geotextile at the time of maximum joint expansion and consequently less stress will be transferred to the AC overlay. This will allow far more thermal cycles to failure in the AC overlay.

3) The use of a high strength geotextile which is less influenced by repeated loads and shows little increase in strain with the increase in thermal cycles should enhance the life of the AC overlay.

10.2 Recommendations for Further Research

a) In this study ISAC was placed over the full length of the PCC slab. In the findings it has been stated that when ISAC was placed under the AC overlay the stress was spread more evenly over a larger area around the joint, with comparatively more stress near the joint and decreasing gradually farther away from the joint. It is felt that the full length of PCC slab need not be covered with ISAC. ISAC should only be placed in the area of the joint where more stress is developed. It is recommended that additional studies be conducted to determine the distance from the joint where the stresses will be low enough to discontinue the ISAC layer on the PCC slab.

b) ISAC should be compared with other presently available reflection cracking control procedures using the same laboratory testing methods.

c) ISAC should be tested in the field. After establishing the point of cut off length of ISAC, appropriate length of ISAC sections should be placed over joints and crack prior to AC overlay placement and the performance of the AC overlay should be evaluated.

APPENDIX A

PREDICTED TEMPERATURE VARIATIONS IN A PAVEMENT DURING THE YEAR IN NORTHERN ILLINOIS AREA

Day of the Year	Temp of Overlay at the Surface (F)			Temp of Overlay at Mid Depth (F)			Temp of ISAC at the Interface (F)			Temp of PCC Slab at Mid Depth (F)		
	Min Temp	Max Temp	Daily Variation	Min Temp	Max Temp	Daily Variation	Min Temp	Max Temp	Daily Variation	Min Temp	Max Temp	Daily Variation
Jan 1	15	32.5	17.5	18	29	11	21	27.5	6.5	24	26.5	2.5
Jan 2	14	32	18	17.5	28	10.5	20.5	26	5.5	23	25	2
Jan 3	13	30	17	16.5	26	9.5	19.5	23.5	4	22	23.5	1.5
Jan 4	13	30	17	16.5	25.5	9	19.5	22	2.5	21.5	23	1.5
Jan 5	13	30	17	16.5	25	8.5	19	21.5	2.5	21.5	22.5	1
Jan 6	13	30	17	16.5	25	8.5	19	21	2	21	22	1
Jan 7	12.5	30	17.5	16	24.5	8.5	19	21	2	21	22	1
Jan 8	12.5	30	17.5	16	24.5	8.5	19	20.5	1.5	21	21.5	0.5
Jan 9	12.5	30	17.5	16	24.5	8.5	19	20.5	1.5	21	21.5	0.5
Jan 10	12.5	30	17.5	16	24	8	19	20	1	20.5	21	0.5
Jan 11	12.5	30	17.5	16	24	8	18.5	20	1.5	20.5	21	0.5
Jan 12	12.5	30	17.5	15.5	24	8.5	18	20	2	20.5	21	0.5
Jan 13	12.5	30	17.5	15.5	24	8.5	18	20	2	20.5	21	0.5
Jan 14	12.5	30	17.5	15.5	24	8.5	18	20	2	20.5	21	0.5
Jan 15	12	30.5	18.5	15	24.5	9.5	17.5	20	2.5	20	20.5	0.5
Jan 16	12	30.5	18.5	15	24.5	9.5	17.5	20	2.5	20	20.5	0.5
Jan 17	13	31.5	18.5	16	24.5	9.5	18	21	3	20.5	21	0.5
Jan 18	13	31.5	18.5	16.5	24.5	9	19	21	2	20.5	21	0.5
Jan 19	13	31.5	18.5	16.5	24.5	9	19	21.5	2.5	20.5	21	0.5
Jan 20	13	31.5	18.5	16.5	24.5	9	19	21.5	2.5	20.5	21	0.5
Jan 21	13	32	19	16.5	24	9.5	19	22	3	20.5	21	0.5
Jan 22	13	32	19	16.5	24	9.5	19	22	3	20.5	21	0.5
Jan 23	13	32	19	16.5	24	9.5	19	22	3	20.5	21.5	1
Jan 24	12	31	19	15.5	24.5	9	18.5	20.5	2	20.5	21	0.5
Jan 25	11.5	31	19.5	15	25	10	17.5	20.5	2.5	20	20.5	0.5
Jan 26	11.5	31	19.5	14.5	25.5	11	17	20	3	20	20.5	0.5
Jan 27	11.5	31	19.5	14.5	25.5	11	17	20	3	20	20.5	0.5
Jan 28	11	31.5	20.5	14	25.5	11.5	17	20	3	20	20.5	0.5
Jan 29	10.5	31.5	21	14	25.5	11.5	16.5	20	3.5	20	20.5	0.5
Jan 30	10	31.5	20.5	13.5	25.5	12	16.5	20	3.5	20	20.5	0.5
Jan 31	11	32.5	21.5	14	26	12	17	20.5	3.5	20	20.5	0.5

Note: Overlay thickness = 2.5 in.

Day of the Year	Temp of Overlay at the Surface (F)			Temp of Overlay at Mid Depth (F)			Temp of ISAC at the Interface (F)			Temp of PCC Slab at Mid Depth (F)		
	Min Temp	Max Temp	Daily Varia–tion	Min Temp	Max Temp	Daily Varia–tion	Min Temp	Max Temp	Daily Varia–tion	Min Temp	Max Temp	Daily Varia–tion
Feb 1	11.5	32.5	21	14.5	26	11.5	17	20.5	3.5	20	20.5	0.5
Feb 2	11.5	32.5	21	14.5	26	11.5	17	20	3	19	20	1
Feb 3	11.5	33	21.5	15	26.5	11.5	17.5	20.5	3	19	19.5	0.5
Feb 4	12	33	21	15	26.5	11.5	17.5	20.5	3	19	19.5	0.5
Feb 5	11.5	33	21.5	15	27	12	17.5	21	3.5	19	19.5	.05
Feb 6	12	33	21	15	27	12	17.5	21	3.5	19	19.5	0.5
Feb 7	13	34.5	21.5	16	28	12	18.5	22	3.5	19	20	1
Feb 8	13	34.5	21.5	16.5	28.5	12	19	22.5	3.5	19	20.5	0.5
Feb 9	13	35	22	16.5	28.5	12	19	23	4	19.5	21	1.5
Feb 10	13.5	35	21.5	17	28.5	11.5	19.5	23	3.5	19.5	21	1.5
Feb 11	13	35	22	16.5	28.5	12	19.5	23.5	4	19.5	21.5	2
Feb 12	13	35	22	16.5	29	12.5	19.5	24	4.5	19.5	21.5	2
Feb 13	13	35	22	16.5	29	12.5	19.5	24	4.5	19.5	21.5	2
Feb 14	14.5	37	22.5	17.5	31	13.5	19.5	26	6.5	19.5	23	3.5
Feb 15	14.5	37.5	23	17.5	32	14.5	20	27.5	7.5	20	23.5	3.5
Feb 16	14.5	38	23.5	17.5	32.5	15	20	27.5	7.5	20.5	24	3.5
Feb 17	14.5	38	23.5	17.5	32.5	15	20	28	8	20.5	24	3.5
Feb 18	14.5	38.5	24	17.5	33	15.5	20	28	8	20.5	24.5	4
Feb 19	15	38.5	22.5	18	33.5	15.5	20.5	28.5	8	20.5	24.5	4
Feb 20	15	39	24	18	33.5	15.5	20.5	28.5	8	21	24.5	3.5
Feb 21	16	41	25	18.5	35.5	17	20.5	30.5	10	21	25.5	4.5
Feb 22	16.5	41.5	25	19	35.5	16	21	31	10	21.5	26	4.5
Feb 23	16.5	42	25.5	19	36	17	21	31	10	21.5	26.5	5
Feb 24	16.5	42	25.5	19	36.5	17.5	21	31.5	10.5	22	26.5	4.5
Feb 25	16.5	42.5	26	19	36.5	17.5	21	31.5	10.5	22	27	5
Feb 26	16.5	42.5	26	19	37	18	21	31.5	10.5	22	27	5
Feb 27	16.5	43	26.5	19	38	19	21	32	11	22.5	27.5	5.5
Feb 28	16.5	43	26.5	20.5	39	18.5	22	32	10	22	27.5	5.5

Note: Overlay thickness = 2.5 in.

Day of the Year	Temp of Overlay at the Surface (F)			Temp of Overlay at Mid Depth (F)			Temp of ISAC at the Interface (F)			Temp of PCC Slab at Mid Depth (F)		
	Min Temp	Max Temp	Daily Varia–tion	Min Temp	Max Temp	Daily Varia–tion	Min Temp	Max Temp	Daily Varia–tion	Min Temp	Max Temp	Daily Varia–tion
Mar 1	18.5	46	27.5	20.5	39	18.5	22	32	10	22	27.5	5.5
Mar 2	19	46.5	27.5	21	40	19	23	32.5	9.5	21.5	27	5.5
Mar 3	19	46.5	27.5	21.5	40.5	19	23.5	33	9.5	22	27.5	5.5
Mar 4	19.5	47	27.5	22	40.5	18.5	23.5	33	9.5	22.5	27.5	5
Mar 5	19.5	47	27.5	22	41	19	23.5	33.5	10	22.5	28	5.5
Mar 6	19.5	47.5	28	22	41	19	24	33.5	9.5	22.5	28	5.5
Mar 7	19.5	47.5	28	22	42	20	24	33.5	9.5	23	28.5	5.5
Mar 8	21	50	29	23	43.5	20.5	24.5	35.5	11	23.5	29.5	6
Mar 9	21.5	50.5	29	23.5	44	20.5	25	36	11	24	30	6
Mar 10	21.5	50.5	29	24	44	20	25.5	36	10.5	24.5	30	5.5
Mar 11	21.5	51	29.5	24	44.5	20.5	25.5	36.5	11	24.5	30.5	6
Mar 12	21.5	51	29.5	24	44.5	20.5	25.5	36.5	11	25	31	6
Mar 13	21.5	51	29.5	24	44.5	20.5	26	37	11	25	31	6
Mar 14	21.5	51.5	30	24	45	21	26	37	11	25.5	31.5	6
Mar 15	23	54	31	25	47	22	26.5	38.5	12	26	32.5	6.5
Mar 16	23.5	54.5	31	26	47.5	21.5	27.5	39	11.5	26.5	33	6.5
Mar 17	23.5	54.5	31	26	47.5	21.5	27.5	39.5	12	27	33	6
Mar 18	23.5	55	31.5	26	48	22	28	39.5	11.5	27	33.5	6.5
Mar 19	23.5	55	31.5	26	48	22	28	40	12	27.5	33.5	6
Mar 20	23.5	55	31.5	26	48	22	28	40	12	27.5	33	6.5
Mar 21	23.5	55.5	32	26	48.5	22.5	28	40.5	12.5	28	33	6
Mar 22	23.5	58	32.5	27	50.5	23.5	29.5	42	12.5	28.5	35	6.5
Mar 23	26	58.5	32.5	28.5	51	22.5	30	42.5	12.5	29.5	36	6.5
Mar 24	26	59	33	28.5	51.5	23	30.5	43	12.5	30	36	6
Mar 25	26.5	59	32.5	29	52	23	30.5	43.5	13	30	36.5	6.5
Mar 26	26.5	59	32.5	29	52	23	31	43.5	12.5	30.5	37	6.5
Mar 27	26.5	59.5	33	29	52.5	23.5	31	43.5	12.5	30.5	37	6.5
Mar 28	26.5	59.5	33	29	52.5	23.5	31	44	13	30.5	37.5	7
Mar 29	28	62.5	34.5	20.5	54.5	24	32	46	14	30.5	38.5	7
Mar 30	28.5	62.5	34	31	54.5	23.5	32.5	46	13.5	32	39	7
Mar 31	28.5	63	34.5	31	55	26	33	46	13	32	39	7

Note: Overlay thickness = 2.5 in.

Day of the Year	Temp of Overlay at the Surface (F)			Temp of Overlay at mid Depth (F)			Temp of ISAC at the Interface (F)			Temp of PCC Slab at Mid Depth (F)		
	Min Temp	Max Temp	Daily Varia–tion	Min Temp	Max Temp	Daily Varia–tion	Min Temp	Max Temp	Daily Varia–tion	Min Temp	Max Temp	Daily Varia–tion
Apr 1	28.5	63	34.5	31	55	24	33	46	13	32	39	7
Apr 2	28.5	63.5	35	31	56	25	33	45	12	31	38	7
Apr 3	29	63.5	34.5	31	56	24.5	33.5	45	11.5	31	38	7
Apr 4	29	63.5	34.5	31.5	56	24.5	33.5	45.5	12	31.5	38	6.5
Apr 5	30	65.5	35.5	32.5	57.5	25	34.5	46.5	12	32	39	7
Apr 6	30.5	66	35.5	33	58	25	35	47	12	32.5	39.5	7
Apr 7	31	66	35	33.5	58.5	25	35	47.5	12.5	33	40	7
Apr 8	31	66.5	35.5	33.5	58.5	25	35.5	47.5	12	33	40	7
Apr 9	31	66.5	35.5	33.5	59	25.5	35.5	48	12.5	33.5	40.5	7
Apr 10	31	66.5	35.5	33.5	59	25.5	35.5	48	12.5	33.5	40.5	7
Apr 11	31	67	36	33.5	59	25.5	35.5	48	12.5	33.5	41	7.5
Apr 12	33	70	37	35.5	61.5	26	35	47	13	34.5	42	8.5
Apr 13	34	70.5	36.5	36.5	62.5	26	38	51	13	35.5	43	7.5
Apr 14	34	70.5	36.5	36.5	62.5	26	38.5	51	12.5	36	43	7
Apr 15	34.5	70.5	36	37	62.5	25.5	38.5	51.5	13	36.5	43.5	7
Apr 16	34.5	71	36.5	37	63	26	39	51.5	12.5	36.5	44	7.5
Apr 17	34.5	71	36.5	37	63	26	39	52	13	37	44	7
Apr 18	34.5	71.5	37	37	63.5	26.5	39	52	13	37	44.5	7.5
Apr 19	36.5	73.5	37	39	65	26	40.5	53.5	13	38	45.5	7.5
Apr 20	37	73.5	36.5	39.5	65.5	26	41	54	13	38.5	46	7.5
Apr 21	37	73.5	36.5	39.5	65.5	26	41.5	54	12.5	39	46	7
Apr 22	37	74	37	39.5	66	26.5	41.5	54.5	13	39	46.5	7.5
Apr 23	37	74	37	39.5	66	26.5	41.5	54.5	13	39.5	46.5	7
Apr 24	37.5	74	36.5	40	66	26	42	55	12	39.5	47	7.5
Apr 25	37.5	74.5	37	40	66.5	26.5	42	55	12	40	47	7
Apr 26	38.5	77.5	39	41	69	28	42.5	57	14.5	40.5	48.5	8
Apr 27	38.5	77.5	39	41.5	69	27.5	43.5	57.5	14	41	49	8
Apr 28	39	78	39	41.5	69.5	28	43.5	57.5	14	41.5	49	7.5
Apr 29	39	78	39	42	69.5	27.5	44	58	14	41.5	49.5	8
Apr 30	39	78	39	42	69.5	27.5	44	58	14	41	49	8

Note: Overlay thickness = 2.5 in.

Day of the Year	Temp of Overlay at the Surface (F)			Temp of Overlay at Mid Depth (F)			Temp of ISAC at the Interface (F)			Temp of PCC Slab at Mid Depth (F)		
	Min Temp	Max Temp	Daily Varia–tion	Min Temp	Max Temp	Daily Varia–tion	Min Temp	Max Temp	Daily Varia–tion	Min Temp	Max Temp	Daily Varia–tion
May 1	39	78	39	42	69.5	27.5	44	58	14	41	49	8
May 2	39	78.5	39.5	42	70	28	44.5	57.5	13	40.5	48	7.5
May 3	40.5	80	39.5	43.5	71.5	28	45.5	57.5	12	41	49	8
May 4	41	80.5	39.5	44	72	28	46	58	12	41.5	49.5	8
May 5	41	80.5	39.5	44	72	28	46	58	12	42	49.5	7.5
May 6	41	80.5	39.5	44	72	28	46.5	58.5	12	42	50	8
May 7	41	81	40	44	72.5	28.5	46.5	58.5	12	42.5	50	7.5
May 8	41.5	81	39.5	44.5	72.5	28	46.5	58.5	12	42.5	50.5	8
May 9	41.5	81	39.5	44.5	72.5	28	46.5	59	12.5	43	50.5	7.5
May 10	42.5	82	39.5	45.5	73.5	28	47.5	59.5	12	43.5	51	7.5
May 11	42.5	82	39.5	45.5	73.5	28	47.5	60	12.5	43.5	51.5	8
May 12	42.5	82	39.5	45.5	73.5	28	48	60	12	44	51.5	7.5
May 13	42.5	82	39.5	45.5	73.5	28	48	60	12	44	52	8
May 14	42.5	82.5	40	45.5	74	28.5	48	60.5	12.5	44.5	52	7.5
May 15	43	82.5	39.5	46	74	28	48.5	60.5	12	44.5	52	7.5
May 16	43	82.5	39.5	46	74	28	48.5	60.5	12	44.5	52.5	8
May 17	45	82.5	40.5	48	74	27	50	62.5	12.5	45.5	53.5	8
May 18	45.5	82.5	40	48.5	75.5	27	50.5	63	12.5	46	54	8
May 19	45.5	86	40.5	48.5	77	28.5	51	63	12	46.5	54.5	8
May 20	46	86	40	49	77.5	28.5	51	63.5	12.5	47	54.5	7.5
May 21	46	86	40	49	77.5	28.5	51	63.5	12.5	47	55	8
May 22	46	86	40	49	77.5	28.5	51.5	63.5	12	47.5	55	7.5
May 23	46	86	40	49	77.5	28.5	51.5	64	12.5	47.5	55	7.5
May 24	47.5	87.5	40	50.5	79	28.5	52.5	65	21.5	48	56	8
May 25	47.5	87.5	40	50.5	79	28.5	53	65	12	48.5	56.5	8
May 26	48	88	40	51	79.5	28.5	53	65.5	12.5	49	56.5	7.5
May 27	48	88	40	51	79.5	28.5	53.5	65.5	12	49	57	8
May 28	48	88	40	51	79.5	28.5	53.5	65.5	12	49.5	57	7.5
May 29	48	88	40	51	79.5	28.5	53.5	66	12.5	49.5	57	7.5
May 30	48	88.5	40.5	51	80	29	53.5	66	12.5	49.5	57.5	8
May 31	49.5	92	42.5	52.5	83	30.5	54	67.5	13.5	50.5	58.5	8

Note: Overlay thickness = 2.5 in.

Day of the Year	Temp of Overlay at the Surface (F)			Temp of Overlay at Mid Depth (F)			Temp of ISAC at the Interface (F)			Temp of PCC Slab at Mid Depth (F)		
	Min Temp	Max Temp	Daily Varia–tion	Min Temp	Max Temp	Daily Varia–tion	Min Temp	Max Temp	Daily Varia–tion	Min Temp	Max Temp	Daily Varia–tion
Jun 1	49.5	92	42.5	53	83	30	54	67.5	13.5	50.5	58.5	8
Jun 2	50.5	92	41.5	53.5	83	29.5	55	68	13	50.5	58.5	8
Jun 3	50.5	92	41.5	53.5	83	29.5	56	68	12	51	59	8
Jun 4	50.5	92.5	42	54	83.5	29.5	56.5	68.5	12	51	59	8
Jun 5	50.5	92.5	42	54	83.5	29.5	56.5	68.5	12	51.5	59.5	8
Jun 6	50.5	92.5	42	54	83.5	29.5	56.5	68.5	12	51.5	59.5	8
Jun 7	51.5	93.5	42	54.5	84.5	30	57	69.5	12	52	60	8
Jun 8	51.5	93.5	42	55	84.5	29.5	57.5	69.5	12	52.5	60.5	8
Jun 9	52	94	42	55	85	30	57.5	70	12.5	52.5	60.5	8
Jun 10	52	94	42	55.5	85	29.5	58	70	12	52.5	61	8.5
Jun 11	52	94	42	55.5	85	29.5	58	70	12	53	61	8
Jun 12	52	94	42	55.5	85	29.5	58	70	12	53	61	8
Jun 13	52	94	42	55.5	85	29.5	58	70	12	53	61	8
Jun 14	53	95	42	56	86	30	58.5	71	12.5	53.5	61.5	8
Jun 15	53	95	42	56.5	86	29.5	59	71	12	54	62	8
Jun 16	53	95.5	42.5	56.5	86.5	30	59	71.5	12.5	54	62	8
Jun 17	53	95.5	42.5	56.5	86.5	30	59.5	71.5	12	54.5	62.5	8
Jun 18	53.5	95.5	42	57	86.5	29.5	59.5	71.5	12	54.5	62.5	8
Jun 19	53.5	95.5	42	57	86.5	29.5	59.5	71.5	12	54.5	62.5	8
Jun 20	53.5	95.5	42	57	86.5	29.5	59.5	71.5	12	54.5	62.5	8
Jun 21	54.5	96.5	42	58	87.5	29.5	60.5	72.5	12	55	63.5	8.5
Jun 22	55	96.5	41.5	58.5	87.5	29	61	72.5	11.5	55.5	63.5	8
Jun 23	55	96.5	41.5	58.5	88	29.5	61	73	12	55.5	63.5	8
Jun 24	55	96.5	41.5	58.5	88	29.5	61	73	12	56	64	8
Jun 25	55	96.5	41.5	58.5	88	29.5	61	73	12	56	64	8
Jun 26	55	96.5	41.5	58.5	88	29.5	61	73	12	56	64	8
Jun 27	55	97	42	58.5	88	29.5	61	73	12	56	64	8
Jun 28	55.5	98.5	43	59	89.5	30.5	61.5	74	12.5	56.5	65	8.5
Jun 29	55.5	98.5	43	59	89.5	30.5	62	74.5	12.5	57	65	8
Jun 30	55.5	98.5	43	59	89.5	30.5	62	74.5	12.5	57	65	8

Note: Overlay thickness = 2.5 in.

Day of the Year	Temp of Overlay at the Surface (F)			Temp of Overlay at Mid Depth (F)			Temp of ISAC at the Interface (F)			Temp of PCC Slab at Mid Depth (F)		
	Min Temp	Max Temp	Daily Varia–tion	Min Temp	Max Temp	Daily Varia–tion	Min Temp	Max Temp	Daily Varia–tion	Min Temp	Max Temp	Daily Varia–tion
Jul 1	55.5	98.5	43	59	89.5	30.5	62	74.5	12.5	57	65	8
Jul 2	55.5	98.5	43	59	89.5	30.5	62	74	12	57	65.5	8.5
Jul 3	55.5	98.5	43	59	89.5	30.5	62	74	12	57.5	65.5	8
Jul 4	55.5	99	43.5	59	90	31	62	74	12	57.5	65.5	8
Jul 5	56	99	43	59.5	90	30.5	62	74	12	57.5	65.5	8
Jul 6	56	99	43	59.5	90	30.5	62.5	74	11.5	57.5	66	8.5
Jul 7	56	99	43	59.5	90	30.5	62.5	74	11.5	57.5	66	8.5
Jul 8	56	99	43	59.5	90	30.5	62.5	74	11.5	57.5	66	8.5
Jul 9	56	99	43	59.5	90	30.5	62.5	74	11.5	58	66	8
Jul 10	56	99	43	59.5	90	30.5	62.5	74	11.5	58	66	8
Jul 11	56	99	43	59.5	90	30.5	62.5	74	11.5	58	66	8
Jul 12	56.5	99	42.5	60	90	30	63	74	11	58	66.5	8.5
Jul 13	57	99	42	60.5	90	29.5	63	74.5	11.5	58.5	66.5	8
Jul 14	57	99	42	60.5	90	29.5	63	74.5	11.5	58.5	66.5	8
Jul 15	57	99	42	60.5	90	29.5	63	74.5	11.5	58.5	66.5	8
Jul 16	57	99	42	60.5	90	29.5	63	74.5	11.5	58.5	66.5	8
Jul 17	57	99	42	60.5	90	29.5	63	74.5	11.5	58.5	66.5	8
Jul 18	57	99	42	60.5	90	29.5	63	74.5	11.5	58.5	66.5	8
Jul 19	57	99	42	60.5	90	29.5	63	74.5	11.5	58.5	67	8.5
Jul 20	57	99	42	60.5	90	29.5	63	74.5	11.5	58.5	67	8.5
Jul 21	57	99	42	60.5	90	29.5	63	74.5	11.5	58.5	67	8.5
Jul 22	57	99	42	60.5	90	29.5	63	74.5	11.5	58.5	67	8.5
Jul 23	57	99	42	60.5	90	29.5	63	74.5	11.5	58.5	67	8.5
Jul 24	57	99	42	60.5	90	29.5	63	74.5	11.5	58.5	67	8.5
Jul 25	57	99	42	60.5	90	29.5	63	74.5	11.5	58.5	66.5	8
Jul 26	57	98.5	41.5	60.5	90	29.5	63	74.5	11.5	58.5	66.5	8
Jul 27	57	98.5	41.5	60.5	90	29.5	63	74.5	11.5	58.5	66.5	8
Jul 28	57	98.5	41.5	60.5	90	29.5	63	74.5	11.5	58.5	66.5	8
Jul 29	57	98.5	41.5	60.5	90	29.5	63	74.5	11.5	58.5	66.5	8
Jul 30	57	98.5	41.5	60.5	90	29.5	63	74.5	11.5	58.5	66.5	8
Jul 31	57	98.5	41.5	60.5	90	29.5	63	74.5	11.5	58.5	66.5	8

Note: Overlay thickness = 2.5 in.

Day of the Year	Temp of Overlay at the Surface (F)			Temp of Overlay at Mid Depth (F)			Temp of ISAC at the Interface (F)			Temp of PCC Slab at Mid Depth (F)		
	Min Temp	Max Temp	Daily Varia–tion	Min Temp	Max Temp	Daily Varia–tion	Min Temp	Max Temp	Daily Varia–tion	Min Temp	Max Temp	Daily Varia–tion
Aug 1	57	98.5	41.5	60.5	90	29.5	63	74.5	11.5	58.5	66.5	8
Aug 2	56.5	97.5	41.5	60	89	29	62.5	74.5	12	58	66.5	8.5
Aug 3	56.5	97.5	41	60	89	29	62.5	74	11.5	58	66.5	8.5
Aug 4	56.5	97.5	41	60	89	29	62.5	74	11.5	58	66.5	8.5
Aug 5	56.5	97.5	41	60	89	29	62.5	74	11.5	58	66.5	8.5
Aug 6	56.5	97	40.5	59.5	89	29.5	62	74	12	58	66.5	8.5
Aug 7	56.5	97	40.5	59.5	89	29.5	62	74	12	58	66.5	8.5
Aug 8	56.5	97	40.5	59.5	89	29.5	62	74	12	58	66.5	8.5
Aug 9	56	96.5	40.5	59.5	88	28.5	62	74	12	58	66.5	8.5
Aug 10	55.5	96.5	41	59	88	29	61.5	74	12.5	57.5	66	8.5
Aug 11	55.5	96	40.5	59	88	29	61.5	74	12.5	57.5	66	8.5
Aug 12	55.5	96	40.5	59	87.5	28.5	61.5	74	12.5	57.5	66	8.5
Aug 13	55.5	96	40.5	59	87.5	28.5	61.5	74	12.5	57.5	66	8.5
Aug 14	55.5	96	40.5	59	87.5	28.5	61.5	74	12.5	57.5	66	8.5
Aug 15	55.5	95.5	40	58.5	87.5	29	61	74	13	57.5	65.5	8
Aug 16	55	95	40	58.5	87	28.5	61	73.5	12.5	57	65.5	8.5
Aug 17	55	95	40	58	87.5	28.5	60.5	73	12.5	57	65	8
Aug 18	55	94.5	39.5	58	87.5	28.5	60.5	73	12.5	57	65	8
Aug 19	55	94.5	39.5	58	87.5	28.5	60.5	73	12.5	57	65	8
Aug 20	54.5	94.5	40	58	87.5	28.5	60.5	73	12.5	57	65	8
Aug 21	54.5	94.5	40	58	87.5	28.5	60.5	73	12.5	57	65	8
Aug 22	54.5	94	39.5	57.5	86	28.5	60	72.5	12.5	57	64.5	7.5
Aug 23	53.5	94	40	57	85.5	28.5	59.5	72	12.5	56.5	64.5	8
Aug 24	53.5	93.5	40	57	85.5	28.5	59.5	72	12.5	56.5	64	7.5
Aug 25	53.5	93.5	40	57	85.5	28.5	59.5	72	12.5	56	64	8
Aug 26	53.5	93.5	40	56.5	85	28.5	59	71.5	12.5	56	64	8
Aug 27	53.5	93	39.5	56.5	85	28.5	59	71.5	12.5	56	63.5	7.5
Aug 28	53.5	93	39.5	56.5	85	28.5	59	71.5	12.5	56	63.5	7.5
Aug 29	53.5	93	39.5	56.5	85	28.5	59	71.5	12.5	55.5	63.5	8
Aug 30	53.5	92.5	39	56.5	84.5	28	59	71	12	55.5	64	8.5
Aug 31	53	92.5	39.5	56	84.5	28.5	58.5	71	11.5	55.5	64	8.5

Note: Overlay thickness = 2.5 in.

Day of the Year	Temp of Overlay at the Surface (F)			Temp of Overlay at Mid Depth (F)			Temp of ISAC at the Interface (F)			Temp of PCC Slab at Mid Depth (F)		
	Min Temp	Max Temp	Daily Varia–tion	Min Temp	Max Temp	Daily Varia–tion	Min Temp	Max Temp	Daily Varia–tion	Min Temp	Max Temp	Daily Varia–tion
Sep 1	53	92.5	39.5	56	84.5	28.5	58.5	71	12.5	55.5	64	8.5
Sep 2	53	92.5	39.5	56	84	28	58.5	71	12.5	55.5	64	8.5
Sep 3	53	92	39	56	84	28	58.5	71.5	13	55.5	64	8.5
Sep 4	53	92	39	56	84	28	58.5	71.5	13	55.5	64	8.5
Sep 5	53	91.5	38.5	56	83.5	27.5	58.5	71.5	13	55	63.5	8
Sep 6	51.5	90.5	39	55	82.5	27.5	57.5	71.5	14	55	63.5	8
Sep 7	51.5	90.5	39	54.5	82.5	28	57	71	14	55	63.5	8.5
Sep 8	51	90	39	54.5	82	27.5	57	71	14	55	63.5	8.5
Sep 9	51	90	39	54.5	82	27.5	57	70.5	13.5	55.5	63	7.5
Sep 10	51	90	39	54.5	82	27.5	57	70.5	13.5	55	63	8
Sep 11	51	89.5	38.5	54	81.5	27.5	56.5	70.5	14	54.5	63	8.5
Sep 12	50.5	89.5	39	54	81.5	27.5	56.5	70	13.5	54.5	62.5	8
Sep 13	49	87.5	37.5	52.5	80.5	27	55.5	68.5	13	54	62	8
Sep 14	48.5	87	38.5	52	79.5	27.5	55	68.5	13.5	54	61.5	7.5
Sep 15	48.5	86.5	38	52	79	27	54.5	68	13.5	53.5	61	7.5
Sep 16	48	86.5	38.5	51.5	79	27.5	54.5	68	13.5	53.5	60.5	7
Sep 17	48	86	38	51.5	78.5	27	54.5	67.5	13	53	60.5	7.5
Sep 18	48	86	38	51.5	78.5	27	54	67.5	13.5	53	60.5	7.5
Sep 19	48	85.5	37.5	51.5	78	26.5	54	67	13	53	60	7
Sep 20	46	83.5	37.5	50	76	26	53	65.5	12.5	52	60	7
Sep 21	45.5	83.5	38	49	76	27	52	65	13	51.5	59.5	8
Sep 22	45.5	83	37.5	49	75.5	26.5	52	65	13	51	59.5	7.5
Sep 23	45.5	83	37.5	49	75.5	26.5	52	64.5	12.5	51	58	7
Sep 24	45.5	82.5	37	49	75	26	51.5	64.5	13	50.5	58	7.5
Sep 25	45.5	82.5	37	49	75	26	51.5	64	12.5	50.5	57.5	7
Sep 26	45	82	37	48.5	74.5	26	51.5	64	12.5	50	57.5	7.5
Sep 27	43	80	37	47	73	26	50	63.5	13.5	49.5	56.5	7
Sep 28	42.5.	80	37.5	46.5	72.5	26	49.5	63.5	14	48.5	55.5	7
Sep 29	42.5	79.5	37	46	72	26	49	63	14	48.5	55.5	7.5
Sep 30	42.5	79.5	37	46	72	26	49	63	14	48	55.5	7

Note: Overlay thickness = 2.5 in.

Day of the Year	Temp of Overlay at the Surface (F)			Temp of Overlay at Mid Depth (F)			Temp of ISAC at the Interface (F)			Temp of PCC Slab at Mid Depth (F)		
	Min Temp	Max Temp	Daily Varia–tion	Min Temp	Max Temp	Daily Varia–tion	Min Temp	Max Temp	Daily Varia–tion	Min Temp	Max Temp	Daily Varia–tion
Oct 1	42.5	79.5	37	46	72	26	49	63	14	48	55.5	7.5
Oct 2	42.5	79	36.5	46	71.5	25.5	48.5	63	14.5	48	55	7
Oct 3	42.5	78.5	36	45	71	25	48.5	62.5	14	48	55	7
Oct 4	41	76.5	36.5	44.5	69.5	25	47.5	61.5	14	48	55	7
Oct 5	40.5	76	35.5	44	69	25	47	61	14	47.5	55	7.5
Oct 6	40.5	76	35.5	44	69	25	47	60.5	13.5	47.5	54.5	7
Oct 7	40.5	75.5	35	44	68.5	24.5	46.5	60	13.5	47.5	54.5	7
Oct 8	40	75.5	35.5	43.5	68.5	25	46.5	60	13.5	47.5	54	6.5
Oct 9	40	75	35	43.5	68	24.5	46	59.5	13.5	47	54	7
Oct 10	40	75	35	43.5	68	24.5	46	59.5	13.5	47	53.5	6.5
Oct 11	39	73.5	34.5	42.5	66.5	24	45.5	58.5	13	46.5	53	6.5
Oct 12	38.5	73	34.5	42	66	24	45	58	13	46	52.5	6.5
Oct 13	38.5	72.5	34	42	65.5	23.5	44.5	57.5	13	45.5	52	6.5
Oct 14	38.5	72.5	34	42	65.5	23.5	44.5	57.5	13	45.5	52	6.5
Oct 15	38.5	72	33.5	42	65	23	44.5	57	12.5	45	51.5	6.5
Oct 16	38.5	72	33.5	41.5	65	23.5	44	57	13	45	51.5	6.5
Oct 17	38	71.5	33.5	41.5	64.5	23	44	56.5	12.5	44.5	51	6.5
Oct 18	36	68.5	32.5	39.5	62	22.5	42.5	54.5	12	44	49.5	5.5
Oct 19	35.5	68	32.5	39	61.5	22.5	41.5	54	12.5	43	49	6
Oct 20	35	67.5	32.5	38.5	61	22.5	41.5	53.5	12	42.5	48.5	6
Oct 21	35	67.5	32.5	38.5	61	22.5	41	53.5	12.5	42	48	6
Oct 22	35	67	32	38.5	60.5	22	41	53	12	42	48	6
Oct 23	35	67	32	38	60.5	22.5	40.5	52.5	12	41.5	47.5	6
Oct 24	35	66.5	31.5	38	60	22	40.5	52.5	12	41.5	47.5	6
Oct 25	33	64	31	36.5	58	21.5	39.5	50.5	12	40.5	46	5.5
Oct 26	32.5	63.5	31	36	57.5	21.5	38.5	50	11.5	40	45.5	5.5
Oct 27	32.5	63	30.5	36	57	21	38.5	49.5	11	39.5	45	5.5
Oct 28	32	63	31	35.5	56	20.5	38	49.5	11.5	39	45	6
Oct 29	32	62.5	30.5	35.5	55	19.5	38	49	11	38.5	44.5	6
Oct 30	32	62	30	35	54	19	37.5	49	11.5	38.5	44	5.5
Oct 31	32	62	30	34.5	52	17.5	37	48.5	11	39	44	5

Note: Overlay thickness = 2.5 in.

Day of the Year	Temp of Overlay at the Surface (F)			Temp of Overlay at Mid Depth (F)			Temp of ISAC at the Interface (F)			Temp of PCC Slab at Mid Depth (F)		
	Min Temp	Max Temp	Daily Varia–tion	Min Temp	Max Temp	Daily Varia–tion	Min Temp	Max Temp	Daily Varia–tion	Min Temp	Max Temp	Daily Varia–tion
Nov 1	32	62	30	34.5	52	17.5	37	48.5	11.5	39	44	5
Nov 2	30.5	58	27.5	33.5	51.5	18	36	48	12	39	43.5	4.5
Nov 3	30.5	58	27.5	33.5	52.5	19	35.5	47.5	12	38.5	43.5	5
Nov 4	30.5	56	25.5	33.5	51	17.5	35.5	46.5	11	38.5	43	4.5
Nov 5	30	56	26	33	50.5	17.5	35.5	46	10.5	38	42.5	4.5
Nov 6	30	55.5	25.5	33	50.5	17.5	35	46	11	37.5	42.5	5
Nov 7	30	55	25	33	50	17	35	45.5	10.5	37.5	42	4.5
Nov 8	28	52	24	31	47.5	16.5	33.5	43.5	10	36.5	41	4.5
Nov 9	27.5	52	24.5	30.5	47	16.5	32.5	43	10.5	35.5	40	4.5
Nov 10	27	51.5	24.5	30	46.5	16.5	32.5	42.5	10	35	39.5	4.5
Nov 11	27	51.5	24.5	30	46.5	16.5	32	42.5	10.5	35	39.5	4.5
Nov 12	27	51	24	30	46	16	32	42	10	34.5	39	4.5
Nov 13	27	51	24	30	46	16	32	42	10	34	38.5	4.5
Nov 14	27	50.5	24.5	29.5	45.5	16	31.5	41.5	10	34	38.5	4.5
Nov 15	26	49	23	29	44.5	15.5	31	40.5	9.5	33.5	38	4.5
Nov 16	25.5	49	23.5	28.5	44	15.5	30.5	40	9.5	33	37.5	4.5
Nov 17	25.5	48.5	23	28.5	44	15.5	30.5	40	9.5	32.5	37	4.5
Nov 18	25.5	48.5	23	28	43.5	15.5	30	39.5	9.5	32.5	37	4.5
Nov 19	25.5	48.5	23	28	43.5	15.5	30	39.5	9.5	32.5	36.5	4
Nov 20	25.5	48	22.5	28	43.5	15.5	30	39.5	9.5	32	36.5	4.5
Nov 21	25	48	23	28	43	15	30	39	9	32	36	4
Nov 22	22	43.5	21.5	25.5	39.5	14	28	36.5	8.5	31	34.5	3.5
Nov 23	21.5	43	21.5	24.5	39	14.5	27	35.5	8.5	29.5	33.5	4
Nov 24	21.5	43	21.5	24.5	38.5	14	26.5	35	8.5	29	33	4
Nov 25	21.5	42.5	21	24.5	38.5	14	26.5	35	8.5	29	32.5	3.5
Nov 26	21.5	42.5	21	24	38	14	26	34.5	8.5	28.5	32.5	4
Nov 27	21.5	42.5	21	24	38	14	26	34.5	8.5	28	32	4
Nov 28	21.5	42	20.5	24	37.5	13.5	26	34	8	28	32	4
Nov 29	20.5	39	18.5	23.5	35	11.5	25.5	33	7.5	27.5	30.5	3
Nov 30	20.5	39	18.5	23	35	12	25	32.5	7.5	27	30	3

Note: Overlay thickness = 2.5 in.

Day of the Year	Temp of Overlay at the Surface (F)			Temp of Overlay at Mid Depth (F)			Temp of ISAC at the Interface (F)			Temp of PCC Slab at Mid Depth (F)		
	Min Temp	Max Temp	Daily Variation	Min Temp	Max Temp	Daily Variation	Min Temp	Max Temp	Daily Variation	Min Temp	Max Temp	Daily Variation
Dec 1	20.5	39	18.5	23	35	12	25	32.5	7.5	27	30	3
Dec 2	20.5	38.5	18	23	34.5	11.5	24.5	32.5	8	27.5	30.5	3
Dec 3	20	38.5	18.5	22.5	34.5	12	24.5	32	7.5	27	30.5	3.5
Dec 4	20	38	18	22.5	34	11.5	24.5	32	8	27	30	3
Dec 5	20	38	18	22.5	34	11.5	24	32	7	27	30	3
Dec 6	18	36	18	21	32	11	23	30	8	26	29	3
Dec 7	17.5	35.5	18	20	32	12	22	30	7.5	25.5	28.5	3
Dec 8	17.5	35.5	18	20	31.5	11.5	22	29.5	8	25	28	3
Dec 9	17.5	35.5	18	20	31.5	11.5	21.5	29.5	7.5	25	28	3
Dec 10	17	35	18	19.5	31	11.5	21.5	29	7.5	24.5	27.5	3
Dec 11	17	35	18	19.5	31	11.5	21.5	29	7.5	24.5	27.5	3
Dec 12	17	35	18	19.5	31	11.5	21.5	29	6	24.5	27.5	3
Dec 13	15.5	32.5	17	18.5	29	10.5	21	27	6	24	26	2
Dec 14	15	32	17	18	28.5	10.5	20.5	26.5	5.5	23.5	25.5	2
Dec 15	15	32	17	18	28	10	20.5	26	5.5	23	25	2
Dec 16	15	32	17	18	28	10	20.5	26	5	23	25	2
Dec 17	15	32	16.5	18	28	10	20.5	25.5	5	22.5	24.5	2
Dec 18	15	31.5	16.5	18	27.5	9.5	20.5	25.5	4.5	22.5	24.5	2
Dec 19	15	31.5	16.5	18	27.5	9.5	20.5	25	4.5	22.5	24.5	2
Dec 20	15	31.5	16.5	18	27.5	9.5	20.5	25	4.5	22.5	24	1.5
Dec 21	15	31.5	16.5	18	27.5	9.5	20.5	25	4.5	22	24	2
Dec 22	15	31.5	16.5	18	27.5	9.5	20.5	25	4.5	22	24	2
Dec 23	15	31.5	16.5	18	27.5	9.5	20.5	25	4.5	22	24	2
Dec 24	15	31.5	16.5	18	27	9	20	24.5	4.5	22	24	2
Dec 25	15	31.5	16	18	27	9	20	24.5	4.5	22	23.5	1.5
Dec 26	15	31	17	18	27	9	20	24.5	4.5	22	23.5	1.5
Dec 27	14	31	17	17.5	26.5	9	20	24	4	21.5	23	1.5
Dec 28	14	31	17	17	26.5	9.5	19.5	23.5	4	21.5	23	1.5
Dec 29	14	31	17	17	26	9	19.5	23	4	21	22.5	1.5
Dec 30	14	31	17	17	26	9	30.5	22.5	3	21	22.5	1.5
Dec 31	14	31	17	17	26	9	30.5	22.5	3	21	22.5	1.5

Note: Overlay thickness = 2.5 in.

APPENDIX B

SHEAR STRENGTH OF RUBBER ASPHALT MIXES
AT
DIFFERENT
TEMPERATURES, RATES OF SHEAR, AND
DISPLACEMENT LEVELS

Type of Rubber Asphalt	Rate of Shear (in/min)	Temp (F)	Shear Stress At Different Shear Displacements (psi)									
			0.01 in. Displa–cement	0.02 in. Displa–cement	0.03 in. Displa–cement	0.04 in. Displa–cement	0.05 in. Displa–cement	0.06 in. Displa–cement	0.07 in. Displa–cement	0.08 in. Displa–cement	0.09 in. Displa–cement	0.1 in. Displa–cement
AC–5	0.05	100	0.1	0.15	0.17	0.2	0.22	0.25	0.27	0.28	0.29	0.3
AC–10			0.1	0.16	0.19	0.22	0.25	0.27	0.28	0.29	0.3	0.3
AC–20			0.15	0.22	0.27	0.32	0.35	0.37	0.4	0.42	0.45	0.47
AC–5		80	0.13	0.25	0.28	0.32	0.35	0.38	0.42	0.45	0.48	0.5
AC–10			0.2	0.3	0.35	0.4	0.45	0.5	0.5	0.55	0.55	0.6
AC–20			0.15	0.3	0.45	0.53	0.6	0.67	0.74	0.82	0.88	0.95
AC–5		60	0.15	0.3	0.42	0.54	0.65	0.75	0.85	0.95	1.1	1.2
AC–10			0.4	0.7	0.9	1.1	1.3	1.4	1.5	1.6	1.7	1.8
AC–20			0.3	0.6	0.9	1.2	1.5	1.8	2.05	2.2	2.3	2.4
AC–5		40	1.1	2.05	2.7	3.4	4.1	4.6	5.2	5.7	6.1	6.4
AC–10			1.8	3.45	4.65	5.7	6.6	7.35	7.9	8.3	8.7	9
AC–20			2.5	5	6.95	8.7	10.2	11.4	12.5	13.4	14.1	14.8
AC–5		20	2.05	4.25	6.35	8.25	9.875	11.2	12.125	12.75	13.25	13.65
AC–10			4.2	8	10.9	13	14.6	15.75	16.65	17.35	17.9	18.3
AC–20			3.2	6.8	10.1	13.2	16.5	19.8	23.05	26.25	29.35	32.1
AC–5		0	2.6	5.5	8.25	11	13.5	16	18	19.375	20.375	21
AC–10			4.5	9	12.8	16	18.9	21.5	23.4	25	26.2	27
AC–20			6.5	13	19	24.5	29	33.3	37	40.8	44.2	47

Shear Stress Of Rubber Asphalt Mixes At Different Temperatures and Displacements @ 0.05 in./min Rate of Shear

Type of Rubber Asphalt	Rate of Shear (in/min)	Temp (F)	Shear Stress At Different Shear Displacements (psi)									
			0.01 in. Displacement	0.02 in. Displacement	0.03 in. Displacement	0.04 in. Displacement	0.05 in. Displacement	0.06 in. Displacement	0.07 in. Displacement	0.08 in. Displacement	0.09 in. Displacement	0.1 in. Displacement
AC–5	0.2	100	0.1	0.15	0.2	0.225	0.25	0.275	0.3	0.325	0.35	0.35
AC–10			0.1	0.15	0.2	0.25	0.3	0.35	0.375	0.4	0.425	0.45
AC–20			0.15	0.2	0.25	0.35	0.4	0.45	0.475	0.5	0.5	0.5
AC–5		80	0.12	0.2	0.28	0.34	0.4	0.44	0.48	0.5	0.53	0.55
AC–10			0.15	0.3	0.45	0.55	0.65	0.75	0.82	0.88	0.92	0.95
AC–20			0.2	0.5	0.75	0.95	1.1	1.2	1.3	1.4	1.5	1.55
AC–5		60	0.4	0.7	0.9	1.1	1.3	1.5	1.7	1.9	2.1	2.3
AC–10			0.6	1.1	1.65	2.1	2.5	2.8	3.2	3.5	3.85	4
AC–20			0.9	1.7	2.4	3.1	3.7	4.3	4.8	5.3	5.75	6.1
AC–5		40	1.95	3.3	4.4	5.3	6.1	6.9	7.5	8	8.4	8.9
AC–10			2.2	4.1	5.8	7.2	8.6	9.8	11	12	13	14
AC–20			4	7.5	11	14.5	18	21.25	24.25	27.25	30.15	32.75
AC–5		20	4.15	9.1	14.4	19.25	23.8	28.55	32.74	36.5	40	
AC–10			5.25	10.5	16	21.5	26.6	31.25	35.8			
AC–20			6	12	18	24	30					
AC–5		0	6.5	13.8	22.5	30.75	40					
AC–10			7	15.5	25	36	48					
AC–20			8.25	18.75	31.25	45	58					

Shear Stress Of Rubber Asphalt Mixes At Different Temperatures and Displacements @ 0.2 in./min Rate of Shear

Type of Rubber Asphalt	Rate of Shear (in/min)	Temp (F)	Shear Stress At Different Shear Displacements (psi)									
			0.01 in. Displa–cement	0.02 in. Displa–cement	0.03 in. Displa–cement	0.04 in. Displa–cement	0.05 in. Displa–cement	0.06 in. Displa–cement	0.07 in. Displa–cement	0.08 in. Displa–cement	0.09 in. Displa–cement	0.1 in. Displa–cement
AC–5	0.5	100	0.1	0.2	0.25	0.275	0.3	0.325	0.35	0.35	0.35	0.35
AC–10			0.12	0.25	0.32	0.36	0.4	0.44	0.48	0.52	0.56	0.6
AC–20			0.15	0.3	0.4	0.45	0.5	0.55	0.6	0.65	0.7	0.75
AC–5		80	0.15	0.25	0.33	0.4	0.45	0.48	0.52	0.56	0.6	0.65
AC–10			0.2	0.4	0.55	0.7	0.85	1	1.1	1.2	1.3	1.4
AC–20			0.4	0.8	1.2	1.4	1.6	1.8	2	2.2	2.4	2.6
AC–5		60	0.6	1.1	1.35	1.6	1.85	2.15	2.4	2.7	3.1	3.4
AC–10			1	1.8	2.5	2.9	3.3	3.7	4.1	4.5	4.9	5.2
AC–20			1.5	2.75	3.8	4.7	5.5	6.2	6.9	7.5	8	8.4
AC–5		40	1.9	3.6	5.1	6.5	7.8	9.2	10.7	12.2	13.6	15.1
AC–10			2.4	4.5	6.6	8.6	10.5	12.3	14	15.7	17.3	18.8
AC–20			3.7	8.4	13.2	17.6	22	26.3	30.6			
AC–5		20	6	13	20	26.25	32.5	38.8	44			
AC–10			7	13.5	20	26.75	33.5	40	46.5	52.5		
AC–20			6.65	14.5	22.75	31.25	40.4					

Shear Stress Of Rubber Asphalt Mixes At Different Temperatures and Displacements @ 0.5 in./min Rate of Shear

Type of Rubber Asphalt	Rate of Shear (in/min)	Temp (F)	Shear Stress At Different Shear Displacements (psi)									
			0.01 in. Displacement	0.02 in. Displacement	0.03 in. Displacement	0.04 in. Displacement	0.05 in. Displacement	0.06 in. Displacement	0.07 in. Displacement	0.08 in. Displacement	0.09 in. Displacement	0.1 in. Displacement
AC–5	1	100	0.1	0.15	0.2	0.28	0.32	0.34	0.35	0.36	0.37	0.37
AC–10			0.1	0.13	0.25	0.35	0.45	0.52	0.58	0.62	0.65	0.65
AC–20			0.15	0.29	0.41	0.5	0.6	0.68	0.75	0.81	0.85	0.88
AC–5		80	0.25	0.45	0.55	0.65	0.75	0.85	0.93	1	1.05	1.1
AC–10			0.3	0.6	0.8	1	1.1	1.2	1.3	1.4	1.5	1.6
AC–20			0.5	0.9	1.3	1.7	2	2.3	2.5	2.7	2.9	3.1
AC–5		60	0.6	1.2	1.7	2.1	2.5	3	3.5	4	4.4	4.8
AC–10			1.2	2.2	3.1	3.9	4.6	5.2	5.8	6.2	6.6	6.95
AC–20			1.4	2.8	4.1	5.3	6.5	7.6	8.6	9.6	10.6	11.6
AC–5		40	2.5	4.8	7.2	9.6	12	14.5	17	19.5	22	24.5
AC–10			4.3	8.2	11.8	15	18	20.7	23.3	25.8	28.2	30.5
AC–20			4.8	9.5	14	18.5	23.2	27.6	32			
AC–5		20	5.5	12	19	27	36					
AC–10			8.5	17.75	26	34	42					
AC–20			10.25	21.75	32	42	51.75					

Shear Stress Of Rubber Asphalt Mixes At Different Temperatures and Displacements @ 1 in./min Rate of Shear

Type of Rubber Asphalt	Rate of Shear (in/min)	Temp (F)	Shear Stress At Different Shear Displacements (psi)									
			0.01 in. Displacement	0.02 in. Displacement	0.03 in. Displacement	0.04 in. Displacement	0.05 in. Displacement	0.06 in. Displacement	0.07 in. Displacement	0.08 in. Displacement	0.09 in. Displacement	0.1 in. Displacement
AC–5	2	100	0.1	0.2	0.25	0.3	0.35	0.4	0.43	0.45	0.47	0.5
AC–10			0.12	0.23	0.33	0.42	0.5	0.57	0.63	0.68	0.72	0.75
AC–20			0.17	0.33	0.47	0.59	0.7	0.8	0.88	0.94	0.98	1.2
AC–5		80	0.2	0.4	0.55	0.7	0.85	0.95	1.08	1.2	1.33	1.45
AC–10			0.3	0.6	0.85	1.1	1.3	1.5	1.7	1.85	2	2.1
AC–20			0.45	0.85	1.4	1.8	2.2	2.6	3	3.4	3.8	4.1
AC–5		60	0.9	1.6	2.2	2.75	3.15	3.7	4.25	4.8	5.4	6
AC–10			1.5	3	4.2	5.1	6	6.7	7.4	8.1	8.8	9.5
AC–20			2.5	4.8	6.8	8.7	10.5	12.1	13.6	15	16.15	17.25
AC–5		40	3	5.8	8.4	11	13.5	16	18.5	21	23.5	26
AC–10			4	8	12	16	20	24	28.2	32.3	36.4	40.5
AC–20			5.4	10.8	16.2	21.6	27	32.4	37.8			

Shear Stress Of Rubber Asphalt Mixes At Different Temperatures and Displacements @ 2 in./min Rate of Shear

Type of Rubber Asphalt	Rate of Shear (in/min)	Temp (F)	Shear Stress At Different Shear Displacements (psi)									
			0.01 in. Displa-cement	0.02 in. Displa-cement	0.03 in. Displa-cement	0.04 in. Displa-cement	0.05 in. Displa-cement	0.06 in. Displa-cement	0.07 in. Displa-cement	0.08 in. Displa-cement	0.09 in. Displa-cement	0.1 in. Displa-cement
AC–5	3	100	0.1	0.15	0.23	0.3	0.37	0.44	0.46	0.48	0.50	0.52
AC–10			0.14	0.26	0.37	0.47	0.55	0.61	0.66	0.7	0.72	0.73
AC–20			0.25	0.5	0.65	0.8	0.9	01	1.08	1.15	1.2	1.25
AC–5		80	0.3	0.5	0.7	0.9	1.1	1.3	1.5	1.7	1.85	2
AC–10			0.45	0.8	1.1	1.4	1.7	1.95	2.15	2.35	2.54	2.7
AC–20			0.6	1.2	1.75	2.15	2.6	3.1	3.5	4	4.35	4.7
AC–5		60	1.2	2.5	3.5	4.5	5.5	6.3	7.1	7.9	8.7	9.3
AC–10			2	3.8	5.4	6.8	8	9.1	10.2	11.1	12	12.8
AC–20			2.6	5	7.3	9.6	12	14.3	16.5	18.6	20.6	22.4
AC–5		40	2.8	5.7	8.6	11.5	14.3	17	19.6	22.2	24.6	26.8
AC–10			4.6	9	13.2	17.6	22	26.2	30.2	34	37.6	41
AC–20			6.7	13.1	19.5	26.1	32.5					

Shear Stress Of Rubber Asphalt Mixes At Different Temperatures and Displacements @ 3 in./min Rate of Shear

APPENDIX C

THEORETICAL SHEAR STRESS AT THE INTERFACE Of PCC SLAB AND AC OVERLAY FOR VARIOUS OVERLAY THICKNESS RESULTING FROM A MOVING VEHICLE

Distance from Center of The Tire Along Y Axis (in.)	Shear Stress At The Interface On XY Plane (psi)	Distance from Center of The Tire Along Y Axis (in.)	Shear Stress At The Interface On XY Plane (psi)
0	43.7	0	43.7
0.5	43.5	–0.5	43.5
1	43.0	–1	43.0
1.5	42.0	–1.5	42.0
2	40.5	–2	40.5
2.5	38.4	–2.5	38.4
3	35.6	–3	35.6
3.5	32.2	–3.5	32.2
4	28.0	–4	28.0
4.5	23.5	–4.5	23.5
5	18.7	–5	18.7
5.5	14.1	–5.5	14.1
6	9.9	–6	9.9
6.5	6.5	–6.5	6.5
7	3.9	–7	3.9
7.5	2.1	–7.5	2.1
8	0.9	–8	0.9
8.5	0.2	–8.5	0.2
9	–0.2	–9	–0.2
9.5	–0.5	–9.5	–0.5
10	–0.7	–10	–0.7
10.5	–0.8	–10.5	–0.8
11	–0.9	–11	–0.9
11.5	–0.9	–11.5	–0.9
12	–0.9	–12	–0.9
12.5	–0.8	–12.5	–0.8

Shear Stress On Horizontal Plane At The Interface For 2.5 in. Thick Overlay

Distance from Center of The Tire Along Y Axis (in.)	Shear Stress At The Interface On XY Plane (psi)	Distance from Center of The Tire Along Y Axis (in.)	Shear Stress At The Interface On XY Plane (psi)
0	37.2	0	37.2
0.5	37.0	–0.5	37.0
1	36.5	–1	36.5
1.5	35.4	–1.5	35.4
2	33.9	–2	33.9
2.5	31.9	–2.5	31.9
3	29.3	–3	29.3
3.5	26.2	–3.5	26.2
4	22.8	–4	22.8
4.5	19.2	–4.5	19.2
5	15.6	–5	15.6
5.5	12.1	–5.5	12.1
6	9.0	–6	9.0
6.5	6.3	–6.5	6.3
7	4.2	–7	4.2
7.5	2.5	–7.5	2.5
8	1.3	–8	1.3
8.5	0.5	–8.5	0.5
9	–0.04	–9	–0.04
9.5	–0.4	–9.5	–0.4
10	–0.6	–10	–0.6
10.5	–0.8	–10.5	–0.8
11	–0.9	–11	–0.9
11.5	–0.9	–11.5	–0.9
12	–1.0	–12	–1.0
12.5	–1.0	–12.5	–1.0

Shear Stress On Horizontal Plane At The Interface
For 3 in. Thick Overlay

Distance from Center of The Tire Along Y Axis (in.)	Shear Stress At The Interface On XY Plane (psi)	Distance from Center of The Tire Along Y Axis (in.)	Shear Stress At The Interface On XY Plane (psi)
0	30.8	0	30.8
0.5	30.6	–0.5	30.6
1	30	–1	30
1.5	29.1	–1.5	29.1
2	27.7	–2	27.7
2.5	26	–2.5	26
3	23.9	–3	23.9
3.5	21.5	–3.5	21.5
4	18.8	–4	18.8
4.5	16	–4.5	16
5	13.2	–5	13.2
5.5	10.5	–5.5	10.5
6	8.1	–6	8.1
6.5	5.9	–6.5	5.9
7	4.1	–7	4.1
7.5	2.6	–7.5	2.6
8	1.5	–8	1.5
8.5	0.7	–8.5	0.7
9	0.2	–9	0.2
9.5	–0.2	–9.5	–0.2
10	–0.5	–10	–0.5
10.5	–0.6	–10.5	–0.6
11	–0.8	–11	–0.8
11.5	–0.9	–11.5	–0.9
12	–1.0	–12	–1.0
12.5	–1.0	–12.5	–1.0

Shear Stress On Horizontal Plane At The Interface
For 3.5 in. Thick Overlay

Distance from Center of The Tire Along Y Axis (in.)	Shear Stress At The Interface On XY Plane (psi)	Distance from Center of The Tire Along Y Axis (in.)	Shear Stress At The Interface On XY Plane (psi)
0	24.47	0	24.47
0.5	24.31	–0.5	24.31
1	23.83	–1	23.83
1.5	23.12	–1.5	23.12
2	22.01	–2	22.01
2.5	20.66	–2.5	20.66
3	18.99	–3	18.99
3.5	17.08	–3.5	17.08
4	14.94	–4	14.94
4.5	12.71	–4.5	12.71
5	10.49	–5	10.49
5.5	8.34	–5.5	8.34
6	6.43	–6	6.43
6.5	4.69	–6.5	4.69
7	3.26	–7	3.26
7.5	2.07	–7.5	2.07
8	1.19	–8	1.19
8.5	0.56	–8.5	0.56
9	0.16	–9	0.16
9.5	–0.16	–9.5	–0.16
10	–0.4	–10	–0.4
10.5	–0.47	–10.5	–0.47
11	–0.63	–11	–0.63
11.5	–0.71	–11.5	–0.71
12	–0.79	–12	–0.79
12.5	–0.79	–12.5	–0.79

Shear Stress On Horizontal Plane At The Interface
For 4 in. Thick Overlay

REFERENCES

1. Wood, W.A.,‘ ‘Reducing Reflection cracking in Bituminous Overlays,” Final Summary Report, National Experimental and Evaluation Program Project No. 10, Federal Highway Report No. FHWA–EP–85–02, 1984.

2. Vyce, J.M., “Reflection Cracking in Bituminous Overlays On Rigid Pavements,” Report No. 109, New York State Department of Transportation, 1983.

3. Lorenz, V. M., “New Mexico Study of Interlayers Used in Reflection Crack Control,”Presented at the Annual Meeting of the Transportation Research Board, January, 1987.

4. Predoehl, N.H., “Evaluation of Paving Fabric Test Installation in California Final Report ,” draft, California Department of Transportation, Translab (1989).

5. Lytton, R.L.,“Use of Geotextiles for Reinforcement and Strain Relief in Asphalt Concrete,”Geotextile and Geomembranes, Vol. 8 (1989).

6. McGhee, K.H., “Efforts to Reduce Reflection Cracking of Bituminous Concrete Overlays of Portland Cement Concrete Pavements,” Report No VHTRC 76–R20, Virginia Highway and Transportation Research Council, Charlottesville, Va. (November 1975).

7. Button, J. W., “Overlay Construction and Performance Using Geotextiles,,” Transportation Research Record 1248: Transportation Research Board, National Research Council, Washington, D.C. (1990).

8. Smith, R.D., "Laboratory Testing of Fabric Interlayers for Asphalt Concrete Paving," Report No. FHWA/CA/TL–84/06, California Department of Transportation, Translab (June 1984)

9. Tyner, H. L. ; Gulden, W. and Brown, D. , "Resurfacing of Plain Jointed Concrete Pavements," Georgia Department of Transportation, paper presented at the annual meeting of the Transportation Research Board, January 1981.

10. Ponniah. E. Joseph, and Palph Haas, R., "Evaluating Alternative Solutions to Reflective Cracking Through Overlays," Transportation Research Record 1215:Pavement Management and Rehabilitation: Transportation Research Board, National Research Council, Washington, D.C. (1989).

11. Coetzee N.F. and C.L. Monismith, "Analytical Study of Minimization of Reflection Cracking in Asphalt Concrete Overlays by Use of a Rubber Asphalt Interlayer." in Transportation Research Record 700: Pavement Evaluation and Overlay Design: A symposium and Related Papers, Transportation Research Board, National Research Council, Washington, D.C. (1979) pp. 100–108.

12. Monismith, C.L. and N.F.Coetzee, " Reflection Cracking: Analysis,Laboratory Studies and Design Considerations,"Proceedings, AAPT, Vol. 49 (1980) pp 268–313.

13. The Asphalt Institute, "Asphalt Overlays for Heavily–Trafficked PCC Pavements", Information Series No. 177, 1981.

14. Barry J. Dempsey, W. Andrew Herlache, and Arti J. Patel, " The Climate–Materials–Structural (CMS) Pavement Analysis Program ".

15. Computer Model CIRCLY, "A computer program for the Analysis of Multiple Complex Circular Loads on Layered Anisotropic Media," by L.J. Wardle.

16. Gulden W. and D. Brown, "Overlays for Plain Jointed Concrete Pavements," Research Project No. 7502, Office of Materials and Research, Georgia Department of Transportation (1984).

17. Knight, N., "Heavy duty Membranes for the reduction of Reflective Cracking in Bituminous Concrete Pavements," Report No. FHWA/PA–85–006, Pennsylvania Department of Transportation (August 1985) 32 pp.

18. Noonan, J.E. and F.R. McCullagh, "Reduction of Reflection Cracking in Bituminous Overlays on Rigid Pavements," Report No. 78, New York State Department Of Transportation, 1980.

19. Knight, N. E., "Sealing Cracks in Bituminous Overlays of Rigid Bases," Presented at Annual Meeting of the Transportation Research Board, January, 1985.

20. Federal Highway Administration, "Crack and Seat Performance," Review Report, Demonstration Projects Divisions and Pavements Divisions, 1987.

21. Voigt, G. F., Carpenter, S. H. and Darter, M. I., "Rehabilitation of Concrete Pavements, Volume 2– Overlay Rehabilitation Techniques," Federal Highway Administration Contract No. DTFH61–85–C–00004, 1987.

22. Pavement Consultancy Services, A Division of Law Engineering Inc., "Guidelines and Methodologies for the Rehabilitations of Rigid Highway Pavements Using Asphalt Concrete Overlays," July 1991.

23. Hensley, M.J., "Open Graded Asphalt Concrete Base for the control of Re-

flection Cracking, Proceedings of the Association of Asphalt Paving Technologists, Volume 49 1980.

24. Morris, G. R., and McDonald, C. H., "Asphalt Roller Stress Absorbing Membranes: Field Performance and State of the Art," Transportation Research Record No. 595, Transportation Research Board, 1976.

25. B. A. Vallerga, G. R. Morris, J. E. Huffman, B. J. Huff, "Applicability of Asphalt Rubber Membranes in Reducing Reflection Cracking."

26. Dean. A. Maurer, and Gerlad. J. Malasheskie, "Field Performance of Fabrics and Fibers to Retard Reflective Cracking," Transportation Research Record 1248: Transportation Research Board, National Research Council, Washington, D.C. (1989).

27. Robert A. Eaton, and Randy N. Godfray, "Reflection Cracking Guides at Thule Air Base," Greenland using AC 2.5 and Fabrics.

28. Bone, A.J., L.W. Crump, and V.J. Roggeveen, "Control of Reflection Cracking in Bituminous Resurfacing over Old Cement and Concrete Pavements," in HRB Proceedings, vol. 33, Highway Research Board, National Research Council, Washington, D.C. (1954) pp. 345–354.

29. Pourkhosrow, G.,"The Evaluation of Non–Woven Fabric: Petromat and Mirafi," Report No. FHWA/OK 8266, Oklahoma Department of Transportation (May 1982) 25 pp.

30. George B. Sherman, "1976 Evaluation of the Philips Petroleum Company's-Product Pertromat." (Jul 1976).

31. Dykes, J.W., "Use of Fabric Interlayers to Retard Reflection Cracking,"

Proceedings, APPT, Vol. 49 (1980) pp. 354–368.

32. Barksdale, R.D., S.F. Brown, and F. Chan, NCHRP Report 315: Potential Benefit of Geosynthetics in Flexible Pavements, Transportation Research Board, National Research Council, Washington, D.C. (November 1989) 56 pp.

33. Ahlrich, R.C., "Evaluation of Asphalt Rubber and Engineering Fabrics as Pavement Interlayers," Misc. Paper GL–86–34 (Untraced Series N–86) (November 1986) 7 pp.

34. Button, J.W. and R.L. Lytton, "Evaluation of Fabrics, Fibers and Grids in Overlays," Proceedings, 6th International Conference on Structural Design of Asphalt Pavements, Vol. 1, Ann Arbor, Mich. (Jul 1987) pp. 925–934.

35. Majidzadeh, K., G.J. Ilves, and V.R. Kumar, "Improved Method to Eliminate Reflection Cracking," Report No. FHWA/RD–86/075, Federal Highway Administration, Washington, D.C. (September 1985).

36. Barry J. Dempsey, "A Heat Transfer Model For Evaluating Frost Action And Temperature Related Effects In Multilayered Pavement Systems, ".

37. American Association of State Highway and Transportation Officials (1986) "AASHTO Guide for Design of Pavement Structures", Washington D.C.

38. DeJong, D. L., M. G. F. Peutz, and A. R. Korswagen, "Computer program BISAR," Koninkijke/Shell – Laboratorium, Amsterdam, the Netherlands, 1973.

39. German, F.P. and R.L. Lytton, "Methodology of Predicting the Reflection Cracking Life of Asphalt Concrete overlays," Report No. FHWA/TX–79/09–207–5, Texas State Department of Highway and Public Transportation, Austin, Tex. (March 1979).

40. Maurer, D.A. and G.J. Malasheskie, "Field Performance of Fabric and Fibersto Retard Reflection Cracking," Report No. 83–8, Pennsylvania Department of Transportation (1988).

41. Button, J.W., J.A. Epps, and R.L. Lytton, "Laboratory Evaluation of Fabricator Reducing Reflection Cracking," Report No. RF 3424–3, Texas Transportation Institute, Texas A&M University (January 1983).

42. Button, J. W. and Epps, J. A., "Evaluation of Fabric Interlayers," Texas Transportation Institute. Texas A & M University. College Station. Nov. 1982.

43. George B. Sherman, "NCHRP Synthesis of Highway Practice 92: Minimizing Reflection Cracking of Pavement Overlays. TRB," National Research Council, Washington, D.C., Sept. 1982.

44. Epps, J.A., and Button, J.W., "The Slippage Question on Airport Pavements," Texas Tansportation Institute, Interim report RF 3424–2.

45. Report on Performance of Fabrics in Asphalt Overlays. FHWA. U.S. Department of Transportation, Sept. 1982.

46. Jacob, T. R.,"Design Parameters for Use of Reinforced Stress Absorbing Membrane Interlayers," Transportation Research Record 1272:Pavement Management and Rehabilitation: Transportation Research Board, National Research Council, Washington, D.C. (1990).

47. Carey, D. E.,"Evaluation of Synthetic Fabrics for the Reduction of Reflection Cracking," Federal Highway Administration Report No. 70–18(B), 1975.

48. Pumphrey, N. D.,' 'Relief Layer Reduces Reflection Cracking," Public Works. July, 1982.

49. Constrantine A. Vokas, C. A. and Stoll, R. D., "Reinforced Elastic Layered Systems," Transportation Research Record 1153:Reinforced Layered Systems: Transportation Research Board, National Research Council, Washington, D.C. (1987).

50. Bathurst, R. J. and Raymond, G. P., "Geogrid Reinforcement of Ballasted Track," Transportation Research Record 1153:Reinforced Layered Systems: Transportation Research Board, National Research Council, Washington, D.C. (1987)

51. P. Joseph, R. Hass, and W. A. Phang. Thermally Associated Fatigue Crack Growth Through Asphalt Overlays: an Experimental Investigation. Proc., Paving in Cold Areas Workshop 3, Ottawa, Ontrio, Canada, 1987.

52. Allen, H.S., "Methods and Materials for Reducing Crack Reflectance," Report No FHWA–MN–RD–84–09, Minnesota Department of Transportation (January 1985) 32 pp.

53. P. Joseph. Low Temperature Reflection Cracking Through Asphalt Overlays. Ph.D. Thesis. University of Waterloo, Waterloo, Ontario, Canada, 1987.